Defining a role for the mesenchymal stem cell secretome in inflammatory response suppression

Marwan Mohammed Merkhan

Submitted For the Degree of Doctor of Philosophy

March 2018

Keele University

Abstract

Human mesenchymal stem cells (hMSCs) have multiple potential roles in regenerative medicine. These roles revolve around the exploitation of their multipotent differentiation potential, their immunogenic privilege, or the broad range of molecules they secrete. The functions of these molecules include stimulation of cell migration during wound repair, activation of endogenous tissue-specific stem cell pools, and suppression of T-cell-based inflammatory responses. hMSCs have been exploited clinically in the treatment of graft versus host disease following bone marrow or organ transplant via systemic administration and in other indications including ischemic heart disease, Crohn's disease, and diabetes mellitus. However, the mechanisms underlying the regenerative potential of hMSCs are still uncertain. Moreover, the effectiveness of hMSCs-based cell therapy has been doubted because the therapeutic actions have often been noticed in the absence of hMSCs homing to the target tissues. Thus, indicating that the level of improvement of diseased tissues is not reciprocal to the observed target tissue homing/differentiation, suggesting that it may play an indirect role in tissue regeneration or it may have a dualistic mode of action.

Irrespective MSCs provide a great promise in the treatment of degenerative disorders and inflammatory ailments. However, there are still many challenges to overcome prior to their widespread clinical application. For instance, their ambiguous paracrine mechanism remains a matter for controversy and exploration; moreover, current *in vitro* cultures have limited success in reflecting many aspects of the *in vivo* niche – including oxygen level. This study focused on the paracrine properties of hMSCs with a particular focus on their role in immunosuppression and anti-inflammation. Coupled to this we explored oxygen-dependent regulation of the paracrine biology of MSCs focussing on a number of important paracrine factors with roles in immunomodulation. Serum free-conditioned media (SFCM) were used as a model to characterize the immune sentinel function of MSCs. Proteomic analysis indicated that SFCM of hMSCs contained various cytokines which may play an important role in the suppression of inflammation and that the composition and

concentration of SFCM was oxygen dependent. Intermittent hypoxia (IH) initiated a stark upregulation of paracrine factor secretion. The therapeutic effectiveness of SFCM was reflected via its efficacy across two *in vitro* cell line models; SFCM suppressed T cell model activation (Jurkat) in an oxygen independent manner while the modulation of macrophage (THP-1) terminal differentiation was oxygen sensitive. Collectively, IH SFCM suppressed the immune response at T cell and antigen presentation levels while air oxygen (21% O_2) cultured hMSC SFCM supressed the immune response at T cell level and maintain the antigen presentation which might elicits the immune response.

These optimized *in vitro*-culture findings support clinical application of hMSCs and/or their secretory factors as a pharmacoregenerative modality for the treatment of non-curative diseases, such as, rheumatoid arthritis, Crohn's disease, myocardial infarction, and advanced critical limb diseases. Moreover, this property may be harnessed to produce an optimized acellular biological product with immunomodulatory actions similar to hMSCs, leading to production of an "off-the-shelf" biological product. The production of such biological products will have important economic considerations in cell-based therapy.

Keywords: mesenchymal stem cell, secretome, conditioned media, regeneration, immune cell, T cell, macrophage, neutrophil, Jurkat cell, THP-1 cell, immunosuppression.

Contents

Figures

Tables

Abbreviations

ABTS	2.2-azino-bis(3-ethylbenzothiazolin-6-sulphonic acid
ACE	Angiotensin converting enzyme
AP-1	Activator protein-1
APC	Antigen presenting cells
BCA	Bicinchononic acid
BMA	Bone marrow aspirate
bNGF	beta-nerve growth factor
BSA	Bovine serum albumin
C5a	Complement component 5a
CCL5	Chemokine (C-C motif) ligand 5
CCR2	chemokine receptor type 3
CCR5	chemokine receptor type 5
CD	Cluster of Differentiation
CFU	Colony forming unit
CFU-F	Colony forming unit-fibroblast
CLRs	C-type lectin receptors
CM	conditioned media
CNTF	Central neurotrophic factor
CTls	Cytotoxic T lymphocytes
DAG	Diacyl glycerol
DAMP	Damage associated molecular pattern
DC	Dendritic cells
dH2O	Deionised water
DMEM	Dulbecco's Modified Eagle Medium
DMSO	Dimethyl sulphoxide
dNTP	deoxy nucleoside triphosphate
EDTA	Ethylene diamine tetra-acetic acid
EGF	Epidermal growth factor
EOTAXIN	eosinophil-specific chemoattractant
ER	Endoplasmic reticulum
ERK	Extracellular-signal-regulated kinase
FBS	Foetal bovine serum
FGF	Fibroblast growth factor
f-MLP	N-Formylmethionine-leucyl-phenylalanine
Fos	FBJ osteosarcoma oncogene
GAPDH	Glyceraldehyde 3-phosphate dehydrogenase
GM	Growth media
GM-	Growth media in absence of stimulant
GM+	Growth media in presence of stimulant

GMCSF	Granulocyte monocyte colony stimulating factor
GvHD	Graft vs. host disease
H2O2	Hydrogen peroxide
HBG2	Haemoglobin G2
HGF	Hepatocyte growth factor
HLADR	Human leucocyte antigen-DR
HLA-G5	Human leukocyte antigen-G5
hMSCs	human mesenchymal stem cells
HO	Haemoxygenase
HRP	Horse raddish peroxidase
HSC	Haematopoeitic stem cell
IBMX	3-Isobutyl-1-methylxanthine
ICAM	Intercellular Adhesion Molecule 1
IDO	Indolamine di-oxygenase
IL	Interleukine
IL10R	Interleukine 10 receptor
IL2R	Interleukine 2 receptor
IFNγ	Interferron gamma
IP-10	C-X-C motif chemokine 10 (CXCL10)
IP3	Inositol trisphosphate
ITS	Insulin-Transferrin-Selenium
JAK	Janus kinases
JNK	Jun N-terminal kinase
JUN	Jun proto-oncogene, AP-1 transcription factor subunit
LIF	Leukemia inhibitory factor
M0	Macrophage 0
M1	Macrophage 1
M2	Macrophage 2
MAPK8	Mitogen-activated protein kinase 8
MCP1	Monocyte Chemoattractant Protein1
MCSF	Monocyte colony stimulating factor
MD	Muscular dystrophy
MEG	Megakaryocyte
MHC	Major histocompatability complex
MIP1	Macrophage inflammatory protein1
MPO	Myeloperoxidase
MS	Multiple sclerosis
mTOR	mammalian target of rapamycin
MTT	3-(4,5-dimethylthiazol-2yl)-2,5diphenyltetrazolium bromide
NADPH	Nicotinamide adenine dinucleotide phosphate
NCM	Non-conditioned media

NEAA	Non-essential amino acid
NETs	Neutrophil extracellular traps
NFATC2	Nuclear factor of activated T-cells, cytoplasmic, calcineurin-dependent 2
NF-kB	Nuclear Factor-Kappa Beta
NK	Natural killer cells
NLRs	NOD-like receptors
NSAIDs	Non-steroidal anti-inflammatory drugs
OD	Optical density
PAI1	Plasminogen activator inhibitor1
PAMP	Pathogen-associated molecular pattern
PBS	Phosphate buffered saline
pD1	Programmed cell death protein 1
PDGF	Platelet-derived growth factor
PGE2	Prostaglandine E2
PHA	Phytohaemaglutinin
PIGF1	Placental growth factor1
PIP2	Phosphatidylinositol 4,5-bisphosphate
PKC	Protein kinase C
PLC	Phospholipase C
PMA	Phorbol myristate acetate
PMN	Polymorphonuclear cells
PPP3CA	Serine/threonine-protein phosphatase 2B catalytic subunit alpha isoform
PRRs	pattern recognition receptors
PSA	Penicillin streptomycin amphotericin
qRTPCR	quantitative Reverse transcription polymerase chain reaction
RANTES	Chemokine (C-C motif) ligand 5
Rela	Reticuloendotheliosis viral oncogene homolog A
RESISTIN	Adipose tissue-specific secretory factor
RTPCR	Reverse transcription polymerase chain reaction
SAPK	stress activated protein kinase
SCF	Stem cell factor
SDS	Sodium dodecyl sulphate
SFCM	Serum-free conditioned media
SFCM-	Serum-free conditioned media in absence of stimulant
SFCM+	Serum-free conditioned media in presence of stimulant
SFNCM	Serum-free non-conditioned media
SFNCM-	Serum-free non-conditioned media in absence of stimulant
SFNCM+	Serum-free non-conditioned media in presence of stimulant
SH2	Src Homology2
STAT	Signal transducer and activator of transcription
TAE	Tris base, acetic acid and EDTA buffer

TCR	T cell receptor
TGFb	Transforming growth factor beta
Th	T helper type T cell
TLRs	Toll-like receptor
TNFa	Tumour necrosis factor alpha
Tregs	T regulatory Type T cells
TYK	Tyrosine kinases
VEGF	Vascular endothelial growth factor
WS	Work station

Publications and presentations

Oral presentations

1- ISTM PG symposium2014/Keele University

MM Merkhan, NR Forsyth. Developing mesenchymal stem cell-based systems for localised inflammatory response suppression.

2- Stem cells in regenerative medicine meeting2015/Robert Jones and Agent Hunt Orthopaedic Hospital/Oswestry

MM Merkhan, NR Forsyth. Hypoxic modulation of the hMSC secretome; a role in dictating immune response.

3- 9th UK MSC meeting2015/university of Manchester

MM Merkhan, NR Forsyth. The role of hMSCs-secretome in attenuating the immune response using Jurkat cells as an *in vitro* model.

4- MSCA2016/Manchester

MM Merkhan, NR Forsyth. Restoration of *in vitro* immune response in IL10 devoided MSCs secretome.

5- TERMIS-EU meeting2016/Sweden

NR Forsyth, MM Merkhan. Mesenchymal stem cell secretome; immunomodulation and oxygen dependency.

6- Regenerative Medicine PhD WebEx Forum2017/GHRC, Oswestry, Keele University

MM Merkhan, NR Forsyth. Mesenchymal stem cell secretome; immunomodulation and oxygen dependency.

7- MSCA2015/Sheffield-Teaser Talk

MM Merkhan, NR Forsyth. Reduced oxygen culture modulates transcription and composition of hMSC secretome.

8- ISTM PG symposium2016/Stoke-On-Trent-Turbo Talk

MM Merkhan, NR Forsyth. IL10: an immunomodulatory component of hMSC secretome.

Poster presentation

1- MSCA2014/Liverpool

MM Merkhan, NR Forsyth. Characterisation of immunomodulatory cytokines of bone marrow derived mesenchymal stem cell secretome.

2- TCES2015/Southampton

MM Merkhan, NR Forsyth. The role of hMSCs-secretome in attenuating the immune response using Jurkat cells as an *in vitro* model.

3- North staffordshire conference centre2015/Stoke-On-Trent

S Premi, MM Merkhan, NR Forsyth. Characterisation of the mechanism of Mesenchymal stem cell-driven immunomodulation.

4- MSCA2015/Sheffield

MM Merkhan, NR Forsyth. Reduced oxygen culture modulates transcription and composition of hMSC secretome.

5- ISTM PG symposium2016/Stoke-On-Trent

MM Merkhan, NR Forsyth. IL10: an immunomodulatory component of hMSC secretome.

6- MSCA2016/Manchester

MM Merkhan, NR Forsyth. Restoration of *in vitro* immune response in IL10 devoided MSCs secretome.

7- TCES2017/Manchester

MM Merkhan, TP Dale, EL Pollard, NR Forsyth. Role of the hMSC-secretome in the modulation of inflammatory lung diseases.

8- Ilas conference2017/Keele University

MM Merkhan, NR Forsyth. Restoration of *in vitro* immune response in IL10 devoided MSCs secretome

Acknowledgments

I would like to sincerely thank my supervisor Prof Forsyth NR for the patient guidance, encouragement, and advice he has provided throughout my time as his PhD student. Thanks for allowing me the freedom to work independently but being supportive when I needed it which eventually make me independent researcher. I have been extremely lucky to have a supervisor who cared so much about my work, and who responded to my questions and queries so promptly.

I would also like to thank all the members of staff at Guy Hilton research centre, including receptionists, lab-technicians, PhD students, post-doc students, Dr Richardson A (my advisor), Dr Kelly C, and all Iraqi PhD students on/off-campus, especially people in Prof Forsyth's group; Dr Dale TP, Dr Al-Azzawi BA, Dr Al-Zubaidi MA, Al-Jumaily RM, Dr Ahmed MA, Younus ZM, Li-Yun Chen, Borg D'Anastasi EL, Bratt JAJ, Kyoseva AY, and Fadayomi IE, guys it was a pleasure to work with you all and without your support this work is not going to see the light.

Thanks are also in order for a number of people outside the ISTM, Including Dr Ibrahim Mohammed Faisal, Dr Moath Kahtan, and Dr Dilbreen Barzanji, without you guys I am not going to be here and I really appreciate what you have done for me. I would like also to thank Dr Mohanad Alfahadi and Mrs Noor Altaan for accommodating me and my family when I have arrived at the UK and helping us to settle down.

I would also like to express my deep gratitude to my beloved wife Maryam for being so helpful and understanding my needs, you spent sleepless nights with and you were always my support in the moments when there was no one to answer my queries. Maram, Moamin, and Yamin (just born!) you are all parts of my heart and you all provide me a spiritual strength throughout my life. Last but not the least, I would like to thank my big family in Iraq: my parents and to my brothers and sisters for supporting me spiritually throughout writing this thesis and my life in general.

The work described in this thesis was principally funded by the Iraqi Ministry of Higher Education and Scientific Research, University of Mosul, and Keele University. Thanks should also go to all other foundations, charity societies, institutions, and organisations in the UK, which are sponsoring or in collaboration with Prof Forsyth's lab and hence participated somehow in fulfilment of this thesis.

Keele UNIVERSITY

Chapter 1

-----Introduction-----

1.1 Mesenchymal stem cells

hMSCs are stromal cells which are widely distributed throughout the body but commonly isolated *in vitro* from; bone marrow, adipose tissues, and umbilical cord blood[1]. They are characterised by a capacity for finite serial passaging expansion, multiple lineage differentiation, and trophic factors secretion together with engraftment potentials, regeneration, and immunoregulatory functions[2,3]. There is some controversy regarding the identity of MSCs; however, the International Society for Cellular Therapy has defined minimal guidelines for MSCs characterisation including; plastic adherence, multi-lineage differentiation into fat, bone, and cartilage, together with a surface expression of stem cell markers (CD73, CD90, and CD105), with lacking expression of haematopoietic markers (CD34, CD45, CD11a, CD19 or CD79a, CD14 or CD11b and histocompatibility locus antigen (HLA)-DR)[4]. MSCs have potential therapeutic value in inflammatory diseases and it has been confirmed that hMSCs mitigate the acute phase of graft versus host disease[5,6], manipulate the early inflammatory response associated with kidney injury[7,8], and improve inflammatory phase of immunological diseases like hepatitis[9], arthritis[10], and organ transplantation[11].

The main role of hMSCs in bone marrow biology is the regulation of homeostasis of the hematopoietic stem cells (HSCs) in an undifferentiated state[12]. MSCs provide an immunosuppression environment within the bone marrow niche, inhibiting autoimmune responses by mature T cells until naïve immune cells are released to the periphery[13]. The immunoregulatory properties of hMSCs, together with the *in vitro* isolation and expansion of MSCs, make these cells an attractive candidate for cell biotherapy. Additionally, hMSCs are characterised by an intrinsic immune-privileged nature, demonstrated by low expression levels of MHCI and no expression of MHCII, protecting them from allogenic reactions and NK cytotoxicity[14].

Stem cells can be primarily categorised based on differentiation potential into 4 categories; totipotent stem cells which have the capacity to differentiate to all possible cell types, for

example, zygote formed at egg fertilisation. Pluripotent stem cells have the ability to differentiate into derivatives of the 3 germ layers (ectoderm, mesoderm, and endoderm), e.g. embryonic stem cells. Multipotent stem cells have the ability to differentiate into multiple cell types of the same family, such as haematopoietic stem cells, which give rise ito red blood cells, white blood cells, and platelets[15,14]. Adult stem cells (ASCs) are thought to be present in all tissues; have been isolated from the bone marrow, brain, liver, lung, fetal blood, umbilical cord blood, kidneys, adipose tissue, and placentas[16]. hMSC from bone marrow were originally characterised by their plastic adherent spindle-shaped cells with a capacity to form colonies called colony-forming unit fibroblasts (CFU-F)[17]. hMSCs are characterised by their multipotent differentiation potential into fat, bone, cartilage, and muscle (Figure 1-1)[18]. Moreover, MSCs trans-differentiation into cell types representative of liver, neuron, and astrocytes has been reported[19].

Recent studies have confirmed the immunomodulatory properties of MSCs. Mouse and human MSCs originating from bone marrow, fetal membrane, placenta, amniotic MSCs, dental pulp or umbilical cord, express MHC class I but not MHC class II antigens[20,21,14]. However, some studies have demonstrated that IFNγ can induce upregulation of MHCII on MSCs derived from bone marrow, placenta, and umbilical cord[22]. The up-regulation of MHC class II by IFNγ does not elicit alloreactive lymphocyte proliferative responses[20,23]. These data are controversial, because the stimulation of MSCs with high-dose of IFNγ can induce the proliferation of allogeneic T cells[24,25,26]. However, high doses of IFNγ have also been noted to reduce the expression of MHCII on MSCs resulting in a loss of the ability of hMSCs to act as antigen-presenting cells[26]. Therefore, it's believed that MSCs can modulate their immunomodulatory properties according to their localised milieu.

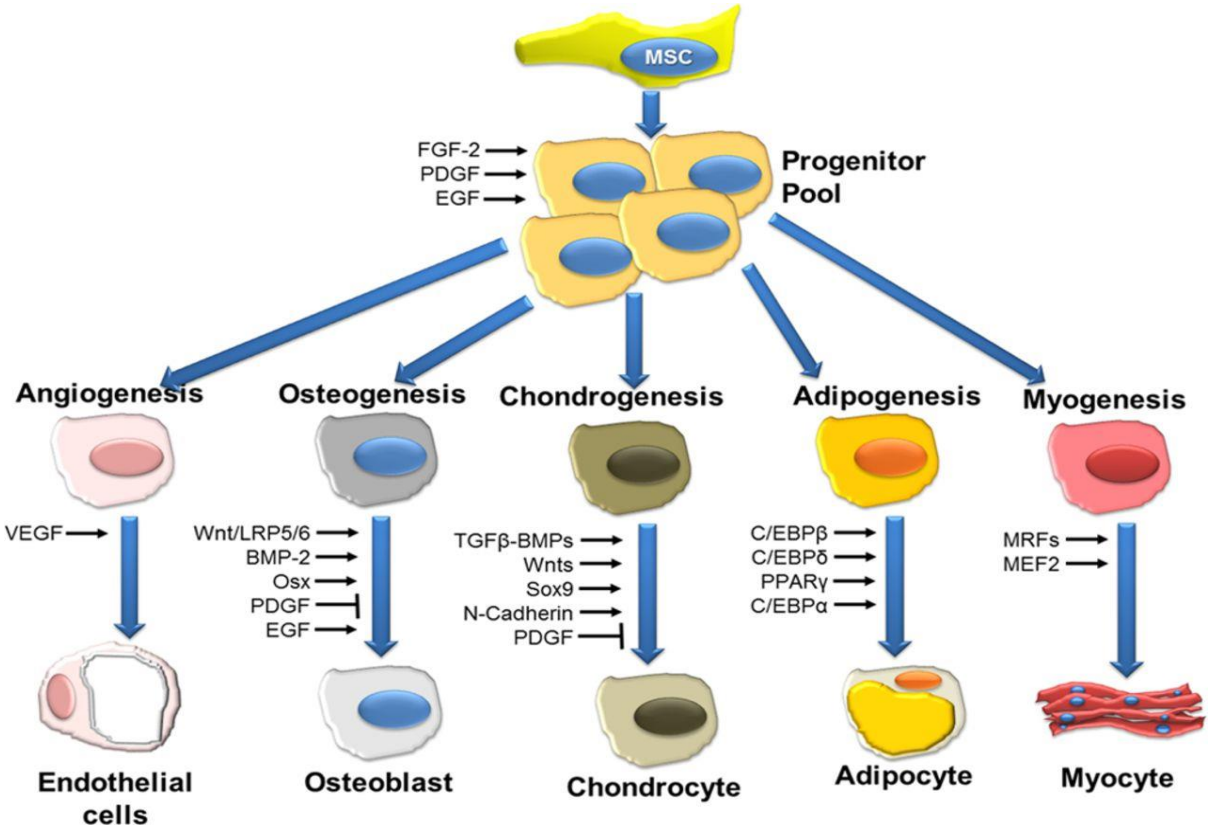

Figure 1-1. Schematic overview of signalling molecules and transcription factors involved in the regulation of differentiation of mesenchymal stem cells (MSCs).

BMP-2 indicates bone morphogenetic protein-2; EGF, epidermal growth factor; FGF-2, fibroblast growth factor-2; LRP5/6, low-density lipoprotein receptor-related protein-5/6; MEF2, myocyte enhancer factor-2; MRF, myogenic regulatory factors; Osx, Osterix; PDGF, platelet-derived growth factor; RUNX2, runt-related transcription factor-2; TGFb, transforming growth factor-β; and VEGF, vascular endothelial growth factor.

Reprinted from Karantalis *et al*, 2015[27] with permission from Circulation Research, License number 4200780800970.

1.2 *In vitro* recreation of bone marrow niche physioxia versus air oxygen tension

The anatomical design of bone marrow is complex. The structure consists of haematopoetic and adipose cells surrounded by sinusoidal vessels. The cells are arranged in a well-organised order with progenitors located in foci away from the vessel sinuses while mature cells are adjacent to the blood stream enabling gradual escape to the blood according to body demands[28]. This organised morphological architecture positions progenitor cells; including MSCs, far away from sinuses under a gradient hypoxic environment (1-6% O_2) depending their location relative to the sinuses[29,30].

In healthy tissue, physiological normoxia (physioxia) is a characteristic feature of the natural *in vivo* environment. MSCs exist within the lower limits of physioxia norms despite their perivascular localization in niches adjacent to blood vessels (Figure 1-2). Tissue oxygen tension is significantly lower than the inhaled exogenous air (21% O_2) and it declines gradually as it passes from the lung to the tissues; ranging between 0.1% - 9% with an average of 2% O_2[31,32,33,34]. This intrinsic low physioxic value may be responsible for the maintenance of MSC plasticity and proliferation capacity [33,29,32]. Recent reports have confirmed that in the presence of reprogramming factors physioxic oxygen levels *in vitro* can promote the generation of induced pluripotent stem cells from human adult somatic cells[35]. Likewise in disease, damage, or disorder states tissue injury can be associated with inflammatory hypoxia due to the activation of a coagulation cascade with an accompanying and subsequent release of MSC chemotactic factors resulting in localisation of migratory MSCs in a transiently hypoxic environment[36]. Some diseases for which MSCs are under current clinical trials including ischemic heart disease are characterised by a dualistic hypoxia; mechanical hypoxia due to narrowing of coronary blood vessels and biochemical hypoxia due to inflammation[37]. However, most research centres culture and characterise stem cells in air oxygen (21% O_2) ignoring the importance of the niche-like physioxic paradigm and its important role in cell metabolic status, integrity, longevity and engraftment potential [38,39,40].

With reference to exposure to different oxygen tensions the journey of the transplanted stem cell; from donor to recipient, could be broadly divided into *in vitro* and *in vivo* stages. The *in vitro* stage involves isolation and expansion while the *in vivo* stage includes both donor (before isolation) and recipient (after transplantation) physioxia[31]. Nevertheless, the physiological environment of the recipient is compounded due to the introduction of an intravenous (IV) dose of hMSCs first into the blood stream and an associated hypoxic shock followed by first-pass pulmonary effect (air oxygen)[41] as the cells pass through the lungs further compounded by the limited free availability of dissolved oxygen in the bloodstream and the likely impact of pathological hypoxia[42]. Tracking the fate cycle of transplanted MSCs

before and after IV infusion suggest that exposure to different oxygen tensions may modulate the paracrine activity of hMSCs and consequently the efficacy of cell-based or cell-free therapy. Moreover, the injured tissues are associated with activation of coagulation cascade which is reciprocally associated with oxygen tension[36]. Interestingly, monocyte-macrophage differentiation ensues alongside the initiation of hypoxia in vicinity to pathological injury[43]. Therefore, culturing hMSCs under either a hypoxic or physioxic environment to mimic the *in vivo* milieu might significantly change MSCs behaviour including their paracrine and immunomodulatory properties.

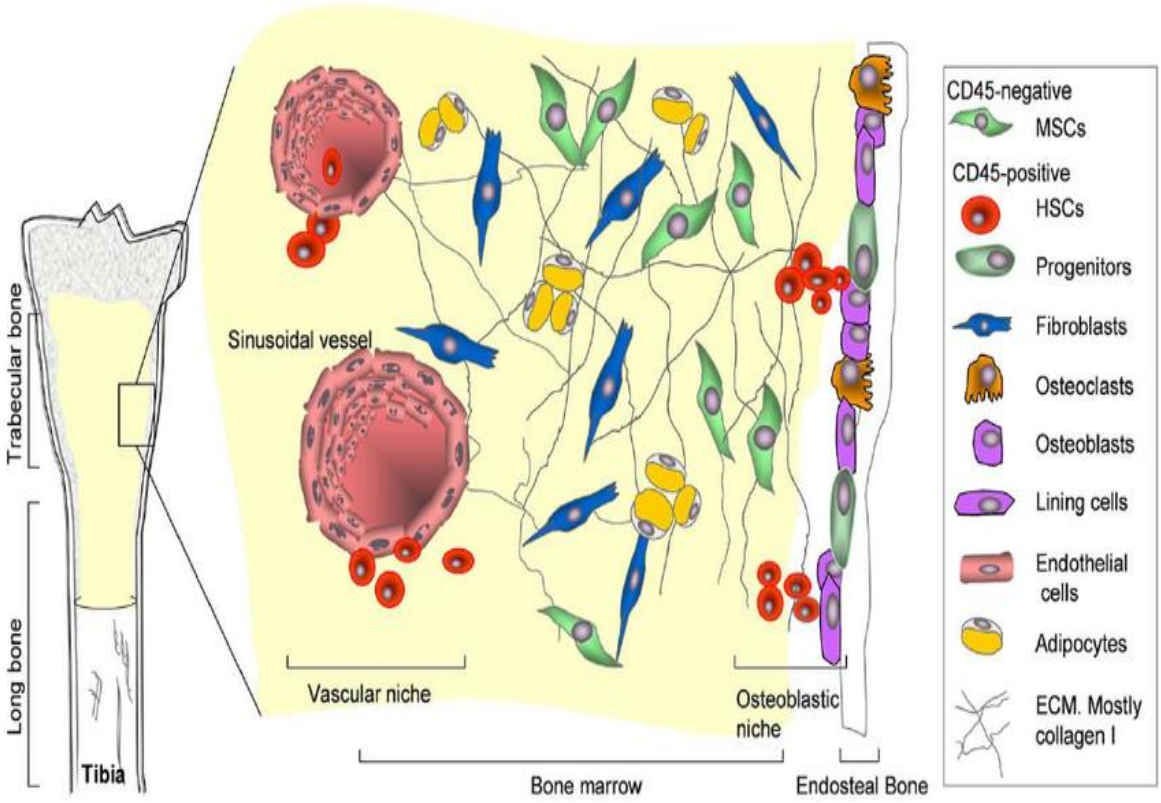

Figure 1-2. The stem cell niches in bone marrow.

In the bone marrow haematopoietic stem cells (HSCs) and their progeny populate the vascular niche which is surrounded by stromal cells derived from MSCs. Comitted progenitors and differentiated cells are distributed in the central and perisinusoidal niches, respectively. Quiescent HSCs are in close association with endosteal osteoclasts and bone-lining cells. As HSCs exit quiescence to proliferative states, they migrate and colonise the subendosteal perivascular niche, interacting with both endothelial cells and pericytes. Subendosteal sinusoid-derived pericytes serve as a source for new osteoprogenitors, which will differentiate into osteoclasts during bone remodelling.

Reprinted from Grassel S *et al*, 2007[44], with permission from Frontiers in Bioscience.

MSCs behaviour in cell culture is different depending on the oxygen tension provided. Air oxygen pressure, 21%, is often referred to as normoxia whilst lower oxygen tensions, between 1% and 5%, are often referred to as hypoxic environments[45]. However, in regard to a cell type found at highest abundance with in the bone marrow, these "hypoxic" environments can in fact be considered to be physiologically normoxic (physioxic) whilst the air oxygen pressure presents a hyperoxic environment to mesenchymal stem cells[46]. Physiological (2% O_2 or 5% O_2) environments promote proliferation of MSCs whilst decreasing differentiation[47]. It was also reported that MSC cell expansion under 1% was lower than at 3%, indicating that there is a lower-limit to the effects of reducing oxygen levels during cell culture. Basciano *et al* (2011)[45] add that lower oxygen tension during culture of MSC inhibits cellular differentiation even in differentiation promoting conditions. MSCs grown in hypoxic (5% O_2) conditions maintain their differentiation potential through more passages than their counterparts cultured in air oxygen, which could be clinically beneficial by increasing the cells that can be yielded from a patient. As well as affecting rates of cell proliferation, changes in oxygen tension also result in changes of gene expression and protein production. MSCs in low oxygen environments upregulate expression of hepatocyte growth factor (HGF) and vascular endothelial growth factor (VEGF)[48]. Lönne *et al* (2013)[49] describe cord blood derived mesenchymal stem cells upregulating expression of fibroblast growth factor 7 (FGF7), VEGF receptor 2, stem cell factor receptor and insulin like growth factor binding proteins 3 and 6 when cultured in lower than air oxygen concentrations. In contrast, air oxygen resulted in upregulation of bone morphogenic protein 4 (BMP4), endothelial growth factor (EGF) and tissue growth factor-b1 (TGFb1). Rhijn *et al* (2013)[50] report that adipose derived mesenchymal stem cells (ASCs) maintain their immunosuppressive properties when cultured under hypoxia (1% O_2). ASCs were able to inhibit stimulation of CD4+ and CD8+ T cell by anti-CD3/CD28 under air oxygen or physioxic environments. However, they did not aim to demonstrate whether either oxygen tension results in more efficient inhibition of the immune response.

The idea of optimisation of *in vitro* culture conditions for MSCs has been a subject of controversy over previous decades. Optimisation of oxygen culture conditions should be cell-specific because physiological oxygen tension ranges from as high as 12% O_2 in arterial blood (though primarily complexed to haemoglobin) reaching virtual anoxic levels of 0.1% O_2 in poorly vascularised tissues including cartilage and brain[51]. Early studies reported a rapid proliferation rate of hMSC in lower than air oxygen tensions, including prolonged exposure to 2% O_2 resulted in 30 times higher cell number and the cell proliferation continued up to passage 7 in comparison to normoxia cultured hMSCs [34,52]. These earlier findings have been taken into consideration for culturing, isolation, and expansion of MSCs in order to optimise the end product for translational therapy.

1.3 Mechanism of oxygen level-induced modulation of hMSC biology

Culture of MSCs in air oxygen is a general laboratory practice though it has been reported that this atmospheric environment is associated with a reduction in proliferation. For instance, fibroblasts isolated from human or mouse show higher proliferation rate at low oxygen levels (3% O_2) before undergoing senescence[53]. In line with this, hMSCs exhibited higher proliferation rates, lower rates of telomere shortening and decreased oxidative stress when cultured in low oxygen tension[54]. The mechanism of oxygen level driven modulation of cellular behaviours is linked to the Hypoxia inducible factors-1a (HIF-1a). Air oxygen induces degradation of HIF-1a while hypoxia stabilises HIF-1a because the prolyl-hydroxylase enzyme uses oxygen as a catalyst cofactor for HIF-1a degradation[32,55]. HIF-1a binds to the RCGTG pentanucleotide present in the nucleic acid sequence of genes of interest, known as the hypoxia responsive element (HRE), and activates a group of genes that promote adaptation and survival. HIF-1 is a heterodimeric complex consisted of two subunits: the constitutively expressed HIF-1b and HIF-1a, which is sensitive to oxygen[53].

Many published *in vitro* proteomic studies conducted on SFCM revealed upregulation of measured bioactive factors in hypoxia (1-5% O_2) over hyperoxia (20% O_2) despite differences in the source of isolated MSCs; adipose[56,57] or bone marrow[58,59,60], and variation

in conditioning periods; short or long. Interestingly, leptin and VEGF; hypoxia markers[58], were reported to be the most sensitive biomolecules to hypoxia by most cells. Alteration of these transcription factors could be linked to HIF-1a pathway; hypoxia stabilises HIF-1a and keeps MSCs in quiescent proliferation status, maximising the transcription of hypoxia-responsive genes[32,55].

1.4 Characterization of hMSCs

1.4.1 Proliferation capacity of MSCs

By seeding bone marrow aspirate into plastic cell culture flasks which contained growth media (Parker's 199), to antibiotics, and foetal calf serum (20%), Friedenstein *et al.* (1970) discovered that bone marrow was comprised of both non-adherent haematopoietic cells and an adherent cell population which represented approximately 1 in 10,000 nucleated cells. These cells have a clonogenic capacity and colonies originate from single cells. After attachment cells start to divide and proliferate into circular colonies[18]. These colonies consist of fibroblastoid cells and are termed Colony Forming Unit–fibroblastic (CFU-f). Moreover, Friedenstein detected that some colonies differentiated *in vitro* into a mass with features identical to bone and cartilage. Subsequent studies indicated that these cells were multipotent and have the capacity to undergo tri-lineage differentiation, into bone, cartilage, and fat cells, and even into muscle cells[61]. Presently these cells are described as mesenchymal stem cells due to their capacity to differentiate into cells of mesenchymal lineages or stromal cells because they are originated from stroma which has a maintenance function in the hematopoietic stem cell (HSC) microenvironment[18]. They have been the focus of extreme argument in relation to whether they are true stem cells or a multipotent progenitor of mesenchymal lineages, thereby it has been given the name "multipotent mesenchymal stromal cells" instead of "mesenchymal stem cells"[62].

The proliferation of MSCs is an important aspect of their biology. To overcome the inherent donor limitations in cell numbers coupled to a requirement to achieve minimum cell numbers for hMSC-based therapy, several cycles of *in vitro* proliferation are required to

achieve the goal. Continuous proliferation is associated with telomere shortening and continuous telomere shortening is associated with cessation of proliferation and loss of viability. A telomere is a sequence of nucleotides that consists of a sequence of repeats of TTAGGG and a complementary DNA sequence, AATCCC. Their maintenance is carried out by telomerase enzyme, telomerase is a reverse transcriptase that restores the DNA repeat[63]. Telomere function is crucial in providing DNA protection from degradation due to continuous replication, however, the telomere undergoes shortening over each cell division cycle due to partial replication at each telomere end per cell division cycle[64,65].

Samsonraj *et al*. 2013, demonstrated that hMSCs undergo telomere shortening with sub-culture and expansion resulting in cessation of proliferation and hence cell senescence[63]. A separate study demonstrated that reduced oxygen culture decreased the rate of hMSCs telomere shortening compared to air oxygen cultured cells confirming that telomere shortening contributed to cell senescence in these telomerase negative cells and that premature senescence in air oxygen was likely linked to oxidative DNA damage occurring at the higher oxygen tension[38]. Moreover, it has been confirmed that both somatic cells and MSCs do not express telomerase activity in comparison to positive control cells[65], indicating that the mechanism of damage of DNA and telomere erosion in air oxygen tension is related to oxidative damage rather than telomere maintenance which is carried out by telomerase enzyme. Unlike somatic cells and MSCs, telomerase immortalised cell lines, cancer cell lines, and ESC display an unlimited proliferation potential [64,65,66]. Reduced oxygen culture systems are described as having an impact on different cell aspects including proliferation, differentiation, and paracrine behaviour[67,51].

1.4.2 Differentiation capacity and markers of MSCs

The current *in vitro* standard used to approve the identity of MSCs is their ability to undergo tri-lineage differentiation into osteocytes, chondrocytes, and adipocytes. This is readily achievable across all three lineages using long established protocols. To produce osteocytes from MSCs, cells should be cultured in a monolayer and incubated with a medium

containing FBS, vitamin C, β-glycerophosphate, and dexamethasone[68]. Exposure of MSCs to osteogenic media leads to mineralisation indicated by osteogenic nodules formation, calcium deposition, alkaline phospahtase expression and via molecular biology techniques including RTPCR of target genes including Runx2 and osteocalcin[18,69,54].

Producing chondrocytes from MSCs can be achieved by first generating a cell pellet. The macro-aggregate is then incubated in a serum-free high-glucose DMEM medium supplemented with dexamethasone, ascorbic acid, sodium pyruvate, L-proline, transforming growth Factor-b (TGFb), and ITS (insulin, transferrin, selenious acid)[70]. The confirmation of chondrogenic differentiation can be achieved morphologically by staining with Alcian blue[71]. Positively labelled regions represent the precipitated proteoglycans, such as, glycosaminoglycans in the cytoplasm of the differentiated cells in response to their exposure to target differentiation media[71]. Further assessment of chondrogenic expression can be achieved via gene expression of Sox5, Sox6, Sox9, aggrecan, and type II collagen[54].
The production of adipocytes from MSCs requires a DMEM medium containing FBS, dexamethasone, insulin, isobutyl methyl xanthine, and indomethacin[72]. Adipocyte differentiation is morphologically confirmed by the presence of lipid vesicles via oil red O staining[73]. Moreover, the adipogenesis is characterised by induction of genetic transcription of peroxisome proliferator-activated receptor gamma (PPAR-γ), C/EBP-α and C/EBP-β, and Wnt signalling[74].

Reports have suggested that some CFU-f have the capacity to differentiate into all three lineages whereas others are restricted to a single lineage e.g. osteogenesis [69,70]. Subsequent studies have demonstrated a hierarchical paradigm of differentiation of human MSCs[75]. Evidence has now accumulated to show that MSCs are actually dissimilar populations with subgroups of different potency[75]. This phenomenon is applicable to both bone marrow MSCs and MSCs from other tissues. Recently, it has been demonstrated that MSCs derived from synovial fluid display varying potency of differentiation into bone and cartilage and that only 30% of the total colonies examined were able to differentiate into fat tissues[76]. Moreover, MSCs placed in appropriate media are described as having a

capacity to differentiate into both skeletal myocytes and tenocytes[77,78], with some studies reported that the MSCs have the capacity to differentiate into non-mesenchymal lineages such as neurons[79].

1.4.3 Immunomodulatory properties of MSCs

MSC-mediated immunoregulation was identified following the observation that MSCs that originated from bone marrow inhibited T cell proliferation[80,81]. This promising evidence directed investigators to consider the likelihood that MSCs may have immunoregulatory effects. To better clarify the action of MSCs on various immunocytes, the following paragraphs provide an overview of each cell class (Figure 1-3).

1.4.3.1 Immunomodulation of innate immune system

1.4.3.1.1 Neutrophils

Neutrophils are the first line defence mechanism against invader particles; they are the most abundant WBC population (40-80%) in circulation[82]. Myeloperoxidase (MPO) is the major neutrophil protein making approximately 5% of its total protein constituents[83]. MPO antibacterial properties emerge following translocation of phagocytosed particles into the phagosome where cytoplasmic granules fuse with the phagosome to release their contents resulting in digestion of engulfed particles[84]. Upon activation, neutrophils engulf foreign particles and undergo respiratory burst, a phenomena of rapid oxygen consumption associated with the release of reactive oxygen species (superoxide radical and hydrogen peroxide) from neutrophils as they come into contact with pathogens[85]. It has been reported that MSCs inhibit respiratory burst and delay IL6-dependent pathways of apoptosis for both naïve and stimulated neutrophils[86]. Moreover, exposure of MSCs to bacterial endotoxins induces chemokine receptor expression and MSC chemotaxis; where they subsequently release inflammatory cytokines and recruit neutrophils in a MIF and IL8 dependent manner. However, MSCs have no influence on the *in vitro* expression of

adhesion molecules in transwell system, neutrophil phagocytosis and neutrophil chemotaxis mediated through IL8, fMLP, or C5a pathways[87].

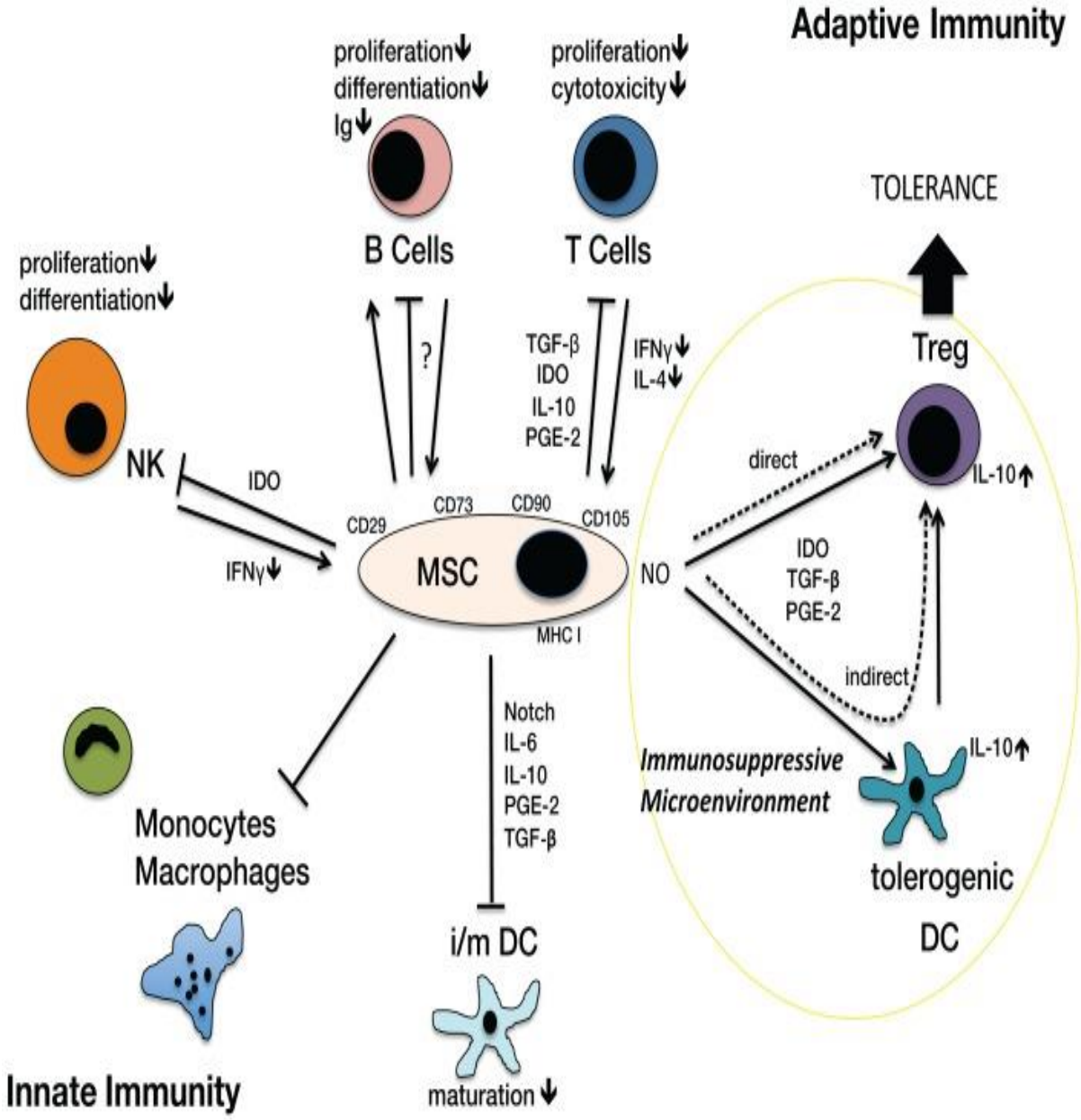

Figure 1-3. Immunological Function of MSCs on different cell types of the innate and adaptive immune system.

Arrows indicate activation, bars indicate blockade of activation, in particular inhibition of proliferation, differentiation, cytotoxicity, maturation. MSCs can directly activate Treg generation. These Tregs play a significant role in the development of tolerance.

Reprinted from Plock *et al*, 2013[88], with permission from Frontiers in Immunology.

1.4.3.1.2 Antigen-presenting cells

The fundamental function of dendritic cells (DCs) is to process and present antigens to resting T cells during DCs maturation. The engaged T cells then induce the immunostimulatory cytokines propagating the immune response. DCs are divided into two lineages, conventional dendritic cells (cDC) with myeloid surface markers and plasmacytoid dendritic cells (pDC) with lymphoid surface markers. The DC maturation is inhibited by MSCs[89] and consequently, the expression of antigens and T cell stimulatory factors, including CD40, CD80, and CD86, are reduced[90], this process is mediated by IL6 secreted by MSCs[91]. Moreover, the growth of DC is intensely affected by the presence of MSCs via the secretion of PGE2 where PGE2 decreases the proportion of cDC while pDC are increased, consequently shifting the immune responses more in the direction of Th2 rather than Th1[92]. Additionally, MSCs lead to impaired maturation, chemotaxis and antigen entrapment and processing by DCs through inhibition of IL2, IL12, IFNγ and TNFa synthesis and increased IL10 production[93,89]. As a direct consequence-lymphocyte stimulation is also inhibited. These effects indicated that MSCs have an inhibitory effect on DC phenotype that can lead to a reduction in effector T cells coupled to an augmented regulatory T cell response[94,95].

1.4.3.1.3 Monocytes/Macrophages

These mononuclear cells, derived from myeloid precursors, are called monocytes while in circulation and macrophages upon entry into tissue. Macrophages are subdivided into M1 and M2 macrophages. MSCs enhanced the differentiation of macrophages towards the M2 class via PGE2, IDO and MSC-derived IL4 and IL10[96,97]. Moreover, the synthesis of pro-inflammatory cytokines, IL1B, IL6, TNFa, and IFNγ, by macrophages were decreased in the presence of MSCs via TGFb1 and PGE2 dependent pathways[98]. In contrast, MSCs intensely increase IL10 (an anti-inflammatory cytokine), which is responsible for enhancing the synthesis of regulatory T cells[96]. However, the debris clearance action or the phagocytosis of macrophage was not affected by MSCs[98,99].

1.4.3.1.4 Natural killer cells (NK cells)

NK cells are the crucial cells of innate immunity during immune responses to viral infections and cancers[100]. The cytotoxic activity of quiescent NK cells is suppressed by MSCs through downregulation of NKp30 and NKG2D (natural-killer group 2, member D) stimulating receptors implicated in NK-cell stimulation and lysis of target cells[101]. Exposure of resting NK cells to activating cytokines, such as interleukin-2 (IL2); promotes either *de novo* expression or an increase of surface density of the activating receptors NKp44, CD69, NKp30, and NKG2D. Naïve NK cells proliferate and gain potent cell-killing effects when stimulated with IL2 or IL15, however, when NK cells are co-cultured with MSCs and cytokine stimulated the latent NK cells, the previously stimulated NK cell proliferation and IFNγ synthesis are inhibited[100,102].

The immunomodulatory effect of MSCs on previously activated NK cells is less potent than against the resting NK cells[101]. The cytotoxic action of NK cells against MSCs is reliant upon the low amount of extracellular expression of MHCI by MSCs and the expression of a number of ligands that are identified by stimulated NK cell receptors[103]. MSCs, both autologous and allogenic, are vulnerable to NK cell mediated cytotoxicity which reciprocally correlates with the expression of MHCI molecules on MSCs[101]. Collectively, these discoveries confirm the presence of a vigorous *in vivo* interaction between MSCs and NK cells where NK cells incompletely suppress pre-activated MSCs without diminishing their intensity to kill MSCs, suggesting that the interaction was entirely regulated by IFNγ level[103].

1.4.3.2 Immunomodulation of adaptive immune system

1.4.3.2.1 T cells

Stimulation of T cell receptors cause proliferation of T cells and initiates numerous actions involving cytokine secretion and cytotoxicity (in the case of CD8+ T cells). MSCs, both autologous and allogeneic, inhibit naïve T cell proliferation by arresting T cells in the G0/G1 phase of the cell cycle[103]. MSCs inhibit T cell apoptosis and support the survival of T cells

that are subjected to overstimulation through the TCR and are committed to undergo CD95–CD95-ligand-dependent activation induced cell death[104]. The antiproliferative action of MSCs on T cells is accompanied by persistence of T cells in latency phase that can be incompletely reversed by IL2 stimulation[105].

Suppression of T cell multiplication by MSCs results in reduced IFNγ synthesis, both *in vitro* and *in vivo*[105]. Stimulation of Th2 cells to increase IL4 synthesis, suggesting a change in T cells from pro-inflammatory status (IFNγ producing) to anti-inflammatory status (IL4 producing)[106]. A key role of T cells is the MHC controlled destruction of virus-infected or allogenic cells, which is regulated primarily by CD8+ cytotoxic T lymphocytes (CTls). MSCs have been demonstrated to down regulate CTl-mediated cytotoxicity[103]. *In vitro*, human MSCs treated by viral peptides or transfected with mRNA derived from tumour cells appeared to be resistant to damage by CTls. Pre-treatment with IFNγ enhanced MSCs cell-surface expression of MHCI factors, however, it was nominal at returning CTl-mediated killing[107,108].

Regulatory T cells, a particular subset of T cells, inhibit the activation of the immune system; maintain homeostasis, and auto-antigen tolerance. MSCs stimulate the synthesis of IL10 by pDCs thereby initiating the production of regulatory T cells[106,109]. Moreover, following co-culture with antigen-specific T cells, MSCs can directly stimulate the proliferation of regulatory T cells via secretion of immune-regulatory HLA-G (HLA-G5 isoform)[103]. Collectively, these demonstrate that MSCs can alleviate the strength of the immune response by suppression of antigen-specific T-cell proliferation and cytotoxicity and by stimulation of the production of regulatory T cell. In the point of view of clinicians, continuous suppression of T cell immune reaction by MSCs would leave the host susceptible to pathogenic microorganisms. Nevertheless, it may be possible that MSCs exhibit active Toll-like receptors (TlRs) which, following contact with microorganism-linked ligands, stimulate multiplication, differentiation and chemotaxis of MSCs and their release of chemokines and cytokines[110,111]. Additionally, it has been revealed that MSCs lose the capacity to inhibit T cell proliferation as a result of impaired Notch signalling after activation

of TLR3 and TLR4[112]. Consequently, it is plausible that the antigenic determinant linked to microorganisms might rescue the T cells from MSCs immunosuppression thereby restoring competent T cell immune-reactivity against invader insults[112]. However, it is also proposed that tissue stromal cells may direct regional immune reaction following exposure to pathogenic offenses[113].

1.4.3.2.2 B cells

Experimental studies performed on the action of MSCs on the B cell show diverse results[114,115,116]. *In vitro* studies revealed that MSCs suppress B cells multiplication, differentiation, and the expression of chemokine receptors[115,117]. It is apparent that these effects rely on the secretion of soluble factors[115] and on cell-cell contact, perhaps mediated by binding between pD1 and its ligands[117]. In contrast, other studies demonstrated that MSCs could maintain the survival, multiplication, and differentiation of the antibody-producing type of B cells from apparently normal subjects[116,118] and from SLE (systemic lupus erythematosus) child patients[116]. Although there is a debate in the *in vitro* studies, it should be highlighted that B cell responses are predominantly T cell mediated and consequently the ultimate result of the interaction between MSCs and B cells *in vivo* could be considerably affected by MSCs dependent inhibition of T cell function. This hypothesis is confirmed by the outcome of the experimental study, using multiple sclerosis paradigms, on autoimmune encephalomyelitis in mice injected with plp-peptide (proteolipid protein peptide). In this paradigm, the *in vivo* synthesis of antigen-specific antibodies was suppressed by injection of MSCs, in addition to a considerable down regulation of plp-specific T cell immune reactions, which confirm that these two episodes were closely correlated[119].

1.5 Inflammation

Inflammation is a physiological response of the immune system to foreign particles. The reaction involves both the innate and adaptive immune system and requires the participation of blood constituents, including plasma proteins, platelets, fluid, and leukocytes. The aim of inflammation is destruction of the invader particles and restoration of normal tissue homeostasis. Inflammation is a tightly integrated process that is orchestrated by biomolecules called cytokines[120]. Inflammation is generally initiated by pathogenic microorganisms known as pathogen-associated molecular patterns (PAMPs), for example, bacterial and viral infections, however, inflammatory processes could be initiated in absence of pathogens and this type is known as damage-associated molecular patterns (DAMPs), for example, Graft vs. Host Disease, arthritic disease, and ischemic heart disease[121]. According to chronicity, inflammation could be acute or chronic, hours versus days, respectively. Neutrophils are the major cells in acute inflammation while macrophage/T cells dealt with chronic stages[120].

Controlled inflammation is considered as beneficial rather than harmful, but when inflammation proceeds and is dysregulated it will lead to organ damage. The initial recognition of invader particles is mediated by tissue resident mast cells and macrophages, leading to release of a group of cytokines, vasoactive amines, eicosanoids, proteolytic products, and chemokines. These bioactive factors mediate local exudation and extravasation of plasma proteins and neutrophils; which are mainly restricted to the systemic circulation. The endothelium lining of the local blood vessels permit selective extravasation of leucocyte and prevents erythrocytes, this selectivity is provided by specific cytokines, chemokines, and adhesion proteins on a surface of leucocytes, endothelial surface, and extravascular spaces[122].

Upon extravasation, neutrophils are activated either by direct contact with invader particles or via released proinflammatory cytokines (Figure 1-8). Neutrophils kill the invader particles by releasing their granule contents, including reactive oxygen and reactive nitrogen species, proteinase 3, cathepsin G, and elastase, resulting in digestion of invader

particles and the damage extended to include localised host environment[123,85]. Proper acute inflammation results in clearance of the infectious agents followed by repair and restoration of function which is mediated mainly by both recruited and tissue resident macrophages[120]. At this stage, the pro-inflammatory prostaglandins were replaced by anti-inflammatory lipoxins. Lipoxins inhibit neutrophil recruitment, stimulate recruitment of monocytes, stimulate dead cell clearance, and initiate tissue resolution and remodelling. TGFb released by macrophage have a crucial role in resolution and remodelling of events[122,124]. If clearance of foreign bodies is not achieved by acute inflammation, the processing proceeds to advanced stages, involving further accumulation of macrophages and T cell activation, however, if these cells fail to remove the invader particles, the inflammation will enter chronic status. Chronic inflammation involves formation of granulation and lymphoid tissue; at this stage the macrophages cover the granuloma as layer in order to protect the host tissues[121,122].

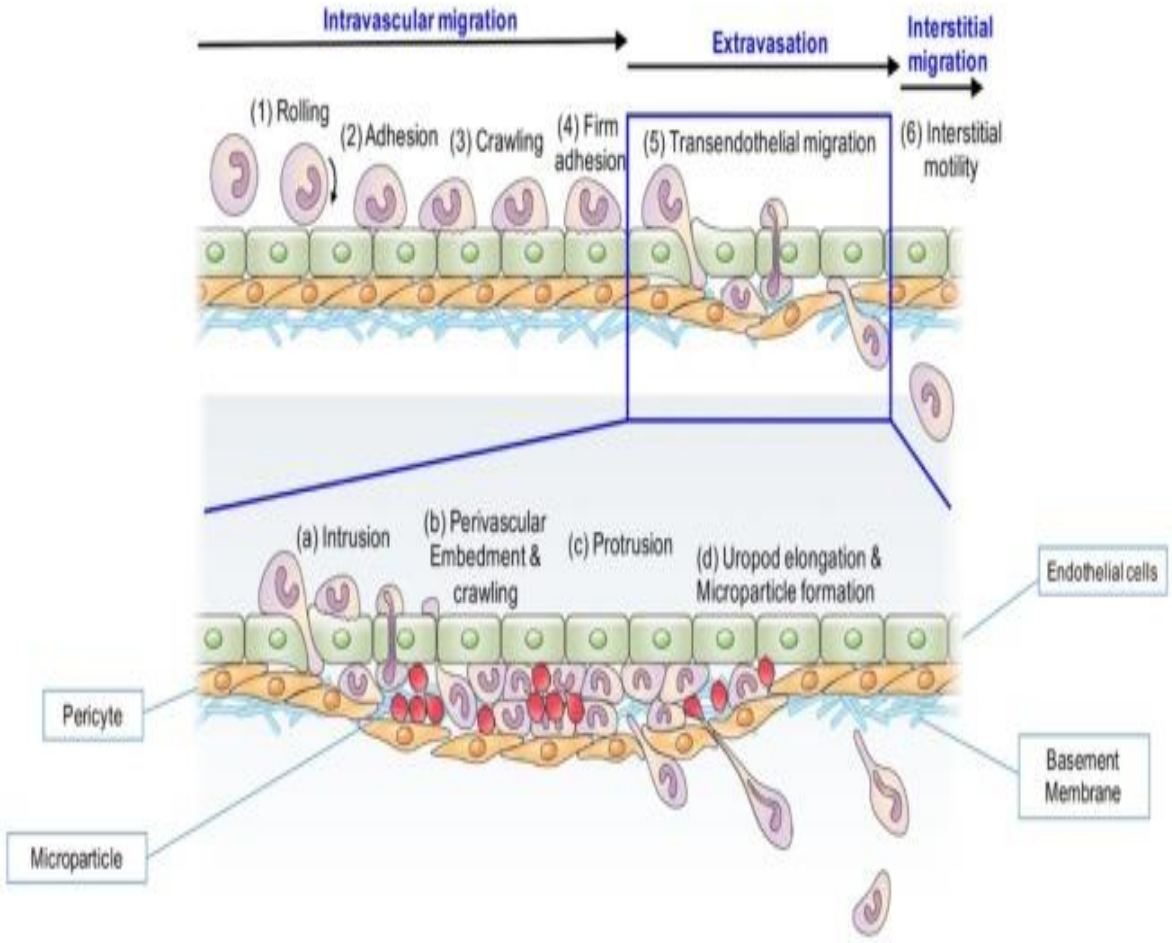

Figure 1-4. Schema of neutrophil extravasation cascade.

In the process of intravascular migration, neutrophil tethers itself to the endothelial cells via (1) rolling, (2) adhesion and (3) crawling. Thereafter neutrophil is (4) firmly adhered to the luminal surface of the vessel. After approaching to the proper site of extravasation, (5) leukocyte transmigrate through the endothelial cells, pericyte and basement membrane. In this process of extravasation, neutrophil undergoes (a) intrusion, (b) perivascular embedment & crawling, (c) protrusion, and then finally (d) uropod elongation & microparticle formation. Microparticles (red dot) are formed in this stage, and usually embedded between endothelial cells and pericytes. When extravasation is over, (6) leukocyte starts interstitial migration.

Reprinted from Park and Hyun *et al*, 2016[125] with permission from Immune Network Journal.

Host cells recognise inflammatory stimuli by their transmembrane receptors called pattern recognition receptors (PRRs), which are expressed by immune cells. The functions of these receptors is to sense the presence of invader pathogens or insults from cellular injury[126]. These receptors recognise a particular structure on the microbial surface called pathogen-associated molecular patterns (PAMPs), or endogenous antigen from host injury called damage-associated molecular patterns (DAMPs)[121]. Examples of PRRs include Toll-like receptors (TLRs), C-type lectin receptors (CLRs), RIG-1-like receptors (RLRs), and NOD-like receptors (NLRs)[120]. The engagement of PRRs with antigen whether from PAMPs or DAMPs molecules result in transmitting the signal down through post-receptor translation pathways to the nucleus. The inflammatory responses are integrated by transcription of these genes and their subsequent protein synthesis of proinflammatory cytokines, such as, TNFa, IL1B, and IL6 are expressed in response to exposure to pathogenic micro-organism[126].

Upon recognition of the antigen, TLRs activate the signalling pathways including NF-kB (nuclear factor kappa-light-chain-enhancer of activated B cells), this transcription factor is distributed in nearly all cell types in an inactive state through their binding to the inhibitor protein, IkB. Upon signal transmission, NF-kB is released from IkB and translocated to the nucleus resulting in transcription of target genes. Transcription of target genes results in expression of proinflammatory cytokines, such as, TNFa, IL1, IL6, and others[120,126]. In addition to these cytokines, chemokines, and costimulatory factors induce recruitment of effector cells, such as neutrophils, monocytes, and macrophages. Neutrophils polarisation

results in the release of their toxic substances by a process known as degranulation, this process necessitates consumption of a higher amount of oxygen and glucose than normal status and is associated with the production of reactive oxygen and nitrogen species, and this situation is called respiratory burst. The products of the reaction are toxic to both invader particles and host tissues in the vicinity resulting in host collateral injury[126].

T cells are the crucial cells of the adaptive immune system. Stimulation of naïve Th cells by antigen-presenting cells results in T cell differentiation into effector types, such as, Th1 cells (pro-inflammatory), Th2 cells (anti-inflammatory), regulatory T-cells (Tregs), and Th17 cells[120]. Th1 cells control host immunity and proinflammatory responses against pathogenic microorganism by the production of IFNγ promoting Th1 differentiation. Th1 releases IL2 and TNFa which stimulate macrophage polarisation and mediate delayed hypersensitivity reactions while Th2 produces anti-inflammatory cytokines; IL4, IL5, IL10, and IL13 that stimulate Th2 differentiation, B cell proliferation/differentiation, reduction of Th1 differentiation, regulation of allergic response, and humoral immunity. Additionally, Treg produces IL10 and TGFb suppressing T cells, NK cells, B cells, and antigen-presenting cells. Treg suppresses Th1 and Th2 proliferation and differentiation[120]. A cascade of immune reaction involving neutrophils, monocytes, and T cells are outlined and summarised in Figure 1-9.

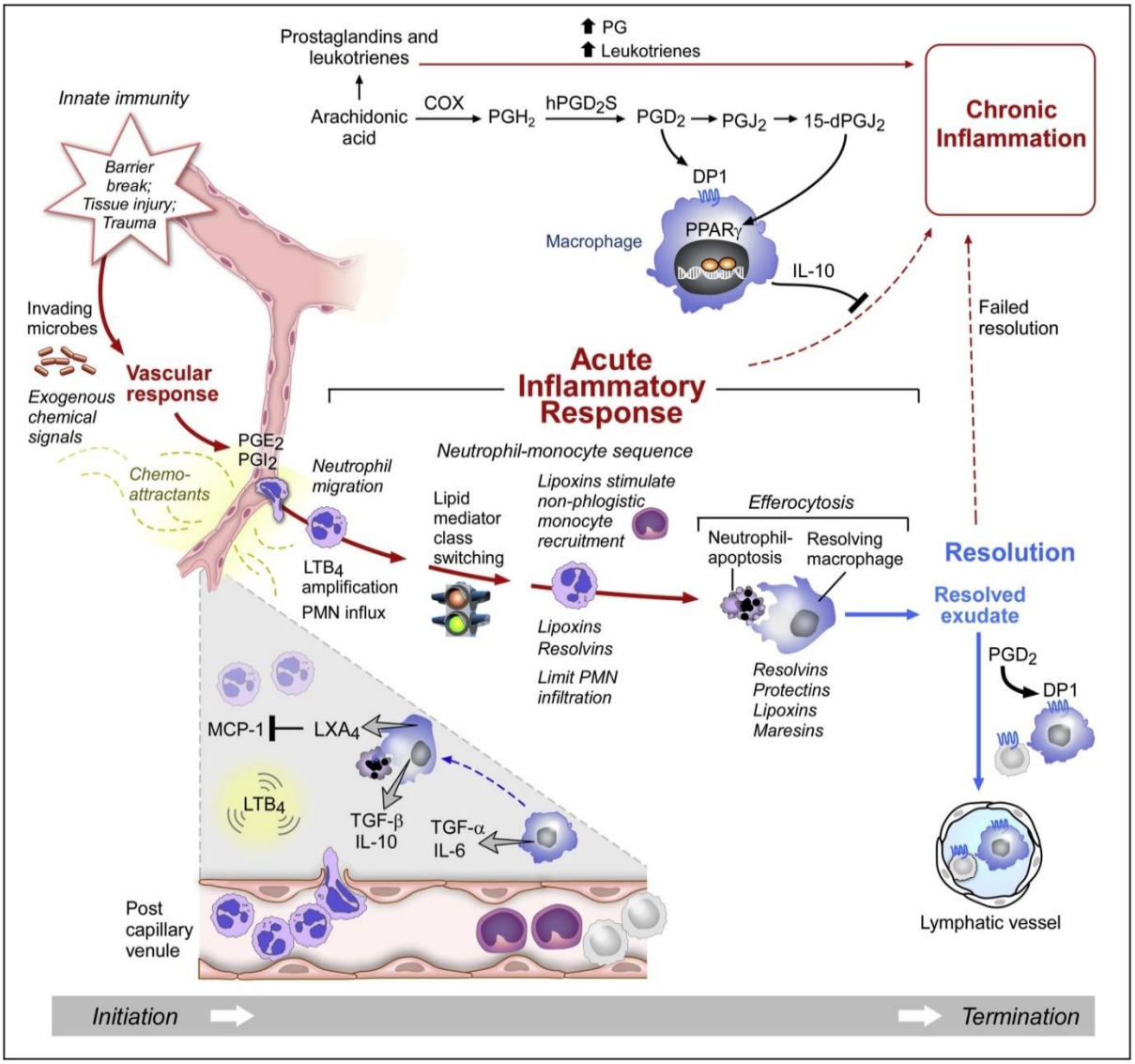

Figure 1-5. Cascade of immune response in acute and chronic inflammation.

Initiation of the acute inflammation ensues with alteration in blood flow stimulated by PGE2 and PGI2, and LTB4, which are produced from arachidonic acid and stimulate PMN recruitment. Excess prostaglandins and leukotrienes contribute to chronic inflammation. Cyclooxygenase (COX) production of PGD2 via human PGD2 synthase (hPGD2s) activates its receptor DP1, a GPCR that stimulates IL10, an anti-inflammatory cytokine, which blocks the path to chronic inflammation. Lipid mediator class switching is the temporal switch in inflammatory exudates that activates lipoxin production. LXA4 regulates MCP1 and monocyte recruitment and stops LTB4-stimulated PMN influx. Lipoxins and resolvins limit further PMN influx to the site and stimulate efferocytosis and the clearance of cellular debris by resolving macrophages.

Reprinted from Buckley *et al*, 2014[124] with permission from Elsevier, License number 4187050083656

1.6 Application of MSCs in regenerative immunity and inflammatory diseases

The mode of regeneration of heart, CNS, liver, skeletal muscle, and other organs is primarily based on the presence/absence of progenitor stem cells and their differentiation and fusion into sites of injury to restore functionality. The reparative programme is based on induction of localised tissue progenitor's stem cells, stimulated reprogramming of other cells to maintain tissue homeostasis, stimulated deposition of exogenous cells to injured organ, and inhibition of endogenous tissue destructive events. Recent studies have mainly focused on regenerative immunity through modulation of immune cell differentiation towards regulatory rather than stimulatory means and thereby directing localised events toward tissue regeneration[127]. The area in which MSCs-immunomodulation could find application includes diseases with underlying immunopathies, including multiple sclerosis, muscular dystrophies, heart failure, and liver fibrosis. In these diseases the effect of MSCs is mainly based on modulation of the immune response toward regulatory via differentiating cells toward Tregs and M2 macrophages.

1.6.1 Multiple sclerosis (MS)

MS is an autoimmune disease associated with an inflammatory defect in the external layer that surrounds the nerve axon and myelin sheath, resulting in a continuous degeneration of the myelin layer. Current studies are focussed on replacing myelinating cells, called oligodendrocytes. Originally, oligodendrocytes are derived from neural stem cells (oligodendrocyte progenitor cells)[127]. Generally, it has been considered that inflammation suppresses regeneration in CNS, however, recent studies confirm that acute induction of inflammation by zymosan particle injection stimulates oligodendrocyte deposition mediating tissue regeneration[128,129] The positive impact of acute inflammation on oligodendrocytes has been approved in zebrafish models confirming that inflammation plays a role in regeneration[130]. Recently, it has been confirmed that activin A exclusively expressed by M2 macrophage promotes re-myelination[131], providing evidence that immunomodulatory products inducing M2 macrophage terminal differentiation might have a clinical application in MS[132].

1.6.2 Muscular dystrophies (MDs)

MDs are a group of muscle breakdown diseases characterised by skeletal muscle wasting overtime, muscle protein abnormalities, and degeneration of muscle tissues. The immune system has complex roles in the pathogenesis of MD. In a mouse model for Duchenne's muscular dystrophy, MDX mice, TGFb synthesis by macrophage stimulated collagen production by fibroblasts and the collagen accumulation is further amplified via pro-fibrotic stimuli resulting in M2 macrophage terminal differentiation[133]. Studies confirmed that macrophage M2 terminal differentiation is vital for muscular regeneration; however, recent studies confirmed that Tregs and eosinophils play a significant role in modulation of muscular regeneration through their influence on satellite and progenitor cells differentiation, respectively[134,135].

1.6.3 Heart failure

Cardiac tissue lacks regenerative capacity and subsequently cardiac ischemia is associated with deposition of non-contractile fibrous tissues to the site of injury by monocytes where subsequently cardiac function is reduced resulting in heart failure[127]. Some studies have suggested that mammalian cardiac tissues have a regeneration capacity, however, there is controversy regarding that presence of cardiac stem cells in the heart and the overall response of the tissue to the cardiac failure is limited recovery of functionality following significant tissue damage[136].

Recent studies exploring the role of immune response in heart failure has resulted in an improvement in our understanding regarding cardiac immunity, these studies have confirmed that the heart has a specific type of myeloid cells and induces a unique immune response to insult[127]. Recognition of monocyte/macrophage subsets and determination of their *in vivo* chemotaxis kinetics to the site of injury will result in advancement of cardiac immunity knowledge with potential to lead to either new management approaches or to explain the mode of action of current therapy, for example, angiotensin-converting-enzyme (ACE) inhibitors. With reference to ACE inhibitors, a current therapy for patients

with cardiac failure and ischemic heart diseases, this might improve cardiac function and reduce the infarct size through anti-inflammatory effects via stimulating specific monocyte/macrophage subsets localisation in cardiac tissues. Moreover, initial cardiac inflammatory stages were associated with deposition of Ly-6C^{hi} monocytes which subsequently exert its regenerative potential through terminal differentiation to Ly-6C^{hi} macrophages[127].

1.6.4 Liver fibrosis

The liver is a unique example of adult solid organ regeneration; however, chronic hepatic diseases are a worldwide major cause of morbidity and mortality. Pro-inflammatory M1 macrophages, Kupffer cells, and deposition in the target tissues promote fibrosis by stimulation of satellite cells. Conversely, M2 regenerative macrophages and NK cells promote regeneration through stimulation of satellite cell apoptosis, and stimulation of Wnt pathway resulting in hepatocyte regeneration[137,138]. Additionally, arginase-1 positive M2 macrophages provide hepatic protection against schistosomiasis infestation, not by phagocytosis, but rather by inhibition of chronic inflammation and suppression of liver fibrosis[139] Current therapeutic modalities focus on the dampening of inflammation and inhibition of fibrosis through stimulation of M2 macrophages.

1.7 Current anti-inflammatory medications and MSCs future perspectives

Tissue injury is associated with infiltration of immune cells in injured tissues resulting in release of reactive biomolecules which contribute to further tissue damage. Moreover, once inflammation becomes chronic, immune cell deposition is associated with further damage and tissue remodelling events. Available therapeutic modalities are mainly focussed on the inhibition of inflammation, such as, corticosteroid, NSAIDs, and anti-TNFa monoclonal antibodies[127]. Recent studies are directed toward investigation of new products with immunoregulatory rather than immunosuppressive effects via stimulation of immune cell differentiation toward Tregs and M2 macrophages to direct the immune response toward tissue repair rather than degeneration. One suggested manner to induce

regenerative immunity is by modulation of immune cell polarisation. Management of spinal cord injury involves a dualistic mode of action through the involvement of monocyte/macrophages or their terminal differentiation M1/M2 macrophages[140].

The creation of new therapeutic modalities in the field of regenerative immunity is hampered by the absence of specific markers to distinguish different subsets of immune cells resulting in a lack of precise knowledge regarding immunobiology in health and disease status. One possible method for the creation of new therapeutic modalities is by exploring different subpopulation of tissue resident immune cells in health and disease, for instance, the cardiac tissue comprises different subclasses of tissue resident macrophages and these subsets vary in their expression markers and functional characteristics[141]. These subsets can be distinguished by their expression of CCR2, Ly-6C, and MHCII; $MHCII^{lo}$ macrophages are responsible for the clearance of debris of injured cardiac tissues by phagocytosis. However, $MHCII^{hi}$ macrophages propagate the immune response beyond phagocytosis by presenting phagocytosed particles to T cells, moreover, $CCR2^{+}$ macrophages aggravate tissue injury through release of a different inflammasome in response to stimuli, including IL1B[127].

These regenerative properties position mesenchymal stem cells at the forefront of a new trend in cell-based therapy by restoring the functionality of damaged tissues and escaping endogenous remodelling events following tissue injury which are most often associated with loss of functionality, however, their immunobiology require further explanation[142,143]. hMSCs exert their mode of action via different aspects including cell trans-differentiation, cell-incorporation, trophic factors, exosome production and mitochondrial translation. Each one of these modes of action has associated drawbacks, cell trans-differentiation and cell-incorporation are queried due to an insufficient amount of hMSCs deposition in target tissues, moreover, exosome production and mitochondrial transfer lack reproducibility in the production of a measurable standardised product regarding quality and quantity of released biological products to generate a standard product. The drawback of the paracrine factor includes their mixture nature of both anti-inflammatory and pro-inflammatory

molecules and this might explain the modest effects achieved with hMSCs translation in clinical trials, for instance, some cytokines/chemokines released by hMSCs could be harmful, such as, IL6 and TNFa[48].

Nonetheless, accumulating data suggests that the paracrine mode of action could be manipulated to overcome some of these limitations via preconditioning or genetic engineering. Moreover, single cytokine or cytokine cocktails could be used to treat certain diseases. However, the hMSCs-based therapy is characterised by a moderate trend of release of trophic factors that are varied based on the localised vicinity suggesting that these cells are performing smartly based on the systemic environment and target diseased tissue environment aiming to establish a physiological environment[48]. Further studies are needed to define these variables and establish optimised methods of culture and preconditioning environments in an attempt to prepare the best biological product for bench to bedside transition in near future.

1.8 Mechanistic immunobiology of MSCs

The molecular mechanism of immunomodulation by MSCs is still incompletely known. However, it is believed that cell-to-cell contact and involvement of soluble factors cooperate to stimulate MSCs-mediated immunomodulation. Initially, MSCs interact with the target cells by means of adhesive molecules, this interaction was confirmed by studies revealing that the inactivation of T cell multiplication by MSCs necessitates binding of an inhibitory factor called programmed cell death 1 (pD1) by its ligands[117]. Numerous soluble inhibitory factors of the immune system are implicated in MSC-associated immunomodulation, these factors are either inducible by MSCs after engagement with target cells, or constitutively produced by MSCs, for example, nitric oxide and IDO which are secreted by MSCs following exposure to IFNγ released by target cells[114,21]. These soluble factors mediate immunomodulation by different pathways, IDO generated from MSCs stimulates the exhaustion of tryptophan, the amino acid which is vital for T cell multiplication, from the localised environment. Moreover, IDO was stated to be vital for the prevention of multiplication of IFNγ-generating Th1 cells[114] which together with PGE2

impeded the function of NK cells[100,114]. Additionally, IFNγ, alone or in combination with the immunostimulatory cytokines (TNF, IL1a or IL1B), promoted mouse MSCs to produce chemokines that attracted T cells and induced nitric-oxide synthase (iNOS) inhibiting T cell activation via the generation of nitric oxide[112]. The vital role of IFNγ is confirmed by mice-MSCs which lack the IFNγ receptor (IFNγR1) and appear to have no immunomodulatory effects[112]. MSCs constitutively produce further soluble agents, for instance, transforming growth factor-b1 (TGFb1), hepatocyte growth factor (HGF), IL10, PGE2, haem oxygenase-1 (HO1), IL6 and soluble HlA-G5[108,144,145] . In addition, the release of some of these soluble agents can be increased by cytokines produced by target cells through their interaction with MSCs. For instance, TNF and IFNγ have been shown to increase the constitutive production of PGE2 by MSCs[106]. Another example of the constitutively produced soluble factor by MSCs is IL6, it was reported that this factor inhibits the respiratory burst and prolong lifespan, by delaying apoptosis, of human neutrophils by stimulating phosphorylation of the transcription factor signal transducer and activator of transcription 3(STAT3)[86]. In addition, it prevents the differentiation of bone marrow haematopoietic stem cells into DCs[91]. An additional factor produced by MSCs is HLA-G5 which has been reported to inhibit T cell multiplication and at the same time suppress the cytotoxicity of NK and T cells[108,146]. IL10, produced following contact between MSCs and stimulated T cells, has a crucial task in promoting the secretion of HLA-G5 by MSCs[146]

1.9 SFCM composition and hypoxic preconditioning

Although the mechanism of action of hMSCs in regeneration is not fully understood, the therapeutic potency is being related to multipotent differentiation, functional incorporation, and secretion of strong paracrine factors[143,147]. However, a number of recent *in vitro* studies[148,149,150,49,151]confirmed that paracrine factors underline the tissue repairing effects of injected MSCs. This has been further supported by *in vivo* studies in Balb/C mice model of excisional wound injury leading to deposition of regulatory macrophages and endothelial progenitor cells to the site of injury [152] and hindlimb injury induced by femoral artery ligation via collateral angiogenesis and limb remodelling [153]. Moreover, it has been reported that IV infusion of SFCM promotes regeneration and inhibits cellular damage in a

rat model of liver injury[154] while localised administration of SFCM to a rat ischemic retinal model restored functionality and reduced damage[155]. Collectively, these confirm that SFCM may become a milestone therapeutic tool or a source for discovery of new bioactive therapeutic molecules.

Proteomic profiling of SFCM has revealed the presence of different biomolecules[156]; which could be categorised into functional groups (Figure 1-4); including pro-inflammatory, anti-inflammatory and pleiotropic cytokines, chemokines, growth factors, and angiogenic factors[157,158,159]. The analysed SFCM is generated from various hMSCs sources, like, adipose tissue, cord blood[159,160], bone marrow aspirate[157,16,20], and stem cell lines[158]. Variation in the outcome of these studies is being probably due to variation in the culturing condition e.g. oxygen tension; hypoxia versus hyperoxia, conditioning periods, and classical monolayer versus 3D conditioning methods[161] (Table 1-1).

Table 1-1. Biomolecules present in conditioned media from MSCs-isolated from different sources and analysed by various techniques.

Source of MSCs	Type of analysis	Measured biomolecules
Bone marrow-derived MSCs [157]	Antibody-array	HGF, IGF1, VEGF, and angiogenin
Adipose-derived MSCs, Wharton's Jelly-derived MSCs[160]	Antibody-based immunoassay	bFGF, VEGF, NGF, SCF, HGF
Cord blood-derived MSCs[159]	Antibody array	GMCSF, IL1b, IL6, IL8, MCP1, VEGF, FGF (4, 7, 9), IP10, and MIP
human embryonic stem cell-derived mesenchymal stem cells[158]	Mass-spectrometry/Antibody-array	CCL (1, 5, 11, 15, 16, 23, 24, 26), CSF (1, 2, 3), CX3CL1, CXCL11, CXCL13, CXCR3, EGF, FGF (4, 6, 9, 17), GDNF, HGF, IFNγ, IGF1, IGFBP1, IL (2, 3, 7, 10, 12B, 13, 16), TNF, VEGF, TGFb

It has been reported that hypoxia (1% O_2) plays a great role in MSCs biology revealed by microarray screening study. Ohnishi *et al*. 2007[162] demonstrated that the expression of many genes were upregulated when rat MSCs were cultured for 24h in 1% O_2 compared to

air oxygen, including factors involved in cell proliferation, such as, pre-D-cell colony–enhancing factor 1, heparin-binding epi-dermal growth factor, VEGF-D, and placental growth factor. In a separate study, it has been demonstrated that culturing adipose derived-MSCs under a hypoxia environment (0.5% O_2) versus normoxia (20% O_2) associated with modulation of some transcription factors measured by microarray screening, including VEGF, MCSF, MIP1, IGFII, HB-EGF, FGF7, and Angiopoietin-like 1[163]. Moreover, bone marrow (BMA) derived and umbilical cord blood (UCB) MSCs respond to hypoxia (1.5% O_2) confirmed by modulation in transcription of via by stabilizing the HIF-1a protein. When their transcriptional profiles were compared, 183 genes in UCB cells and 45 genes in BMA were specifically modulated by hypoxia; some of these genes included known hypoxia-responsive targets such as BNIP3, PGK1, ENO2, and VEGFA, and other genes not previously described to be regulated by hypoxia. Several of these genes, namely CDTSPL, CCL20, LSP1, NEDD9, TMEM45A, EDG-1, and EPHA3 were confirmed to be regulated by hypoxia using quantitative reverse transcriptase polymerase chain reaction[164].

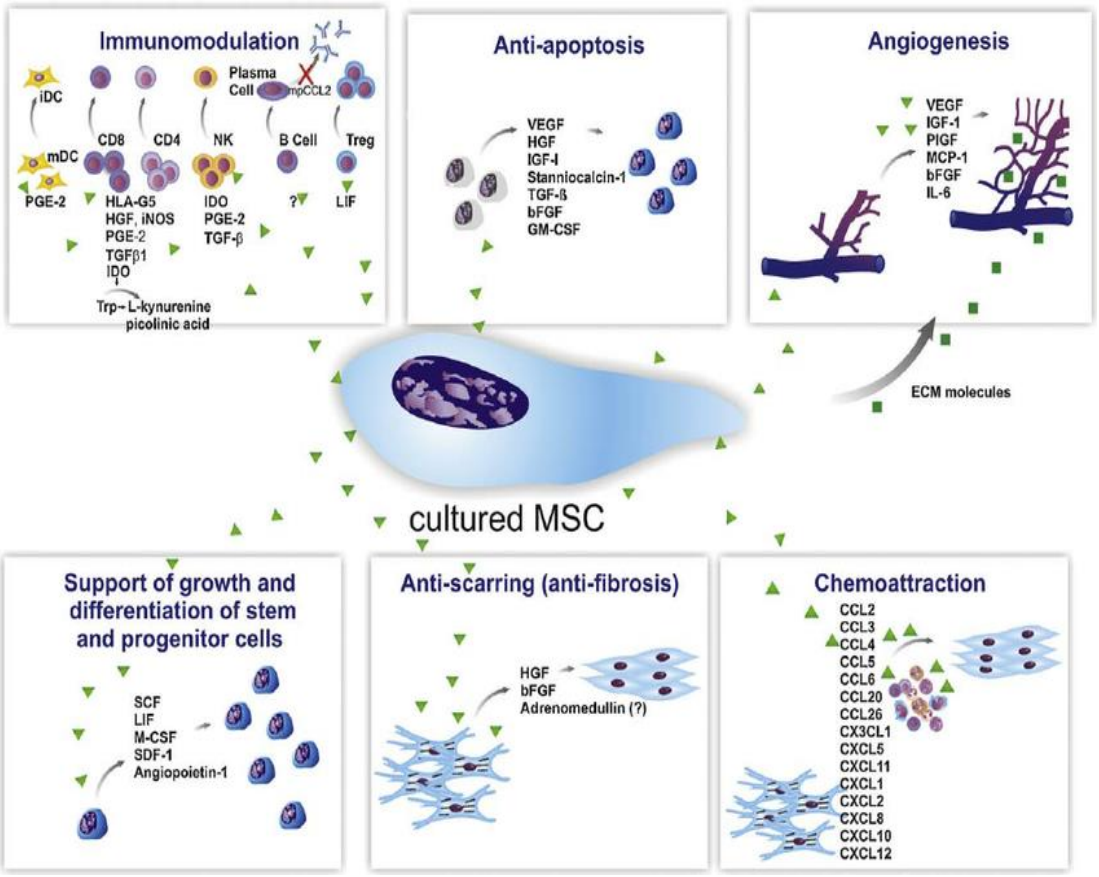

Figure 1-6. Paracrine effects of cultured MSCs.

The secretion of a broad range of bioactive molecules is now believed to be the main mechanism by which MSCs achieve their therapeutic effect and it can be divided into six main categories: immunomodulation, anti-apoptosis, angiogenesis, support of the growth and differentiation of local stem and progenitor cells, anti-scarring and chemoattraction. The immunomodulatory effects of MSCs consist of inhibition of the proliferation of CD8+ and CD4+ T cells and natural killer (NK) cells, suppression of immunoglobulin production by plasma cells, inhibition of maturation of dendritic cells (DCs) and stimulation of the proliferation of regulatory T cells. The secretion of PGE2, HLAG5, HGF, iNOS, IDO, TGFb, LIF and IL10 contributes to this effect. MSCs also limit apoptosis, and the principal bioactive molecules responsible for this are VEGF, HGF, IGF1, stanniocalcin-1, TGFb and GM-CSF. In addition, MSCs stimulate local angiogenesis by secretion of extracellular matrix molecules, VEGF, IGF1, PIGF, MCP1, bFGF and IL6, and also stimulate mitosis of tissue-intrinsic progenitor or stem cells by secretion of SCF, LIF, M-CSF, SDF-1 and angiopoietin-1. Moreover, HGF and bFGF (and, possibly, adrenomedullin) produced by MSCs contribute to inhibition of scarring caused by ischemia. Finally, a group of at least 15 chemokines produced by MSCs can elicit leukocyte migration to the injured area, which is important in normal tissue maintenance.

1.10 Cytokine receptor and mechanism of action

Transformation of information in an organism is carried out by protein biomolecules. The formation of the protein-receptor complex is central in processing the signal. The signalling pathways are arranged in a cascade of events following engagement of ligand with the receptor's extracellular domain. Upon ligand-receptor engagement, the receptor becomes activated and transmits the signal from the extracellular to intracellular compartment resulting in stimulation of post-receptor translation pathways[166]. The engagement of the cytokine to its receptor is followed by activation of post-receptor translation pathway associated Janus kinases (JAKs). JAK, in turn, activate and phosphorylate signal transducer and activator of transcription (STAT) transcription factors resulting in modulation of gene transcription, alteration of cellular behaviours, and a cascade of reactions which ultimately determine cell fate. The majority of cytokine mechanism of action is based on JAK/STAT signalling pathways; however, some cytokines are based on activation of Akt and Erk pathways for their mechanism of action. The post-receptor translation pathways is based on Ligand-mediated oligomerisation or preformed receptor reorganisation, these models are the central concepts in the cytokines mode of action[167].

Cytokines transmit their signal through complex receptor subunits which fall into different categories based on the subtype family of receptors shared between the groups; for instance, IL6, IL11, ciliary neurotrophic factor, cardiotrophin-1, cardiotrophin1 and the cytokines leukemia inhibitory factor and oncostatin M share gp130. Similarly, IL3, IL5 and GMCSF share a subunit of the IL3 receptor. Moreover, the IL2γ receptor is the shared subunit for IL2, IL4, IL7 and IL15. This receptor sharing phenomena allows subfamily classifications of cytokines and might underpin their functional cross-reactivity[166]. Information about cytokines and cytokine receptors is accumulating, however, its noteworthy to mention some general examples to spotlight on the identity of cytokine receptors in general; such as, IL4, IL10, IL13, and TGFb, which are the focus of this research. The IL10 receptor is a complex structure consisting of tetramers of two principle ligand-binding subunits (IL10RA or IL10R1) and two accessory signalling subunits (IL10RB or IL10R2) (Figure 1-5). Engagement of IL10 ligands to their specific receptor extracellular domain of IL10R1 results in activation and phosphorylation of the receptor-associated JAK1 (Janus kinase1) and TYK2 (Tyrosine Kinase2), which is intrinsically associated with IL10R1 and IL10R2 in inactive status, respectively. These enzymes phosphorylate characteristic tyrosine moieties (Y446 and Y496) on the receptor's intracellular domain of the IL10R1 chain. Upon phosphorylation of these tyrosine moieties; their flanking peptide sequences function as a docking site for the inactive latent cytoplasmic protein, Signal Transducer and Activator of Transcription3 (STAT3). STAT3 binds to these sites via its Src Homology2 (SH2) domain which is in turn tyrosine-phosphorylated by the receptor-associated JAKs. The STAT3 homodimerises and translocates to the nucleus compartments where it engaged with high-affinity SBE (STAT Binding Elements) in the promoters of different IL10-responsive genes. STAT3 increase transcription of anti-apoptotic and genes of cell-cycle events including, BCLXL, CyclinD1, CyclinD2, Cyclin-D3, and Cyclin-A, Pim1, cMyc, and p19 (INK4D)[168].

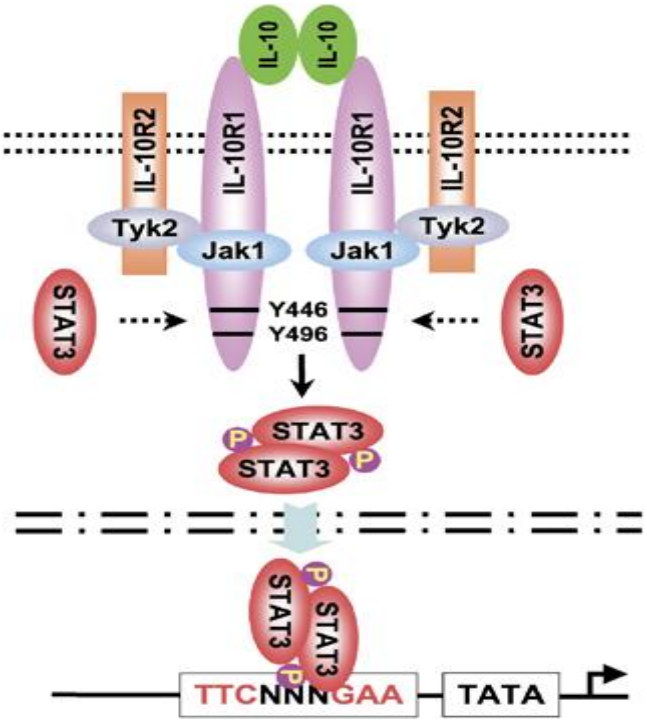

Figure 1-7. The IL10 receptor and a simplified version of signalling from this receptor.

The functional receptor complex is composed of two subunits each of IL10R1 and IL10R2. The Janus tyrosine kinases JAK1 and Tyk2 associate with the cytoplasmic tails of the receptor and phosphorylate tyrosine residues in IL10R1, to which STAT3 is recruited. STAT3 homodimers translocate into the nucleus and bind to STAT elements in several immune response genes, including IL10 itself and the SOCS genes.

IL4 and IL13 cytokines have 25% structural similarity, and they are characterised by a receptor overlapping phenomena via sharing same receptor subunit (IL4Rα) for their signal transduction, IL4 binds to the IL4 receptor α subunit that is a component of both the type I (IL4 receptor α and γc) and type II receptor (IL4 receptor α and IL13 receptor α1), whereas IL13 is recognised by the IL13 receptor α1 of the type II receptor (Figure 1-6)[169]. IL13 also binds to the IL13 receptor α2 chain with greater affinity than to IL13α1. IL13 receptor α2 lacks a transmembrane-signalling domain and as a consequence functions as a decoy receptor to downregulate IL13 signalling. γc activates Janus kinase (JAK) 3 and IL13 receptor α1 activates tyrosine kinase 2 (TYK2) and JAK2. Activated JAKs phosphorylate STAT6 which, upon dimerization, translocates to the nucleus where it binds to the promoters of the IL4 and IL13 responsive genes associated cell polarisation pathway, therefore, IL13 could induce many functional properties of IL4[170]. The signal started with the engagement of the

ligand to a second receptor subunit either γC or IL13Rα1 subunit. Despite their structural similarities, the engagement of the γC subunit is limited only to IL4; but not IL13, while IL13Rα1 could interact with both IL4 and IL13 to form immunological complexes. An additional IL13Rα2 subunit exists known as a "decoy receptor" and stimulation of which is associated with no response because this subunit lacks the transmembrane signalling domain[171]. The difference between IL4 and IL13 is the sequence of engagement to these receptor subunits; IL4 interacts with IL4Rα followed by interaction with IL13Rα1, an effect which is reversed in case of IL13 ligand[170].

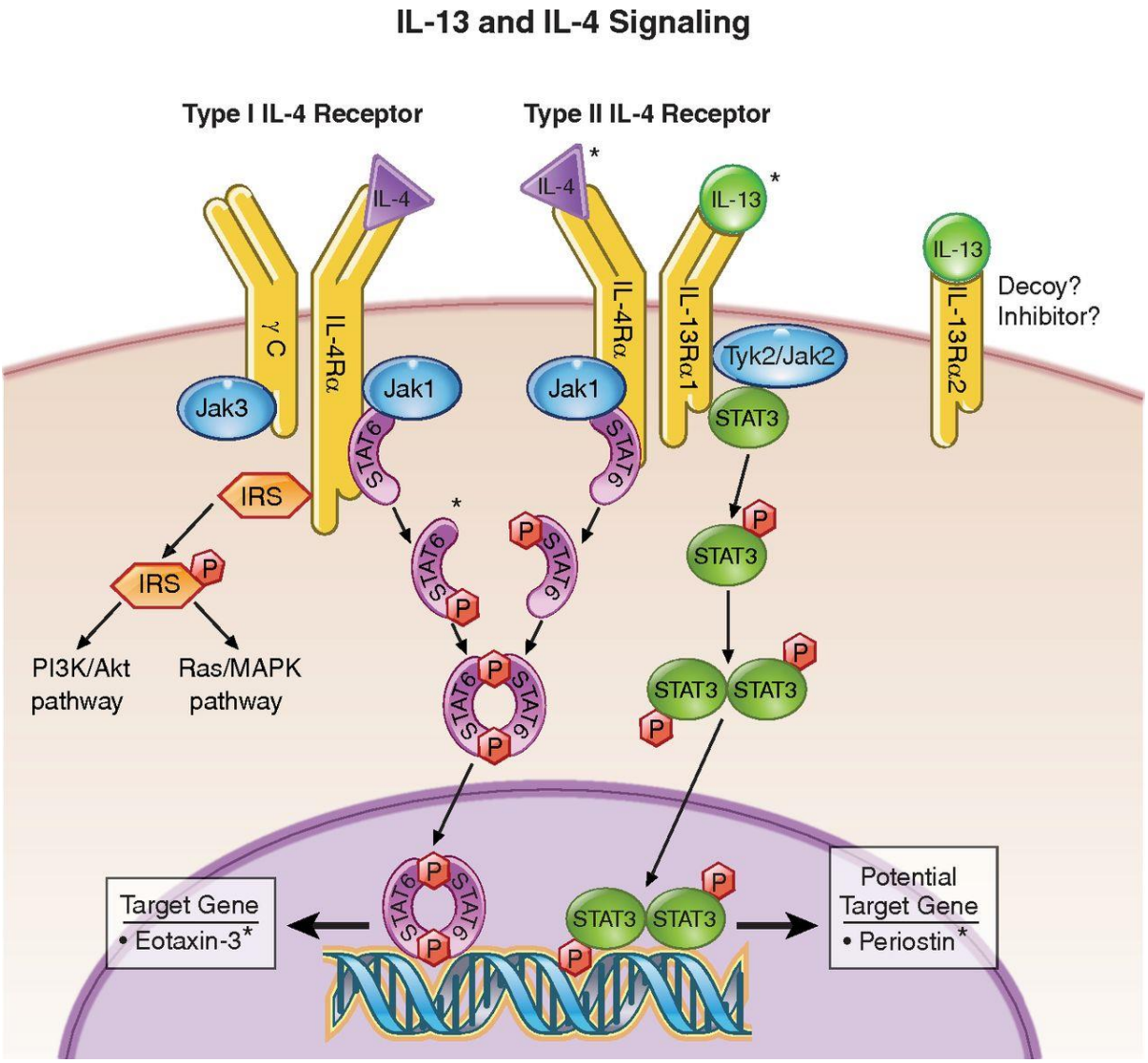

Figure 1-8. Interleukin (IL)-13 and IL-4 signaling pathway.

When the receptor subunits IL-4Rα and IL-13Rα1 bind to their respective ligands, heterodimerization occurs (IL-4Rα-IL-13Rα1 or IL-4Rα-γC), which enhances Janus kinase (JAK) activity. Subsequently, signaling molecules such as signal transducer and activator of transcription (STAT) 6 and STAT3 are phosphorylated and activated. STAT6 and STAT3 are transcription factors that can initiate transcription of target genes including eotaxin-3 and, potentially, periostin. IRS can initiate other pathways such as PI3K/Akt and Ras/mitogen-activated protein kinase (MAPK), which can regulate survival and proliferation. The function of IL-13Rα2 is unclear but may operate as a decoy or inhibitor.

Reprinted from Cheng *et al*, 2012[169], with permission from American journal of physiology. Gastrointestinal and liver physiology

TGFb receptor is slightly different from other cytokines (Figure 1-7). The signalling is initiated by the binding of TGFb to its receptors which are serine and threonine kinases; the cell membrane TbRI (type 1) and TbRII (type 2) receptors. Ligand-receptor engagement produces receptor heterocomplexes and thereby the TbRII activate threonine and serine moieties by their phosphorylation in the TTSGSGSG motif of TbRI which results in its activation. The phosphorylated TbRI phosphorylates and recruits R-Smad proteins, Smad2/3 for TGFb and activin signalling while Smad1/5/8 are for BMP signalling, forming a heterocomplex with the Co- Smad, Smad4. The signalling is then translated by translocation of Smad complexes to the nucleus to control transcription of the target genes catalysed by co-factors[172].

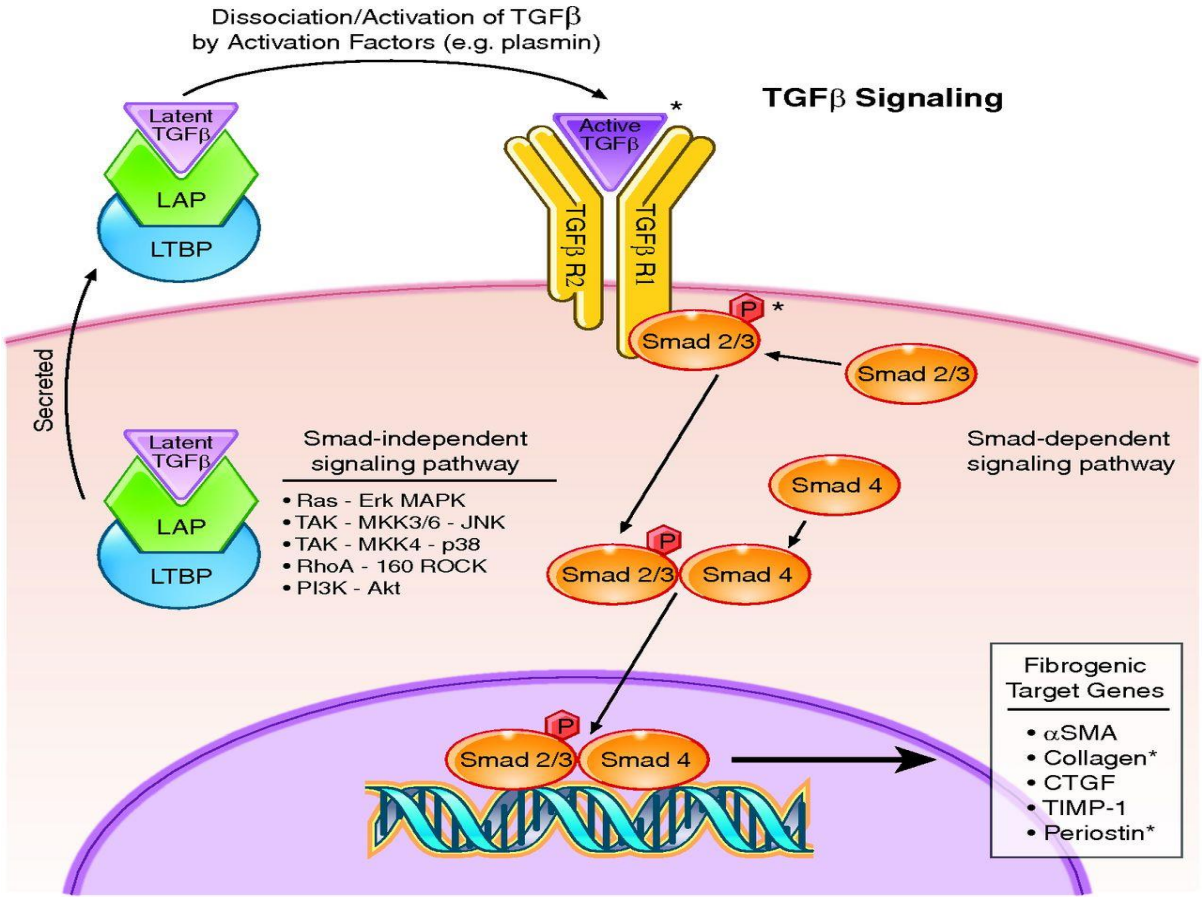

Figure 1-9. Transforming growth factor (TGFb) signalling pathway.

TGFb is a pleiotropic cytokine that mediates fibrosis by inducing fibrogenic target genes. TGFb is generally secreted as part of a large latent complex bound to latency-associated protein and latent-TGFb-binding protein. The active TGFb binds its receptor to initiate Smad-dependent and independent signalling. TGFb can also induce a number of Smad-independent pathways such as Ras, TGFb-activated kinase, RhoA, and phosphatidylinositol-3-kinase, thereby adding to its pleiotropic effects.

Reprinted from Cheng *et al*, 2012[169], with permission from American journal of physiology. Gastrointestinal and liver physiology

1.11 Role of hMSCs in suppression of inflammation

Chronic diseases share inflammation as an underlying pathology. According to the duration of persistence (hours versus days), inflammation is either acute or chronic, respectively. Neutrophils are the principle cell during acute inflammation while macrophages/T cells involved in chronic inflammation[120]. Broadly macrophages are of two types, M1 and M2, expressing distinct surface markers and secretome profiles; they also activate distinct

subsets of T cells based on the received signal and localised tissue milieu[173]. The M1 macrophage subtype characterised by releasing a strong pro-inflammatory cytokines (e.g. TNFa, IL12, and IL1B), strong antimicrobial action, and present their antigen to Th1 subsets of T cells[174]. Localised environment plays a great role in modulation of macrophage phenotype, for instance, a proinflammatory factors including lipopolysaccharide, IFNγ, and GMCSF promote M1 phenotype polarisation and subsequently interaction with Th1 subsets of T cells[175]. Whereas M2 macrophage subtype characterised by releasing strong anti-inflammatory cytokines (e.g. IL10), expression of high amount of mannose scavenger receptor (CD206), and polarised in response to fungal or helminthic infection, apoptotic cells, immune complexes and complement component, moreover, polarisation could be triggered by MCSF, IL4, IL13, IL10, and TGFb. Finally, M2 polarised macrophage stimulates a Th2 subset of T cells[176,175].

MSCs emerged as a therapeutic tool for inflammatory diseases following *in vitro* suppression of T cell proliferation in a mixed lymphocyte reaction[81]. The suppression is broad spectrum involving mitogens, peptide antigens, and alloantigen induced T cell proliferation and CD3/CD28 antibodies mediated T cell activation[177]. Additionally, MSCs suppresses pharmacological activation of intracellular pathways of T cell, confirming that the mechanism of inhibition is a non-T cell receptor-based pathways[178], the suppression involve different T cell subtypes including both CD4+ and CD8+ as well as naïve T cells[80]. In addition to *in vitro* evidence, *in vivo* suppression has been confirmed in experimental baboon animal model of skin graft[81]. The suppression of T cell through transwell system confirm that MSCs exerts its immunosuppressive activity through a paracrine mechanism[80]. Moreover, it has been found that MSCs stimulate macrophage differentiation favourably toward M2 rather than M1 resulting in immunoregulation[179]. However, MSCs show discrepant results on neutrophil behaviours and functionality[82,86,87].

1.12 Aims and Objectives

The primary aims of this study were:

- Establishment of cellular models to recreate the *in vitro* immune response using Jurkat T cell line and THP-1 monocyte cell line; polarisation of cell lines were achieved using chemical stimuli, such as, PMA/PHA.
- Optimisation of hMSCs culture condition via recreation of niche mimic hypoxia model by culturing hMSCs and immune cell lines in both physioxia versus air oxygen incubators.
- Exploring the therapeutic effectiveness of SFCM via their immunosuppression and stimulation of regeneration.
- Analysis of SFCM to identify the biomolecules responsible about immunomodulation and regeneration. Investigation the potential mode of action of candidate biomolecule(s) confers immunosuppression.

Keele UNIVERSITY

Chapter 2

-----Materials & Methods-----

2.1 Materials

Table 2-1. List of materials, catalogue numbers and suppliers (UK distributers).

	Catalogue number	Supplier
3,3-dimethoxybenzidine	10269880	Fisher Scientific
(3-(4,5-dimethylthiazol-2yl)-2,5diphenyltetrazolium bromide (MTT)	M6494	Life Technologies
2.2-azino-bis (3-ethylbenzothiazolin-6-sulphonic acid(ABTS)	A3219	Sigma-Aldrich
3-isobutyl-1-methylxanthine (IBMX)	I7018	Sigma-Aldrich
Acetic acid	A6283	Fisher Scientific
Acetone	A/0560/17	Fisher Scientific
Agarose	BP1356-500	Fisher Scientific
Agarose	BP1356-500	Fisher Scientific
Alcian blue	A3157	Sigma-Aldrich
Alizarin red S	A5533	Sigma-Aldrich
Ascorbic acid phosphate	A8960	Sigma-Aldrich
Bicinchoninic acid	B9643-1L	Sigma
B-mercaptoethanol	10368072	Fisher Scientific
Bovine serum albumin (BSA)	BP9703-100	Fisher Scientific
copper sulphate	C2284	Sigma
Crystal violet	HT90132-1L	Sigma-Aldrich
Cytokine array	EA-4002	Signosis
Dexamethasone	D2915	Sigma-Aldrich
Dimethyl sulfoxide	D/4121/PB08	Fisher Scientific
Direct load wide range DNA marker	D7058	Sigma-Aldrich
DPX mounting medium	360294H	Analar
Dulbecco's Modified Eagle Medium (DMEM)	BE12-709F	Lonza
Ethanol (absolute)	E0650/17	Fisher Scientific
Ethidium bromide	E1510	Sigma-Aldrich
Ethylene diamine tetra-acetic acid (EDTA)	BP2482-1	Fisher Scientific
FBS (foetal bovine serum)	FB-1001G/500	Biosera
Fibronectin	F0895	Sigma-Aldrich
Foetal bovine serum	FB-1001G/500	Biosera
Gel loading buffer	G2526	Sigma-Aldrich
Giemsa	48900-1L-F	Sigma
Hemin	H9039-1G	Sigma-Aldrich
Human IL-10 standard ELISA kit	900-M21	PeproTech
Hydrogen peroxide (H_2O_2)	216763	Sigma-Aldrich
IL10 ELISA KIT	900-M21	PeproTech
IL2 ELISA KIT	900-K12	PeproTech
IL4 ELISA KIT	900-M14	PeproTech
Indomethacin	I7378	Sigma-Aldrich
Industrial methylated spirits	I99050	Genta Medical

Insulin	I9278	Sigma-Aldrich
Insulin, Transferrin, Selenium (ITS)	I3146	Sigma-Aldrich
Isopropanol	P/7500/17	Fisher Scientific
L-Glutamine	BE17-605E	Lonza
L-Proline	P5607	Sigma-Aldrich
May-Grunwald	205435-25G	Sigma-Aldrich
Methanol	M/3900/17	Fisher Scientific
Non-essential amino acids	BE13-114E	Lonza
Oil Red O	O0625	Sigma-Aldrich
Penicillin, streptomycin, amphotericin B	BE17-745E	Lonza
Phorbol myristate acetate (PMA)	P8139-5MG	Sigma-Aldrich
Phosphate buffered saline	BE17-516F	Lonza
Phycoerythrin conjugated antibodies CD105	130-098-845	Miltenyi Biotec
Phycoerythrin conjugated antibodies CD14	130-098-167	Miltenyi Biotec
Phycoerythrin conjugated antibodies CD19	130-098-168	Miltenyi Biotec
Phycoerythrin conjugated antibodies CD197	130-098-124	Miltenyi Biotec
Phycoerythrin conjugated antibodies CD204	130-107-061	Miltenyi Biotec
Phycoerythrin conjugated antibodies CD206	130-099-732	Miltenyi Biotec
Phycoerythrin conjugated antibodies CD25	130-101-428	Miltenyi Biotec
Phycoerythrin conjugated antibodies CD34	130-098-140	Miltenyi Biotec
Phycoerythrin conjugated antibodies CD36	130-100-149	Miltenyi Biotec
Phycoerythrin conjugated antibodies CD45	130-098-141	Miltenyi Biotec
Phycoerythrin conjugated antibodies CD73	130-097-932	Miltenyi Biotec
Phycoerythrin conjugated antibodies CD86	130-098-198	Miltenyi Biotec
Phycoerythrin conjugated antibodies CD90	130-098-906	Miltenyi Biotec
Phycoerythrin conjugated antibodies HLA-DR	130-098-177	Miltenyi Biotec
Phycoerythrin conjugated antibodies IgG1isotype	130-098-849	Miltenyi Biotec
Phycoerythrin conjugated antibodies IgG2a isotype	130-098-849	Miltenyi Biotec
Phycoerythrin conjugated antibodies REA isotype	130-104-612	Miltenyi Biotec
Phytohaemaglutinin (PHA)	L166	Sigma-Aldrich
PIGF ELISA KIT	900-K307	PeproTech
QIAGEN RTPCR KIT	210210	Qiagen
QIAshredder mnispin columns	79656	Qiagen
Recombinant human IL10	200-10	PeproTech
Recombinant human IL13	200-04	PeproTech
Recombinant human IL4	200-04	Peprotech
RNase Zap	R2020	Sigma-Aldrich
RNeasy mini kit	74104	Qiagen
Rosewell Park Memorial Institute (RPMI1640)	12-918F	Lonza
sodium chloride (NaCl)	S7653	Sigma-Aldrich
Sodium pyruvate	S8636	Sigma-Aldrich
TNFa ELIZA KIT	900-K25	PeproTech
Transforming growth factor B3	100-36E	Peprotech
Tris-Acetate-EDTA (TAE) buffer (50X) (2 M Tris Acetate, 100 mM Na2EDTA)	EC-872	National Diagnostics
Trypsin/Versene(EDTA)	BE02-007E	LONZA

Tryptan blue	T8154	Sigma-Aldrich
Tween 20	66368	Analar
Ultrapure distilled water DNAse free	10977-035	Gibco
VEGF ELISA KIT	900-M10	PeproTech
β-glycerophosphate	G9422	Sigma-Aldrich

2.2 General cell culture methodology

2.2.1 Cell lines

The primary human mesenchymal stem cells (hMSCs) and the cell lines that were used in the experiments are tabulated below (Table 2-2).

Table 2-2. Primary cells and cell lines.

Cells	Description	Source
hMSCs (BMA-14)	Derived from Human Bone Marrow, Male, Age - 20 years	Lonza, USA, code 1M-125, Lot No. 0000400307
hMSCs (BMA-15)	Derived from Human Bone Marrow, Female, Age - 36 years	Lonza, USA, code 1M-125, Lot No. 0000419250
hMSCs (BMA-16)	Derived from Human Bone Marrow, Male, Age - 29 years	Lonza, USA, code 1M-125, Lot No. 0000444715
Jurkat	Human acute leukemic T cells	Laboratory stock
THP-1	Human acute monocytic leukaemia cells	

2.2.2 Cell culture techniques

2.2.2.1 hMSC isolation

hMSCs were isolated and expanded from human bone marrow aspirates (BMA) by a plastic adherent culture technique following a previously published methodology[180,181]. A total of 3 human BMA (BMA14 and BMA15, and BMA16) from 3 different donors were purchased from Lonza, USA and processed for experimentation (Table 2-2). Whole BMA was seeded at a density of 10^5 mononuclear cells/cm^2 on 10 ng/ml fibronectin-coated T75 tissue culture flasks in 15ml of growth media (GM) which consist of DMEM supplemented with 5% FBS, 1% L-glutamine, 1% non-essential amino acids (NEAA) and 1% Penicillin-Streptomycin-Amphotericin B (PSA) and incubated at 37°C in presence of 5% CO_2/95% air in either a 2% O_2 or 21 %O_2 incubator or a 2% O_2 work station. For fibronectin coating, 10ml of 10ng/ml

fibronectin solution in PBS was added to each T75 flask and incubated for 2 hours at room temperature. Before use, fibronectin solution was discarded, and the growth media was added. The whole bone marrow containing non-adherent (mononuclear cells) and adherent cells (hMSC) were maintained in a continuous culture for three weeks in a humidified incubator at 37°C in the presence of 5% CO_2 and 95% air and different oxygen tensions. After 7 days of culture half of media was removed and replaced with antibiotic-free GM. On the second week, whole media was discarded, cells were rinsed once with PBS and growth media was added (15 ml/T75 flask). At the end of the third week, it was possible to identify CFU-F derived from single hMSC.

2.2.2.2 hMSCs expansion

hMSC were cultured in T75 culture flasks in GM with media changed twice weekly until confluent. Once confluent hMSC were washed once with PBS, the PBS aspirated from the T75 and 3ml of 1% trypsin/EDTA in PBS solution added to detach the cells from the culture plastic. Once the cells had detached from the T75 flask, 3ml of hMSC culture media was added to the trypsin/EDTA/cell suspension to quench the effects of trypsin. The media-cell suspension was then placed into a 15ml centrifuge tube and centrifuged for 3 minutes at 180g. After 3 minutes had elapsed the supernatant was aspirated from the centrifuge tube to leave a cell pellet. The cell pellet was then re-suspended in 2ml of GM and 1ml of the cell suspension was added to two, T75 flask with a further 14ml of hMSC media added. hMSC were then cultured with a twice-weekly media change until confluent.

2.2.2.3 Culturing cell lines

Cell lines used in this study were; Jurkat cells and THP-1 cells (Table 2-2). Cells were rapidly thawed at 37^{o}C following removal from liquid nitrogen, re-suspended in 10ml of media, centrifuged at 180g for 3min, and the supernatant removed. Cells were then re-suspended and incubated in antibiotic-free GM; DMEM supplemented with 10% FBS, 1% L-glutamine, 1% NEAA. Jurkat cells were cultured in both 21% O_2 and 2% O_2 whereas THP-1 cells failed to proliferate at the lower level (Figure 2-1). Therefore, we explored 10% O_2 as an alternative hypoxic environment for these cell lines.

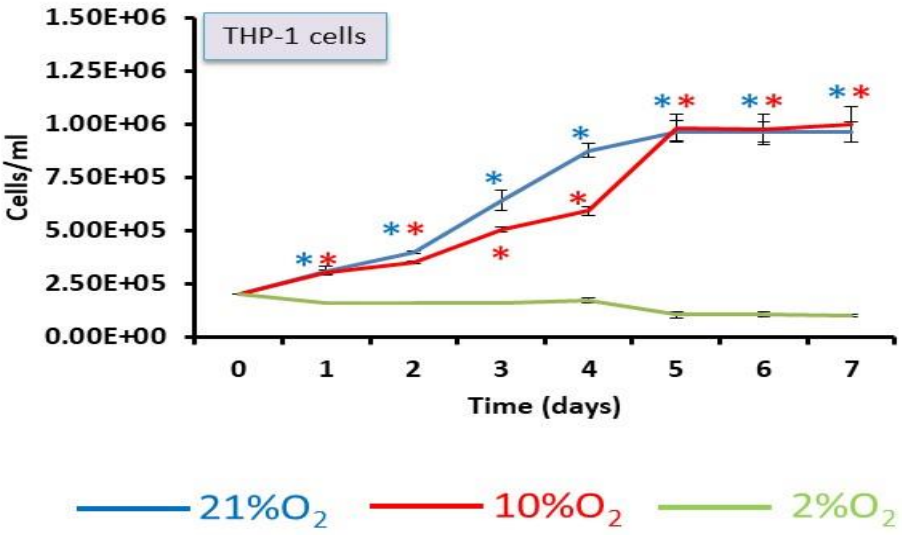

Figure 2-1. Growth curve of THP-1 cells in GM over a 7-day period in 21% O_2, 10% O_2, and 2% O_2.

THP-1 cells failed to proliferate in 2% O_2, compared to both 21% O_2 and 10% O_2. Cell lines were cultured in 21% O_2 and 10% O_2 for subsequent experimentation. Data expressed as mean±SD each result represent a replicate of 3 independent experiments (n=3). One-way ANOVA were conducted with Tukey's test to determine pairwise significant difference, *P<0.001, * colour indicates that the growth curve in relevant condition is significantly higher than 2% O_2.

2.2.2.4 Cell line sub-culturing and expansion

For sub-culturing Jurkat and THP-1 cell lines, confluent T75 flasks of these cells were centrifuged at 180g for 3 min, the supernatant removed, and the cell pellet re-suspended in fresh GM and split at 1:4 ratios into T75 tissue culture flasks. Media changes were performed twice per week. These cells were seeded at a density of $1x10^5$ cells/ml in 15 ml T75 flasks. The media changed twice per week based on their population doubling time (2-3 days), and reseeded again at same seeding density of $1x10^5$ cells/ml.

2.2.2.5 Cell line cryopreservation

Following expansion, cells were cryopreserved for future use. A confluent flask of cells was centrifuged, supernatant removed, and the cell pellet re-suspended in a cryopreservation solution composed of 10% DMSO in FBS. Cell concentration for cryopreservation was $2x10^6$ cells per ml of DMSO-FBS solution. For freezing, the cryovials passed through two stages,

transient freezing in Mr. Frosty freezing container stored in -80 freezers for 24hrs before being permanently transferred to liquid nitrogen.

2.2.3 Preparation of SFCM of hMSC

hMSCs (P0 to P3) were grown to 70% confluency in T75 tissue culture flasks in GM. The 70% confluent T75 tissue culture flasks were washed twice with 15ml PBS and once with 15ml serum free non-conditioned media (SFNCM) and then 20ml of SFNCM added and incubated for 24 hours[182] in normal culture condition (37ºC, 5% CO_2 and 95% air) under different oxygen tension (21% O_2, 2% O_2 and 2% O_2 work station). After 24 hours of culture, media were collected in 50ml centrifuge tubes. To remove cell debris, if any, SFCM media was centrifuged for 3 minutes at 200g, the supernatant was collected and stored at -80ºC. Prior use, SFCM was sterile filtered through a 0.2µm cellulose acetate syringe filter.

2.3 *In vitro* immune cell line activation

As per manufacturer instructions, $5x10^5$Jurkat cell/ml was activated by the addition of 50ng of Phorbol Myristate Acetate (PMA) plus 1µg of Phytohaemaglutinin (PHA), while THP-1 cells were activated by addition of PMA alone. PMA is structurally similar to diacylglycerol (DAG), and consequently stimulates the intracellular pathways of PKC which are usually activated during *in vivo* binding of extracellular pathological ligands triggering phospholipase C (PLC) enzyme. Activation of PLC results in enzymatic degradation of phosphatidylinositol 4,5-bisphosphate (PIP_2) to diacylglycerol and inositol 1,4,5-trisphosphate (IP_3). Calcium catalyses the degradation of PIP_2, PHA provides a potential bottleneck step for calcium release from endoplasmic reticulum resulting in augmentation of PMA-induced immune cell activation as indicated by IL2 secretion by Jurkat cells. The activation was performed for Jurkat and THP-1 cells cultured in GM, SFNCM, and SFCM.

2.4 Viability/proliferation assay

2.4.1 Cell count for Jurkat and THP-1 cells

Cell counts were performed for the cell lines in a triplicate over 7 days to determine the rate of cell growth at a seeding density of $2x10^5$cell/ml, using a haemocytometer. Cell counts were performed on the cells in different conditions, including, activated and inactivated cells in their GM, SFNCM, and SFCM and under different oxygen tensions, 2% O_2, 10% O_2, and 21% O_2. For counting an equal volume of sample and trypan blue were loaded into the haemocytometer cell in 4 external squares of counting chamber, cells were then counted under a microscope. A mean count was determined from the 4 corner regions to give the number of cells per 0.1 µL. To determine the number of cells/mL and the total cells the mean number of cells/0.1 µL was multiplied by 10^4 and the total number of mL of cell suspension respectively. If trypan blue was used the dilution factor was also taken into account in the calculation. For THP-1 cells, the total cell count is a summation of suspension and adherent cells, the adherent cells were counted after being detached using trypsin.

2.4.2 MTT cell proliferation assay

The MTT (3-[4,5-dimethylthiazol-2-yl]-2,5 diphenyl tetrazolium bromide) assay is based on the conversion of MTT into formazan crystals, by NAD(P)H-dependent cellular oxidoreductase enzyme expressed by living cells, which determines mitochondrial activity. Since for most cell populations, the total mitochondrial activity is related to the number of viable cells, this assay is broadly used to measure the *in vitro* cytotoxic effects of drugs on cell lines or primary patient cells.

To determine cell proliferation, MTT was performed on the three cell lines in a triplicate of three T25 flasks for 7 days. The MTT was performed on the cells in different conditions, including, activated and inactivated cells in their usual GM, SFNCM, and SFCM, and under different oxygen tensions, 2% O_2, 10% O_2, and 21% O_2.

To perform MTT assay for Jurkat and THP-1 cells, the cells were seeded in a triplicate of 3 T25 flasks at a concentration of $2x10^5$cells/ml, every day on 8 consecutive days, then MTT

were performed on individual flasks. A 100µl cells of each day were placed in a row of 96-well plate and 10µl of MTT solution was added to each well, the MTT solution was prepared by dissolving the powder in PBS to obtain concentration of 5mg/ml; then sterile filtered, the plate was incubated at 37°C after addition of MTT for 4 hours, then 50µl of DMSO was added to each well to dissolve formazan crystals and the plate was incubated again for 45 minutes then the optical density of each well was determined by reading at 570nm using plate reader.

2.5 Morphological/histological assessment

2.5.1 Trilineage differentiation

Trilineage differentiation of hMSCs was performed by plating $5x10^4$ cells/well in 24 well plates, each 3 wells were labelled for a certain lineage and 3 wells as a control for each lineage. The plates were incubated with GM overnight, then the next day the media was changed to differentiation media (DM). The media of the wells were changed two times per week for a period of 3 weeks. The composition of DM is outlined in (Table 2-3)

For chondrogenesis, the micromass culture system was used. Briefly, 1×10^5 hMSC were re-suspended in 7µl of complete media and dropped in the centre of a 24-well plate as a micromass and cultured for 2 hours in the humidified incubator in the standard culture condition allowing them to adhere to the culture surface. Micromasses were then replenished with chondrogenic differentiation media and cultured in standard culture conditions for three weeks with media change every two days. For control, micromasses were cultured with complete growth media for the same duration.

Table 2-3. The composition of trilineage differentiation media

Osteogenic media content	Final Conc.
Ascorbic acid	50µM
Beta glycerophosphate	10mM
Dexamethasone	0.1µM
FBS	10% v/v
NEAA	1%v/v
L-glutamine	1%v/v
DMEM media	…….
Adipogenic media content	Final Conc.
Dexamethasone	0.5µM
IBMX (3-Isobutyl-1-methylxanthine)	0.5mM
Insulin	10µg/ml
Indomethacin	100µM
FBS	10% v/v
NEAA	1%v/v
L-glutamine	1%v/v
DMEM media	…….
Chrondrogenic media content	Final Conc.
ITS (insulin, transferrin, selenite)	1%v/v
Dexamethasone	0.1µM
Ascorbic acid	50µM
L-proline	40µg/ml
Sodium pyruvate	1%v/v
TGF-B3 (transforming growth factor-B3	10ng/ml
FBS	1%v/v
NEAA	1%v/v
L-glutamine	1%v/v
DMEM media	…….

2.5.1.1 Stain preparation

1% Alizarin Red solution was prepared by dissolving 0.5g of Alizarin Red in 50ml of dH_2O. The solution was filtered with 0.4µm porous filter paper before use. Oil Red O solution was prepared by first preparing a stock solution by dissolving 0.175g of Oil Red O powder in 50 ml of 100% isopropanol. The stock solution was then filtered with 0.4µm filter paper. Oil Red O working solution was prepared by adding 3 ml of stock solution to 2ml of dH_2O. 1% Alcian Blue solution was prepared by dissolving 0.5g of Alcian Blue 8GX in 50ml of 3% acetic

acid to prepare 1% Alcian Blue solution (pH 1.5). The solution was filtered using a 0.4µm porous paper filter.

2.5.1.2 Evaluation of trilineage differentiation by histological staining

After three weeks, the differentiated hMSC lineage was confirmed by histological staining. The mineral deposition by differentiated osteoblasts, lipid accumulation in adipocytes, and proteoglycan-rich matrix accumulation in chondrocytes was detected by classical histological stains; Alizarin Red, Oil Red O, and Alcian Blue, respectively, following standard protocols. Firstly, the media were removed from all wells, followed by twice washing with dH_2O, then fixed by 0.5ml/well of 10% formalin for 30 minutes incubated at room temperature, then formalin was discarded and the adipogenic wells and their controls were washed twice with isopropanol and the other wells were washed twice by dH_2O. Then for osteogenic wells and their control, 500µl/well of Alizarin Red solution was loaded and incubated for 10 minutes at room temperature. After incubation, Alizarin Red solution discarded, and samples were then washed three times with tap water to remove excess dye. For adipogenic wells and their controls, 500 µl/well of Oil Red O working solution was loaded and incubated for 10 minutes at room temperature. After incubation, Oil Red O was discarded, and samples were washed three times with isopropanol. Images should be taken immediately for the adipogenic wells. Finally, to stain chondrogenic wells and their control, 500µl/well of Alcian Blue was loaded and incubated overnight at room temperature. Samples were washed three times with dH_2O to remove excess stain and images were captured by an inverted light microscope attached with a colour CCD camera.

2.5.2 Cytospin

In order to identify the morphological appearance of the Jurkat T cells in GM, SFNCM, and SFCM, the cytospin technique was used where the cells were centrifuged under high-speed annealing the cells on a slide in a monolayer form which improves their morphological appearance. To prepare cytospin slides, $5x10^4$ cells were centrifuged and the supernatant removed, following which, the pellets were washed twice in cold PBS solution and then the pellets diluted with 1ml of PBS solution. Then the slides were placed into an appropriate metal template and the filter paper was fixed to the cytofunnel, then the cytofunnel fixed

to the slide by the metal template. The cells were then pipetted into the cytofunnel and centrifuged by cytospin-centrifuge at 300g for 2 minutes. Slides were then removed from the filter and cytofunnel and examined under the microscope to make sure that the cells were annealed properly. Slides were air dried for 15 minutes and fixed with 95% ethanol for 15 minutes. Following air drying, the slides were flooded with an excess amount of May-Grunwald for 5 minutes and the slides were then washed and followed by staining with a surplus of Giemsa stain for 15 minutes, then the slides were washed with tap water to remove any excess stain. Xylene mounting agent was placed over the slides to fix the cover slides. Images were captured for these slides and cell surface area was calculated for 100 cells using ImageJ software (NIH). For adherent THP-1 cell to the bottom of the wells, the cells were stained with May-Grunwald and Giemsa stain. THP-1 cells were scored into pancake and spindle shaped cells.

2.6 Genetic assay

2.6.1 Ribonucleic acid extraction and processing

2.6.1.1 Cell pellet preparation

To conduct genetic study, the cell lines (Jurkat and THP-1 cells) were cultured in $GM^{\pm PMA}$, $SFCM^{\pm PMA}$, and $SFNCM^{\pm PMA}$. Pellets of cells at day 0 to day 7 in $GM^{\pm PMA}$, $SFCM^{\pm PMA}$, and $SFNCM^{\pm PMA}$ were collected, centrifuged (180g for 3min), and freezed in -80°C for subsequent RNA extraction.

2.6.1.2 Cell lysis and RNA extraction

RNA lysates were obtained by addition of 350µl of lysis buffer (ß-mercaptoethanol: RLT lysis buffer at ratio 1:100) to the pellets. The lysis buffer-cell suspension was then transferred into a QIAshredder spin column, which was placed into a collection tube. The column/ collection tube was then centrifuged for 2 minutes at 1800g. After 2 minutes the shredder column was removed and 350µl of 70% ethanol added to the collection tube, then the solution transferred into the RNeasy mini-column. The collection tube/column was then centrifuged at 1800g for 15 seconds and the flow-through discarded. 700µl of buffer RW1

(supplied as part of the Qiagen RNeasy Kit) was placed into the RNeasy mini-column; this was then centrifuged for 15 seconds at 1800g and the flow-through discarded. 500µl of RPE buffer was then added to the RNeasy mini-column and centrifuged again for 15 seconds at 1800g, flow-through discarded and 500µl of RPE buffer added again and centrifuged for 2 minutes at 1800g. The column was then placed into a new collection tube and centrifuged at 1800g for 2 minutes to remove excess ethanol. The RNeasy mini-column was then placed into a new 1.5ml collection tube and 15µl of RNase-free water added and left to stand for 5 minutes prior to being centrifuged for 1 minute at 1800g. The flow-through was then pipetted directly back onto the RNeasy minicolumn and allowed to stand for a further 5 minutes and then centrifuged for 1 minute at 1800g. The RNeasy mini-column was then discarded and the flow through retained for quantification and subsequent gene expression analysis. Samples were frozen at -80°C until analysis could be undertaken.

2.6.1.3 Quantitative analysis of RNA extraction

After RNA extraction quantitative analysis of the RNA sample was performed using Nanodrop (ND-2000) spectrophotometer to enable correct RNA sample concentration for RTPCR (25ng/µl). Briefly, 1µl of RNA sample was loaded onto the pedestal analysis stand and read using the RNA quantification tool as part of the ND-2000 software. RNA concentration (ng/ml), 260/280 260/230 measurements were recorded. Pre and post sample analysis the Nanodrop pedestal was cleaned before each sample run (all samples were kept on ice whilst RNA quantitative analysis was performed). The dilution equation ($C_1*V_1=C_2*V_2$) was applied to each reading to calculate the dilution of RNA samples to the 25ng/µl required for RTPCR. (C_2=25ng/µl, V_2=50µl, C_1=provided by Nanodrop and V_1=the required volume of the sample to be diluted to 50µl to provide the RTPCR-desired concentration of 25ng/µl).

2.6.2 Reverse transcription polymerase chain reaction

2.6.2.1 Preparation of reaction mix

The PCR reaction tubes were set up to contain 1µl of the sample to be amplified along with 11.5µl of the reaction mix (including enzyme, gene-specific primers and reaction mix) (Table 2-4). The reaction tubes are then capped and placed in the thermal cycler for the PCR reaction to be initiated. Once the PCR reaction was complete the reaction tubes where removed from the thermal cycler, and the content mixed with 1µl of gel loading solution using a fresh pipette tip for each of the samples.

Table 2-4. PCR reaction mix volumes

Chemical	Sample Mix Volume	Blank Mix Volume
Qiagen-one step RTPCR buffer 5x	2.5µl	2.5µl
dNTP mix	0.5µl	0.5µl
Q solution	0.5µl	0.5µl
RNase free H_2O	3.5µl	3.5µl
Forward Primer	1µl	1µl
Reverse Primer	1µl	1µl
Enzyme mix	0.1µl	0.1µl
Sample (RNA)	1µl	0µl
RNA free H_2O	0µl	1µl

2.6.2.2 Thermocycler set up

The gene amplification was performed on the DNA Engine thermal cycler (GENEFLOW). The cycle temperature, time and number of cycles used in the amplification of the specific genes shown in the following table.

Table 2-5. RTPCR thermal cycler set up for primer annealing

Sub Cycle	Temperature	Time	Number of cycles
cDNA Synthesis	50ºC	30 mins	1
pre-denaturing	95ºC	15 mins	1
Denaturing	94ºC	1 mins	39 cycles
Annealing	* Gene specific	30secs	39 cycles
Extend	72ºC	30secs	39 cycles
Extend	72ºC	10mins	1
Extend	15ºC	∞	1
* Gene specific temperature for annealing			

2.6.2.3 Primer sequences design

The primers for this study were designed using human gene sequences from NCBI Gene Viewer. Designed primers (Table 2-6) were evaluated in NCBI Primer-BLAST to check binding specificity. Customised primer sets were purchased from Invitrogen, UK. RTPCR was performed with a one-step protocol.

Table 2-6. RTPCR primer sequences.

Gene ID	Sense sequence (5' to 3')	Antisense sequence (3' to 5')	size
GAPDH	GAGTCAACGGATTTGGTCGT	GATCTCGCTCCTGGAAGATG	225
IL2	CCAGGGACTTAATCAGCAAT	TGTTTTAAGTGGGAAGCACT	184
IL2RA	AAGGAACCATGTTGAACTGT	CTTCTCTTCACCTGGAAGG	251
IL2RB	GTGTACTTGCTGATCAACTG	CTGAGTAGGGGTCGTAAGTA	385
IL2RG	GAGATCCACCTCTACCAAAC	TTCCACAGAGTGGGTTAAAG	337
NFATAC2	GCTTGACTTCTCCATCCTC	GGCTGGTCTTCCACATCT	385
PPP3CA	CACTCGCTACCTCTTCTTAG	AGTCAAAGGCATCCATACAG	220
Erk	GCCTAAGGAAAAGCTCAAAG	GTCAAAGTGGATAAGCCAAG	230
Fos	TAGGGAGGACCTTATCTGTG	TGCTACTAACTACCAGCTCT	165
JNK1	GTTTGCCACAAAATCCTCTT	TCATCTAACTGCTTGTCAGG	180
Jun	ACTCCCCTAACCTCTTTTCT	CATCGCACTATCCTTTGGTA	236
NF-kB1	TATTTCAACCACAGATGGCA	CCATTTGTGACCAACTGAAC	223
Rela	ATCAATGGCTACACAGGACCA	CTGCTCTTCTTGGAAGGGGTT	270
MAPK8	TCTTTGCCAAGTGATTCAGA	ACAGACCATAAATCCACGTT	291
IL10RA	AGTCACTTCCGAGAGTATGA	TAGACCACATCCCCTTGTTA	175
IL10RB	CTCCCCAGTATGACTTTGAG	AAGGCGTACTTTGTCTTCTT	259
L32	TCCCTTCTCTCTTCCTCG	GAATCTTCTACGAACCCTGT	206
CCL5	GGATTTCCTGTATGACTCCCG	TTTGTAACTGCTGCTGTGTG	268
CCR5	CCCGTAAATAAACCTTCAGAC	AGATGAACACCAGTGAGTAG	372
IL8	CACAAACTTTCAGAGACAGC	GTCCACTCTCAATCACTCTC	266
MCP1	TCGCGAGCTATAGAAGAATC	AATAAAACAGGGTGTCTGGG	232
MIP1A	GGTTTCAGACTTCAGAAGGAC	GCTCGTCTCAAAGTAGTCAG	260
IL1B	ATTCTCTTCAGCCAATCTTCA	TATCCCATGTGTCGAAGAAG	372
IL12B	GCCATTAAAGAATTCTCGGC	AGATGAGCTATAGTAGCGGT	223
TNFa	TCTCTCTAATCAGCCCTCTG	CAGATAGATGGGCTCATACC	389
IL10	TCAGCAGAGTGAAGACTTTC	CCTTGCTCTTGTTTTCACAG	270
bNGF	GAGAGCGCTGGGAGC	GCTGTGATCAGAGTGTAGAA	200
FGFb	CGACCCTCACATCAAGCTA	CGTAACACATTTAGAAGCCAGT	263
GMCSF	AAAGGCTAAAGTTCTCTGGA	CCTGGAGGTCAAACATTTCT	224
IGF-1	TAAGGAGGCTGGAGATGTAT	GATCTGCAGACTTGCTTCT	209
IL12A	GCCTAAATTCCAGAGAGACC	TCATCAATAACTGCCAGCAT	208
Leptin	TCGGGCCGCTATAAGAG	GTGACTTTCTGTTTGGAGGA	266
SCF	ACCATTTATGTTACCCCCTG	AGTGTTGATACAAGCCACAA	300
VEGF	CTGGAGCGTGTACGTTG	GAGTCTCCTCTTCCTTCATTT	382

2.6.2.4 Agarose gel

The 2% agarose gel was prepared 1 hour prior to electrophoresis by adding 2g agarose (electrophoresis quality) to 100ml of 1 x TAE (20ml 50xTAE buffer is added to 980ml of dH_2O to get a working concentration of 1 x TAE buffer). This was heated using a laboratory microwave set to full power until the agarose was fully dissolved and the solution was completely clear. Once the agarose was dissolved 5µl of Ethidium bromide solution was added, and the solution poured into the gel tray and allowed to solidify with a gel comb in place for 1hr.

2.6.2.5 Electrophoresis

The comb was removed from the gel and the gel with the mould placed in the electrophoresis tank containing excess 1x TAE buffer ensuring the buffer completely covers the gel. The wide range ladder loaded into the first well and samples were loaded in all other wells allowing for a blank (including enzyme, gene specific primers and reaction mix but without RNA sample) and second wide range ladder to be placed in the final well. Samples and blanks were loaded at a volume of 6µl per well with fresh pipette tips for each sample and blank. The wide range ladders were loaded at a volume of 6µl. The electrophoresis tank was then connected to the Biorad Powerpac 1000 (100Volts/400mAMPS/37W) and allowed to run for 1hr.

2.6.2.6 Gel imaging

After the allotted 1hr for electrophoresis, the Powerpack was switched off and the gel removed from the tank. Gels were imaged on the GelDoc-It^2 imager and focused using UVP software. Once the gel was focused the image was printed and saved.

2.6.3 Microarray

A previous study performed by our group Kay *et al*[183] showed that hMSCs global gene expression was altered in different oxygen tensions (21% O_2, 2% O_2 and 2% O_2 workstation). In the present study we exploited those datasets further with a focus on the 31 bioactive markers identified on the protein arrays. The affymetrix expression values specific to these

31 bioactive factors were selected using UCSC Genome browser home (https://genome.ucsc.edu) and then uploaded into the Online Microarray Data Mining tool (http://www.arraymining.net/R-php-1/ASAP/microarrayinfobiotic.php) to produce the heatmap. The heatmap shows green-dark-red colour ranges indicating expression, no expression, and repression, respectively. Furthermore, factors with more than one affymetrix value were averaged and plotted in a bar chart.

2.7 Proteomic assay

2.7.1 Total protein assay

To quantify total protein, a bicinchoninic acid assay is used. The assay relies on the production of a cupric-protein complex in basic media, followed by reduction of cupric to cuprous. The reduction process is reciprocal to the amount of protein present. In an alkali environment, the formed cuprous reacts with the bicinchoninic acid resulting in a formation of a bluish-purple coloured complex to be detected at an optical density of 570nm (Figure 2-2A). A total protein assay was performed on conditioned media generated from MSCs. The standard was prepared using 3mg/ml of bovine serum albumin (BSA) followed by serial dilutions to prepare 12 samples of different concentrations, following which 10µl of the standard or samples were loaded into the 96-well plate, then 100µl of reagent were added to each well of the standards and samples. The reagent was prepared by mixing 4% copper sulphate solution with the bicinchoninic acid solution at a ratio of 1:50 respectively. The plate was incubated at 37°C for 1hr then the optical density determined by reading at 570nm using plate reader. The concentrations of unknown samples were determined from the interpolation of the standard calibration curve (Figure 2-2B).

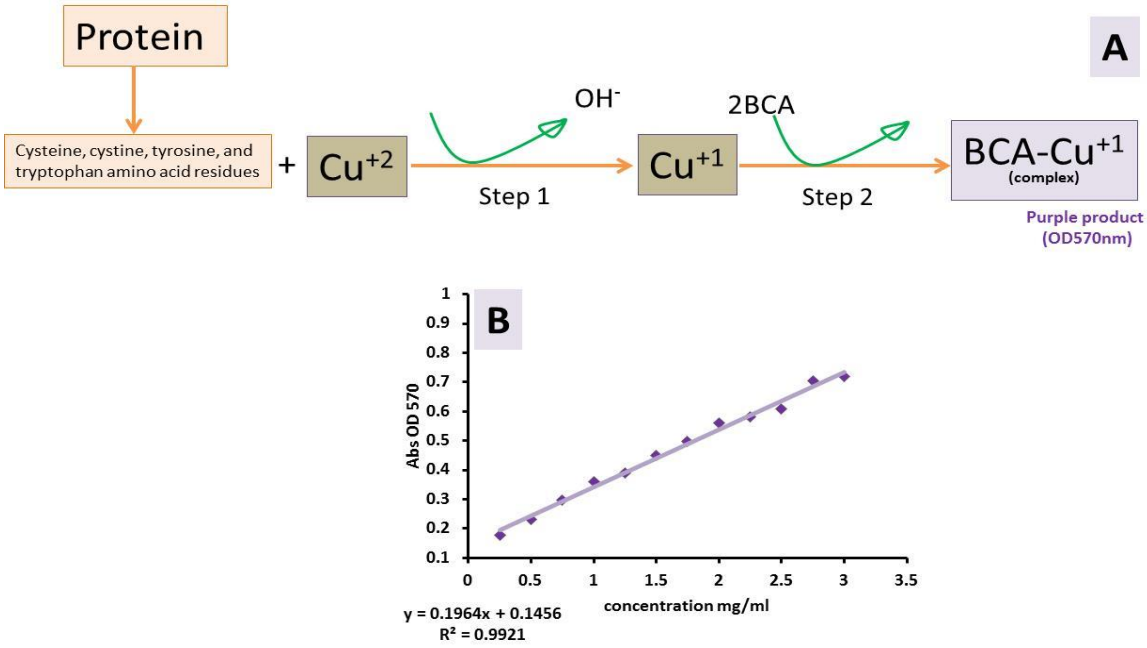

Figure 2-2. BCA total protein assay principle and standard curve.

(A) A schematic diagram describing 2-steps of BCA total protein assay in presence of cupric sulphate as a catalytic subunit resulting in the formation of purple protein-BCA-cupper complex, the signal intensity is reflecting the protein quantity. (B)The standard curve of BCA assay using a serial dilution of BSA, the concentrations of unknown samples from cell lysate were determined from the interpolation of X-axis of the standard curve, data expressed as mean±SD (n=3). Interpolation of x-axis was used for determination of protein concentrations of unknown samples.

2.7.2 Flow cytometry

Cell surface marker expression was performed by flow cytometery for hMSCs isolated from bone marrow for identity confirmation, THP-1 cells at day 0 and day 3 in GM$^{\pm PMA}$, SFCM$^{\pm PMA}$, and SFNCM$^{\pm PMA}$. The principle of the assay is based on the passage of a stream of fluid containing the target cells, which are labeled with fluorochrome molecule specific for a certain antibody, through an optic system. The optic system consists of a laser beam to illuminate the cell particles and optic filters to direct the resulting light signal from a stained population at the interrogation point toward specific detectors. The detectors transfer the emitted light into an electronically processed format to be further analyzed by computer software system (Figure 2-3). For adherent cells like hMSCs, 90% confluent T75 flasks, under different oxygen tensions, were utilized to perform the FACs. The flasks were washed with 10ml PBS, following which 3ml of 10% trypsin/EDTA in PBS were added to harvest the cells. The flasks were examined under microscope to ensure detachment, then 10ml of

fresh media was added to neutralize the action of trypsin, then the whole solution was transferred into 15ml tubes, centrifuged at 300g for 3min, supernatant removed and the pellet washed with excess amount of FACS buffer added. The buffer consists of 0.075% of EDTA and 0.5% of BSA dissolved in PBS solution. The solution divided equally into several Eppendorf tubes; based on the number of antibodies included in the tested panel (Table 2-5). The tubes were again centrifuged at 300g for 5 min, the supernatant removed, and the cell pellets re-suspended in 1µl of antibodies in a 100µl of FACS buffer with gentle pipetting. The stained cells were incubated in the dark in the refrigerator for 10min and then centrifuged. The supernatant was removed, and the pellets were washed with 1ml of FACS buffer with gentle pipetting and then centrifuged at 300g for 10min. Then the supernatant was aspirated completely and finally the cell pellets were resuspended in 200µl of PBS for analysis by flow cytometry. For THP-1 (suspension cells); same steps are carried out without trypsinization. Results were analysed using a Cyflogic software.

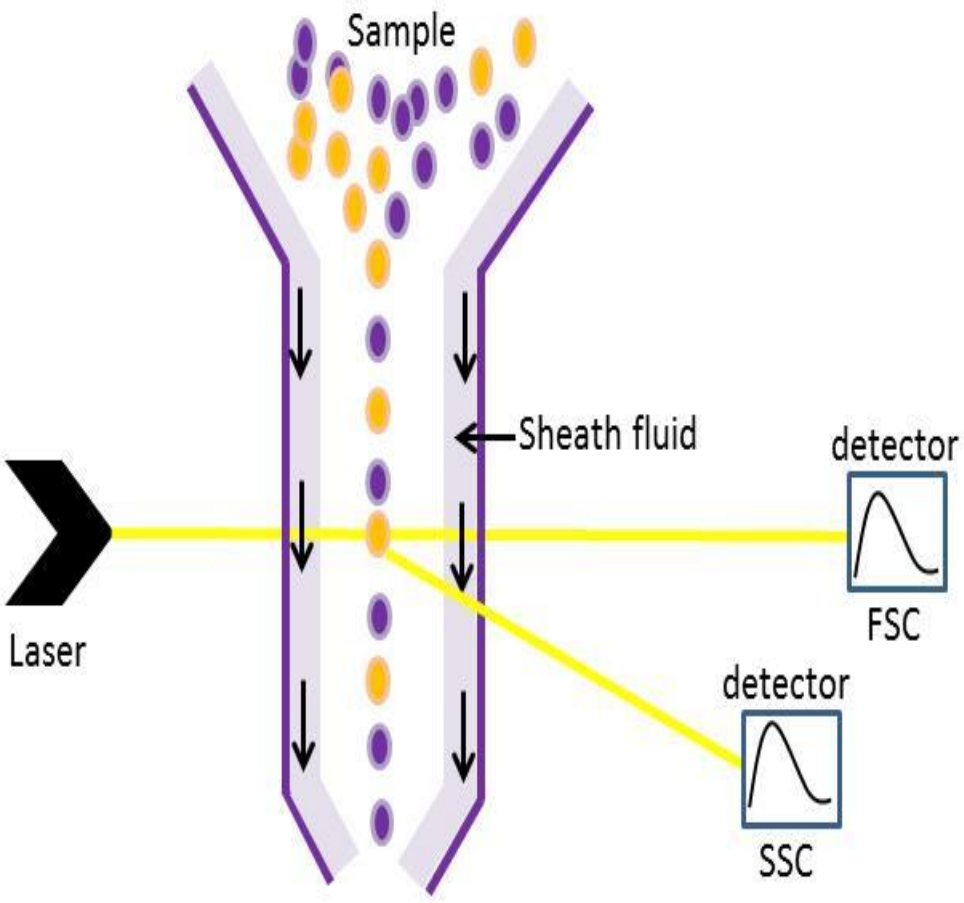

Figure 2-3. Schematic diagram describing the principle of flow cytometry.

The sheath fluid mobilises the cell suspension directing them through laser beam as a single event per time, during which both forward (FSC) and side (SSC) scattered light is recorded, as well as fluorescence emitted from stained cells. When the laser beam strikes the stream, the majority of the photons will pass through unobstructed. Some of these photons will diverge slightly, primarily via light diffraction, from their path as they contact the membranes of passing cells. A detector is placed in line with the laser path (on the opposite side of the stream) and this "scattered" light is collected. Because of the nature of its collection, this parameter is referred to as Small Angle Light Scatter (SALS), Forward Angle Lights Scatter (FALS), or, most commonly, Forward Scatter (FSC). Forward scatter is proportional to cell size; the bigger the cell, the more light is scattered, the higher the detected signal. As cells are translucent, many photons will pass through the cytoplasm. If the photon strikes an organelle (ER, nucleus, etc), the photon will be reflected at a larger angle than those generated by the forward scatter phenomenon. In a typical cytometer, a second detector is placed perpendicular to the laser path to collect light scattered in this manner. This is known as Wide Angle Light Scatter (WALS), Orthogonal Light Scatter (OLS), 90° Lights Scatter, or, commonly, Side Scatter (SSC). Side scatter is proportional to cell complexity; the more organelles/bits inside the cytoplasm, the lighter scatter, the higher the detected signal.

Table 2-7. Antibody panel

Cells	Types	Antibody markers
hMSCs	Positive markers	CD73, CD90, CD105
	Negative markers	CD14, CD19, CD34, CD45, HLA-DR
THP-1	Positive markers	CD45, CD105, HLADR
	Negative markers	CD14, CD19, CD25, CD34, CD73, CD86, CD90, CD197, CD206, CD204
	Negative markers	CD10, CD197, HLADR
Isotype control	IgG1 for CD19, CD25, CD73, CD86, CD90, CD105, CD206	
	IgG2a for CD14, CD34, CD36, CD45, HLA-DR	
	REA for CD197, CD204	

2.7.3 Human cytokine ELISA plate array I (colorimetric)

2.7.3.1 Principle of the assay

Cytokine array was conducted on SFCM collected from 21% O_2, 2% O_2, and WS environments using a cytokine colorimetric plate array (Signosis). The 96-well clear plate was divided into 3 sections, and each section has 4 columns for one sample. In each section, 31 specific cytokine capture antibodies were pre-coated onto 31 wells, respectively, and one blank well (Figure 2-4). The sample, conditioned media, was incubated on the cytokine ELISA plate, and the captured cytokine proteins were subsequently detected with a cocktail of biotinylated detection antibodies. The test sample was allowed to react with pairs of two antibodies, resulting in the cytokines being sandwiched between the solid phase and enzyme-linked antibodies. After incubation, the wells were washed to remove unbound-labelled antibodies. An HRP substrate, TMB, was added to result in the development of a blue colour. The colour development was then terminated by the addition of Stop Solution changing the colour to yellow. The concentrations of the cytokines were directly proportional to the colour intensity of the test sample. Absorbance was measured spectrophotometrically at 450nm.

2.7.3.2 Assay procedure

Firstly, the 3 sections of the plate were labelled as 21% O_2, 2% O_2, and WS SFCM, then the film over the plate was removed and 100µl of each conditioned media were loaded into their desired 32-wells using multichannel pipette, then the plate was incubated for 2 hours at room temperature with gentle shaking. After 2 hours, the plate was forcibly inverted over the waste container to expel the contents, then the plate was washed by adding 200µl of diluted assay wash buffer, the washing process was repeated two times for a total of three washes. After each wash, the liquid was completely removed by firmly tapping the plate against a clean tissue. When the washing process was completed, 100µl of diluted biotin-labelled antibody mixture was added to each well and incubated for 1 hour at room temperature with gentle shaking. Then, the liquid was removed, and the washing process was repeated in the same way as above. Subsequently, a 100µl of the diluted streptavidin-HRP conjugate was added to each well and incubated for 45 minutes at room temperature

with gentle shaking. Then, the liquid was discarded, and the washing process was repeated in the same way as above except that in the third washing step the plate was incubated for 10 minutes at room temperature with gentle shaking then the liquid was removed. Following which 100µl of the substrate was added to each well and incubated for 30-40 minutes, in this step the colour of the liquid inside the wells were blue, then, 50µl of stop solution was added to each well, in this step the colour of the liquid was changed from blue to yellow. The optical density was determined at 450nm using plate reader. This assay procedure was repeated four times.

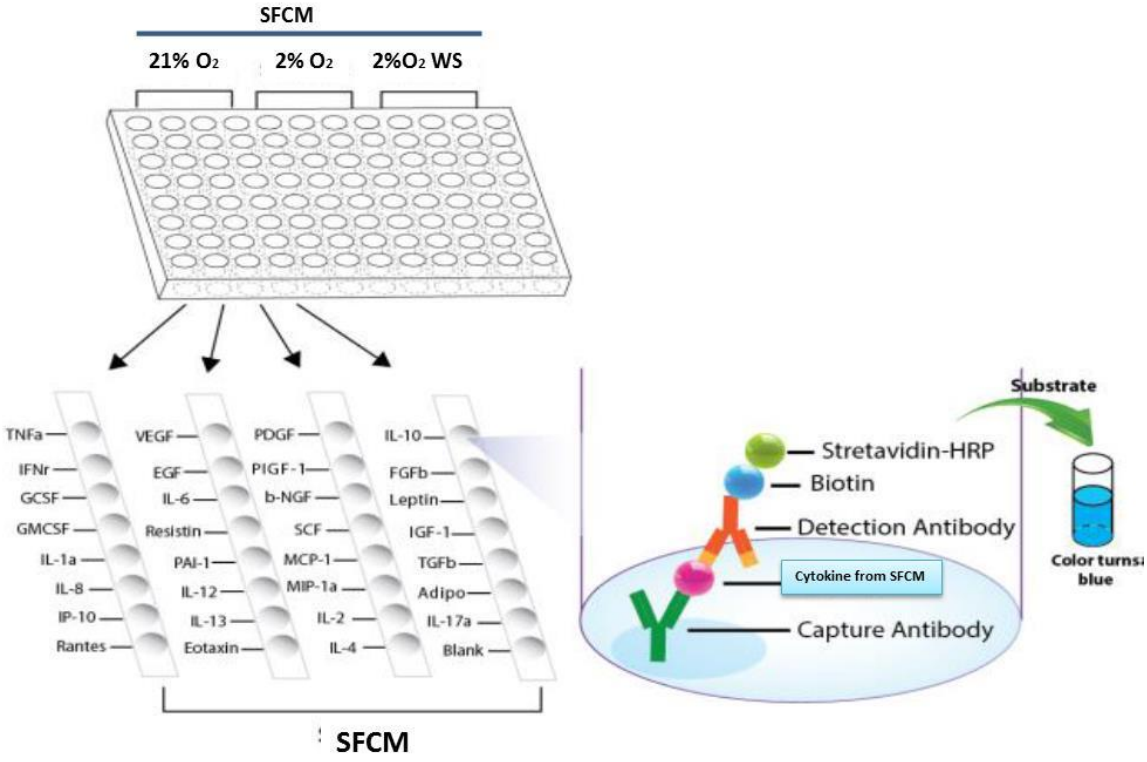

Figure 2-4. Schematic diagram of human Cytokine ELISA plate array.

The diagram summarizes the steps of the reaction of different materials provided by the kit, the captured cytokine proteins in the SF-CM detected with a cocktail of biotinylated detection antibodies. The test sample is allowed to react with pairs of two antibodies, resulting in the cytokines being sandwiched between the solid phase and enzyme-linked antibodies. After incubation, the wells were washed to remove unbound-labelled antibodies. A substrate was added to result in the development of a blue colour. The colour development is then stopped by the addition of stop solution changing the colour to yellow. Reading performed at an optical density of 405nm.

2.7.4 ELISA assay

Cytokine array was validated by focussed detection of IL2, IL4, IL10, TNFa, PIGF1, and VEGF. Standard serial dilutions and SFCM in triplicate were loaded into an overnight pre-coated surface with a capture antibody specific to these 6 cytokines and blocked for 1 hour by 1% BSA-blocking buffer, followed by a 2-hour incubation with diluted detection antibody mixture and 30 minutes with diluted avidin-HRP conjuate. Each step was accompanied by discarding the contents forcibly and 4 times of washing with diluted detergent buffer. The washing buffer was prepared from 0.05% Tween-20 in PBS. Finally, an enzymatic reaction initiated by addition of an ABTS-substrate (2,2'-Azino-bis (3-ethylbenzothiazoline-6-sulfonic acid)) leading to bluish-green colour development within 5-15 minutes during which a visible signal was detected at 405nm via plate reader. The concentrations of unknown samples were determined by the interpolation of the standard calibration curves for each component (Figure 2-5). ELISA assay has been conducted on culture media collected from polarised Jurkat T cells and THP-1 monocyte cells for detection of IL2 and TNFa/IL10, respectively. The tested culture media has been collected from polarised Jurkat or THP-1 cell line models cultured in GM, SFNCM, SFCM, $SFNCM^{+Ligand(s)}$, and $SFCM^{+antiLigand(s)AB}$. The interpolation of unknown samples has been achieved using the standard curve for each individual cytokine (Figure 2-5).

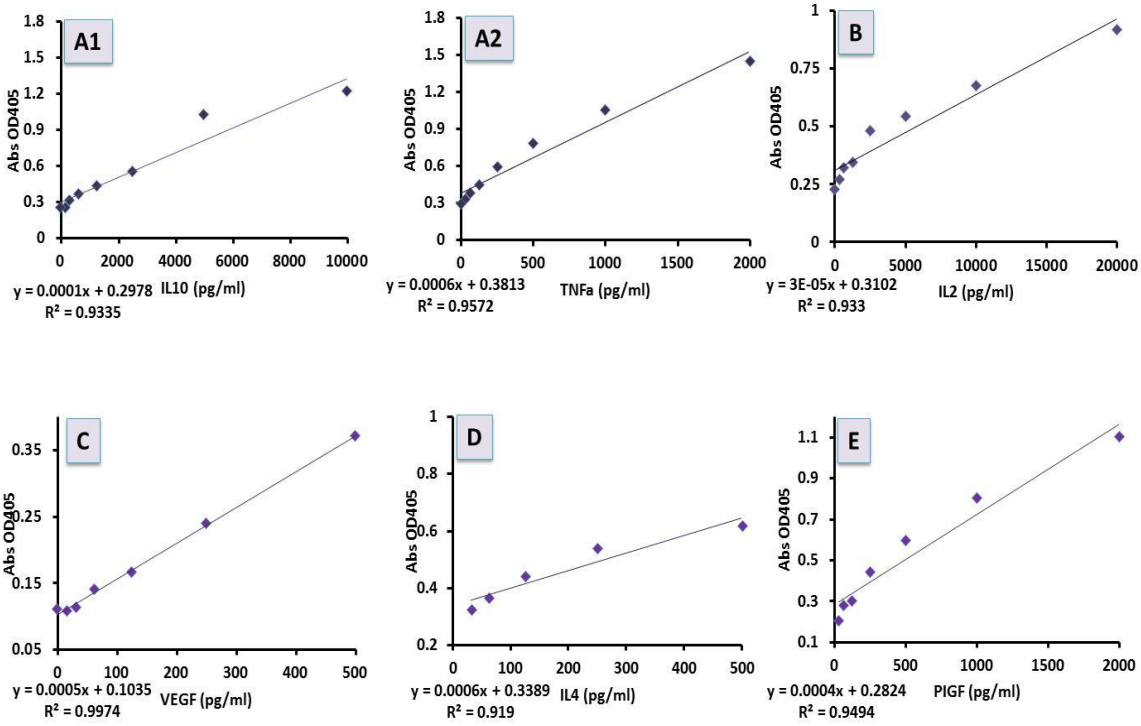

Figure 2-5. Standard curves used to interpolate the concentrations of detected cytokines.

These were IL10 and TNFa secreted from THP-1 cells (A) and IL2 secreted from Jurkat T cells (B) following their exposure to PMA or PMA/PHA in different culture conditions. These standard curves (A-E) has been considered for interpolation of IL10, TNFa, IL2, IL4, PIGF, and VEGF cytokines in SFCM to validate the array profiling. The intensity of visible signal determined at optical density 405nm and is reciprocally related to the concentration of cytokine standard and represents a replicate of 3 samples.

2.8 Cytokine challenging

This study sought to identify if the immunosuppression of SFCM was cytokine-driven. We selected 4 anti-inflammatory cytokines from the cytokine array as targets for SFCM mediated immunosuppression, including IL4, IL10, IL13, and TGFb. To identify the candidate biomolecule(s), these cytokines were individually tested on the cell line models in SFNCM and a cytomix is considered to account for the IL4/IL13 receptor overlapping phenomena. Moreover, these cytokines were individually or in combination (IL4/IL13) blocked from SFCM with their specific rabbit polyclonal antibodies. The doses were identified via dose-response curve via testing a serial dilution of individual cytokine in SFNCM on the target cell line models. For Jurkat T cells, MTT was conducted after 24-hrs of cell exposure to a serial doses of IL4 (0-10000 pg/ml), IL13 (0-10000 pg/ml), IL10 (0-50 ng/ml), and TGFb (0-100 ng/ml), the toxic doses were ignored and a highest non-toxic doses of each [(IL4 and IL13 (250pg/ml), IL10 (1ng/ml), and TGFb (5ng/ml)] was considered as a target dose in subsequent experiments (Figure 2-6). However, the adherent cell counts at day 3 were considered as a target response for THP-1 following their exposure to these anti-inflammatory cytokines and accordingly the doses were selected. The lowest concentration of these cytokines which induce THP-1 adherence and used in subsequent experimentation, including [(IL4/IL13 (20ng/ml), and IL10/TGFb (5ng/ml)] used either alone or in combinations (Figure 2-7). In the subsequent steps, these cytokines were blocked in SFCM either alone or in combinations using an excess amount of rabbit polyclonal antibodies. To neutralise these cytokines from SFCM, different concentrations of their specific antibodies were used based on the target cytokine. For example, IL10 was neutralised by 2µg/ml of anti-human IL10, IL4 neutralised by 100ng/ml anti-human IL4, and IL13 neutralised by 200ng/ml anti-human IL13.

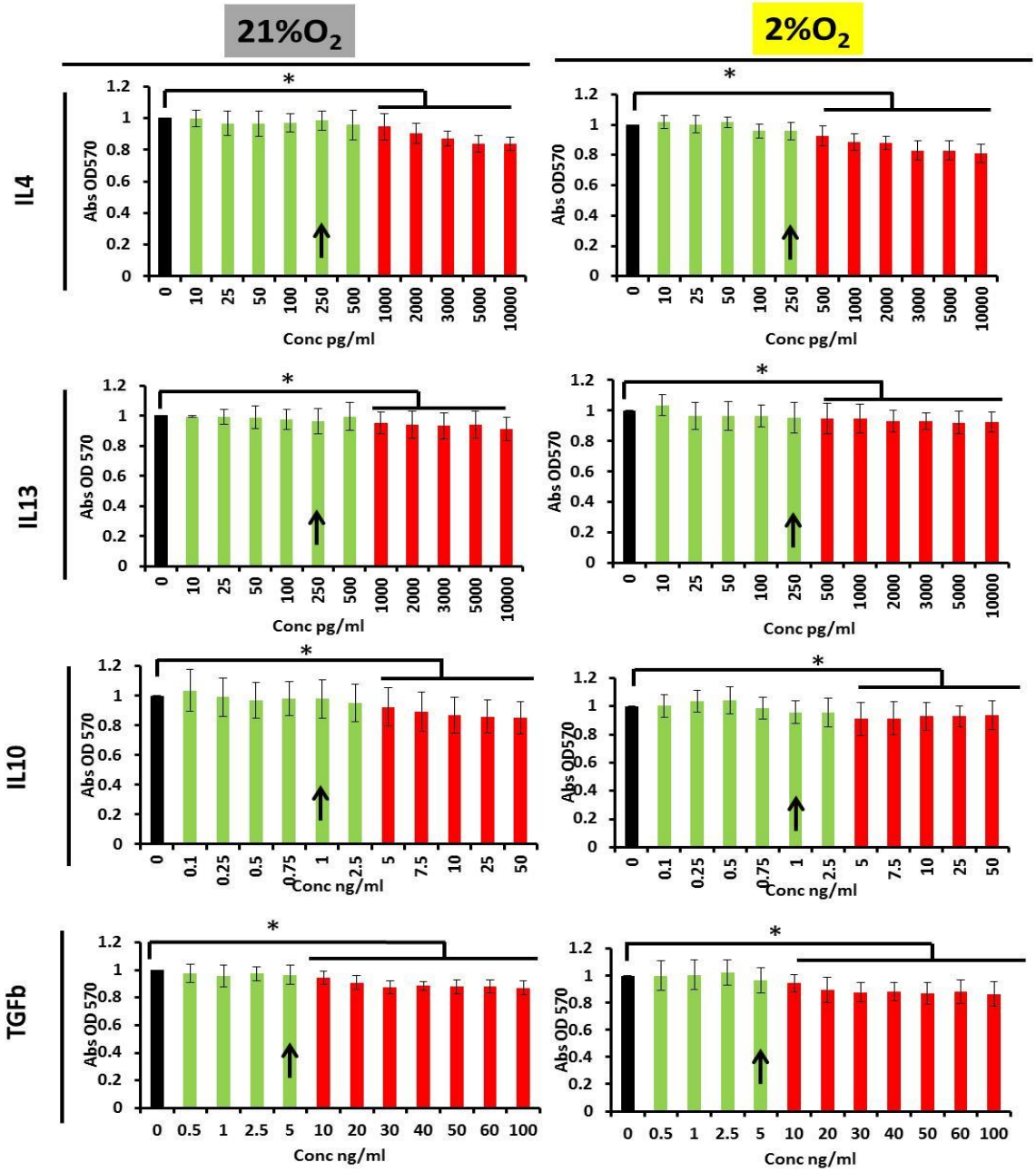

Figure 2-6. Dose response MTT-based proliferation assay of Jurkat T cells for selected anti-inflammatory prominent cytokines.

IL4, IL13, IL10, and TGFb were added to SFNCM in normoxia and hypoxia, Data expressed as mean±SD, each result represent a replicate of 3 independent experiments (n=3). Two-sample t-test were conducted to determine the significant difference, *P<0.05 in comparison to cytokine devoid SFNCM control group, arrow indicate used concentration in subsequent experiments Black bar=control group, green bar=non-toxic dose, and red bar=toxic dose.

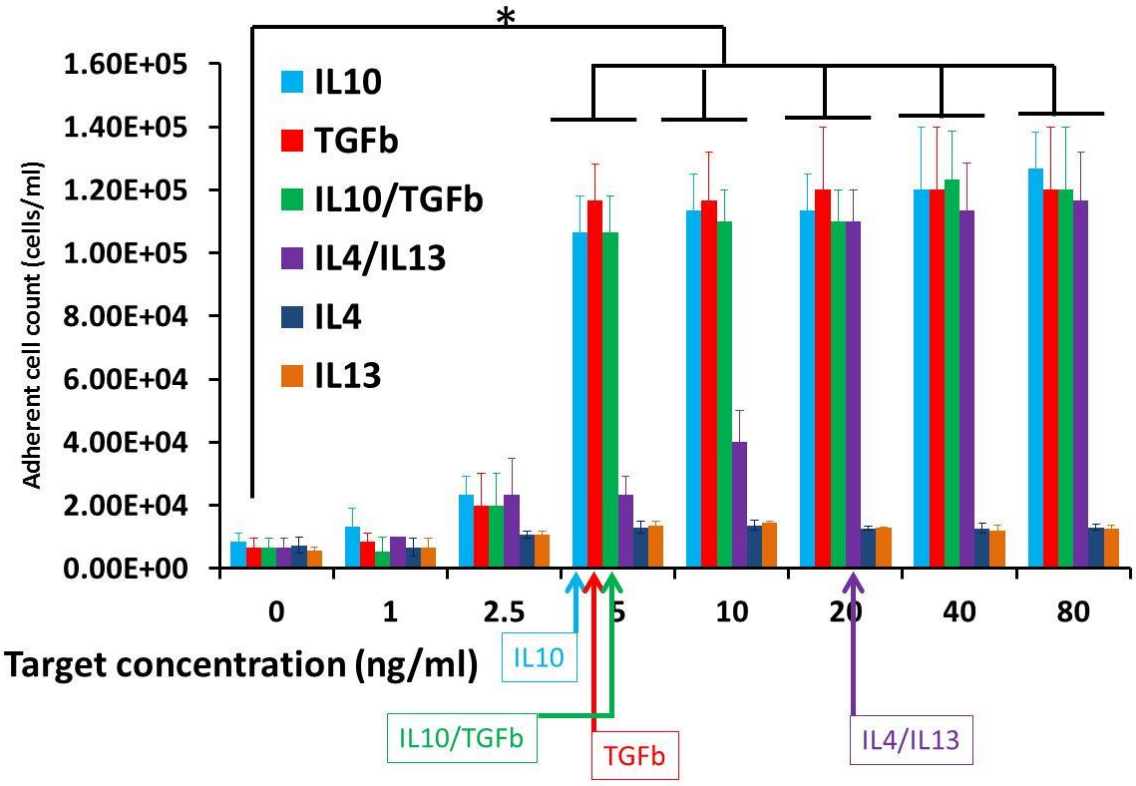

Figure 2-7. Dose-response curve of target anti-inflammatory cytokines (IL4, IL10, IL13, and TGFb) on THP-1^{+PMA} cells based on adherent cell count.

THP-1^{+PMA} cells were cultured in 24-wellplates and exposed to different doses of target cytokines for a period of 3 days and the response was determined as an adherent cell counted over different doses. The target dose of these cytokines (IL4=20ng/ml, IL10=5ng/ml, IL13=20ng/ml, and TGFb=5ng/ml) were determined and used for subsequent experiments. IL4/IL13 are combined to induce adherence (no action achieved with single cytokine). * P<0.001 when compared to control (cytokine devoid SFNCM). Data expressed as mean±SD each result represent a replicate of 3 independent experiments (n=3). Two-sample t-test were conducted to determine the significant difference, arrows indicated the doses used in subsequent experiments.

2.9 Justification of experimental duration of cell line models:

In the present study, the therapeutic effect of SFCM was tested on two *in vitro* cell line models (Jurkat cells and THP-1 cells). The experiments were carried out over 7 days period due to the following reasons. Firstly, the population doubling time (PDT) of Jurkat cells and THP-1 cells were within 3 days in GM; PDT for Jurkat cells [21% O_2 (2.1 days) and 2% O_2 (2.2 days)] and PDT for THP-1 cells [21% O_2 (3 days) and 10% O_2 (3 days)]. However, our target media are serum-free (SFNCM and SFCM), which were associated with extension of PDT;

PDT for Jurkat cells [$SFNCM^{21\%O2}$ (5 days), $SFNCM^{2\%O2}$ (5.2 days), $SFCM^{21\%O2}$ (9.5 days), and $SFCM^{2\%O2}$ (4 days)] and PDT for THP-1 cells [$SFNCM^{21\%O2}$ (5.5 days), $SFNCM^{10\%O2}$ (4.4 days), $SFCM^{21\%O2}$ (5.2 days), and $SFCM^{10\%O2}$ (6 days)]. Therefore, we have extended our experiments to cover 7 days. Secondly, the paracrine activity of Jurkat cells (IL2 release) and THP-1 cells (IL10/TNFa release) were maximum with first 2 days, however, we sought to track the fate of activation of our cell line model and to ensure that Jurkat cells are not re-stimulated in SFCM after suppression and THP-1 phenotype (M1 and M2) is not changed (transdifferentiation).

2.10 Data collection and statistical analysis

The BMA were collected from 3 donors (Table 2-2) on different timepoints. The generated SFCM was utilised for the subsequent experiments. Data in Chapter 3 were collected from replicates of SFCM generated from BMA14, BMA15, and BMA16 (n=3). Each set of experiments were conducted independently on SFCM collected from these donors. Data were normalised to either blank or SFNCM and expressed as mean±SD. One-way ANOVA were conducted using Graphpad Prism 6 (CA, USA) with Tukey's multiple comparison test were used to determine pairwise statistical significance ($p \leq 0.05$ was considered significant), with further analysis performed in Microsoft Excel Spread-sheets application. The microarray data were extracted from previously published results. The original data were collected from RNA of 4 different donors (n=4). However, we performed our statistics on 31 genes matching our cytokine array. Log expression was taken for individual sample. Data were expressed as mean±SD. One-way ANOVA were conducted with Tukey's multiple comparison test were used to determine pairwise statistical significance ($p \leq 0.05$ was considered significant).

In Chapter 4 and 5, SFCM collected from BMA15 (Chapter 4) and BMA16 (Chapter 5) were freezed in -80 and used for subsequent experiments. All experiments were conducted in replicates of 3 independent samples. For cell count and MTT, cells were seeded in 3 flasks, cell count performed every day on the 3 flasks (n=3), while for MTT, a 100µl/well of cell suspension from each flask was transferred to a row (12 well) of 96-wellplate (n=36). Data

were expressed as mean±SD. Two-sample t-test was conducted using Graphpad Prism 6 (CA, USA) to compare SFNCM vs. SFCM.

For ELISA, the culture media were analysed, the media was collected from replicates of 3 flasks following cell activation. Samples from each flask was transferred into 3 wells (n=9). Data were expressed as mean±SD. One-way ANOVA were conducted using Graphpad Prism 6 (CA, USA) with Tukey's multiple comparison test were used to determine pairwise statistical significance ($p \leq 0.05$ was considered significant). Fold upregulation was considered for those timepoints which were associated with highly significant differences.

Flow cytometry was conducted on THP-1 cells. The cells were seeded in 3 independent flasks. Flow cytometry was conducted on each sample at day 3 following exposure to SFCM or a cytokine. Data were expressed as mean±SD. One-way ANOVA were conducted using Graphpad Prism 6 (CA, USA) with Tukey's multiple comparison test were used to determine pairwise statistical significance ($p \leq 0.05$ was considered significant). Fold upregulation was considered for those timepoints which were associated with highly significant differences.

Chapter 3

Physioxia alters human mesenchymal stem cell secretome constituent components

3.1 Introduction

Mesenchymal stem cells (MSCs), first identified approximately 50 years ago, have a growing role in regenerative medicine as a treatment for various diseases and disorders[177,96]. In spite of this the precise mechanisms of action remain unclear though likely related to all or a combination of the following; multipotent differentiation, functional incorporation, immunomodulation, and secretion of paracrine factors[177,143,147]. Proteomic profiling of serum-free conditioned media (SFCM) from human MSCs (hMSCs) has revealed the presence of a range of pleiotropic biomolecules[156] within the secretome including VEGF, GMCSF, IL10, and leptin[58,164]. However, precise SFCM composition can vary confusing interpretation where variations can result from hMSC source, e.g. adipose tissue, cord blood[159,160], bone marrow aspirate[157,16,20], stem cell lines[158], applied culture conditions, conditioning periods, and classical monolayer versus 3D conditioning methods[161].

Various *in vitro* studies have reported beneficial effects of hMSC SFCM supporting the paracrine hypothesis of the regenerative potential of hMSCs, for instance, CM promotes proliferation and migration of alveolar epithelial cells[150] and facilitates *in vitro* wound closure model using keratinocyte and fobroblast cell lines[151]. Topical application of SFCM displayed beneficial effects in a Balb/C mouse model of excisional wound injury via recruitment of regulatory macrophages and endothelial progenitor cells to the site of injury[152] and SFCM has improved function recovery in a hindlimb injury induced by femoral artery ligation through induction of collateral angiogenesis and limb remodelling[153]. Moreover, it has been reported that IV infusion of SFCM promotes regeneration and inhibits cellular damage in a rat model of gentamicin-induced liver injury through accelerating proliferation and inhibition of apoptosis[154]. Further localised administration of SFCM in a rat ischemic retinal model restored functionality and reduced the damage via inhibition of retinal cell apoptosis and attenuation of ischemic effects[155]. Collectively, these suggest that SFCM may become a milestone therapeutic tool or a source for discovery of new bioactive therapeutic molecules (Figure 3-1).

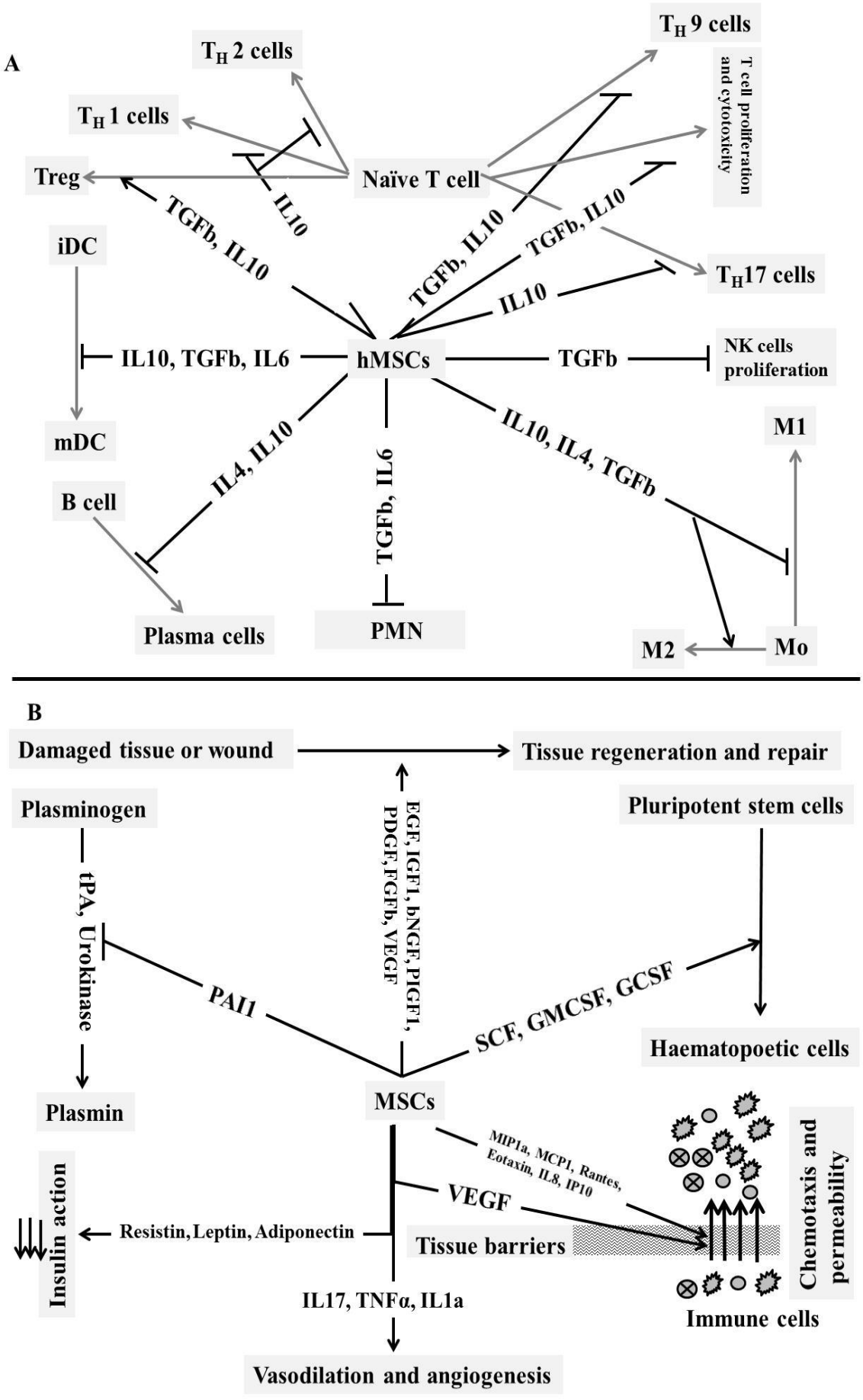
A
T_H 9 cells
T_H 2 cells
T cell proliferation and cytotoxicity
T_H 1 cells
Treg
Naïve T cell
IL10
TGFb, IL10
TGFb, IL10
TGFb, IL10
iDC
IL10
T_H17 cells
IL10, TGFb, IL6
hMSCs
TGFb
NK cells proliferation
M1
mDC
IL4, IL10
TGFb, IL6
IL10, IL4, TGFb
B cell
Plasma cells
PMN
M2
Mo
B
Damaged tissue or wound
Tissue regeneration and repair
Plasminogen
EGF, IGF1, bNGF, PIGF1, PDGF, FGFb, VEGF
Pluripotent stem cells
tPA, Urokinase
PAI1
SCF, GMCSF, GCSF
Haematopoetic cells
Plasmin
MSCs
MIP1a, MCP1, Rantes, Eotaxin, IL8, IP10
VEGF
Insulin action
Resistin, Leptin, Adiponectin
Tissue barriers
Chemotaxis and permeability
IL17, TNFα, IL1a
Immune cells
Vasodilation and angiogenesis

Figure 3-1. Schematic diagram describing the possible regenerative paracrine potential of the detected bioactive factors in SFCM.

The prominent action of SFCM has been noted on immune cells and inflammatory responses of the immune system due to injuries or antigenic insults. The detected bioactive factors dictated to thwart the immune response providing an anti-inflammatory environment which encourages regenerative healing mainly through angiogenesis, tissue regeneration, chemotaxis and inhibition of immune cells activation and differentiation. (A) The role of hMSCs bioactive factors in the immunomodulation, IL10 and TGFb play a crucial role in suppression of immune cell proliferation and differentiation providing overwhelming evidence that MSCs secretome could be used as a therapeutic modality in certain immune diseases. (B) Regenerative potential of hMSCs secretome through releasing growth factors, chemotactic factors and angiogenic factors into the localised environments promoting the healing process. Arrows indicate activated pathways while T-bars indicated inhibited pathways.

The role of oxygen in stem cell biology has been described variously[51,184,35,49]. Physioxia is an inherent feature of the *in vivo* niche environment in which hMSCs are resident drawing largely from the sinusoidal blood network characteristic of bone marrow[185,186,29]. Physioxia is significantly lower than inhaled exogenous air (21% O_2) and it declines gradually as it passes from the lung to the tissues; ranging between 0.1%- 9% with an average of 2% O_2[29,31]. Also important to note is that the journey of a transplanted stem cell from donor to recipient can be broadly divided into *in vitro* and *in vivo* stages. The *in vitro* stage features isolation and expansion under non-physiological conditions while the *in vivo* stage includes both donor (before isolation) and recipient (after transplantation) physiological environments[31]. The immediate physiological environment of the recipient will vary according to the preferred delivery method but focussing on one currently applied intravenous delivery methodology the hMSC dose arrives into the physioxic blood stream having previously experienced a long-term association with air oxygen[41,42].

Applying an increasingly *in vivo*-like physioxia to *in vitro* hMSC culture modulates the transcriptome but it remains to be determined if this manifests itself via an altered secretome composition[183]. An altered secretome would likely impact on the reparative action of SFCM and would likely better reflect the behaviour of hMSCs and/or their secretome following transplant into *in vivo* tissues. A range of control parameters can be applied to mimic conditions both before isolation and after transplantation drawing comparisons to standard *in vitro* culture conditions.

3.2 Aim

Explore the role of different oxygen tensions on the secretome composition of hMSCs using air oxygen (21% O_2) versus both intermittent hypoxia (2% O_2) and physioxia (2% O_2 workstation) models (Figure 3-2).

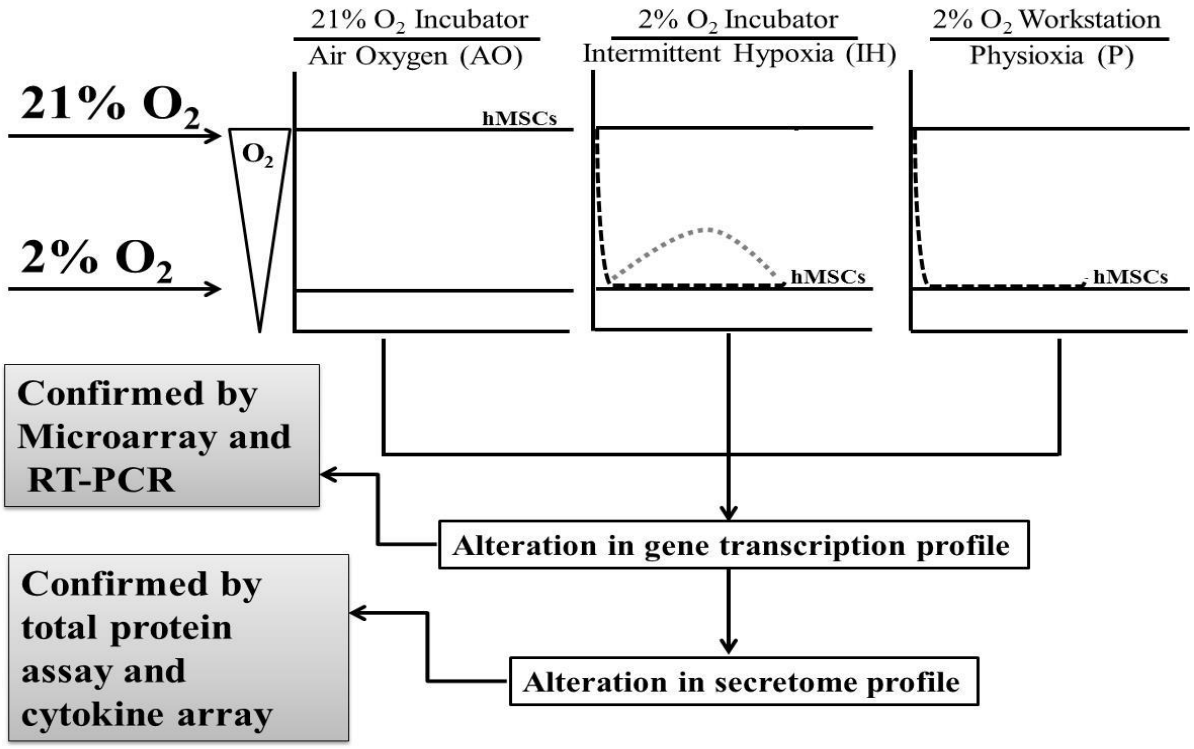

Figure 3-2. Schematic diagram for *in vitro* hypoxic model

The diagram is describing the impact of fluctuation of *in vitro* oxygen tension on hMSCs paracrine signalling during their culturing, isolation and expansion. hMSCs and SFCM were collected under these oxygen tensions and used for subsequent experimentation. The 21% O_2 incubator (air oxygen) shows no fluctuation of oxygen at cellular level during seeding, changing media or passaging or opening and closing incubator doors while 2% O_2 incubators (physioxia) were associated with fluctuation of oxygen concentration at cellular level during seeding, changing media or passaging, additionally the 2% O_2 model (intermittent hypoxia) is associated with oxygen swinging due to door opening and closure phase. These variations in oxygen level associated with changing in hMSCs transcriptome and consequently secretome profile. Grey dotted line (……) indicates oxygen fluctuation due to opening and closure of incubator doors, black dotted line (------) indicates oxygen downregulation during seeding, changing media and passaging, and solid line refer to 21% O_2 (upper) and 2% O_2 (lower) levels.

3.3 Functional classification of biomolecules present in SFCM

Table 3-1. Cytokines of MSCs secretome.

Anti-inflammatory cytokines		Pro-inflammatory cytokines	
IL4	Interleukin4[187]	IFNγ	Interferon r[156]
IL10	Interleukin10[156]	TNFa	Tumour necrosis factor a[156]
IL13	Interleukin13[156]	IL1a	Interleukin-1a[156]
TGFb	Transforming growth factorb[156]	IL2	Interleukin-2[156]
		IL12	Interleukin-12[156]
		IL17a	Interleukin-17a[188]

Hematopoetic cytokines[156]		Growth and trophic factors[156]	
GCSF	Granulocyte colony- stimulating factor	EGF	Epidermal growth factor
GMCSF	Granulocyte-macrophage-colony–stimulating factor	IGF1	Insulin-like growth factor-1
SCF	Stem cell factor	bNGF	b-nerve growth factor
		PIGF	Placental growth factor
		PDGF	Platelet-derived growth factor
		FGFb	Basic Fibroblast growth factor
Chemokines			
MIP1a (CCL3)	Macrophage inflammatory protein-1α (Chemokine (C-C motif) ligand 3)[189]		
MCP1 (CCl2)	monocyte chemotactic protein 1 (chemokine (C-C motif) ligand 2)[156]		
Rantes (CCL5)	regulated on activation, normal T cell expressed and secreted (Chemokine (C-C motif) ligand 5)[156]		
Eotaxin (CCL11)	eosinophil chemotactic protein (C-C motif chemokine 11)[156]		
IL8 (CXCL8)	Interleukin-8[156]		
IP10 (CXCL10)	Interferon gamma-induced protein 10 (C-X-C motif chemokine 10)[190]		

Adipokines[191]	
Resistin	adipose tissue-specific secretory factor (ADSF) or C/EBP-epsilon-regulated myeloid-specific secreted cysteine-rich protein (XCP1)
Leptin	
Adipo	Adiponectine
PAI1	Plasminogen activator inhibitor-1

Others		
Angiogenic factor	VEGF	Vascular endothelial growth factors[156]
Pleiotropic cytokine	IL6	Interleukin-6[156]

Anti-inflammatory cytokines

IL4. Mainly released by CD4+ T cells, basophils, and mast cells it stimulates differentiation of CD4+ T cells into Th2 cells and inhibits their differentiation into Th1 cells. IL4 acts as a growth factor for T cells, B cells, and mast cells and stimulates MHCII expression by B cells. In rheumatic patients, IL4 suppresses the production of several pro-inflammatory factors, such as MIP1a, TNFa, IL1, IL6, and IL8 by synovial tissues. Additionally, IFNγ and IL4 antagonise each other. IL4, acts as a pleiotropic cytokine, influencing Th cell differentiation toward Th2 resulting in subsequent release of IL4 and IL10 by Th2. IL4 suppresses Th1 differentiation, downregulates IL12 production by macrophages, recruits and polarises mast cells, stimulates B cell production of antibodies, suppresses macrophage cytotoxicity, inhibits parasite killing, and inhibits macrophage NO production[192].

IL10. Produced by activated B cells, activated CD4+ T cells, and activated CD8+ T cells. It has a broad range of inhibitory activities inhibiting IFNγ synthesis by activated T cells, antigen induced T cell proliferation, monocyte-MHCII expression induced by IL4/IFNγ, and IL2-induced IFNγ production by NK cells. In addition to above it inhibits IL2 and IFNγ production by Th1 cells, monocyte/macrophage proinflammatory cytokine production, such as, TNFa, MIP1a, MIP2a, TNFa, IL1, IL6, IL8, IL12, and GCSF[168]. IL10 is a potent inhibitor for MHCII expression, the B7 costimulatory molecule, and CD14 expression which is a LPS recognition signalling molecule. IL10 inhibits nuclear factor kB (NF-kβ) nuclear translocation after LPS stimulation and promotes degradation of messenger RNA for the proinflammatory cytokines[193]. Moreover, IL10 decreases surface expression of TNF receptors and increase the sloughing of TNF receptors into the circulation[194]. Low lung concentrations of IL10 in patients with acute lung injury indicate that ARDS is more likely to develop[195]. The

administration of IL10 in experimental animal models of endotoxemia improves survival. Human volunteers given IL10 after endotoxin challenge suffer fewer systemic symptoms, neutrophil responses, and cytokine production than placebo-treated control subjects[196]. Furthermore, it has been reported that IL10 knockout mice acquires chronic inflammatory enteritis that similar to inflammatory bowel disease in humans[194]. This confirms that IL10 plasma concentrations are important in limiting the inflammatory signal to gut-associated bacteria, therefore, IL10 is in clinical trials for inflammatory bowel disease[193,168].

IL13. An anti-inflammatory cytokine produced by activated T cells, it inhibits the NF-kB pathway and the synthesis of pro-inflammatory cytokines, such as, IL1B, IL6, IL8, and TNFa by monocytes in response of lipopolysaccharide. IL4 and IL13 share 25% structural similarities in their amino acid sequences, their receptor shows polymorphism, and they share STAT6 as a post-receptor translation pathway. In addition IL13 increases expression of MHCII and integrin and decreases CD14 and Fcγ receptors[193].

TGFb. Produced by T cells, monocytes, and platelets it exists in 3 isoforms TGFb1, TGFb2, and TGFb3, each encoded by separate genes but binding to the same receptor. It inhibits proliferation of T cells and NK cells. Upon tissue exposure to insult, the localised platelets degranulate and release TGFb. TGFb starts to recruit leucocytes to the site of injury initiating the first step of chronic inflammation. TGFb then stimulate its own synthesis by leucocyte; stimulate extracellular matrix deposition, and integrin expression stimulating cell adhesion. Similar to IL10, TGFb1 inhibits monocytes/macrophages activation; however, TGFb is less potent than IL10 in inhibition of macrophages IL1 production. TGFb exert its activity based on tissue localised cytokine environment, therefore, presence of other cytokines changes the immune response to TGFb thereby TGFb could modulate the active immune response into resolution and healing[193].

Pro-inflammatory cytokines

TNFa. Produced by polarised monocyes/macrophages, fibroblasts, mast cells, T cells, and NK cells, TNFa and IL1 share proinflammatory activity on target tissues. IL1 and TNFa induce fever directly via production of PGE2 by endothelial blood vessels of the hypothalamus or indirectly via stimulation of IL1 synthesis. Moreover, TNFa shares some of its proinflammatory activity with IL6 and IL11 via induction of acute phase protein by liver. In

addition to their paracrine activity, TNFa, TNFb, IL1, and IL6 have endocrine systemic effects during their acute production as in bacterial septicaemia. Systemic release of these cytokines is responsible for fever and hypertension; a characteristic features of septic shock[191].

IFNγ. The interferons are a family of proinflammatory cytokines, the most common of this family is IFNγ which is produced by activated T cells and NK cells. IFNγ stimulates MHCI and II expression by nucleated cells and stimulate phagocytosis[193].

IL1a. Produced by phagocytes, keratinocytes, fibroblasts, activated T and B cells, IL1 stimulates T cell proliferation, stimulates PGE2 synthesis by endothelial blood vessels of the hypothalamus resulting in fever, and stimulates histamine release from mast cells leading to vasodilation[193].

IL2. Produced by activated T cells and results in proliferation of T cells, B cells, and NK cells, and stimulates proinflammatory cytokine secretion by activated target cells with increased surface MHCII expression[197].

IL12. Is produced by professional antigen-presenting cells, such as, B cells, macrophages, and dendritic cells. IL12 activity includes stimulation of cytotoxic T cells, stimulation of NK cell cytotoxicity, and stimulation of proliferation of polarised T cells and NK cells. IL12 synthesis is blocked by IL4 and IL10 and the proinflammatory activity of IL12 on Th1 maturation is inhibited by IL4[193].

IL17a. Produced by activated T cells and stimulates IL6 and IL8 synthesis and increase ICAM-1 expression by activated fibroblasts[193].

Growth factors (SCF, EGF, IGF1, bNGF, PIGF1, PDGF, FGFb, VEGF)

Upon injury platelets degranulate releasing their contents, including growth factors such as: EGF, PDGF and TGFb[156]. PDGF acts with IL1 to stimulate recruitment of neutrophils to the site of an injury[193]. In the presence of TGFb, the monocyte is polarised to form the macrophage resulting in augmentation of the immune response and debris formation[191].

FGF, EGF, TGFb, and PDGF are released by macrophages and stimulate granulation tissue formation[193]. VEGF and FGF are released from platelets and stimulate endothelial cell proliferation and blood vessel formation[198]. Furthermore, FGF, TGFb and PDGF stimulate fibroblast transition to myofibroblasts which align with the extracellular matrix[193].

Colony stimulating factors (GCSF and GMCSF)

When monocytes, T cells, fibroblasts, and endothelial cells are activated by IL1 and TNFa, they produce MCSF and GMCSF. MCSF and GMCSF stimulate neutrophils while GMCSF stimulates both eosinophils and mononuclear phagocytes[193]. In the lungs, alveolar macrophages produce 3-fold higher GMCSF level than other macrophages and the released GMCSF play a role in the pathophysiology of inflammatory phase accompanying asthma[175].

Chemokines (IL8, MIP1a, MCP1, IP10, Rantes, Eotaxin)

These factors control immune cell migration and immune cells allocation, they are crucial for immune cell movements in health and disease status. They induce chemotaxis of neutrophils, monocytes, lymphocytes, basophils, and eosinophils toward the site of injury. [190]. So far, more than 30 chemokines have been characterised, however, IL8 is the most extensively studied cytokine and therefore serves as a prototype to which newly discovered chemokines are compared[48]. IL8 is neutrophil chemotactic factor, it stimulates neutrophils and other granulocyte chemotaxis, the mechanism of chemotaxis involves increased surface expression of the adhesion protein on target cells, including intracellular adhesion molecule, ICAM-1 and endothelial leukocyte adhesion molecule, ELAM-1, and thereby stimulating neutrophil attachment to the endothelium lining of the blood vessels resulting in their diapedesis through the vessel wall[193]. MCP1 is produced by monocytes and its production is enhanced by proinflammatory cytokines, it functions as a chemoattractant for the mononuclear cells. MIP1a and MIP1b stimulate chemotaxis of mononuclear cells and they are produced by monocytes and T cells[199]. Eotaxin is a specific chemoattractant produced by activated epithelial and endothelial cells and induces chemotaxis of eosinophils. IP10 is a chemoattractant which stimulates NK cells and CD8+ T cells trafficking.[156,200]

Adipokines (Leptin, Resistin, Adiponectin, and PAI1)

Produced by adipose tissues and macrophages localised within the adipose tissues[201]. They have a metabolic role influencing insulin resistance and stimulation of obesity. Leptins function as an appetite suppressor hormone and as a mediator for inflammation induced by other cytokines[202]. Resistin increases insulin resistance in skeletal muscle and liver[203]. Adiponectin is an anti-inflammatory adipokine, it inhibits macrophage function[191].

Pleiotropic factors

IL6 is a pleiotropic cytokine produced by firoblasts, phagocytes, and T cells. It stimulates acute phase protein release by the liver, stimulates B cell maturation to antibody-producing plasma cells, participates in T cell polarisation and differentiation, stimulates IL2 and IL2 receptor expression, and blocks TNFa production[193]. IL6 controls the synthesis of some pro-inflammatory and anti-inflammatory cytokines, reduces the synthesis of IL1, TNFa, IFNγ, GMCSF, and MIP2, has no effect on IL10 and TGFb, and stimulates glucocorticoid production[191].

3.4 Methods

Primary hMSCs were isolated from human BMA as outlined in section 2.2.2.1 while SFCM were generated using standard SFNCM as described in section 2.2.3. Identity of the recovered cells was documented by conducting tri-lineage differentiation and flow cytometry as discussed in section 2.5.1 and 2.7.2, respectively. Various assays were performed on hMSCs and SFCM including proteomic and transcriptional analysis investigated in different oxygen tensions. RNA was isolated from hMSCs as previously described in section 2.6.1 and isolated RNA was subsequently used for RTPCR using primers customised in NCBI (section 2.6.2.3). Total protein composition of SFCM was quantified by BCA total protein assay (section 2.7.1) and hybridised onto cytokine array plates (section 2.7.3). Cytokines contained within the array and brief descriptions of each are outlined in table 3-1. Six cytokines of which are randomly selected to quantify using an ELISA based technique (section 2.7.4). Previously obtained RNA microarray global gene expression data

was reanalysed to identify the differences between oxygen tensions and their effect on cytokine gene expression at a quantitative level (section 2.6.3). Relative percentage increase (RPI) of any gene in certain condition versus other conditions was determined by this equation (RPI=[(X-Y)/Y]*100, those showing RPI>20% upregulation between conditions were plotted in Venn diagram and considered for comparison. Proteins showing significant modulation at array level were selected to conduct RTPCR (section 2.6.2).

3.5 Statistical analysis

Statistical analysis was conducted using Graphpad Prism 6 (CA, USA) and with further analysis performed in Microsoft Excel Spread-sheets application. One-way ANOVA were conducted with Tukey's multiple comparison test were used to determine pairwise statistical significance ($p \leq 0.05$ was considered significant). A ($P<0.05$) was estimated to indicate statistical significant differences between groups.

3.6 Results

3.6.1 Functional differentiation of hMSCs

The identity of hMSCs was confirmed by functional differentiation and flow cytometry (Figure 3-3). Fluorescence-activated cell sorting (FACs) was conducted to detect the presence of positive surface markers and absence of negative surface markers followed by analysis with Cyflogic software. The isolated hMSCs from BMA were positive for surface markers [CD73 (91.1±6.8, 94.9±7.6, 96.5±2.2), CD90 (80.9±16, 87.3±16.4, 88.5±13.7), CD105 (81.2±19, 81.4±27, 90.2±11.5)] and negative for haematopoietic markers [CD14 (7±2.6, 9.1±3.7, 7.5±1.4), CD19 (4.4±1.4, 5.6±0.5, 8.6±4.7), CD34 (5.1±0.55, 6.2±0.7, 7.8±2.4), CD45 (6±1.2, 10.1±3.1, 7.9±2.6), HLADR (9±6.4, 8.5±2.9, 7.4±2.1)], for hMSCs in 21% O_2, 2% O_2 and 2% O_2 workstation, respectively.

The isolated cells were successfully differentiated into adipocytes, chondrocytes, and osteocytes upon *in vitro* exposure to differentiation inducing media. The triglyceride vesicles and osteogenic nodules were more abundant in 2% O_2 and 2% O_2 workstation than 21% O_2 and blue stained glycosaminoglycans observed in all oxygen tensions.

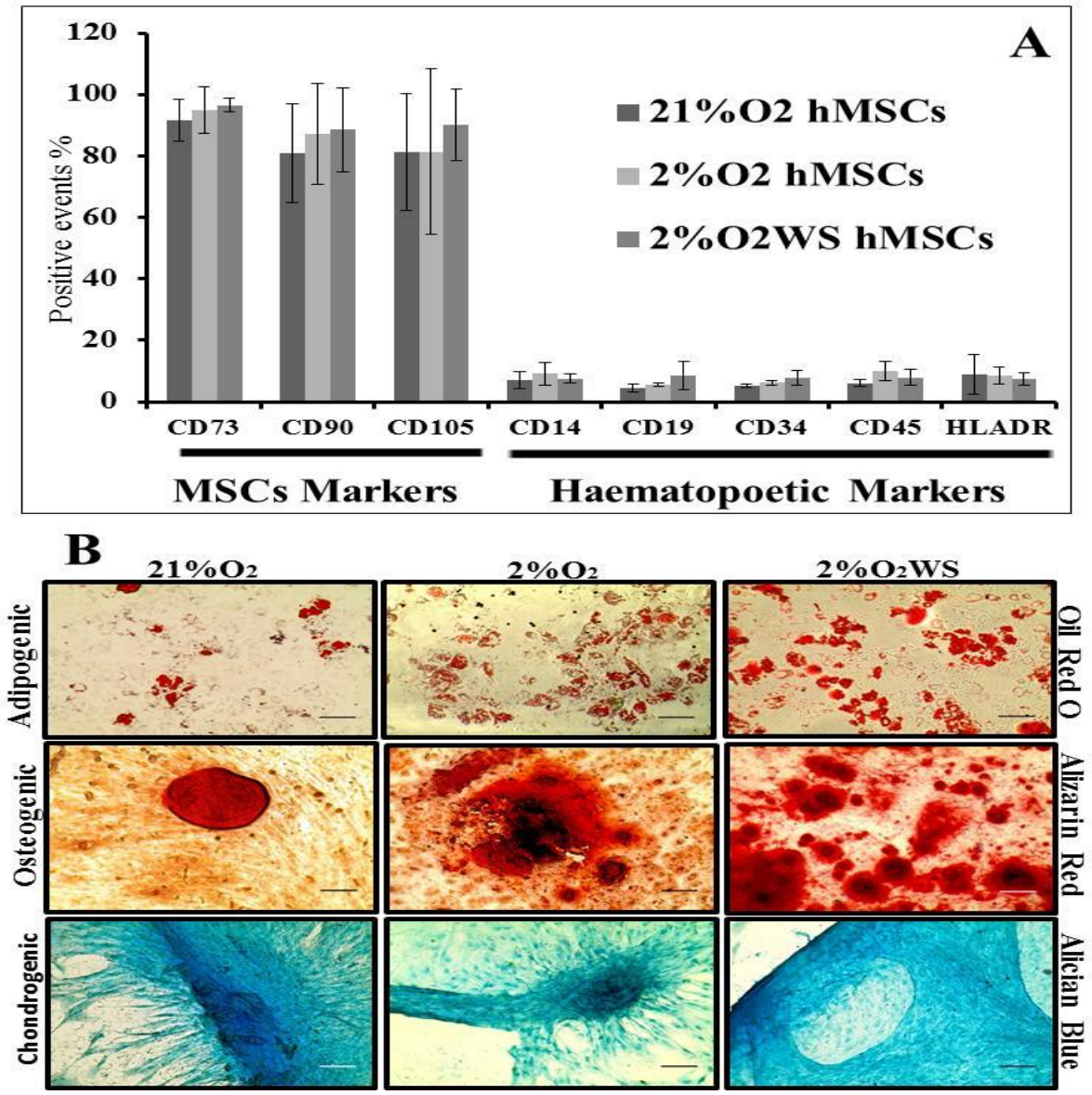

Figure 3-3. Identity of hMSCs isolated from bone marrow aspirate of 3 different donors cultured in 21% O_2, 2% O_2 and 2% O_2WS

(A) Confirmation of hMSCs positive (CD73, CD90, CD105) and negative marker (CD14, CD19, CD34, CD45, HLADR) expression. (B) Confirmed differentiation into adipogenic, osteogenic and chondrogenic lineages. Adipogenic and osteoenic differentiation were conducted on monolayer cell culture while micromass of (50000 cells/drop) was used for chondroenic differentiation.

3.6.2 Transcriptional assessment of hMSCs

hMSCs were isolated and recovered in 21% O_2, 2% O_2, and 2% O_2 WS and transcriptional analysis performed on RNA extracted from hMSC under these different oxygen tensions. The affymetrix expression values specific to these 31 bioactive factors were selected using UCSC Genome browser home and then uploaded into ArrayMining-Online Microarray Data Mining, to produce the heatmap (Figure 3-4A and C). The heatmap show green-dark-red color ranges indicating expression, no expression and repression, respectively. The heatmap indicates that the gene induction is higher in 2% O_2 and 21% O_2 in comparison to the 2% O_2WS, with more abundant red and reddish-dark colour in the later; indicating the lowest range of gene expression in 2% O_2WS. Moreover, the heatmap shows that samples from three experimental conditions cluster together more strongly than across groups.

The gene expression profile showed more than 20% relative percentage upregulation in some genes in both 2% O_2 and 2% O_2WS over 21% O_2 (Figure 3-4B); namely TGFb (71.10%, 47.33%), bNGF (65.86%, 47.03%), MIP1a (33.97%, 28.27%), MCP1 (39.22%, 96.24%) and Leptin (107.79%, 94.34%), respectively. Moreover, EGF showed 23.40% increase in 2% O_2WS over 21% O_2. While 21% O_2 shows 20% relative percentage upregulation over 2% O_2 and 2% O_2WS in some other genes; namely IL1a (52.5%, 86.49%), IGF1 (38.85%, 58.30%) and IL8 (79.27%, 127.5%), respectively. Moreover, FGFb showed 22.14% increase in 21% O_2 over 2% O_2. Finally, 2% O_2WS induced more than 20% relative percentage upregulation over 2% O_2 in some genes FGFb (22.29%), GMCSF (27.15%), MCP1 (29.05%) and IL8 (52.85%). Primers were designed for bioactive factors with significance differences (between hypoxia condition versus normoxia) at protein levels of either $p<0.1$ or $p<0.05$ (see Figure 3-5A). RTPCR results indicated that MCP1, SCF, Leptin, IGF1, FGFb, and bNGF were clearly expressed with intense bands in 21% O_2, 2% O_2, and 2% O_2 WS. However, IL10 and MIP1a were entirely below the detection limits in 2% O_2WS versus intense band expression in 21% O_2 and weak band expression in 2% O_2. Moreover, VEGF, GMCSF, IL12A, IL12B, TNFa were below the detection limits in 21% O_2 versus clear band expression in 2% O_2WS and 2% O_2 (Figure 3-4D).

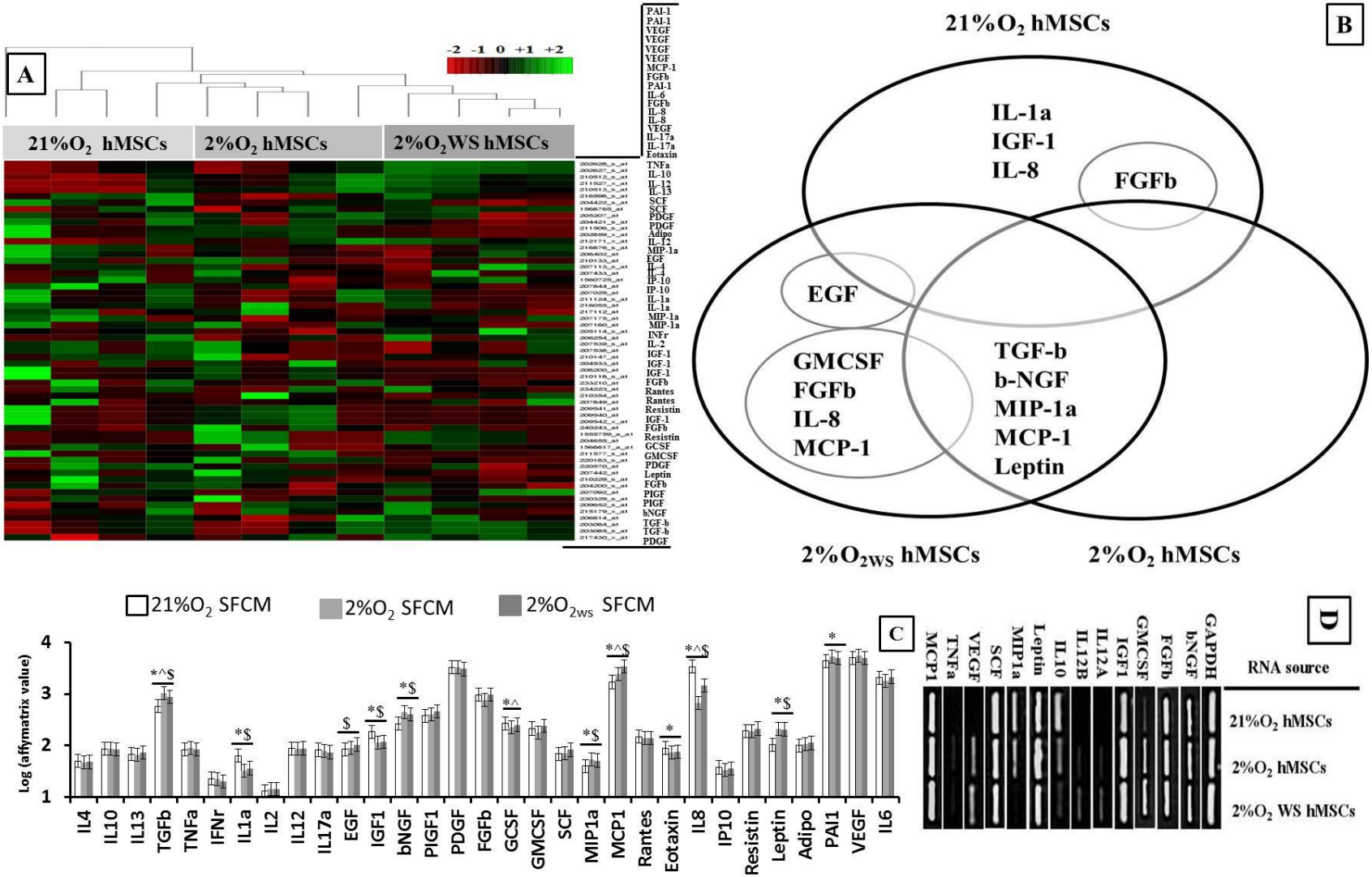
A
-2 -1 0 +1 +2
21%O2 hMSCs
2%O2 hMSCs
2%O2WS hMSCs
B
21%O2 hMSCs
IL-1a
IGF-1
IL-8
FGFb
EGF
GMCSF
FGFb
IL-8
MCP-1
TGF-b
b-NGF
MIP-1a
MCP-1
Leptin
2%O2WS hMSCs
2%O2 hMSCs
C
21%O2 SFCM
2%O2 SFCM
2%O2ws SFCM
Log (affymatrix value)
IL4
IL10
IL13
TGFb
TNFa
IFNr
IL1a
IL2
IL12
IL17a
EGF
IGF1
bNGF
PIGF1
PDGF
FGFb
GCSF
GMCSF
SCF
MIP1a
MCP1
Rantes
Eotaxin
IL8
IP10
Resistin
Leptin
Adipo
PAI1
VEGF
IL6
D
MCP1
TNFa
VEGF
SCF
MIP1a
Leptin
IL10
IL12B
IL12A
IGF1
GMCSF
FGFb
bNGF
GAPDH
RNA source
21%O2 hMSCs
2%O2 hMSCs
2%O2 WS hMSCs

Figure 3-4. Bioactive panel transcript analysis across multiple hMSC samples.

The affymetrix expression values specific to these 31 bioactive factors were selected using UCSC genome bowser home. (A) The selected affymetrix values uploaded individually into arraymining-online microarray data mining tool, to produce the heatmap. Each column represent one sample and each 4 columns represent 4 experiments (n=4) related to specific oxygen tension, the heatmap show green-dark-red colour ranges indicating expression, no expression and repression, respectively, The dendrogram on the top of heatmap indicates that the clustering is better in hypoxia (2% O_2 and 2% O_2WS) in comparison to 21% O_2 (B) the log of average values of affymetrix data of the 31 bioactive factors, error bars indicate ±SEM, One-way ANOVA conducted with Tukey's multiple comparisons test to determine pairwise statistical significance, *^$ $p<0.05$, * 21% O_2 versus 2% O_2, ^ 21% versus 2% O_2WS and $ 2% O_2 versus 2% O_2WS. (C) Venn diagram showing more than 20% relative percentage upregulation of some genes in certain oxygen tension versus others. (D) RTPCR of 13 specific genes which demonstrated differential regulation at protein level.

3.6.3 Proteomic assessment of SFCM

The total protein content of SFCM was determined by Smith assay or bicinchoninic acid total protein assay. Analysis in triplicate of three independent samples using 96-wellplates, indicated that the normalized total protein concentration (ng/ml) of 2% O_2 SFCM (361±50.03) was significantly higher ($p<0.05$ and $p<0.001$) than that of the 2% O_2WS SFCM (247.67±49.24) and 21% O_2 SFCM (123.33±25.17), respectively. Similarly, total protein concentration of 21% O_2 SFCM was significantly lower ($p<0.05$) than 2% O_2WS SFCM (Figure 3-5C).

The presence of bioactive factors in SFCM was assessed qualitatively with a colorimetric cytokine array (Figure 3-5A). The overall result clearly indicated that 2% O_2 had potentiated the hMSCs to synthesize and secrete bioactive factors to a greater extent than in 21% O_2. However, 2% O_2 WS displayed discrepancies with regards to the two other samples and presented a mid-point overall. Bioactive factors which showed more than 2 fold upregulation in 2% O_2 in relation to 21% O_2 were Rantes (47 fold), EGF (5.61 fold), IL2 (5.29 fold), bNGF (4.79 fold), IL17a (4.5 fold), GCSF (4.36 fold), Adiponectin (2.70 fold), IP10 (2.62 fold), VEGF (2.43 fold), IL6 (2.30 fold), and IGF1 (2.03 fold). Moreover, 2% O_2 WS showed greater than 2 fold upregulation over 21% O_2 with Rantes (6.5 fold), GCSF (3.76 fold), IP10 (3.19 fold), EGF (3.15 fold), IL17a (3 fold), Adiponectin (2.15 fold), and IL2 (2.14 fold).

Notably 2% O_2 also showed more than 2 fold upregulation over 2% O_2 WS with Rantes (7.23 fold), bNGF (3.11 fold), IL2 (2.47 fold), MCP1 (2.38 fold), and IL4 (2.30 fold).

These bioactive factors were sub-classified into 9 functional groups, according to previously published articles, including anti-inflammatory cytokines (IL4, IL10, IL13 and TGFb), pro-inflammatory cytokines (TNFa, IFNγ, IL1a, IL2, IL12, and IL17a), Growth factors (EGF, IGF1, bNGF, PIGF1, PDGF, FGFb), haematopoetic factors (GCSF, GMCSF, SCF), chemokines (MIP1a, MCP1, Rantes, Eotaxin, IL8, IP10), adipokines (Resistin, Leptin, Adiponectin), fibrinolytic factor (PAI1), angiogenic factor (VEGF), pleiotropic factor (IL6). The percentage of each functional group was determined and plotted as pie charts (Figure 3-5B). These indicated differences between the fractions of each subclass in relation to other functional group in same and across oxygen tensions (Figure 3-5B). The percentage of these functional groups were: anti-inflammatory cytokine (28%, 20%, 18%), pro-inflammatory cytokines (12%, 13%, 17%), growth factors (19%, 20%, 17%), haematopoetic factors (12%, 13%, 14%), chemokines (13%, 16%, 15%), adipokines (8%, 7%, 7%), fibrinolytic factor (3%, 3%, 3%), angiogenic (4%,5%, 6%) and pleiotropic factor (1%,3%,3%) in 21% O_2 SFCM, 2% SFCM and 2% O_2WS SFCM, respectively.

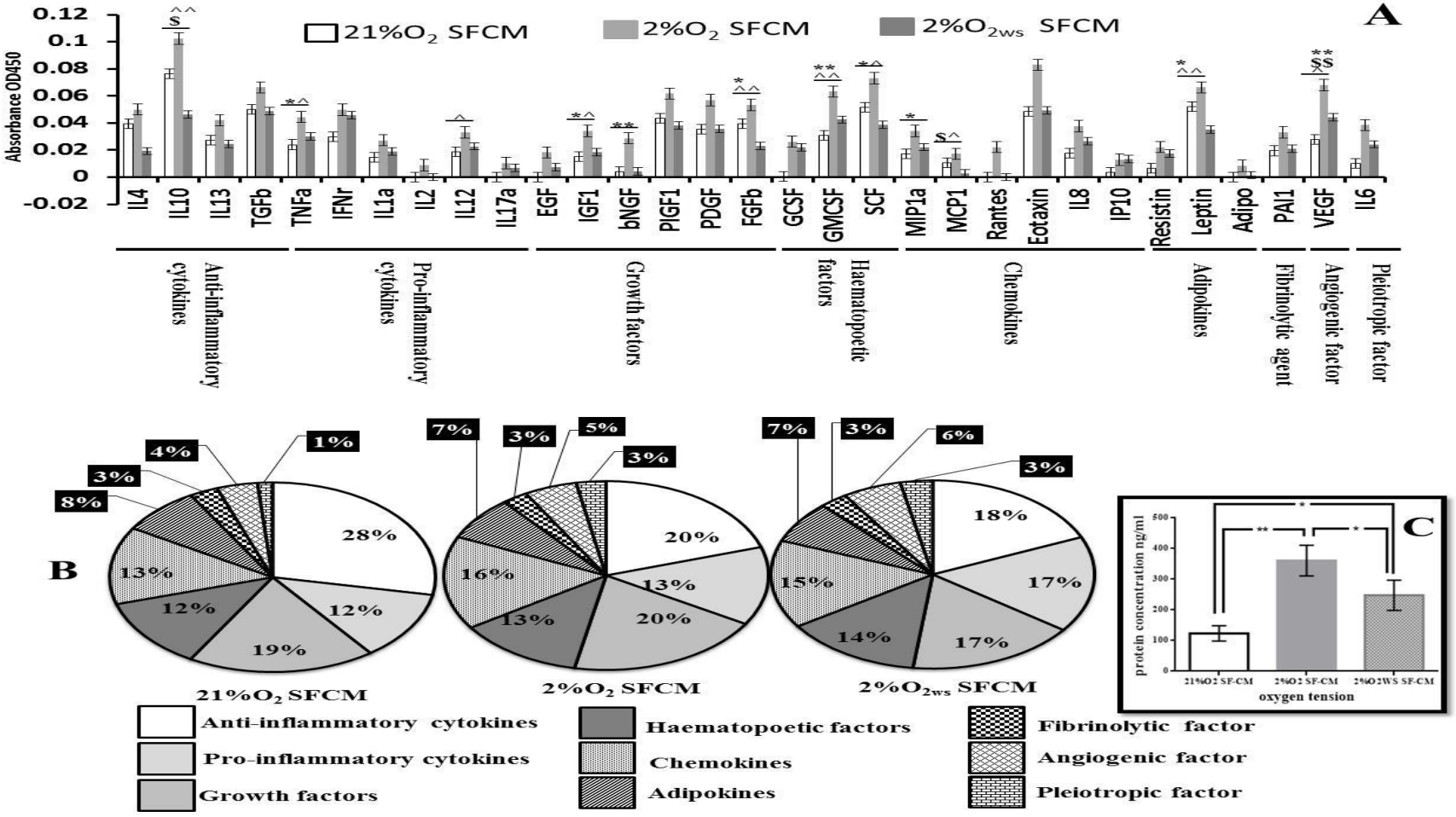
A
21%O2 SFCM
2%O2 SFCM
2%O2ws SFCM
Absorbance OD450
0.12
0.1
0.08
0.06
0.04
0.02
0
-0.02
IL4
IL10
IL13
TGFb
TNFa
IFNr
IL1a
IL2
IL12
IL17a
EGF
IGF1
bNGF
PlGF1
PDGF
FGFb
GCSF
GMCSF
SCF
MIP1a
MCP1
Rantes
Eotaxin
IL8
IP10
Resistin
Leptin
Adipo
PAI1
VEGF
IL6
Anti-inflammatory cytokines
Pro-inflammatory cytokines
Growth factors
Haematopoetic factors
Chemokines
Adipokines
Fibrinolytic agent
Angiogenic factor
Pleiotropic factor
B
28%
12%
19%
12%
13%
8%
3%
4%
1%
20%
13%
20%
13%
16%
7%
3%
5%
3%
18%
17%
17%
14%
15%
7%
3%
6%
3%
21%O2 SFCM
2%O2 SFCM
2%O2ws SFCM
Anti-inflammatory cytokines
Pro-inflammatory cytokines
Growth factors
Haematopoetic factors
Chemokines
Adipokines
Fibrinolytic factor
Angiogenic factor
Pleiotropic factor
C
protein concentration ng/ml
500
400
300
200
100
0
21%O2 SF-CM
2%O2 SF-CM
2%O2WS SF-CM
oxygen tension

.

Figure 3-5. Proteomic assessment of hMSCs secretome.

(A) Cytokine array of SFCM generated from independent donors (n=4) using colorimetric array expressed as mean±SEM, One-way ANOVA conducted with Tukey's multiple comparisons test to determine pairwise statistical significance *^$ P<0.1 and **^^$$ P<0.05, * 21% O_2 versus 2% O_2, ^ 21% versus 2% O_2WS and $ 2% O_2 versus 2% O_2WS. (B) bioactive factors sub-classified into 9 functional groups and the proportion of cytokine functional group in relation to each other in the same oxygen tension determined, results expressed as a percentage of the summation of each functional group in relation to other. (C) Total protein content of SFCM, the results were normalised to SFNCM. One-way ANOVA conducted with Tukey's multiple comparisons test to determine pairwise statistical significance, data expressed as mean±SD, (n=3), * P<0.05 and ** P<0.001.

The qualitative assessment was validated by quantitative ELISA for 6 randomly selected bioactive factors including; IL2, IL4, IL10, TNFa, PIGF1, and VEGF (Figure 3-6). The results followed a similar pattern to the qualitative assessment with 2% O_2 generally presenting higher expression levels than both 2% O_2 WS and 21% O_2. The concentration (pg/ml) of IL4 in 2% O_2 (100.80±9.03) and 21% O_2 (60.40±13.22) were significantly higher ($p<0.05$) than the values noted for 2% O_2WS (25.96±25.88); with no significant difference existing between the 2% O_2 and the 21% O_2. Similarly, the concentration (pg/ml) of IL10 in 2% O_2 (813.27±57.85) and 21% O_2 (757.28±5.75) were significantly higher ($p<0.05$) than the concentration noted in 2% O_2WS (576.09±15.87); with no significant differences existing between the 2% O_2 and the 21% O_2. The concentration (pg/ml) of VEGF in 2% O_2 (289.82±2.32) and 2% O_2WS (293.23±21.30) were significantly higher ($p<0.05$) than 21% O_2 (262.15±9.81) with no significant difference existing between 2% O_2 and 2% O_2WS or 2% O_2WS versus 21% O_2. The concentration of (pg/ml) of PIGF1 in 2% O_2 (1668.49±197.29) was again significantly higher ($p<0.05$) than 21% O_2 (1068.99±99.05) with no significant difference existing between 2% O_2WS and either 2% O_2 or 21% O_2.

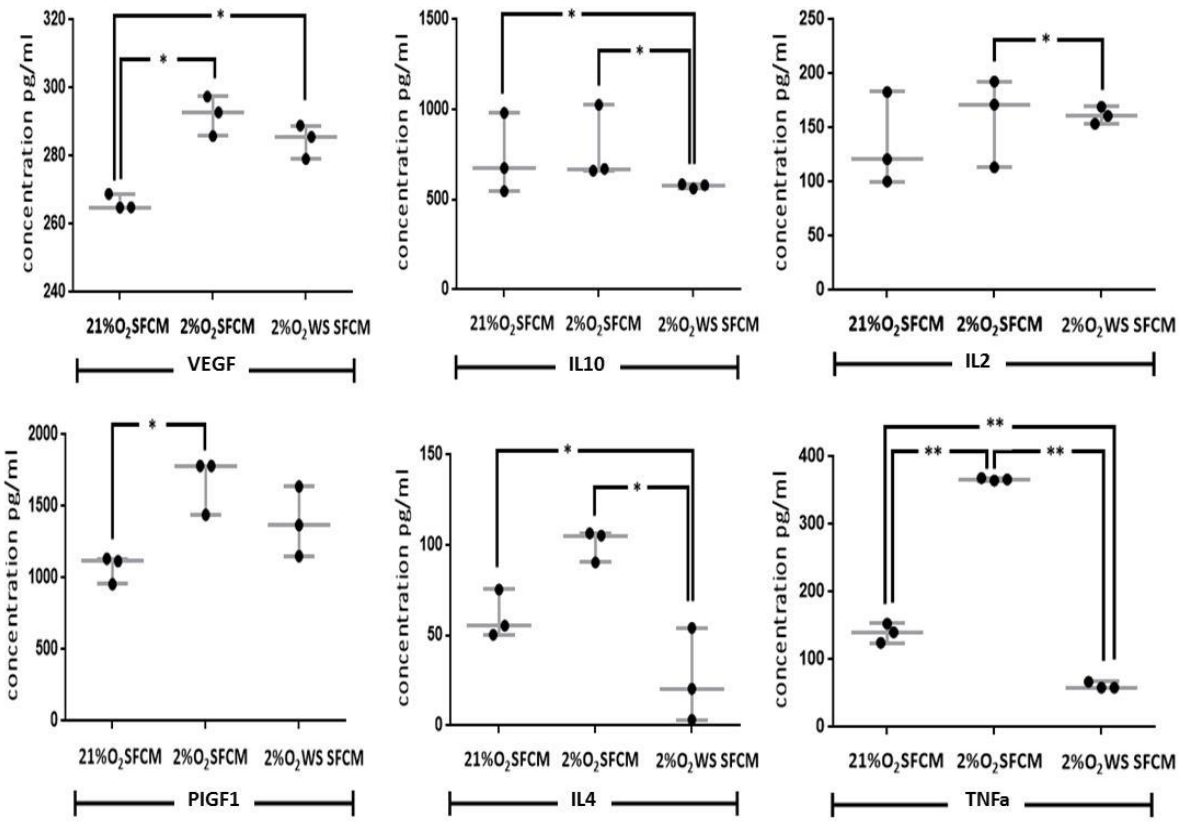

Figure 3-6. ELISA of IL2, IL4, IL10, TNFa, VEGF, and PIGF1 in hMSC SFCM.

Data expressed as interquartile ranges (the box lengths), extreme values (whiskers) the horizontal bar across the box indicates the median and the ends of the vertical lines indicates the minimum and maximum data values. The results were collected from the SFCM generated from the three bone marrow aspirates (n=3). One-way ANOVA conducted with Tukey's multiple comparisons test to determine pairwise statistical significance, * $p<0.05$, ** $p<0.001$.

3.7 Discussion

Various *in vitro* studies[148,149,150,49,151] and preclinical animal studies[152,153,154,155] have reported a beneficial effect of SFCM which supports the paracrine hypothesis of the regenerative potential of hMSCs. These findings hold the possibility of creation of cell devoid biotherapy, bypassing all cell-transplant associated limitations and obstacles coupled with easiest manufacturing processes of production, banking, handling, and transportation[204]. Therefore, many research centres are focusing on SFCM as a model to study the efficacy of hMSCs on various degenerative disorders[161,205,206,207], in an intention to transfer this biological product to clinical settings to substitute the cell-based therapy. However, these studies[157,159,160,16,20] have been cultured their MSCs in ambient oxygen

tension and the generated conditioned media have been collected over different period of time. Moreover, various techniques have been used to analyse the conditioned media either neat or diluted; resulting in various outcome. In the previous studies[58,45] oxygen tension seems to have a pivotal role affecting the proliferation, differentiation, and transcription, therefore, this study designed to partially identify the role of oxygen tension on the transcriptome and secretome profile of some bioactive molecules; using a highly sensitive ELISA-based detection technique.

The anatomical design of bone marrow is complex structure consisting of haematopoetic and adipose cells surrounded by sinusoidal vessels, the cells are arranged in well-organised order with a progenitors located in foci away from the vessel sinuses while mature cells are adjacent to the blood stream and they escape to the blood gradually according to body demand[28], this organised morphological architecture render progenitor cells; including MSCs, to be localised far away from sinuses under gradient hypoxic environment (1-6% O_2) depending on its location from the sinuses[29,30]. In an attempt to replicate *in vivo* oxygen-restrictions the hMSCs in the present study were cultured *in vitro* in a chronic hypoxia (~2% O_2) environment provided via a hermetic workstation with all culture processing being performed in this oxygen restrictive environment. However, in order to expose hMSCs to a wider range of oxygen tension; to mimic *in vivo* ischemic injury[208], a pathological hypoxia model was also created by culturing cells in a hypoxia incubator with intermittent air flushing due to open/shut phase of the incubator doors with all culture processing being performed under an atmospheric environment. Both hypoxia model (2% O_2 and 2% O_2WS) were compared to hyperoxia (21% O_2) cultured mesenchymal stem cells (Figure 3-2). Collectively, these full scan models together might accurately reflect the possible practical effects of oxygen on modulation of proteomic spectrum during clinical application of hMSCs and/or the potency of SFCM as a biotherapy.

Recent *in vitro* publications support the hypothesis of positive impact of hypoxia on growth kinetics of MSCs and delayed replicative senescence possibly through reduction in mitochondrial respiration and subsequently the generation of reactive oxygen species providing better genetic stability and delayed telomere shortening[38]. In the present study, the selected genes for the measured bioactive molecules show relatively better hierarchical clustering under chronic hypoxia and pathological hypoxia when compared to hyperoxia;

which shows a disordered dendrogram configuration. This is despite that the heat map shows a higher expression in both pathological hypoxia and hyperoxia when both are compared to chronic hypoxia, while when the probesets or variants of each gene where averaged with each other, the results show higher expression of some genes (TGFb, bNGF, MIP1a, MCP1, Leptin, and GMCSF) in 2% O_2WS and 2% O_2 versus 21% O_2, and the later shows higher levels of IL1a, IGF1, and IL8 in comparison to the formers (Figure 3-4C). The discrepancy of gene expression between 2% O_2 and 21% O_2 in our sample has been described by another microarray study[58] which was conducted in sever hypoxia (0.5% O_2) and hyperoxia (21% O_2) and concluded that there is better reproducibility in gene expression under hypoxia.

The majority of previously published studies have reported that hypoxia positively mediates upregulation of chemotactic and growth factors in the MSCs secretome[36,58,209]. In agreement with our findings there is an upregulation in the transcription of VEGF, MIP and Leptin and downregulation of IGF1 in severe hypoxia in comparison to hyperoxia in microarray data of bone marrow-derived hMSCs[58,164]. Conversely, our sample shows no change in PIGF1 and upregulation in MCP1 versus upregulation in PIGF1 and downregulation in MCP1 in the comparative studies[58,164]. The hypoxia-induced transcriptional modulation in our sample is not unique to the bone marrow derived hMSCs[58], a comparative study[164] comparing umbilical cord blood- and bone marrow-derived hMSCs shows overlapping in transcription of hypoxia-responsive genes between both sources, similarly, adipose-derived MSCs show upregulation in some transcription factors in hypoxia when compared to hyperoxia[163]. Furthermore, this phenomenon is not limited to the human species confirmed by hypoxia-induced upregulation in the transcription of different factors from MSCs isolated from male Lewis rats[162], which showed more than 3 fold upregulation in VEGF (8.2), TGFb (3.2), IL1B (3.1), MCP1 (7.4), MIP (5.5), and PIGF1 (3.4).

Similarly, proteomic profiling explored a positive impression of 2% O_2 on the bioactive factors and identified a marked upregulation of individual components in SFCM of 2% O_2 over 2% O_2WS and 21% O_2, confirmed by upregulated total protein content of the SFCM of 2% O_2 over 2% O_2WS and 21% O_2. Many published *in vitro* proteomic studies conducted on SFCM have revealed upregulation of measured bioactive factors in hypoxia over hyperoxia

despite differences in the source of isolated MSCs; adipose[56,57] or bone marrow[58,59,60], and variation in conditioning periods; short or long. Transient hypoxic exposure of adipose-derived MSCs[56]; shows more than one fold upregulation of some measured cytokines (GMCSF, IL6, VEGF, IGF1, and TGFb1), likewise, their prolonged hypoxic exposure demonstrates upregulation in (GCSF, GMCSF, IGF, MCSF, PDGF, and VEGF) and downregulation in EGF. Correspondingly, analysis of SFCM from BMA revealed that hypoxia substantially induces the production of some measured biomolecules (bFGF, VEGF, IL6, IL8, PIGF) with no changes being reported with others (IGF1, MCP1, TGFb1, and IL1)[59,60]. Interestingly, leptin and VEGF; hypoxia markers[58], were reported to be the most sensitive biomolecules to hypoxia by most cells. Alteration of these transcription factors could be linked to HIF-1a pathway; hypoxia stabilises HIF-1a and keeps MSCs in quiescent proliferation status, maximising the transcription of hypoxia-responsive genes[32,55].

It has been reported that, the application of critical environment; pathological hypoxia, on *in vitro* cultured MSCs might be responsible for stimulation of normal cellular compensatory mechanisms resulting in upregulation of the secreted proteins; providing a defence mechanism to protect the cells from the harsh environment and prolong its survival[153,56,54]. For instance, in ischemic injuries; like coronary arterial stenosis, the tissue hypoxia is accompanied by upregulated release of certain growth factors resulting in collateral angiogenesis[153]. However, chronic hypoxia mitigated the synthesis and secretion of bioactive factors in comparison to pathological hypoxia, validating the intrinsic behaviour of MSCs in their endogenous natural niche environment under constant and consistent gradient oxygen tension and further subsidises the *in vivo* paracrine hypothesis of MSCs. Unfortunately, limited or no data are available regarding MSCs culturing under chronic hypoxia for comparison, validation of this hypothesis necessitate *in vivo* demonstration of same secretory factors by transplanted MSCs.

Keele UNIVERSITY

Chapter 4

Evaluating the role of hMSC SFCM in a T-cell activation model

4.1 Introduction

hMSCs emerged as a therapeutic tool for inflammatory diseases following the demonstration of *in vitro* suppression of T cell proliferation in a mixed lymphocyte reaction[81]. The suppression is broad spectrum involving mitogens, peptide antigens, and alloantigen-induced T cell proliferation and CD3/CD28 antibody mediated T cell activation[177]. Additionally, MSCs suppressed pharmacological activation of intracellular pathways of T cell, confirming that the mechanism of inhibition was a non-T cell receptor-based pathway[178]. The suppression involves different T cell subtypes including both CD4+ and CD8+ as well as naïve T cells[80]. In addition to *in vitro* evidence, *in vivo* suppression has been confirmed in experimental baboon animal model of skin graft[81]. The suppression of T cells through transwell systems confirms that MSCs exert their immunosuppressive activity through a paracrine mechanism[80].

T cell activation is a complex process involves cell membrane events, cytoplasmic events, and nuclear events. The membrane events started with the recognition of processed peptide antigen on MHCII of the APCs by TCR complex[210]. The interaction started by engagement of TCR complex with the peptide presented on the surface of APCs leads to the initiation of multiple signalling pathways resulting in activation, proliferation, and differentiation[211]. To achieve an immune response the T cell requires an accessory signalling pathway to be activated and unless otherwise engaged the T cell undergoes anergy resulting in unresponsiveness[212]. Among the costimulatory molecules, CD28 and CD152 provide the most potent accessory signals[212]. The activation of the canonical transcription pathway based on the collaboration of three distinct nuclear signalling; Nuclear Factor-Kappa Beta (NF-κB), Activator protein-1 (AP-1), and nuclear factor of activated T cells (NFAT), altogether achieve T cell effector function[197,213]. These nuclear events are preceded by cytoplasmic events, including post-receptor translation pathways which involve phosphorylation of a group of cytoplasmic enzymes and protein biomolecules including phospholipase C (PLC). PLC catalyses the cleavage of phosphatidylinositol 4,5-biphosphate (PIP2) into inositol 1,4,5,-triphosphate (IP3) and diacylglycerol (DAG)[213]. These later biomolecules are a potential bottleneck step in the

subsequent steps of the immune response and mimicking or tackling of which will impact the immune response (Figure 4-1).

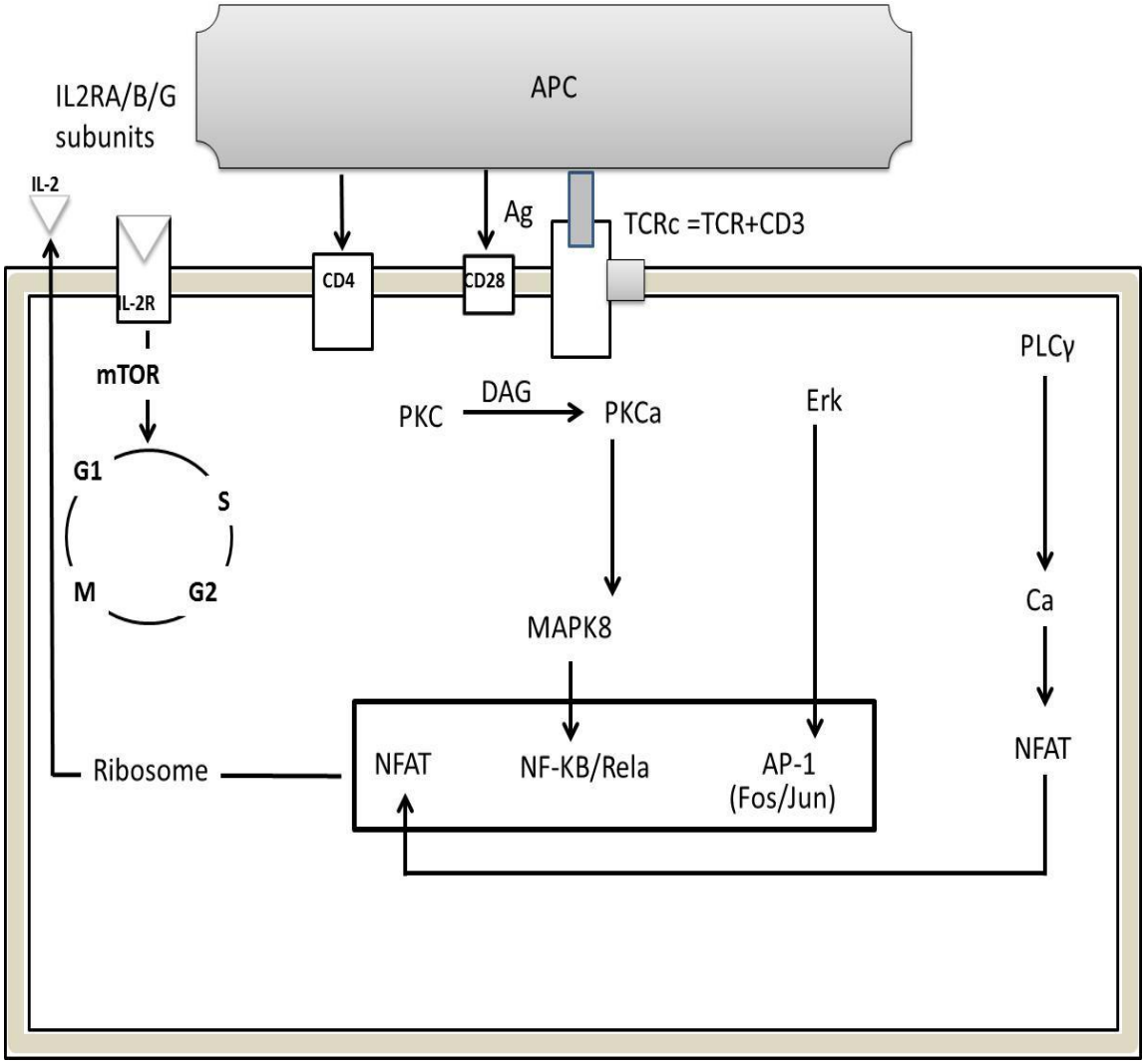

Figure 4-1. A schematic diagram describing the canonical T cell signalling pathways.

Genes transcripted during T cell stimulation by antigen-loaded on surface of antigen-presenting cells (APCs) are indicated, these pathways include, Calcineurin pathway (NFATAC2/PPP3CA), JNK pathway (JNK/Jun), RAS pathway (Erk/Fos), PKC pathway (NF-kB/Rela), and MAPK pathway (MAPK8), the end result is stimulation of transcription and synthesis/release of IL2 and IL2 in turn will binds to its surface IL2-receptor on engaged T cell, resulting in stimulation of mTOR pathway with subsequent proliferation.

DAG induces the protein kinase C (PKC) enzyme while IP3 induces a cytoplasmic calcium release from endoplasmic reticulum with subsequent calmodulin/calcineurin pathway activation culminating in transcription of NFAT. The transcription of NFAT is crucial in the synthesis of IL2, IL4, and IL5[197]. PKC together with other protein tyrosine kinases can

activate mitogen-activated protein kinases (MAPKs), including extracellular-regulated kinase (Erk), Jun N-terminal kinase (JNK)/stress activated protein kinase (SAPK) and p38/Mpk2[213]. Additionally, PKC induces the Ras/Raf/Erk signalling pathway via $p21^{Ras}$ activation pathway. The activated MAPKs participate in cytoplasmic events while the activated Erk translocates to the nucleus inducing AP-1 pathway transcriptional factors; including Jun/Fos[197]. Activated NFAT and AP-1 together form a transcriptional activation complex, this complex bind to the promoters of cytokine genes inducing their transcription. In addition to NFAT and AP-1 signalling pathways, both Ras and PI3-K dependent signalling pathways induce the polarisation of NF-kB signalling pathway inducing further strong transcription of promotor of cytokines genes[214].

Upon activation, naïve T cells undergo polarisation with subsequent IL2 production (Figure 4-1). The released IL2 binds to an IL2 cell surface receptor of engaged T cell inducing mTOR pathway resulting in progression of cell cycle and T cell proliferation[212,215]. During cell cycle progression, the localised cytokine microenvironment determines the fate of differentiation of the T cell into either Th1 or Th2 cells. For instance, the presence of the pro-inflammatory cytokine IL12 in the surrounding vicinity promotes Th1 differentiation while IL4 mediates Th2 differentiation[192]. Likewise, the presence of IL10 in the T cell milieu promotes differentiation toward Treg[194]. It has been confirmed that these cytokines promote their action through latent proteins involving Janus Kinase (JAK) and signal transducer and activator of transcription (STAT)[168]. Different anti-inflammatory cytokines; such as, IL4, IL10, and IL12, use various post-receptor translation pathways to induce their effector function; such as, STAT6, STAT3, and STAT4, respectively[213].

Jurkat an immortalised acute leukemic cell line which has been used by many immunologists as a standard surrogate for T cell[197,104]. Jurkat cells are polarised upon exposure to a combination of phorbol ester and a co-stimulator molecule; either ionomycin or phytohaemaglutinin (PHA), yielding a robust IL2 release. Phorbol myristate acetate (PMA), a structural homologue for DAG, mediates its stimulation via activation of PKC resulting in the production of low amount of IL2 which is strongly accentuated by the addition of PHA. In the present study the Jurkat cell line is used as a model to test the

efficacy of SFCM in the suppression of immune response via conducting a proliferation assay on Jurkat T cells and quantification of the amount of IL2 secretion as an activation marker. In an attempt to identify the cytokine(s) mediating the immunosuppressive effect of SFCM, cytokines with prominent anti-inflammatory activity, and identified in Chapter 3, are added individually to SFNCM or blocked from SFCM using their specific neutralising polyclonal antibody.

4.2 Aims

The primary aims of this chapter were to:

- Develop an *in vitro* polarised T cell line model by stimulating immortalised Jurkat T cells using PMA/PHA as an activation tool.
- Testing the efficacy of SFCM in suppression of immunological aspects (proliferation and polarisation) at cellular level compared to SFNCM.
- Determine the mechanism of action of SFCM by testing the efficacy of main cytokines with prominent anti-inflammatory properties on Jurkat T cell line and eventually neutralising these cytokines either individually or in combination with their specific polyclonal antibodies to identify the restoration potential.

4.3 Methods

Primary hMSCs were isolated from human BMA as described in 2.2.2.1 and SFCM generated using standard SFNCM as described in section 2.2.3. The identity of the recovered cells was documented via tri-lineage differentiation and flow cytometry as described in section 2.5.1 and 2.7.2, respectively. Various assays were performed on Jurkat cells cultured in GM, SFNCM, and SFCM, including proliferation assay (cell count and MTT), polarisation assay (IL2 ELISA), RTPCR, and morphological assessment (cell surface area), as described in sections 2.4, 2.7.4, 2.6.2, and 2.5.2, respectively. These parameters were measured in both polarised and non-polarised Jurkat T cells and in both pathological hypoxia (2% O_2) and air oxygen (21% O_2) tensions. The polarisation of Jurkat T cells was achieved using PMA/PHA as per section 2.3. Selected cytokines from cytokine array

(Chapter 3) with prominent anti-inflammatory properties were tested on Jurkat T cells to determine their inhibitory activity based on selected non-toxic dose according to dose-response curve as described in section 2.8. To identify the mechanism of SFCM, these cytokines were individually blocked from SFCM using specific polyclonal antibodies for each individual cytokine. The experimentations were performed over a 7-day period to achieve full modulation of the response; including a stationary phase for cell count, baseline proliferation for MTT, and baseline IL2 secretion for PMA/PHA-induced activation. For transcriptional analysis RNA was isolated using Qiagen RNA isolation kits as described in section 2.6.1. The proliferation of Jurkat T cells was indicated by MTT as a relative proliferation by normalising all values to day 0. The concentration of IL2 already present in SFCM was subtracted from day 0 IL2 results of Jurkat culture media activated in SFCM. The restoration of immune response achieved by IL10 neutralisation necessitates confirmation of IL10 receptor subunits gene expression, including RTPCR conduction on Jurkat RNA as described in section 2.6.2.

4.4 Statistical analysis

Statistical analysis was conducted between SFCM and SFNCM using a two-sample t-test for most of the measured parameters, whereas for more than 2 groups one-way ANOVA with Tukey's multiple comparisons test to determine pairwise statistical significance, $p \leq 0.05$ was considered significant. The analysis was performed using using Graphpad Prism 6 (CA, USA). Unless otherwise stated all values quoted in the results are mean ± standard deviation.

4.5 Results

4.5.1 Characterisation of Jurkat T cell line in GM

4.5.1.1 Morphological assessment of Jurkat T cells in GM

We first sought to conform that we had a reliable Jurkat activation model to base our subsequent experimentation on. To do this Jurkat cells were activated by seeding $2x10^5$ cells/ml in GM and exposed to (50ng/ml of PMA and 1µg/ml of PHA) in both normoxia (21% O_2) and hypoxia (2% O_2) environments over 7-days period compared to control non-treated group. Morphological assessment of Jurkat T cells following on from polarisation explored changes in cell surface area (μm^2). To achieve this, we scored 100 cells per 3 fields on each slide for replicates of 3 slides. This demonstrated that the surface area was slightly increased following on from activation with PMA/PHA over a 7-day period (Figure 4-2). However, there was no significant difference between the polarised and non-polarised conditions at earlier time-points (0-4), day-4 [21% O_2 ($GM^{-PMA/PHA}$=200±25 and $GM^{+PMA/PHA}$=236±41) and 2% O_2 ($GM^{-PMA/PHA}$=206±18 and $GM^{+PMA/PHA}$=273±38) (P>0.05)]. Significant differences emerged at day-5 and thereafter [21%O_2 ($GM^{-PMA/PHA}$=206±24 and $GM^{+PMA/PHA}$=253±41) and 2% O_2 ($GM^{-PMA/PHA}$=206±29 and $GM^{+PMA/PHA}$=274±37) (p<0.05)] in both oxygen tensions (Figure 4-2C)

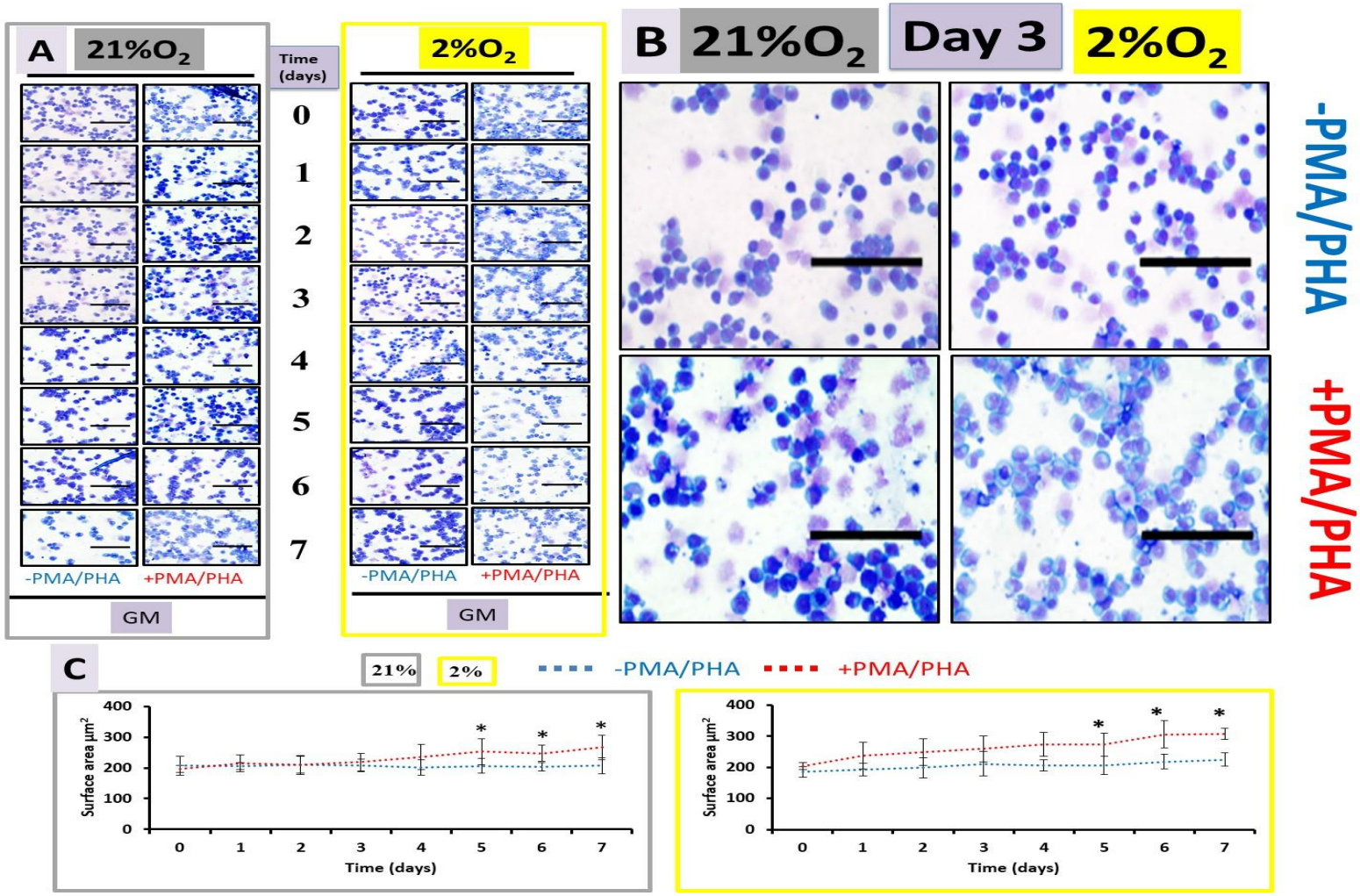
A
21%O2
Time (days)
2%O2
0
1
2
3
4
5
6
7
-PMA/PHA
+PMA/PHA
GM
B
21%O2
Day 3
2%O2
-PMA/PHA
+PMA/PHA
C
21%
2%
-PMA/PHA
+PMA/PHA
Surface area µm2
Time (days)

Figure 4-2. Jurkat activation results in an increased surface area.

A cytospin results of Jurkat T cells in $GM^{\pm PMA/PHA}$ in both normoxia (21% O_2) and hypoxia (2% O_2) environments over 7-days period. The Jurkat T cells were cultured and samples from each day were cytospinned, fixed, and stained with Giemsa-May-Grunwald's stain. (A and B) representative images for each slide at each time-point (n=3), scale bar 100µm, (C) Surface area (μm^2) of Jurkat T cells in $GM^{\pm PMA/PHA}$, data expressed as mean±SD of 3 spots for each slide for a total of 3 slides. Two-sample t-test conducted to compare the two groups, *p<0.05.

4.5.1.2 Proliferation and polarisation of Jurkat T cell in GM

We had determined that PMA/PHA activation resulted in an increase in Jurkat cell surface area. We next sought to determine if activation had an effect on either proliferation via either cell count or MTT. In the absence of PMA/PHA, cell count showed a trend of lag phase, log phase, and finally stationary phase at day-4 [21% O_2 (1750000±86602)] or day 6 [2% O_2 (1733333±57735)] (Figure 4-3A). In the presence of PMA/PHA there was a significant (p<0.05) reduction of proliferation at all time-points particularly at the start of the polarisation phase at day-2, $GM^{-PMA/PHA}$ [21% O_2 (766666± 76376)] and 2% O_2 (487777± 63098)] versus $GM^{+PMA/PHA}$ [21% O_2 (320000± 43588)] and 2% O_2 (276666± 20816)] and onward (Figure 4-3A). The growth potential was further confirmed by MTT which showed significantly lower proliferation potential in the presence of PMA/PHA as compared to the control non-treated group (Figure 4-3B). In the absence of PMA/PHA, MTT was upregulated at day-3 [21% O_2 (1.9±0.07) and 2% O_2 (2.65±0.26)] followed by a decline (p<0.05) thereafter reaching minimum at day-7 [21% O_2 (1.15±0.05) and 2% O_2 (1.55±0.1)]. Addition of PMA/PHA to the Jurkat T cells was associated with a reduction in proliferation when compared to non-treated control group, MTT day-3 [21% O_2 (1.65±0.1) and 2% O_2 (1.62±0.1)]. Moreover, polarisation of Jurkat T cells by PMA/PHA resulted in production or release of IL2 (pg/ml) over 7-days reaching a maximum at day-2 [21% O_2 (8303±707) and 2% O_2 (10134±1398) (p<0.05)] and which declined thereafter reaching a minimum at day-7 [21% O_2 (3368±429) and 2% O_2 (3892±224)] (Figure 4-3C).

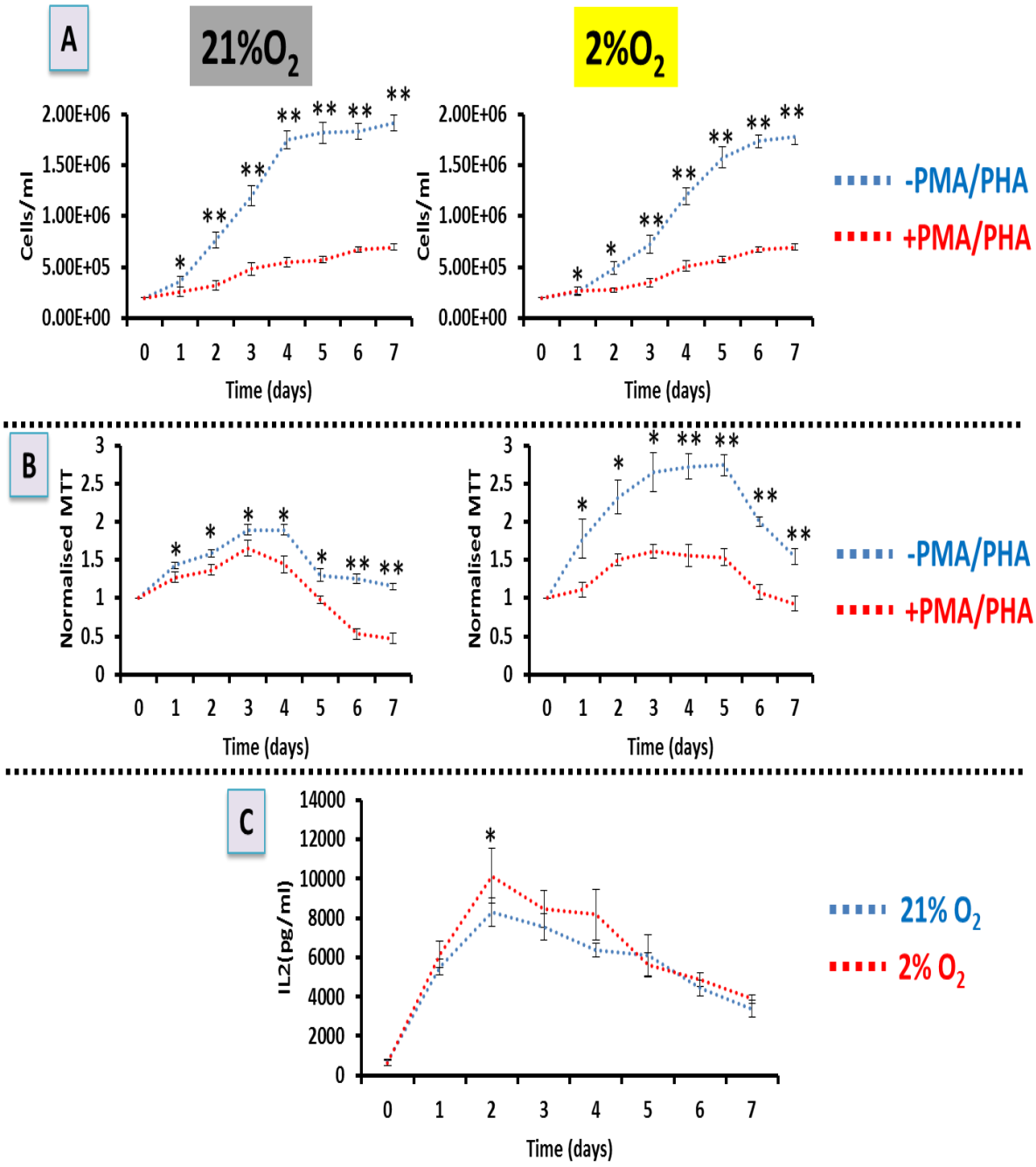

Figure 4-3. PMA/PHA stimulation results in suppression of proliferation and induction of polarisation.

The proliferation and activation of Jurkat T cells were characterised in $GM^{\pm PMA/PHA}$ in hypoxia (2% O_2) and normoxia (21% O_2) over 7-days period. The proliferation of Jurkat T cells was assessed using haemocytometer-based cell count from 3 independent flasks (n=3) (A) and confirmed by colorimetric MTT assay on the three samples using 96-wellplates (n=36) (B). The polarisation and differentiation of Jurkat T cells were confirmed by detection of IL2 concentration (C) in cell culture media from replicates of 3 independent samples (n=9) in presence of PMA/PHA in both hypoxia (2% O_2) and normoxia (21% O_2). Two-sample t-test conducted to compare different groups. Data expressed as mean±SD, *p<0.05, **p<0.001.

4.5.1.3 Gene expression of Jurkat T cell activation pathways in GM

To confirm that the Jurkat T cell was expressing T cell activation pathway genes, a semi-quantitative RTPCR was conducted on RNA isolated from Jurkat T cells cultured in $GM^{+PMA/PHA}$ in both hypoxia (2% O_2) and normoxia (21% O_2) environment. The results indicated that these genes were expressed in these different culture conditions and environments, noting that the intensity for some of these genes was modulated over a 7-day period compared to time 0 (-PMA/PHA), including IL2, IL2RA, IL2RB, IL2RG, NFATAC2, JNK, and Erk with no observable alterations occurring with either PPP3CA, Fos, Jun, NF-kB, Rela, and MAPK8, indicating that PMA/PHA could simulate the *in vivo* stimulation of T cells by pathogenic antigen (Figure 4-4).

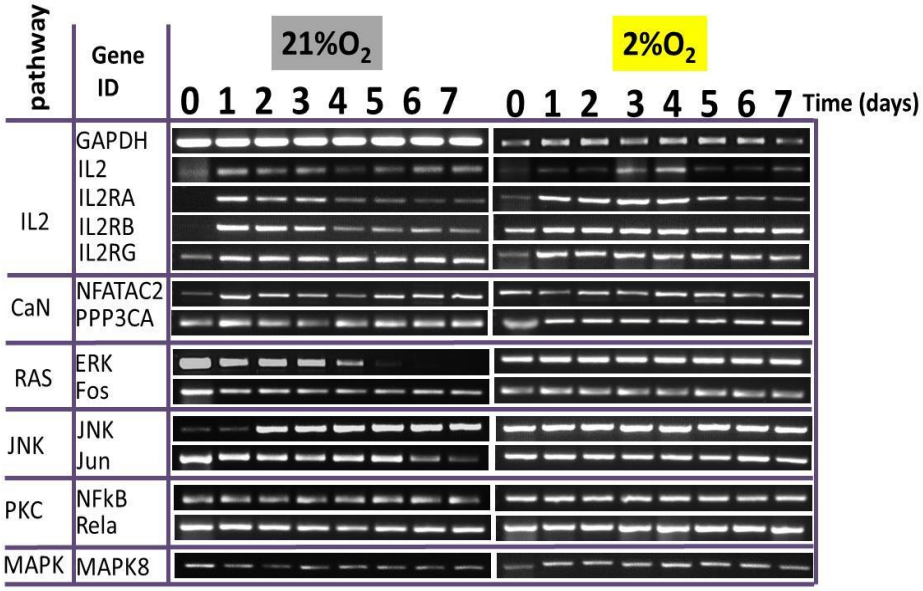

Figure 4-4. PMA/PHA modulates gene expression of Jurkat T cell line.

Semi-quantitative RTPCR for RNA from Jurkat T cells in $GM^{+PMA/PHA}$ in both normoxia (21% O_2) and hypoxia (2% O_2) environments over 7-days period. PMA/PHA induced stimulation of genes linked to Jurkat T cell activation pathways in GM in comparison to GAPDH, including Calcineurin pathway (NFATAC2/PPP3CA), JNK pathway (JNK/Jun), RAS pathway (Erk/Fos), PKC pathway (NF-kB/Rela), and MAPK pathway (MAPK8).

4.5.2 Effect of SFCM on the morphology of Jurkat T cells

The morphological assessment of Jurkat T cells following polarisation in SFNCM versus SFCM was assessed. The results indicated that the surface area (μm^2) was slightly increased with the incorporation of PMA/PHA over 7-days period in SFNCM (Fig. 4-5A). However, there was no notable differences between the polarised and non-polarised conditions at earlier time-points (0-4), day-4 [21% O_2 ($SFNCM^{-PMA/PHA}$=208±26 and $SFNCM^{+PMA/PHA}$=236±35) and 2% O_2 ($SFNCM^{-PMA/PHA}$=205±32 and $SFNCM^{+PMA/PHA}$=239±33)], whereas from day-5 onwards significance emerged [21% O_2 ($SFNCM^{-PMA/PHA}$=210±23 and $SFNCM^{+PMA/PHA}$=250±18) and 2% O_2 ($SFNCM^{-PMA/PHA}$=208±27 and $SFNCM^{+PMA/PHA}$=241±19) ($p<0.05$)] and thereafter in both oxygen tensions. These differences were minimised in SFCM showing with no significant differences between polarised versus non-polarised culture conditions at day-5 [21% O_2 ($SFCM^{-PMA/PHA}$=206±21 and $SFCM^{+PMA/PHA}$=225±14) and 2% O_2 ($SFCM^{-PMA/PHA}$=203±13 and $SFCM^{+PMA/PHA}$=218±30) ($P>0.05$)]. These results suggest that SFCM has blocked the increase in surface area associated with activation by PMA/PHA.

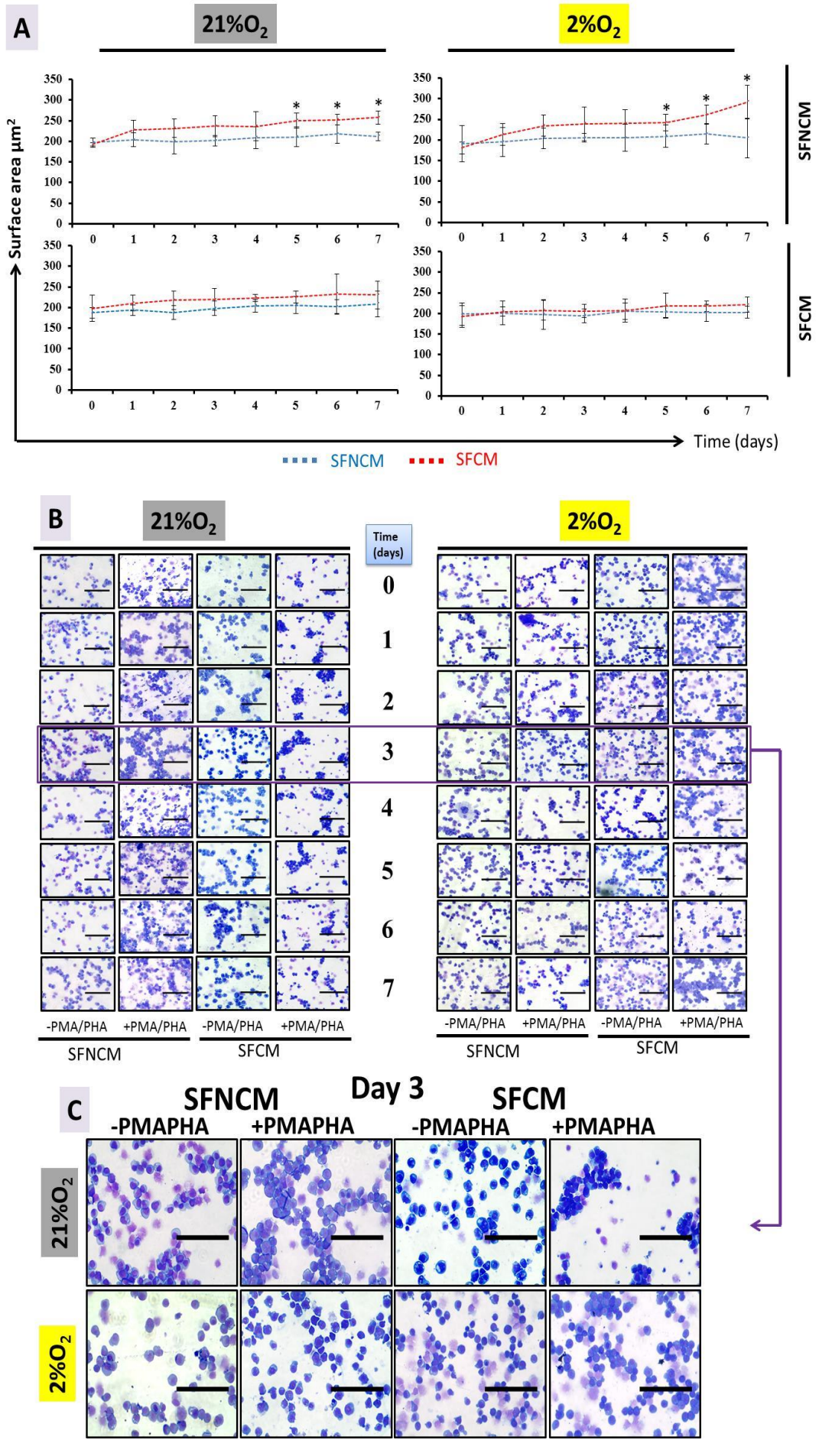
A
21%O2
2%O2
SFNCM
SFCM
Surface area µm²
Time (days)
SFNCM
SFCM
B
21%O2
2%O2
Time (days)
0
1
2
3
4
5
6
7
-PMA/PHA
+PMA/PHA
SFNCM
SFCM
C
Day 3
SFNCM
SFCM
-PMAPHA
+PMAPHA
21%O2
2%O2

Figure 4-5. SFCM protects Jurkat T cells from PMA/PHA-induced morphological changes.

Cytospin results of activated/non-activated Jurkat T cells in SFNCM versus SFCM in both normoxia (21% O_2) and hypoxia (2% O_2) over 7-days period. Jurkat T cells were cultured and samples from each day were cytospinned, fixed, and stained with Giemsa-May-Grunwald's stain. (A) Surface area (μm^2) of Jurkat T cells in SFNCM versus SFCM, data expressed as mean±SD (n=3) of 3 spots for each slide for a total of 3 slides, *$p<0.05$ (B) representative images for each slide at each time-point (C) day-3 enlarged to show clear cells with large central nucleus resulting in minute cytoplasm a characteristic feature of T cells, scale bar 200µm.

4.5.3 A role for IL10 in SFCM-induced immunosuppression

4.5.3.1 IL10 and proliferation of non-polarised Jurkat T cells

4.5.3.1.1 Growth curve suppressed by IL10

In vivo T cell stimulation via antigen presentation on the surface of APCs is associated with IL2 production and subsequent proliferation leading to the launch of the immune response. However, *in vitro* polarisation of Jurkat T cells by PMA/PHA resulted in abrogation of proliferation and production/release of IL2. In SFNCM, the growth curve followed the normal pattern of lag, log, and achieved stationary phase at day-4 (21% O_2=530000±17616 and 2% O_2=507000±30600), whereas the maximal growth curve in SFCM was significantly lower than that of SFNCM with maximum differences achieved at stationary phase in day-4 (21% O_2=243000±25166 and 2% O_2=223000±5770) (Figure 4-6A). In an attempt to identify specific biomolecule(s) responsible for this phenotype; cytokines with prominent anti-inflammatory properties were tested individually including; IL4, IL10, and IL13. The result show that these cytokines individually added at certain concentration (see section 2.8 and Figure 2-6) induced suppression of proliferation by non-polarised Jurkat T cells in SFCM-comparable manner in both normoxia (21% O_2) and hypoxia (2% O_2) environment, day-4 [(NCM/NCM^{+IL4}~2 fold), (NCM/NCM^{+IL10} >2 fold), and (NCM/NCM^{+IL13} >2 fold)] (Figure 4-6B).

To specifically identify the biomolecules responsible for suppression of proliferation in SFCM the cytokines (IL4, IL10, and IL13) were individually blocked by their specific polyclonal antibodies (see section 2.8). IL10 blockage in SFCM induced a restoration of

proliferation in both normoxia (21% O_2) and hypoxia (2% O_2) environments, day-4 (NCM/$CM^{+antiIL10}$ ~1 fold). IL4/IL13 blockage was associated with no restoration of proliferation in either (21% O_2) and hypoxia (2% O_2) environments, day-4 [(NCM/$CM^{+antiIL4}$ ~2 fold) and (NCM/$CM^{+antiIL13}$ ~2fold)], suggesting that IL10 serves as a strong anti-inflammatory in SFCM in comparison to others tested and that the presence of IL10 in SFCM is associated with suppression of proliferation regardless of presence or absence of both IL4/IL13 (Figure 4-6A and 4-10). Moreover, it has been reported that the IL4/IL13 ligands share some structural and functional properties and chemostabilise each other via their binding sites on the receptors. In the present study IL4/IL13 are blocked from SFCM with their specific polyclonal antibodies resulting in failure to reverse the suppressed proliferation induced by SFCM, day-4 (NCM/$CM^{+antiIL4+antiIL13}$ ~2 fold) (Figure 4-10). Additionally, TGFb failed to inhibit proliferation of non-polarised Jurkat T cells in SFNCM, day-4 (NCM/NCM^{+TGFb}~1 fold). These results indicate that activation of T cells model mainly linked to presence or absence of IL10 (Figure 4-11).

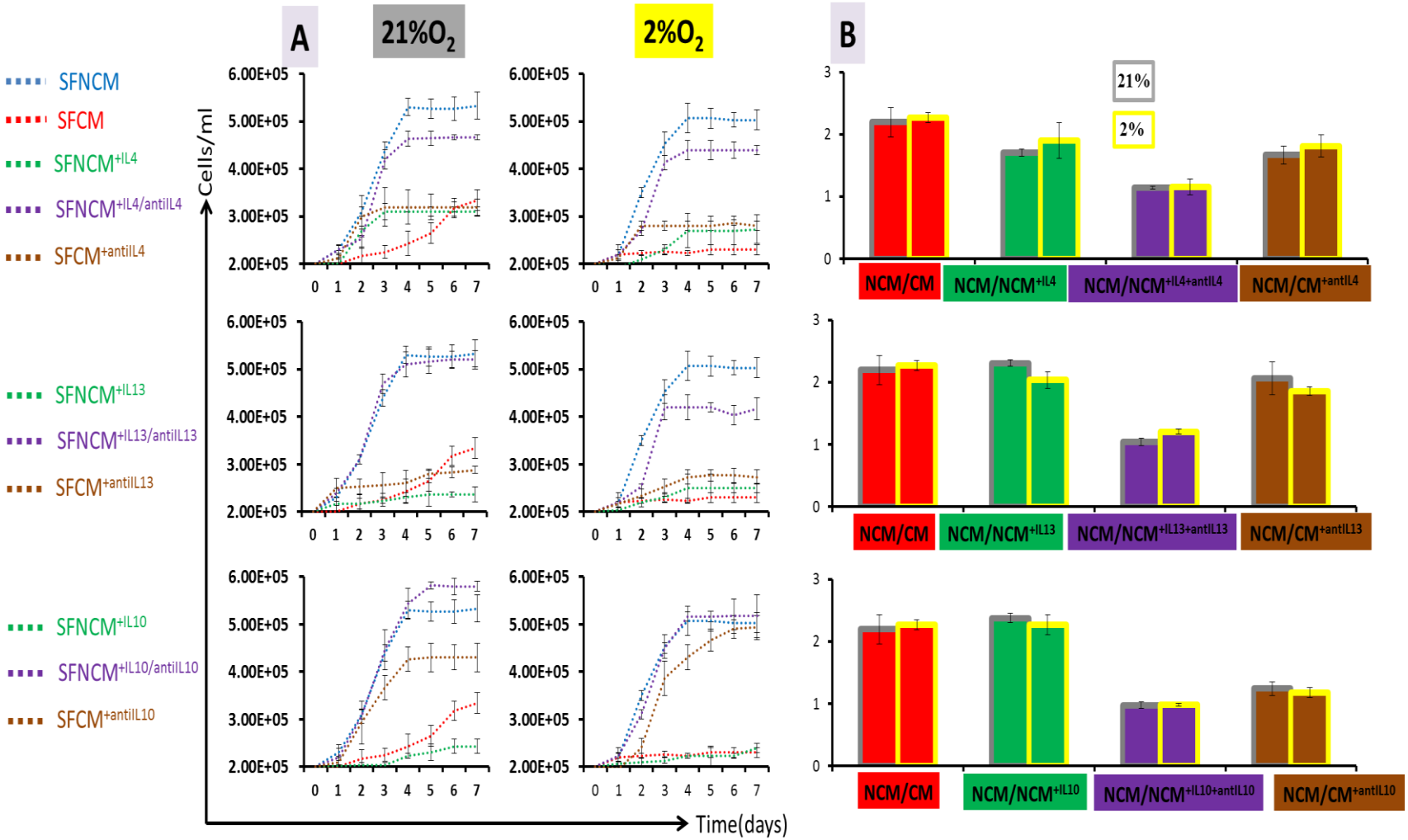
A
21%O2
2%O2
B
SFNCM
SFCM
SFNCM+IL4
SFNCM+IL4/antiIL4
SFCM+antiIL4
SFNCM+IL13
SFNCM+IL13/antiIL13
SFCM+antiIL13
SFNCM+IL10
SFNCM+IL10/antiIL10
SFCM+antiIL10
Cells/ml
Time(days)
6.00E+05
5.00E+05
4.00E+05
3.00E+05
2.00E+05
0 1 2 3 4 5 6 7
21%
2%
NCM/CM
NCM/NCM+IL4
NCM/NCM+IL4+antiIL4
NCM/CM+antiIL4
NCM/NCM+IL13
NCM/NCM+IL13+antiIL13
NCM/CM+antiIL13
NCM/NCM+IL10
NCM/NCM+IL10+antiIL10
NCM/CM+antiIL10

Figure 4-6. Proliferation of non-polarised Jurkat T cells restored in IL10-devoid SFCM based on cell count.

Growth curve of non-polarised Jurkat T cells in different conditions (SFNCM, SFCM, $SFNCM^{+Ligand}$, $SFNCM^{+Ligand/antiLigand\ AB}$, and $SFCM^{+antiLigand\ AB}$) in normoxia (21% O_2) and hypoxia (2% O_2) environments over 7-days periods. The growth curves were obtained by haemocytometer-based cell count. SFCM and $SFNCM^{+IL10}$ produce static growth curve and extend the population doubling time in comparison to exponential growth curve and reduced population doubling time in SFNCM. Conversely, neutralization of IL10 action by an excess amount of rabbit polyclonal IL10 antibodies resulted in partial restoration in growth curve and reduce the population doubling time in both SFCM or $SFNCM^{+IL10}$ compared to SFNCM. The plateau growth curve in SFNCM between days 5-7 is might be related to exhaustion in nutritional substances. Data expressed as mean±SD, each result represent a replicate of 3 independent experiments (n=3). (A) Growth curve of non-polarised Jurkat T cells (B) fold of change achieved by dividing the result in day-4-SFNCM by relevant conditions. Data expressed as mean±SD (n=3).

4.5.3.1.2 MTT suppressed by IL10

In SFNCM we noted that proliferation (MTT) increased gradually reaching a maximum at day-4 (21% O_2=1.95±0.1 and 2% O_2=1.8±0.13), whereas the proliferation in SFCM was significantly lower than that of SFNCM at all time-points, day-4 (21% O_2=1.2±0.06 and 2% O_2=1.2±0.12) (Figure 4-7A). Following on from our previous observations we sought to identify if either IL4, IL10, or IL13 played a prominent role in suppression of proliferation. This demonstrated that these cytokines (see section 2.8 and Figure 2-6) individually induced suppression of proliferation by non-polarised Jurkat T cells in a SFCM-comparable manner in both normoxia (21% O_2) and hypoxia (2% O_2) environments, day-4 [(NCM/NCM^{+IL4}~2 fold), (NCM/NCM^{+IL10}~2 fold), and (NCM/NCM^{+IL13}~2 fold)] (Figure 4-7B).

To specifically identify the biomolecule responsible for immunosuppression in SFCM, these cytokines were again individually blocked by their specific polyclonal antibodies. This demonstrated that IL10 neutralisation in SFCM induced restoration of proliferation in both normoxia (21% O_2) and hypoxia (2% O_2) environments, day-4 ($NCM/CM^{+antiIL10}$ ~1 fold). Conversely, IL4/IL13 neutralisation was associated with no restoration of proliferation in either normoxia (21% O_2) and hypoxia (2% O_2) environments, day-4 [($NCM/NCM^{+antiIL4}$~2 fold), and ($NCM/CM^{+antiIL13}$~2 fold)]. Taken together this suggests that IL10 in SFCM is associated with suppression of proliferation. This suppression occurs irrespective of IL4 and

IL13 activity (Figure 4-7 and 4-10). IL4/IL13 were blocked from SFCM with their specific polyclonal antibodies because IL4/IL13 ligands show structural similarities and receptor overlapping. This resulted in a SFCM which continued to suppress proliferation induced by SFCM, day-4 (NCM/$CM^{+antiIL4+antiIL13}$ ~2 fold) (Figure 4-10). Additionally, TGFb failed to inhibit proliferation of non-polarised Jurkat T cells in SFNCM, indicating that activation of T cells model mainly linked to presence or absence of IL10 in SFCM, day-4 [(NCM/NCM^{+TGFb} ~1 fold) (Figure 4-11).

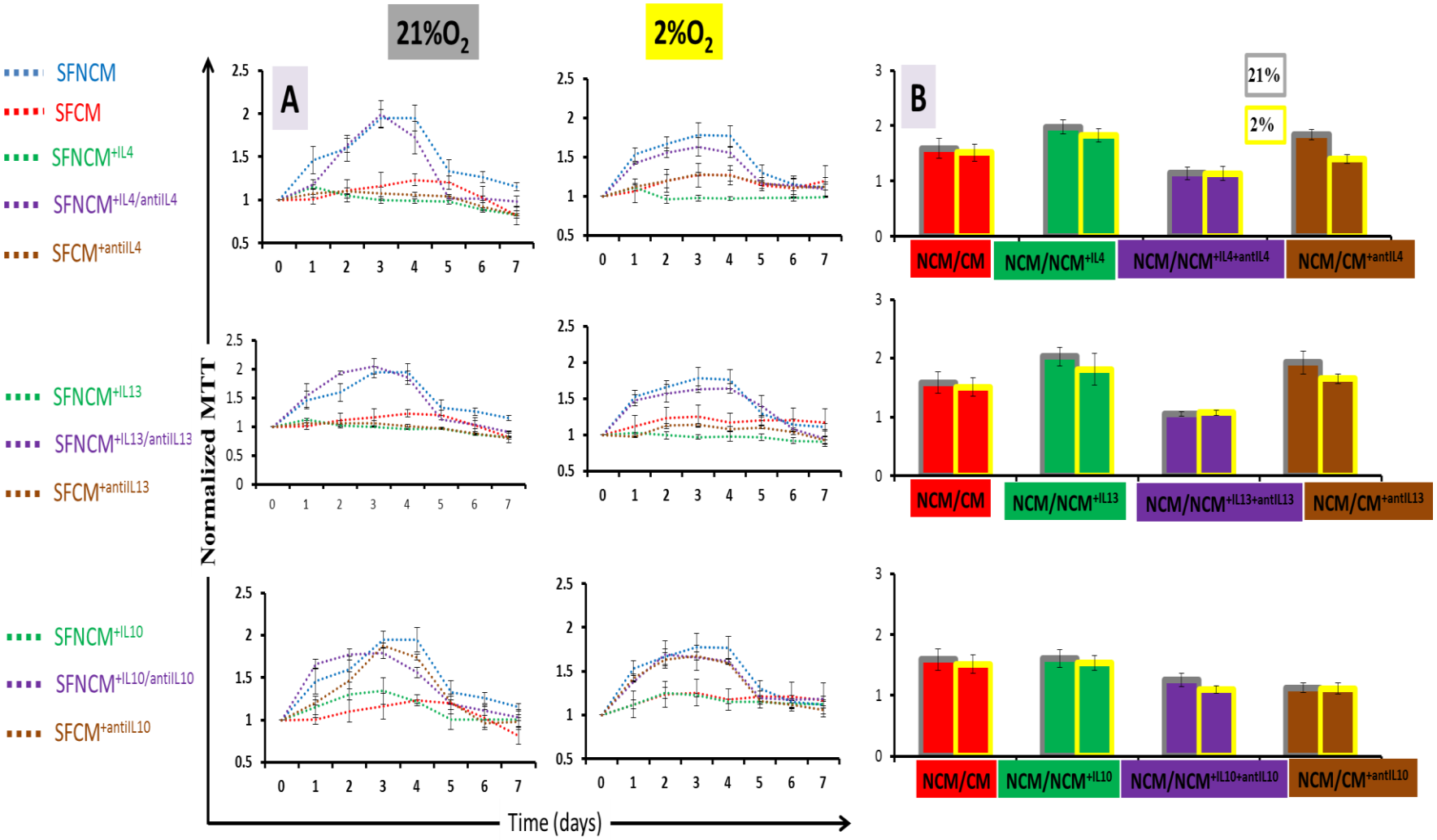
21%O2
2%O2
A
B
SFNCM
SFCM
SFNCM+IL4
SFNCM+IL4/antiIL4
SFCM+antiIL4
SFNCM+IL13
SFNCM+IL13/antiIL13
SFCM+antiIL13
SFNCM+IL10
SFNCM+IL10/antiIL10
SFCM+antiIL10
Normalized MTT
Time (days)
21%
2%
NCM/CM
NCM/NCM+IL4
NCM/NCM+IL4+antiIL4
NCM/CM+antiIL4
NCM/NCM+IL13
NCM/NCM+IL13+antiIL13
NCM/CM+antiIL13
NCM/NCM+IL10
NCM/NCM+IL10+antiIL10
NCM/CM+antiIL10

Figure 4-7. Proliferation of non-polarised Jurkat T cells restored in IL10-devoid SFCM based on MTT

Proliferation assay of non-polarised Jurkat T cells in different conditions (SFNCM, SFCM, $SFNCM^{+Ligand}$, $SFNCM^{+Ligand/antiLigand\ AB}$, and $SFCM^{+antiLigand\ AB}$) in normoxia (21% O_2) and hypoxia (2% O_2) environments over 7-days periods. The proliferation measure was obtained by conducting MTT assay at each time point followed by their subsequent normalisation to time 0. SFCM and $SFNCM^{+IL10}$ inhibited the proliferation in comparison to SFNCM. Conversely, neutralization of IL10 action by an excess amount of rabbit polyclonal IL10 antibody resulted in partial restoration in proliferation in both SFCM and $SFNCM^{+IL10}$ compared to SFNCM. The declined proliferation in SFNCM between days 5-7 is might be related to exhaustion in nutritional substances. Data expressed as mean±SD, each result represent a replicate of 3 independent experiments (n=3). (A) Normalised MTT value of non-polarised Jurkat T cells (B) fold of change achieved by dividing the result in day-4 SFNCM by relevant conditions.

4.5.3.2 IL10's role in the proliferation of polarised Jurkat T cells

4.5.3.2.1 Growth curve suppressed by IL10

We next sought to explore if IL10 had a role in the reduced proliferation rate of PMA/PHA-polarised Jurkat T cells following on from our earlier observation. To do so Jurkat T cells were seeded at density of $2x10^5$ cell/ml exposed to (50ng/ml of PMA and 1µg/ml of PHA) in both normoxia (21% O_2) and hypoxia (2% O_2) environments over 7-days period. These experimentations were performed in different culture conditions (SFNCM, SFCM, $SFNCM^{+Ligand}$, $SFNCM^{+Ligand/antiLigand\ AB}$, and $SFCM^{+antiLigand\ AB}$). The cell count revealed similar patterns of suppression of proliferation were noted in either SFCM or $SFNCM^{+Ligand}$ cells compared to SFNCM or $SFNCM^{+Ligand+antiLigand}$ with a slight restoration (~1 fold) achieved with neutralisation of either anti-inflammatory cytokines (Figure 4-8, 4-10, and 4-11).

4.5.3.2.2 MTT suppressed by IL10

MTT assay was then conducted on PMA/PHA-polarised Jurkat T cells where proliferation appeared to be reduced when compared to non-polarised Jurkat T cells. Similar patterns of suppression of proliferation were noted in both SFCM or $SFNCM^{+Ligand}$ cells compared to SFNCM or $SFNCM^{+Ligand+antiLigand}$ with no restoration (~1 fold) achieved following neutralisation of either anti-inflammatory cytokines (Figure 4-9, 4-10, and 4-11).

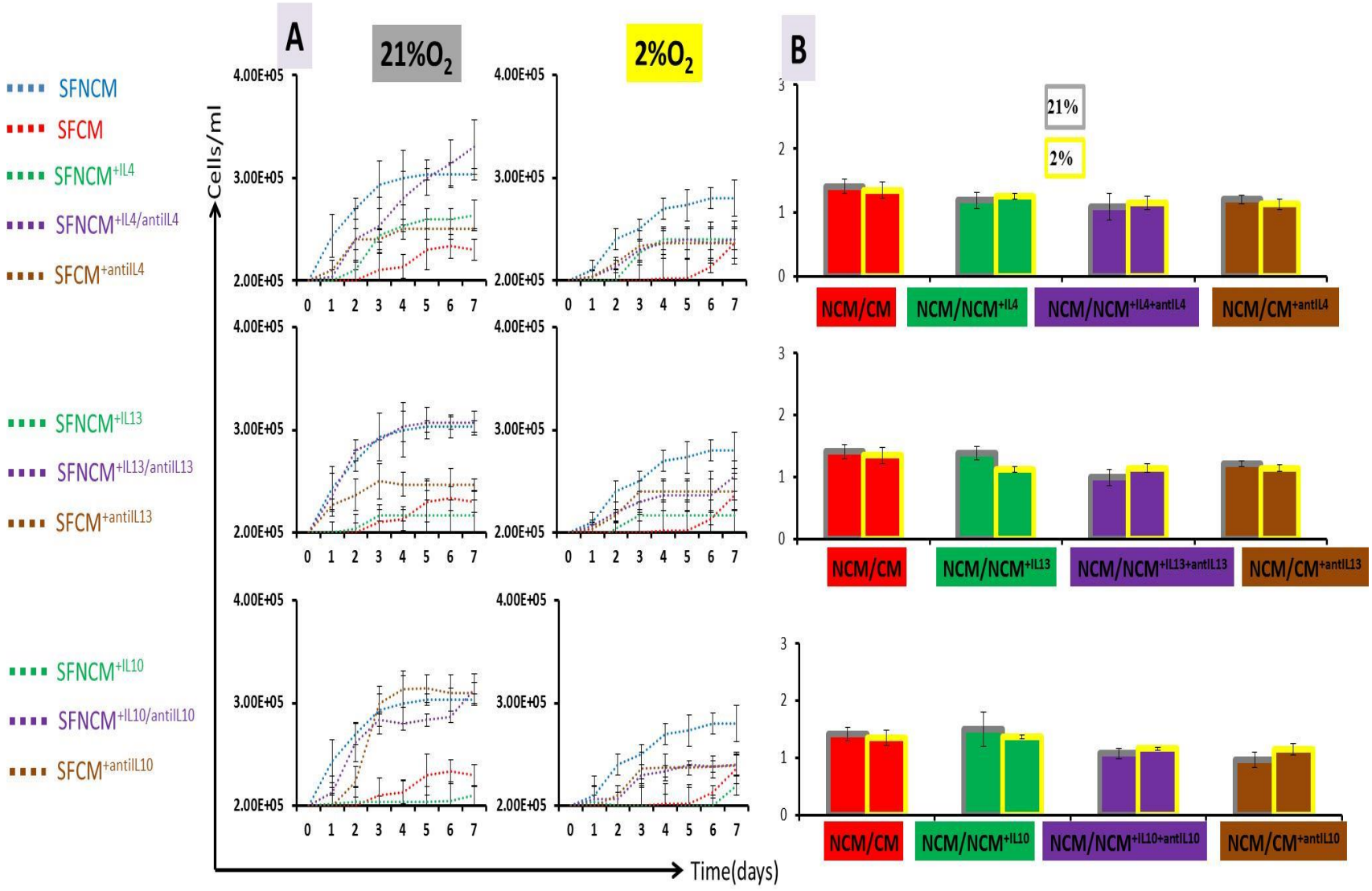
A
21%O2
2%O2
B
SFNCM
SFCM
SFNCM+IL4
SFNCM+IL4/antiIL4
SFCM+antiIL4
SFNCM+IL13
SFNCM+IL13/antiIL13
SFCM+antiIL13
SFNCM+IL10
SFNCM+IL10/antiIL10
SFCM+antiIL10
Cells/ml
Time(days)
4.00E+05
3.00E+05
2.00E+05
0 1 2 3 4 5 6 7
21%
2%
NCM/CM
NCM/NCM+IL4
NCM/NCM+IL4+antiIL4
NCM/CM+antiIL4
NCM/NCM+IL13
NCM/NCM+IL13+antiIL13
NCM/CM+antiIL13
NCM/NCM+IL10
NCM/NCM+IL10+antiIL10
NCM/CM+antiIL10

Figure 4-8. Proliferation of polarised Jurkat T cells restored in IL10-devoid SFCM based on cell count.

Growth curve of polarised Jurkat T cells in different conditions (SFNCM, SFCM, SFNCM$^{+Ligand}$, SFNCM$^{+Ligand/antiLigand\ AB}$, and SFCM$^{+antiLigand\ AB}$) in normoxia (21% O_2) and hypoxia (2% O_2) environments over 7-days periods. The growth curve was obtained by haemocytometer-based cell count. (A) Growth curve of polarised Jurkat T cells (B) fold of change achieved by dividing the result in day-4 SFNCM by relevant conditions. Data expressed as mean±SD, each result represent a replicate of 3 independent experiments (n=3).

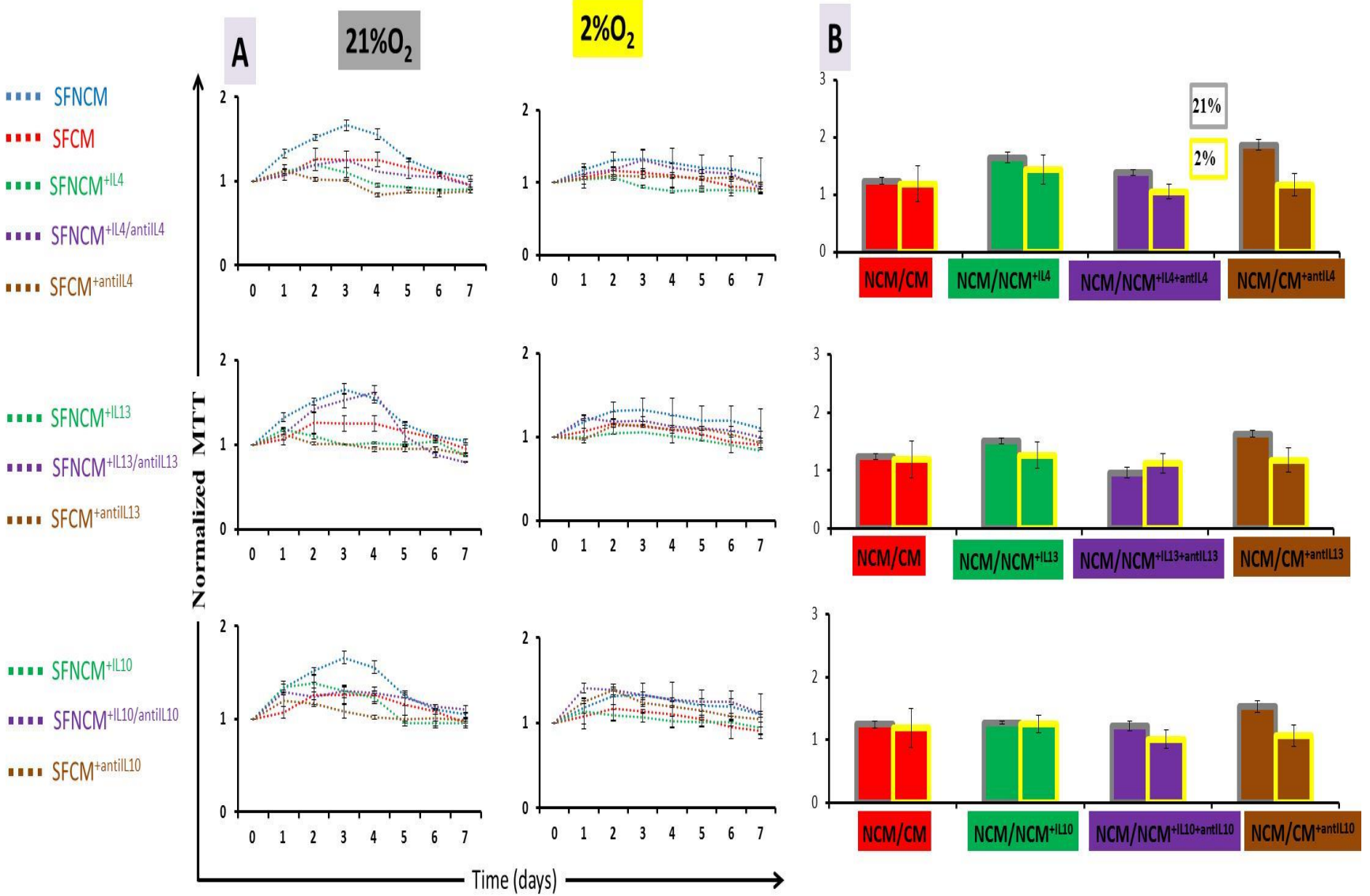
A
21%O2
2%O2
B
SFNCM
SFCM
SFNCM+IL4
SFNCM+IL4/antiIL4
SFCM+antiIL4
SFNCM+IL13
SFNCM+IL13/antiIL13
SFCM+antiIL13
SFNCM+IL10
SFNCM+IL10/antiIL10
SFCM+antiIL10
Normalized MTT
Time (days)
21%
2%
NCM/CM
NCM/NCM+IL4
NCM/NCM+IL4+antiIL4
NCM/CM+antiIL4
NCM/NCM+IL13
NCM/NCM+IL13+antiIL13
NCM/CM+antiIL13
NCM/NCM+IL10
NCM/NCM+IL10+antiIL10
NCM/CM+antiIL10

Figure 4-9. Proliferation of polarised Jurkat T cells restored in IL10-devoid SFCM based on MTT.

Proliferation assay of polarised Jurkat T cells in different conditions (SFNCM, SFCM, SFNCM$^{+Ligand}$, SFNCM$^{+Ligand/antiLigand\ AB}$, and SFCM$^{+antiLigand\ AB}$) in normoxia (21% O_2) and hypoxia (2% O_2) environments over 7-days period. The proliferation was obtained by conducting MTT assay at each time point and their subsequent normalisation to time 0. The declined proliferation in SFNCM between days 5-7 is probably related to exhaustion in nutritional substances. Data expressed as mean±SD, each result represent a replicate of 3 independent experiments (n=3). (A) Normalised MTT value of non-polarised Jurkat T cells (B) fold of change achieved by dividing the result in day-4 SFNCM by relevant conditions. Data expressed as mean±SD (n=3).

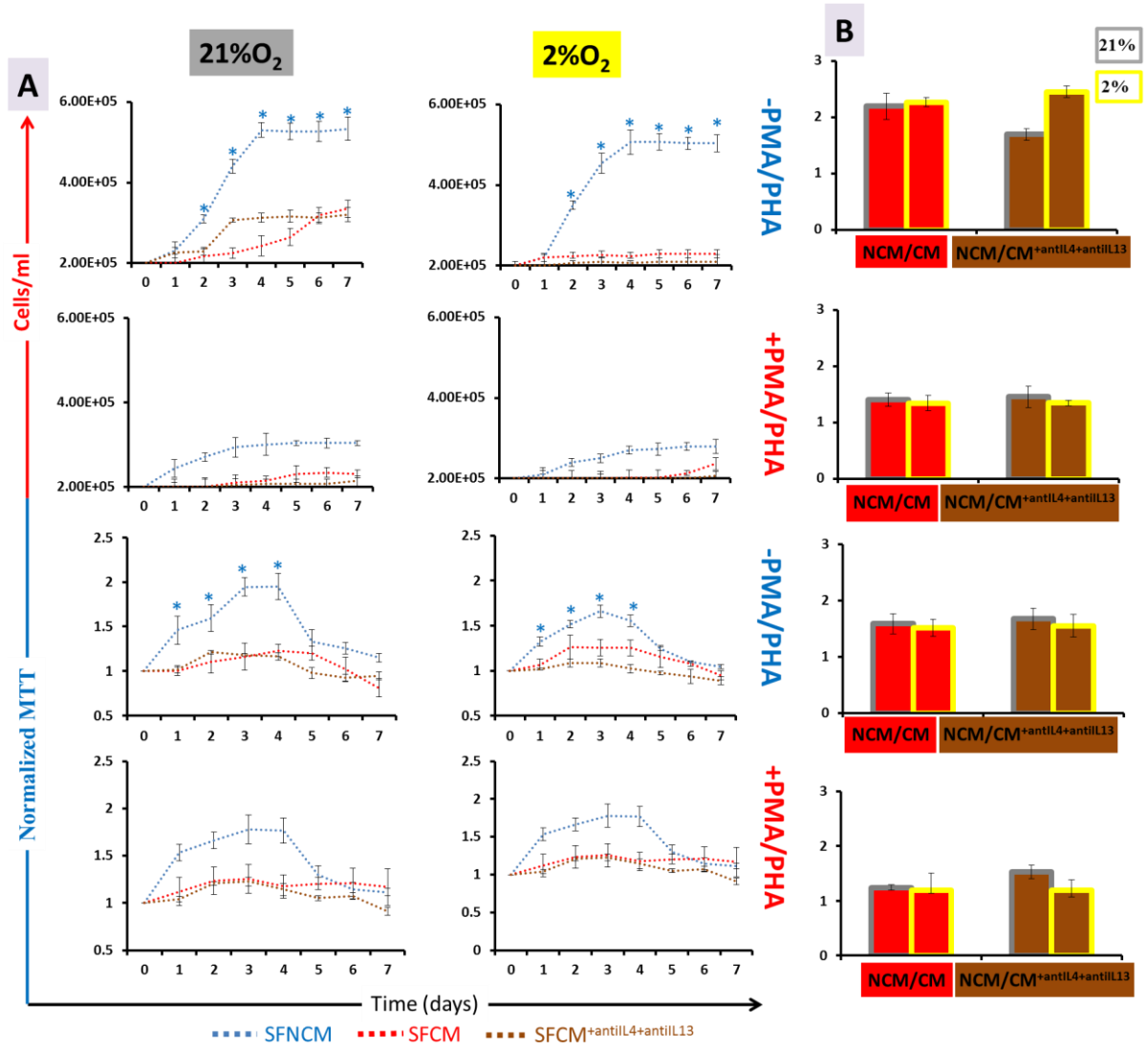

Figure 4-10. IL4/IL13-devoid SFCM failed to restore proliferation.

Proliferation assay of polarised and non-polarised Jurkat T cells in SFCM$^{\pm antiIL4 \pm antiIL13}$ compared to SFCM in normoxia (21% O_2) and hypoxia (2% O_2) environments over 7-days periods. The growth curves were obtained by haemocytometer-based cell count and the results were confirmed by MTT assay. SFCM$^{\pm antiIL4 \pm antiIL13}$ suppressed proliferation of polarised and non-polarised Jurkat T cells in both normoxia (21% O_2) and hypoxia (2% O_2). (A) proliferation assays including cell count and MTT (B) fold of change achieved by dividing the result in day-4 SFNCM by relevant conditions. Data expressed as mean±SD each result represent a replicate of 3 independent experiments (n=3). One-way ANOVA were conducted with Tukey's test to determine pairwise significant difference, *p<0.001, * colour indicates the significant difference is between the relevant culture condition compared to others.

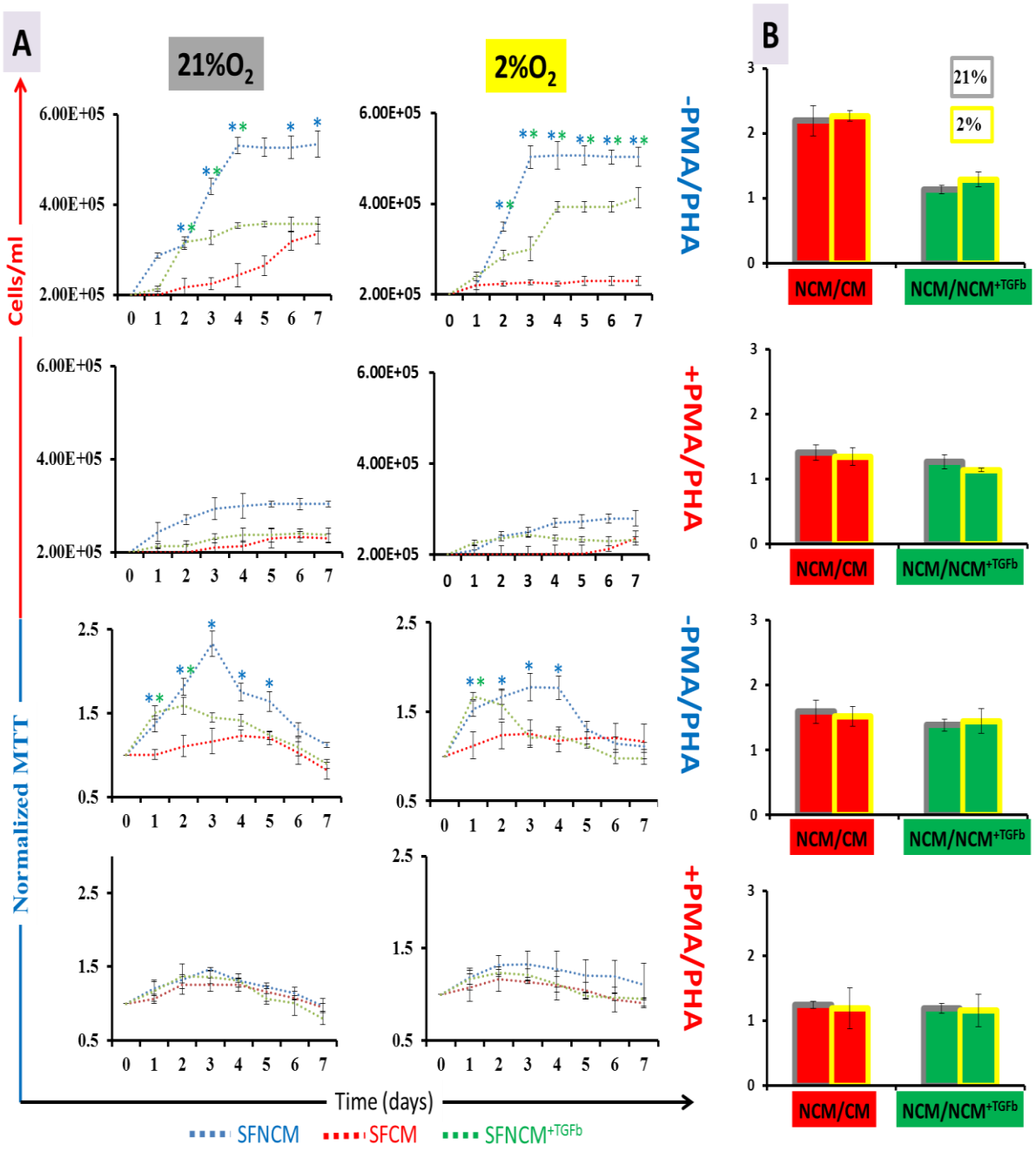

Figure 4-11. TGFb failed to suppress proliferation

Proliferation assay of polarised and non-polarised Jurkat T cells in SFNCM$^{\pm TGFb}$ compared to SFCM in normoxia (21% O_2) and hypoxia (2% O_2) environments over 7-days period. The growth curve was obtained by haemocytometer-based cell count and the results were confirmed by MTT assay. TGFb slightly suppressed proliferation of polarised and non-polarised Jurkat T cels in both normoxia (21% O_2) and hypoxia (2% O_2). (A) proliferation assays including cell count and MTT (B) fold of change achieved by dividing the result in day-4 SFNCM by relevant conditions. Data expressed as mean±SD, each result represent a replicate of 3 independent experiments (n=3). One-way ANOVA were conducted with Tukey's test to determine pairwise significant difference. *p<0.001, * colour indicates the significant difference is between the relevant culture condition compared to others.

4.5.3.3 IL10 role in polarisation of Jurkat T cells

In vivo T cell stimulation occurs following antigen presentation on the surface of the antigen presenting cells and is associated with IL2 production where subsequent proliferation leads to launching of the immune response. In contrast, *in vitro* polarisation of Jurkat T cells by PMA/PHA results in an abrogation of proliferation and production or release of IL2 (pg/ml). We had previously demonstrated that IL2 release from polarised Jurkat cells was equivalent in both normoxia (21% O_2) and hypoxia (2% O_2) and now sought to explore if SFCM impacted on its release following activation. We noted a retention of IL2 release following PMA/PHA treatment over 7-days which reached a maximum in SFNCM at day-2 [21% O_2 (5305±211) and 2% O_2 (5347±327)] and declined thereafter reaching a minimum at day-7 [21% O_2 (258±75) and 2% O_2 (145±32)]. However, SFCM suppressed IL2 secretion by polarised Jurkat T cells in comparison to SFNCM in both normoxia (21% O_2) and hypoxia (2% O_2), day-2 [21% O_2 (2461±178) and 2% O_2 (1625±159)] (Figure 4-12A).

Following on from our earlier observations surrounding IL10, IL4, and IL13 we next explored whether any or all these cytokines displayed a capacity to block IL2 release. This indicated that the cytokines when individually added at certain concentration (see section 2.8 and Figure 2-6) induced blockage of IL2 secretion by polarised T cell model in SFCM-comparable manner in both normoxia (21% O_2) and hypoxia (2% O_2) environment, day-2 [(NCM/NCM^{+IL4} >2 fold), (NCM/NCM^{+IL10}>2 fold), and (NCM/NCM^{+IL13}>2 fold)] (Figure 4-12B). In addition, neutralisation of these cytokines individually by their ligand specific polyclonal antibodies resulted in restoration of IL2 secretion in SFNCM, day-2 [(NCM^{+IL4}/$NCM^{+IL4+antiIL4}$ <2 fold), (NCM^{+IL10}/$NCM^{+IL10+antiIL10}$<2 fold), and (NCM^{+IL13}/$NCM^{+IL13+antiIL13}$<2 fold)] (Figure 4-12B). Further to this IL10 neutralisation in SFCM induced restoration of IL2 secretion, day-2 (NCM/$CM^{+antiIL10}$ <2 fold) while IL4/IL13 neutralisation was not associated with restoration of IL2 secretion, day-2 [(NCM/$CM^{+antiIL4}$ >2 fold) and (NCM/$CM^{+antiIL13}$>2 fold)]. This suggests that IL10 in SFCM is associated with suppression of IL2 secretion regardless of presence or absence of both IL4/IL13 (Figure 4-12). To address IL4/IL13 polymorphism, we simultaneously blocked IL4 and IL13 from SFCM with their specific polyclonal antibodies. This again resulted in a failure to reverse the blockage of IL2 secretion, day-2 (NCM/$CM^{antiIL4/anti13AB}$~8 fold) (Figure 4-13). Additionally, TGFb failed to inhibit IL2 secretion

by polarised Jurkat T cells in SFNCM (Figure 4-14), day-2 (NCM/NCM^{+TGFb} <2 fold), indicating that activation of T cells model mainly linked to presence or absence of IL10. These results together with the previous IL2/IL10 Jurkat gene expression confirmed that the polarisation of an immune cell line model in SFCM is mainly linked to IL10 ligands suggesting the importance of IL10 post-receptor signalling pathway.

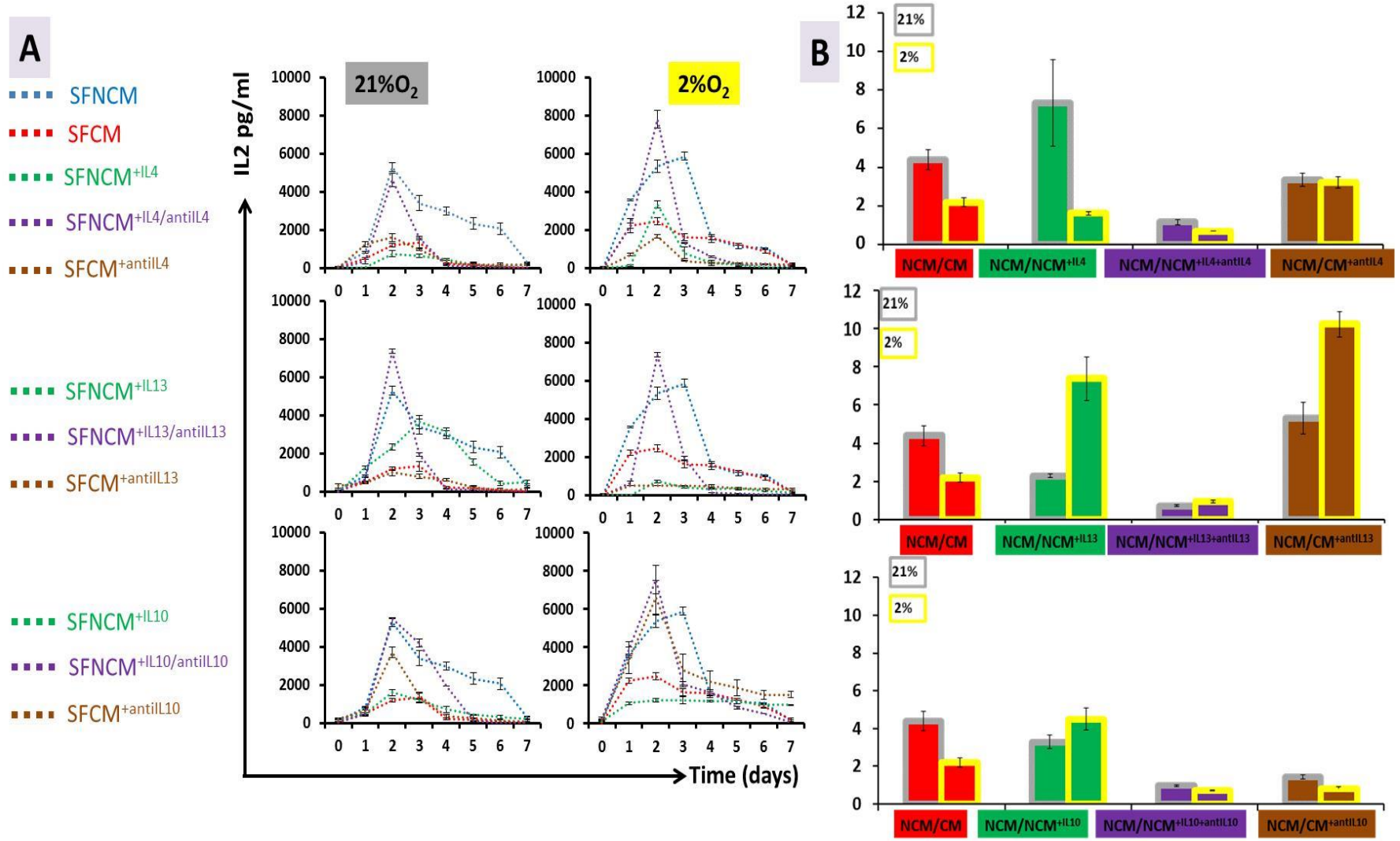
A
SFNCM
SFCM
SFNCM+IL4
SFNCM+IL4/antiIL4
SFCM+antiIL4
SFNCM+IL13
SFNCM+IL13/antiIL13
SFCM+antiIL13
SFNCM+IL10
SFNCM+IL10/antiIL10
SFCM+antiIL10
IL2 pg/ml
21%O2
2%O2
Time (days)
B
21%
2%
NCM/CM
NCM/NCM+IL4
NCM/NCM+IL4+antiIL4
NCM/CM+antiIL4
NCM/NCM+IL13
NCM/NCM+IL13+antiIL13
NCM/CM+antiIL13
NCM/NCM+IL10
NCM/NCM+IL10+antiIL10
NCM/CM+antiIL10

Figure 4-12. IL10-devoid SFCM restored IL2 secretion.

ELISA-based IL2 detection in T cell (Jurkat) culture media following *in vitro* activation. (A) IL2 assay for the media of activated Jurkat cells cultured in different conditions (SFNCM, SFCM, SFNCM$^{+Ligand}$, SFNCM$^{+Ligand/antiLigand\ AB}$, and SFCM$^{+antiLigand\ AB}$) in normoxic (21%$O_2$) and hypoxic (2%$O_2$) oxygen tension. IL2 secretion was blocked by SFCM itself and IL4, IL13, and IL10 when individually added to non-conditioned media. When these cytokines were neutralised individually in SFCM with their specific antibodies, the immune response was restored in IL10-devoided SFCM, irrespective of oxygen condition, following activation when compared to SFNCM. (A1) IL2 concentration (pg/ml) in Jurkat culture media over 7-days following activation. Data expressed as mean±SD, each result represent a replicate of 3 independent experiments (n=3). (A2) Day-2 fold of changes in IL2 concentration in SFNCM divided by the concentration in SFCM (red bar), SFNCM$^{+Ligand}$(green bar), SFNCM$^{+Ligand/antiLigand\ AB}$ (purple bar), and SFCM$^{+antiLigand\ AB}$ (brown bar)

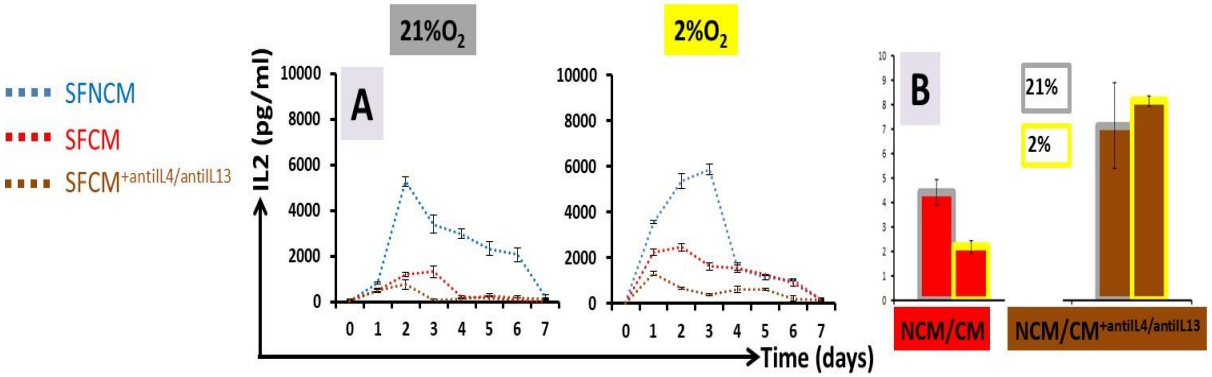

Figure 4-13. IL4/IL13-devoid SFCM failed to restore IL2 secretion.

ELISA IL2 assay for the media of activated Jurkat cells cultured in different conditions (SFNCM, SFCM, SFNCM$^{+antiIL4/antiIL13}$) in normoxic and hypoxic oxygen tension. IL2 secretion was blocked by SFCM when compared to SFNCM. To overcome IL4 receptor polymorphism and IL4/IL13 receptor overlapping, both IL4 and IL13 blocked from SFCM leading to no restoration of IL2 secretion from Jurkat cells. (A) IL2 concentration (pg/ml) in Jurkat culture media over 7-days following activation. Data expressed as mean±SD, each result represent a replicate of 3 independent experiments (n=3). (B) Day-2 fold of changes in IL2 concentration in SFNCM divided by the concentration in SFCM (red bar), SFNCM$^{+antiIL4/antiIL13}$ (brown bar).

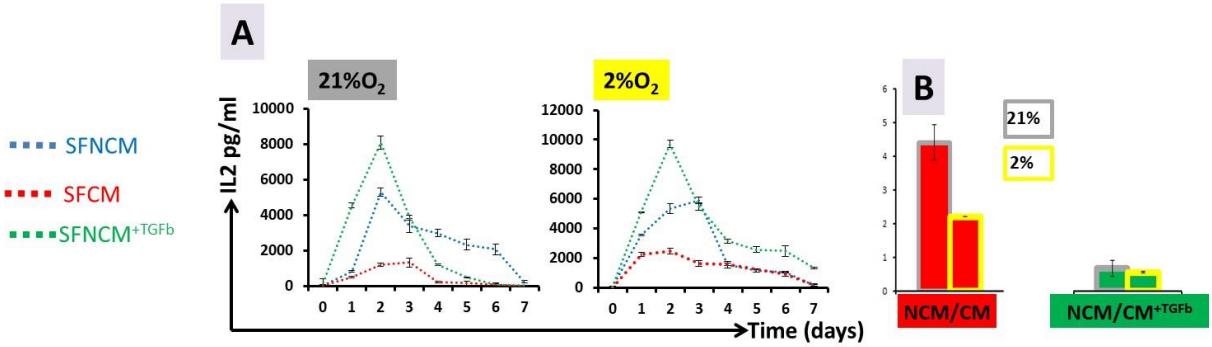

Figure 4-14. TGFb failed to suppress IL2 secretion.

ELISA IL2 assay for the media of activated Jurkat cells cultured in different conditions (SFNCM, SFCM, SFNCM^{+TGFb}) in normoxic and hypoxic oxygen tension over 7-days period. IL2 secretion was blocked by SFCM, while TGFb potentiated IL2 secretion in SFNCM, irrespective of oxygen condition, following activation when compared to SFNCM. (A) IL2 concentration (pg/ml) in Jurkat culture media collected from replicates of 3 independent samples (n=9) over 7-days following activation. (B) Day-2 fold of changes in IL2 concentration in SFNCM divided by the concentration in SFCM (red bar), SFNCM^{+TGFb} (green bar).

4.5.4 SFCM modulated the gene transcription of Jurkat T cell activation pathway

4.5.4.1 IL2-linked genes

To confirm that Jurkat T cell is expressing IL2, IL2-receptor subunit genes, and IL10-receptor subunit genes, a semi-quantitative RTPCR was conducted on RNA isolated from Jurkat T cells cultured in SFCM$^{\pm PMA/PHA}$ and SFNCM$^{\pm PMA/PHA}$ in both normoxia (21% O_2) and hypoxia (2% O_2) environment. The results showed that these genes were expressed in these different culture conditions and environments, these data suggest that Jurkat T cells simulate the T cells in term of IL2 and IL2 receptor subunits expression and that IL10 receptor expression was found in Jurkat T cells (Figure 4-15).

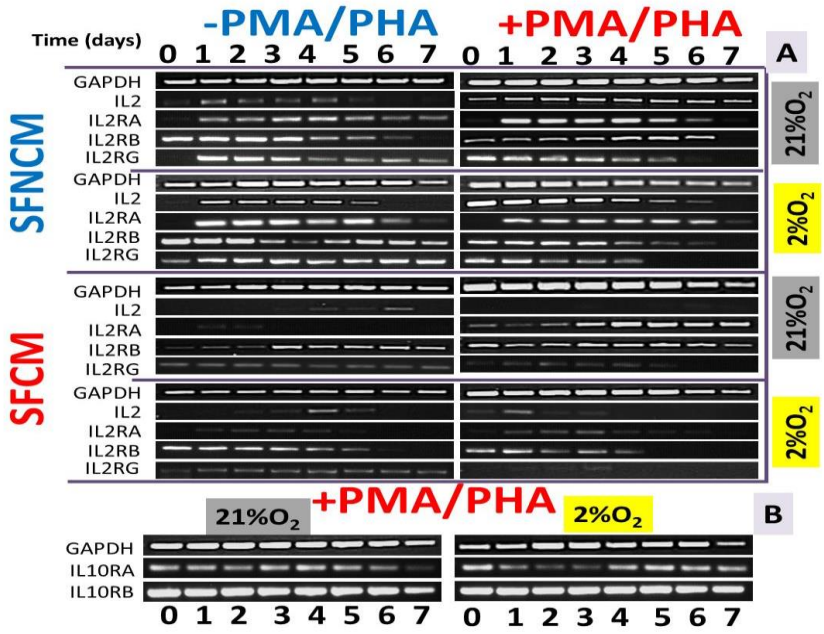

Figure 4-15. SFCM modulates IL2 and IL2 receptor linked genes.

Semi-quantitative RTPCR for activated Jurkat cells showing IL2, $IL2^{receptor}$ and $IL10^{receptor}$ genes. (A) RTPCR for RNA from Jurkat T cells in $SFNCM^{\pm PMA/PHA}$ versus $SFCM^{\pm PMA/PHA}$ in normoxia (21% O_2) and hypoxia (2% O_2) oxygen tension resulting in downregulation of IL2 and $IL2^{receptor}$ subunits gene in SFCM versus SFNCM in comparison to GAPDH (B) RTPCR for $IL10^{receptor}$ (subunit A and B) confirming that IL10 receptor subunits expressed by Jurkat cells in both normoxia (21% O_2) and hypoxia (2% O_2) in post-activation phase.

4.5.4.2 T cell signalling pathway

The T cell activation involves signalling through different T cell pathways resulting in upregulation of certain genes including calcineurin pathway (e.g. NFATAC2/PPP3CA), JNK pathway (e.g. JNK/Jun), RAS pathway (e.g. Erk/Fos), PKC pathway (e.g. NF-kB/Rela), and MAPK pathway (e.g. MAPK8). Induction of these pathways is associated with synthesis and release of IL2 by T cells. Jurkat T cells were stimulated with PMA/PHA resulting in modulation of these pathways and IL2 release. Individual genes were selected from each pathway and a semi-quantitative RTPCR conducted on these genes using primers customised in NCBI. The results showed that SFCM downregulated some of these genes in comparison to polarised Jurkat T cells cultured in SFNCM. In calcineurin pathway, hypoxia (2% O_2) collected Jurkat RNA cultured in SFCM produced faint bands of NFATAC2 and PPP3CA genes in comparison to normoxia (21% O_2) collected SFCM and SFNCM. Similarly, SFCM cultured Jurkat displayed reduced expression of Jun with little effect on JNK gene. In

line with that, the RAS pathway is suppressed by SFCM indicated by suppressed bands of Erk and Fos with hypoxia (2% O_2) collected SFCM induce stronger suppression in comparison to normoxia (21% O_2) collected SFCM. Comparably, PKC pathway was affected indicated by NF-kB/Rela bands suppression in SFCM versus SFNCM. Despite that MAPK8 is upregulated by polarisation induced by PMA/PHA, SFCM showed an only weak effect on MAPK8 band suppression, however, MAPK8 band suppression was achieved in non-polarised T cells cultured in SFCM versus SFNCM (Figure 4-16).

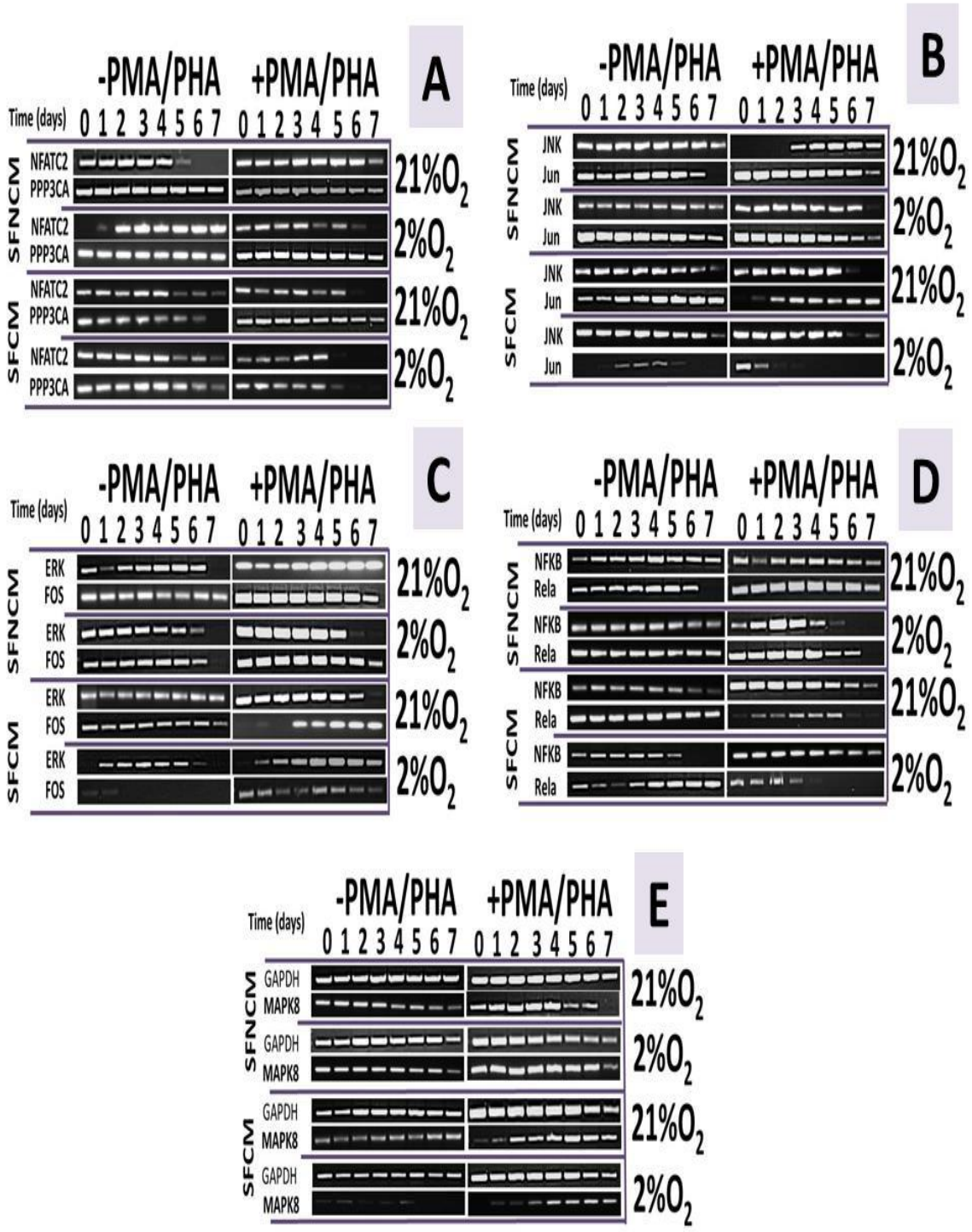

Figure 4-16. SFCM modulates the gene expression of T cell pathway.

Semi-quantitative RTPCR for RNA from Jurkat T cells in SFNCM$^{\pm PMA/PHA}$ versus SFCM$^{\pm PMA/PHA}$ in normoxic and hypoxic oxygen tension over 7-days period, resulting in downregulation of genes linked to Jurkat T cell activation pathways in SFCM versus SFNCM in comparison to GAPDH. (A) Calcineurin pathway (NFATAC2/PPP3CA). (B) JNK pathway (JNK/Jun). (C) RAS pathway (Erk/Fos). (D) PKC pathway (NF-kB/Rela). (E) MAPK pathway (MAPK8).

4.6 Discussion

The application of hMSCs in clinical settings is an attractive prospect due to their characteristic proliferation and incorporation properties[4,3]. Most of these clinical trials are applied to the immune-mediated diseases including Crohn's disease, diabetes mellitus, GvHD, hepatitis, and rheumatoid arthritis[177]. However, their first pass pulmonary engraftment potential makes the mode of action questionable[41,216]. Recent *in vitro* and *in vivo* studies have confirmed that the regenerative mode of action of hMSCs is partially linked to the release of trophic factors rather than their functional incorporation [148,149,153,155]. However, the released trophic factors are a mixture of different biomolecules with various functions, including pro-inflammatory, anti-inflammatory and pleiotropic cytokines, chemokines, growth factors, and angiogenic factors[157,158,159]. The concentration of these cytokine varies depending on the source of hMSCs, their isolation and culture protocol[159,16,160]; some of which is reflective of their *de novo* synthesis while others are present in sufficient quantities suggesting that the mode of action could be linked to a candidate molecule(s). The present report describes the mode of action of hMSCs secretome by testing the efficacy of SFCM itself and IL4, IL10, IL13, and TGFb anti-inflammatory cytokines on Jurkat T cell line.

In the present study, oxygen is an important factor for culture and experimentation for both hMSCs and *in vitro* immune response model. Hypoxia is a characteristic feature of hMSCs niches, which are under continuous gradient oxygen exposure depending on localised tissue microenvironment, such as, bone marrow (1-6% O_2), adipose tissue (2-8% O_2), and neural tissues (1-8% O_2)[32]. The oxygen tension is higher in most endogenous tissues compartments (4-14% O_2) but still less than that of ambient oxygen tension (~21% O_2)[31]. Additionally, the inflammation zone is under a pathological hypoxia due to activation of the coagulation cascade and subsequently, the activation of immune cells ensue under this pathological hypoxia environemnt[36]. In this study SFCM were generated and collected in a 21% O_2 and 2% O_2 environment to simulate the *in vivo* bone marrow environment and the created *in vitro* immune response model. Various *in vitro* and *in vivo* studies have reported the importance of 2% O_2 collected SFCM in comparison to air oxygen SFCM[60,152]. These studies have revealed that recreation of *in vivo* environment in the culture and

application of collected SFCM from 2% O_2 stimulate the *in vitro* healing of injury model and promotes *in vivo* tissue regeneration. In the present study, MSCs were isolated and continuously sub-cultured in both normoxia (21% O_2) and hypoxia (2% O_2) conditions, the conditioned media generated were transferred to comparable oxygen tension of the T cell line model.

T cell responses to stimuli are associated with modulation in different cell aspects, including morphology, polarisation, gene expression, and proliferation. Following their engagement in the immunological synapse, T cell morphology change is mediated by an increase in cytoplasmic calcium concentration with subsequent modulation of calcium signalling pathways, these changes have been reported in the *in vitro* model of both activated T cell and Jurkat cells[217]. The polarisation of engaged T cell is associated with activation of post-receptor translation pathways leading to translocation of activated latent protein into the nucleus with subsequent DNA transcription of proinflammatory cytokine genes, including IL2[215] (Figure 4-17). These pro-inflammatory cytokines promote T cell proliferation and determine their differentiation fate. In this study, Jurkat T cell was used as T cell model of the immune response using PMA/PHA as activation tools. *In vitro* exposure of Jurkat T cells to PMA/PHA result in activation of the cells indicated by IL2 secretion, gene expression, abrogation of proliferation, and increase in their surface area. It has been reported that cell line exposure to mitogenic stimuli results in their differentiation and suppression of their proliferation[197]. Jurkat T cells showed normal proliferation in growth media, the proliferation curve pass through lag, log and stationary phase in non-stimulated GM while with their activation the exponential log phase disappeared, and the cells reach plateau directly after the lag phase showing no log and stationary phase. RTPCR gene expression following activation of Jurkat T cells by PMA/PHA in GM confirmed that PMA/PHA induced modulation in several genetic pathways including IL2, IL2RA, IL2RB, IL2RG, NFATAC2, JNK, and Erk with no changes happened with PPP3CA, Fos, Jun, NF-kB, Rela, and MAPK8, indicating that PMA/PHA could simulate the *in vivo* stimulation of T cells by pathogenic antigen[213].

It has been reported that the immunosuppressive activity of MSCs is mainly mediated through soluble factors. There is a controversy about the signalling biomolecules responsible for immunosuppression making the exact mechanism of action questionable[218,14]. Cell-cell contact is not the fundamental requirement for immune response suppression and secretion of soluble factors is the requirement to achieve the immunosuppression[14]. However, the secretome profile is a mixture of complex protein-based bioactive factors, including stem cell factor (SCF), IL6, IL8, IL10, IL12, IFNγ, PGE2 (prostaglandin E2), vascular endothelial growth factor (VEGF), macrophage colony-stimulating factor (M-CSF), hepatocyte growth factor (HGF) and transforming growth factor -b1 (TGFb1)[16,156,219,158].

Di Nicola et al. confirmed that in the *in vitro* immunosuppressive activity of MSCs could be reverted through blocking the effects of both TGFb and HGF[80]. However, neutralisation of either TGFb or HGF individually results in minimal restoration of the immune response, while their combinations (TGFb/HGF) achieve a comparable immunosuppression to MSCs[220]. Failure to achieve immunosuppression with TGFb alone has been reported by different *in vitro* studies[23,221,90]. A study done by Mori et al. concluded that TGFb mediates its action synergistically with HGF through JNK-dependent Smad2/3 phosphorylation at their promotor regions[222]. In the present study, TGFb was used to induce immunosuppression, the result confirmed that TGFb have no role in SFCM-mediated immunosuppression; Jurkat T cells proliferate in $SFNCM^{+TGFb}$ and produced IL2 during activation with PMA/PHA when compared with SFCM confirming that TGFb alone have no immunosuppressive properties. However, cyclosporine A, a potent immunosuppressive agent, show elevated level of intracellular TGFb with upregulation of its receptor suggesting that its mechanism of action is mainly linked to TGFb[223]. These discrepant studies indicate that there is a relationship between the mode of action of TGFb and HGF and explain the failure to respond to TGFb added to SFNCM in the present study.

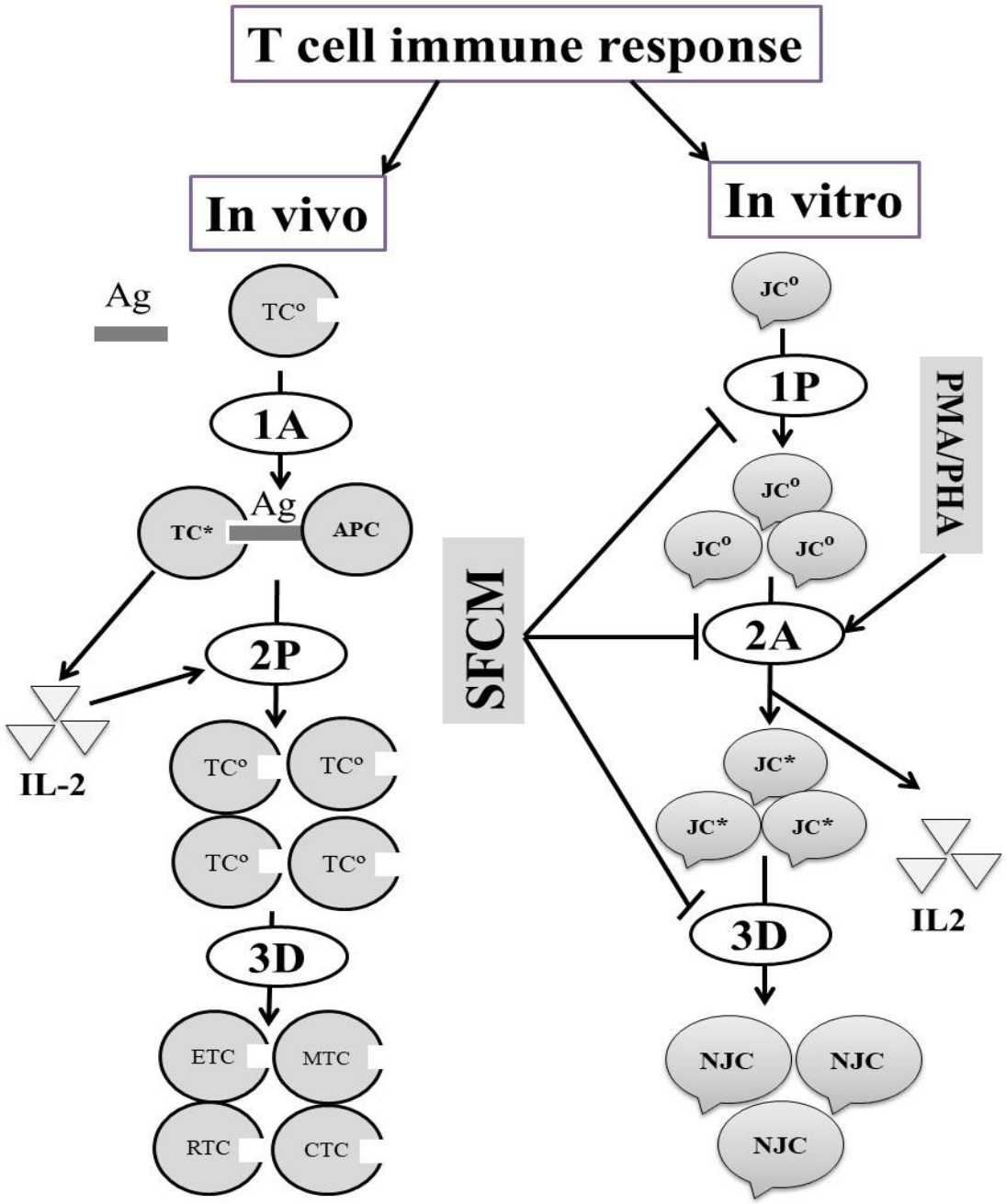

Figure 4-17. Schematic diagram simplifying the stages of T cell activation *in vivo* (left diagram) and *in vitro* (right diagram).

The *in vivo* stages start with resting T cell which upon antigenic (Ag) stimulation undergo activation (A) indicated by IL2 secretion and clonal expansion (P) with subsequent differentiation (D) while *in vitro*, the T cell line (Jurkat cells) are already proliferating in culture media while exposure to PMA/PHA leads to their activation and abrogation of proliferation associated with IL2 secretion and differentiation, the *in vitro* model were tested for the action of SFCM on both proliferation and polarisation. JC (Jurkat cells), NJC (non-Jurkat cells), PMA (Phorbol Myristate Acetate), PHA (Phytohaemaglutinin), CTC (cytotoxic T cells), RTC (regulatory T cells), ET (effector T cells), MTC (memory T cells), APC (antigen-presenting cells), TC (T cells), *stimulated cell, ° Naïve cell.

Naïve T cells proliferation carried out by IL2 and CD25 (IL2 receptor alpha subunit (IL2Ra)), while their maturation is under control of different cytokines, including IL2, IL12, and IFNγ which promote Th1 differentiation and IL4, IL5, IL9, IL10, and IL13 which promote Th2 differentiation[171]. Hence, IL4 and IL13 are part of the differentiation mechanism of the T cells, these two cytokines have 25% structural similarities, and they are characterised by receptor overlapping phenomena via sharing same receptor subunit (IL4Rα) for their signal transduction, therefore, IL13 could induce many functional properties of IL4[170,171]. The signal started with the engagement of the ligand to a second receptor subunit either γC or IL13Rα1 subunit. Despite structural similarities, the engagement of the γC subunit is limited only to IL4; but not IL13, while IL13Rα1 could interact with both IL4 and IL13 to form immunological complexes. An additional IL13Rα2 subunit exists known as a "decoy receptor" and stimulation of which is associated with no response because this subunit lacks the transmembrane signalling domain[171]. The difference between IL4 and IL13 is the sequence of engagement to these receptor subunits; IL4 interacts with IL4Rα followed by interaction with IL13Rα1, an effect which is reversed in case of IL13 ligand[171,170]. In the present study, the immunosuppression achieved by either IL4 or IL13, when individually tested on Jurkat T cells, confirmed by suppression of proliferation and reduction of IL2 production. However, neutralisation of IL4/IL13 individually or together induced no restoration in the immunosuppressive activity of SFCM, suggesting that alternative pathways could be responsible for the immunomodulation achieved by SFCM. Dupilumab, human monoclonal antibody, is a new therapeutic approach for the treatment of asthmatic patients and its mechanism based on the targeting both IL4 and IL13; the mechanism of this antibody is based on the inhibition of IL4/IL13 engagement with the α subunit of IL4 receptor[224]. Despite successful immunosuppression achieved by dupilumab and failure to achieve immune response restoration following IL4/IL13 neutralisation in SFCM, their participation in immunosuppression is not negligible indicated by suppression of proliferation and revoked IL2 secretion by Jurkat T cells. The reasonable explanation for this phenomenon is the cytokine cross-reactivity and receptor affinity (Figure 4-18), taking into consideration that SFCM is a mixture of different cytokines and most cytokines which are present in SFCM, such as, IL2, IL4, IL7, IL9, IL15, and IL21 show IL4 receptor sharing[170].

The response of Jurkat T cells to IL4 and IL13 varies in an oxygen-dependent manner. The suppression of immune response indicated by the reduction in IL2 secretion is more potent in normoxia (21% O_2) than that in hypoxia (2% O_2), indicating that hypoxia (2% O_2) diminishes the IL4 efficacy. Conversely, hypoxia (2% O_2) potentiates the efficacy of IL13 on the suppression of IL2 in comparison to normoxia (21% O_2) environment. However, the effect of IL4 and IL13 on Jurkat T cells proliferation is completely different from that of polarisation indicated by the higher potency of IL4 in the reduction of proliferation in hypoxia (2% O_2) compared to normoxia (21% O_2). Despite that, the neutralisation of IL4/IL13 from SFCM by specific polyclonal antibodies reduced the proliferation slightly better in normoxia (21% O_2) compared to hypoxia (2% O_2). These data indicate that *in vivo* translation of either SFCM or these bioactive factors individually might be associated with different response to *in vitro* results which could be related to hypoxia (2% O_2) itself because hypoxia (2% O_2) induces HIF-1a pathway while normoxia (21% O_2) blocks HIF-1a pathway and participate in the modulation of immune response[213]. HIF-1a induction promotes the generation of Tregs and directs the immune response toward suppression, indicating that the differences achieved in this study between normoxia (21% O_2) and hypoxia (2% O_2) response to the tested cytokines are mainly linked to HIF-1a pathway.

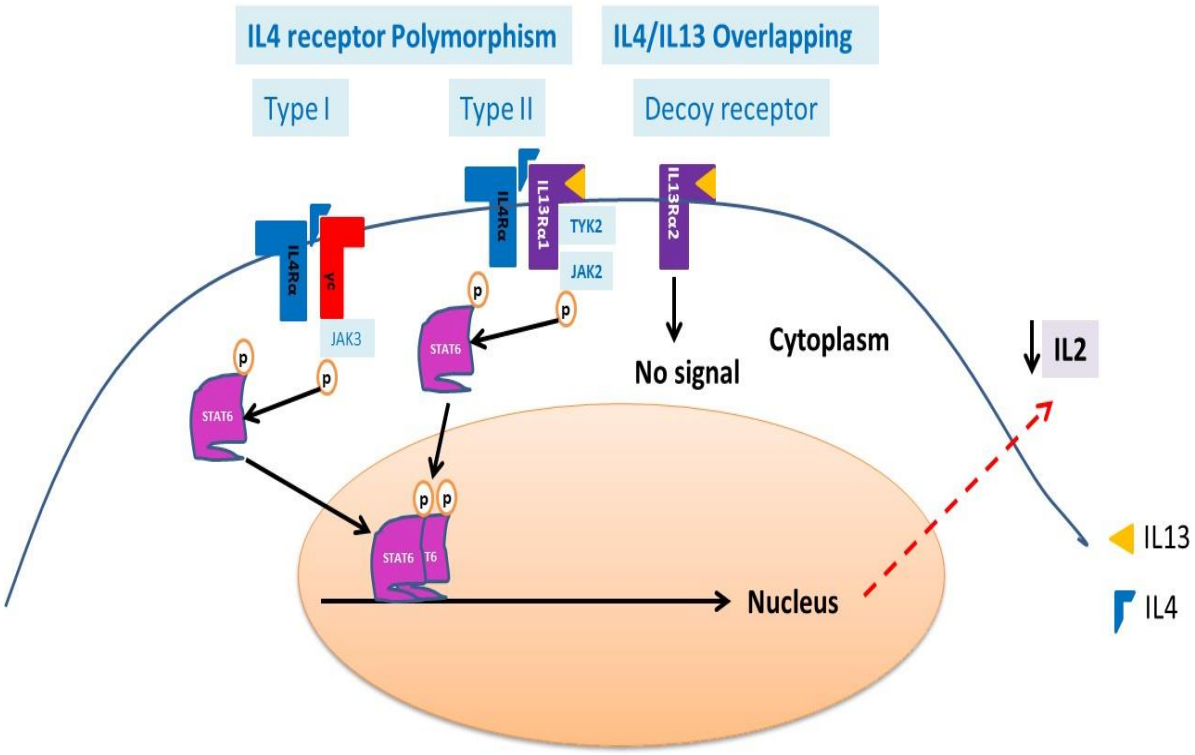

Figure 4-18. Schematic diagram of the IL4 and IL13 signal transduction pathways.

IL4 binds to the IL4 receptor a subunit that is a component of both the type I (IL4 receptor α and γc) and type II receptors (IL4 receptor α and IL13 receptor α1), whereas IL13 is recognised by the IL13 receptor α1 of the type II receptor. IL13 also binds to the IL13 receptor α2 chain with greater affinity than to IL13α1. IL13 receptor α2 lacks a transmembrane-signalling domain and consequently functions as a decoy receptor to downregulate IL13 signalling. γc activates Janus kinase (JAK) 3 and IL13 receptor α1 activates tyrosine kinase 2 (TYK2) and JAK2. Activated JAKs phosphorylate STAT6 which, upon dimerization, translocates to the nucleus where it binds to the promoters of the IL4 and IL13 responsive genes associated IL2 Jurkat cell activation via PMA/PHA stimuli.

IL4/IL13 share the same post-receptor latent proteins and translation pathway (STAT6), and the translocation of this second messenger protein to the nucleus results in transcription of anti-inflammatory genes[171,170]; moreover, pharmacological targeting of either cytokine alone achieved limited therapeutic activity in comparison to combined therapy[171]. However, IL10 mediates its immunosuppressive activity through a distinct (STAT3) post-receptor translation pathway[168]. Various reports have mentioned that IL10 have the unique capacity to block the synthesis of proinflammatory cytokines, including TNFa, IFNγ, IL1B, and IL6[168,194]. Moreover, the fact that IL10 post-receptor translation pathways involve induction of more than one post-receptor translation pathways including STAT1, STAT3, and STAT5. STAT1 and STAT5 are not involved directly in IL10 receptor stimulation, however, their knockout is associated with modulation of the cellular response to IL10[194]. These controversial results are conflicting, and clarification required further documentation of the immunosuppression activity of SFCM through IL10 receptor blocking or JAK1 knockout rather than simple polyclonal antibody neutralisation (Figure 4-19)

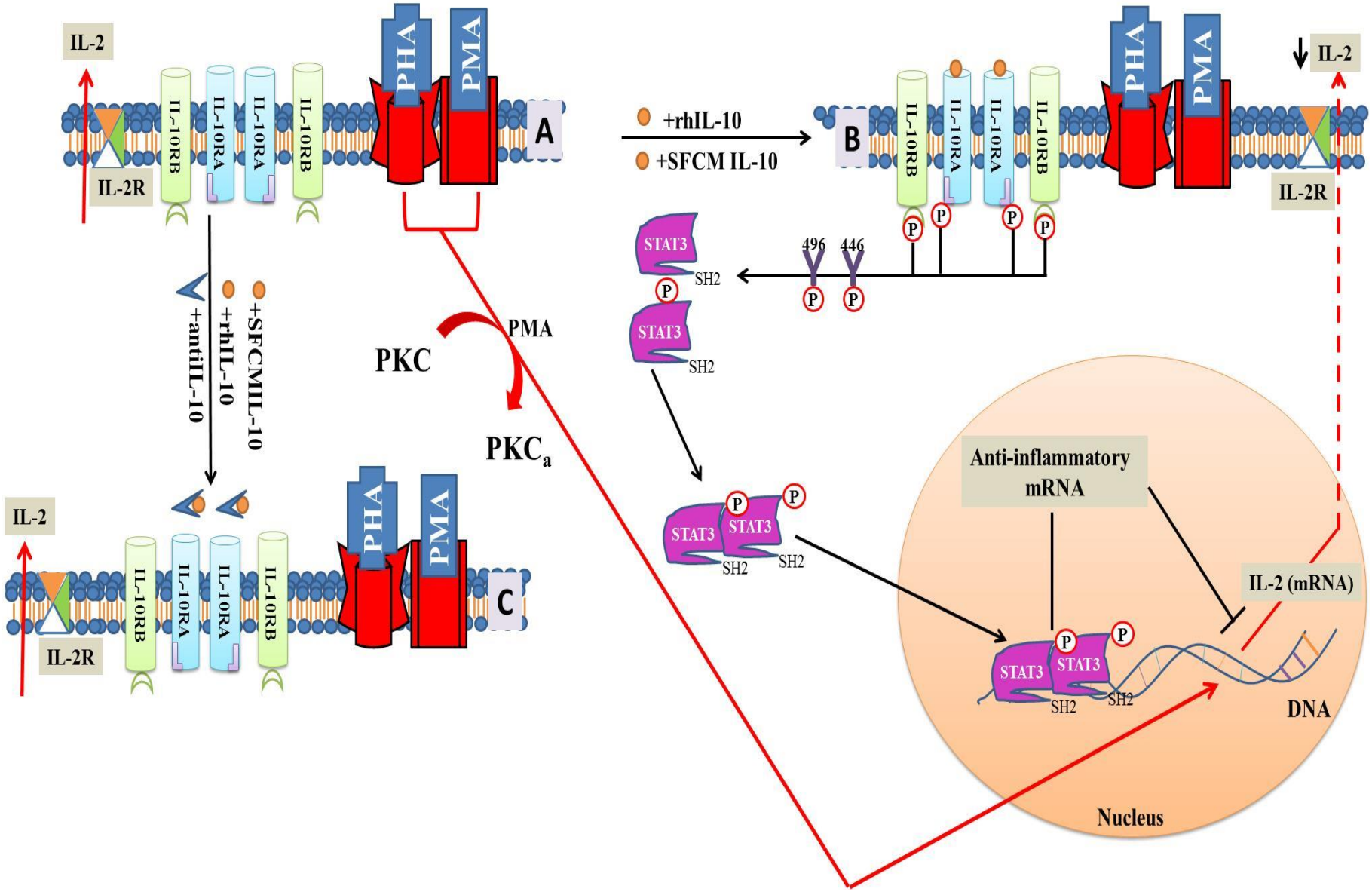
IL-2
IL-2R
IL-10RB
IL-10RA
IL-10RA
IL-10RB
PHA
PMA
A
+antiIL-10
+rhIL-10
+SFCMIL-10
PKC
PMA
PKCa
+rhIL-10
+SFCM IL-10
B
IL-2
IL-2R
STAT3
SH2
496
446
P
Anti-inflammatory mRNA
IL-2 (mRNA)
DNA
Nucleus
C

Figure 4-19. Structure and function of the IL10 receptor.

Functional IL10 receptor complexes are tetramers composed of two ligand-binding subunits (IL10RA) and two accessory signalling subunits (IL10RB). Binding of IL10 to the extracellular domain of IL10RA results in a cascade of reaction leading to STAT3 homodimerization and translocation to the nucleus with subsequent transcription of DNA leading to inhibition of IL2 gene transcription and abrogation of the immune response. (A) Schematic diagram describing the *in vitro* inflammatory response model using Jurkat cell plus PMA/PHA indicated by IL2 secretion; (B) IL10 receptor stimulation by its specific ligand from SFCM or exogenously added recombinant human IL10 (rhIL10) to the serum-free culture media resulted in stimulation of IL10 post-receptor translation pathway (STAT3) leading to inhibition of IL2 synthesis/secretion by Jurkat cells; (C) Contrariwise, neutralization of IL10 action by excess amount of rabbit polyclonal IL10 antibody resulted in restoration of IL2 secretion in both SFCM or $SFNCM^{+IL10}$.

Tryptophan is an important amino acid for T cell viability and functionality, tryptophan catabolised by indoleamine 2,3-dioxygenase (IDO) into Kynurenine depleting the availability of tryptophan for T cell resulting in inhibition of T cell proliferation and functionality[225]. IDO participated in the immunosuppression activity of MSCs, however, the activation of IDO is dependent on the localised pro-inflammatory environment[218]. Various studies reported that the engraftment of MSCs to the target diseased tissue is associated with their activation and IDO expression due to their exposure to proinflammatory cytokines including TNFa, IFNγ, and IL2[21,97]. However, in the present study, the SFCM were collected from resting MSCs because the cells used were isolated from commercially ordered bone marrow aspirates and SFCM were collected without previous priming with proinflammatory factors. Therefore, this study confirmed that the immunosuppressive activity of MSCs exerted by soluble factors and the suppression is achieved with both polarised and non-polarised MSCs indicating a likely non-IDO suppression pathway.

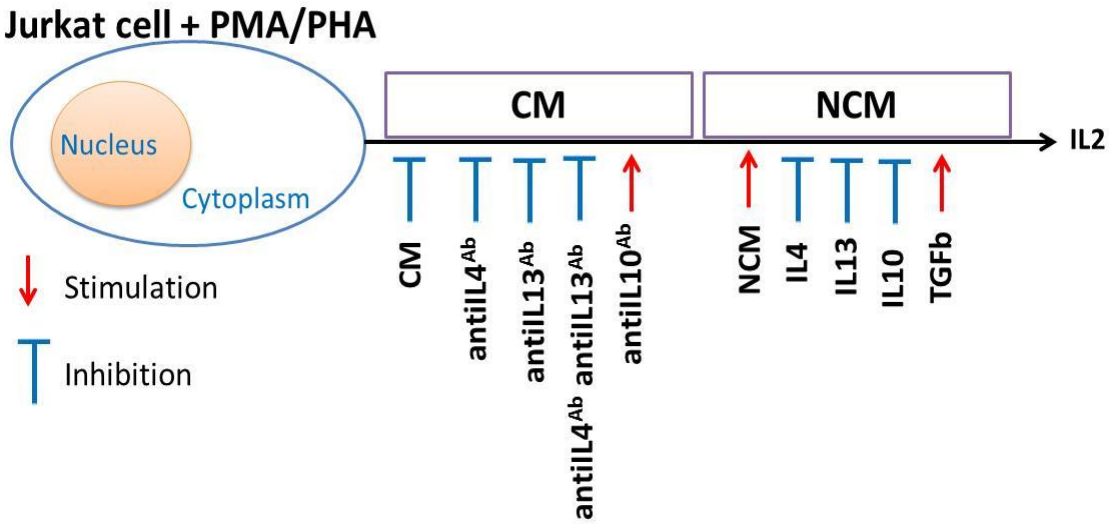

Figure 4-20. Schematic diagram summarizing the inhibitory and stimulatory activity of differently targeted cytokine biomolecules on Jurkat T cell IL2 activation marker.

IL4, IL10, IL13 inhibit IL2 secretion while TGFb slightly potentiated IL2 secretion. Reversal of IL2 secretion solely achieved in SFCM$^{+antiIL10\ AB}$.

Collectively, the present findings support the suggestion that IL10 plays an immunosuppressive role in Jurkat T cell proliferation and activation by reducing the secretion of IL2 (Figure 4-20). However, the molecular sites targeted by SFCM in order to achieve this effect remain unidentified; moreover, the present study is incompletely excluding the role of IL4/IL13 ligands in the immunosuppression achieved by SFCM. In addition, further investigation is required to determine the underlying mechanism(s) by which MSCs exert their immunomodulatory effect.

Keele UNIVERSITY

Chapter 5

hMSCs secretome reprograms macrophage differentiation in oxygen dependent manner

5.1 Introduction

Chronic diseases share inflammation as an underlying pathology. According to the duration of persistence; hours versus days, inflammation is either acute or chronic, respectively. Neutrophils are the principle cell during acute inflammation while macrophages/T cells are involved in chronic inflammation[120]. Inflammation is classified according to the causative factor, whether microbial or non-microbial, into pathogen-associated molecular pattern (PAMP) or damage associated molecular pattern (DAMP), respectively[121]. Broadly macrophages are of two types, M1 and M2, expressing distinct surface markers and secretome profiles; they also activate distinct subsets of T cells based on the received signal and localised tissue milieu[173]. The M1 macrophage subtype is characterised by the release of strong pro-inflammatory cytokines (e.g. TNFa, IL12, and IL1B), strong antimicrobial action, and presentation of their antigens to Th1 subsets of T cells[174]. Localised environment plays a great role in modulation of the macrophage phenotype, for instance, the proinflammatory factors including lipopolysaccharide, IFNγ, and GMCSF promote M1 phenotype polarisation and subsequently interaction with Th1 subsets of T cells[175]. M2 macrophage subtype is characterised by the release of strong anti-inflammatory cytokines (e.g. IL10), expression of high amount of mannose scavenger receptor (CD206), and polarised response to fungal or helminthic infection, apoptotic cells, immune complexes, and complement component. Moreover, polarisation can be triggered by MCSF, IL4, IL13, IL10, and TGFb. Finally, M2 polarised macrophages stimulate the Th2 subsets of T cells[176,175].

Access to the primary macrophage is limited by *in vitro* proliferation and the requirement of invasive techniques (tissue biopsy or bronchoscopy) for collection[226]. To overcome these obstacles and to meet the large scale requirement of cells for *in vitro* experimentation a monocyte cell line model was used; the THP-1 cell which is stimulated *in vitro* by PMA into a functional macrophage through stimulation of the protein kinase C pathway[227]. The present study tested the efficacy of SFCM, collected from MSCs cultured in 21% O_2 and 2% O_2, on modulation of THP-1 differentiation towards M1/M2 differentiation via analysis of surface marker expression and secretome profile. In an attempt to identify the mode of

action, the activity of selected biomolecules were neutralised in SFCM, such as, IL4, IL10, IL13, and TGFb, based on previously published data which confirm their contribution into THP-1 differentiation into macrophage[173].

5.2 Aim

The primary aims of this chapter were to:

- Develop an *in vitro* THP-1 macrophage differentiation.
- Testing the efficacy of SFCM in induction of macrophage terminal differentiation and investigation the role of SFCM in direction of macrophage differentiation toward M1 or M2 lineages.
- Identifying the influences of SFCM collected from 2% O_2 versus 21% O_2 on macrophage M1/M2 phenotype differentiation.
- Identification of individual cytokine roles in modulation of macrophage differentiation.

5.3 Methods:

Primary hMSCs were isolated from human BMA as outlined in section 2.2.2.1 with SFCM subsequently generated using standard SFNCM as described in section 2.2.3. The identity of the recovered cells was documented by conducting tri-lineage differentiation and flow cytometry as discussed in section 2.5.1 and 2.7.2, respectively. Various assays were performed on THP-1 cells cultured in GM, SFNCM, and SFCM, including histological assays, cellular assays, and molecular assays. Histological assay, pancake versus spindle cell shapes for morphological assessment, were used as a marker for M1/M2 lineage differentiation as described in section 2.5.2. Cellular assays included cell count, adherent cell count, and MTT to confirm proliferation as outlined in section 2.4. Molecular assays include IL0/TNFa ELISA, surface marker flow cytometry, RTPCR are as described in section 2.7.4, 2.7.2, and 2.6.2, respectively. These parameters were measured in both activated and non-activated THP-1 cells and in 21% O_2 and 10% O_2. The activation of THP-1 cells were achieved using PMA as described in section 2.3.

Selected cytokines identified from the cytokine array (described in Chapter 3) were tested on THP-1 cells to determine their potential M1/M2 differentiation activity following on from dose-response curve as described in section 2.8. To identify the mechanism of SFCM, these cytokines were individually blocked from SFCM using specific polyclonal antibodies as described in section 2.8, and surface marker expression at day-3 and secretome profile at days 1 and 2 were considered as M1/M2 lineage differentiation markers. The experimentation was performed over a 7-day period to achieve full modulation of the response; including the stationary phase for cell count, baseline proliferation for MTT, and baseline TNFa/IL10 secretion for PMA-induced activation. For genetic study RNA was isolated using Qiagen RNA isolation kits as described in section 2.6.1. Proliferations of THP-1 cells indicated by MTT were assessed as a relative proliferation by normalising all values to day-0. The concentration of IL10/TNFa already present in SFCM was subtracted from day-0 IL0/TNFa to achieve normalisation for results of THP-1 culture media activated in SFCM. Day-3 was considered as a time-point for flow cytometry based on the secretome results achieved within day-1 (high IL10) and day-2 (high TNFa) for M2 and M1 markers, respectively. Positive and negative surface markers were included to confirm that any subsequent changes are related to the SFCM or introduced/blocked cytokines to culture media.

5.4 Statistical analysis

Statistical analysis was conducted between SFCM and SFNCM using a two-sample t-test for most of the measured parameters, whereas for more than 2 groups one-way ANOVA with Tukey's multiple comparisons test to determine pairwise statistical significance, $p \leq 0.05$ was considered significant. The analysis was performed using Graphpad Prism 6 (CA, USA). Unless otherwise stated all values quoted in the results are mean ± SD.

5.5 Results

5.5.1 Characterisation of THP-1 cell line in GM

5.5.1.1 Proliferation of THP-1 cell in GM

We have characterised the effects of PMA on various cellular/molecular aspects of THP-1 cell line including proliferation/viability, morphological aspects, and gene expression profile. The effects of PMA on THP-1 cell line were determined based on the total cell count and MTT assay (Figure 5-1). To do this THP-1 cells were seeded at a density of $2x10^5$ cells/ml in GM and exposed to (50ng/ml of PMA) in both 21% O_2 and 10% O_2 environments over 7-days period compared to control non-treated group. In absence of PMA, the growth curve followed the standard pattern of lag, log, and stationary phase over a 7-day period. However, in the presence of PMA, the growth curve plateaued showing only a slight increase in proliferation with time (Figure 5-1A). Total cell counts (cell/ml) were significantly higher ($p<0.001$) in GM^{-PMA} over a 7-day period when compared to GM^{+PMA} in both 21% O_2 and 10% O_2. The maximum difference appeared at day-5 when stationary phase was reached [21% O_2 (GM^{-PMA} = 12000±2645 and GM^{+PMA} = 120000±10000) and 10% O_2 (GM^{-PMA} = 15000±5000 and GM^{+PMA} = 203000±5773)]. These results were confirmed by performing the MTT assay which revealed that in the absence of PMA, MTT was slightly increased reaching a maximum at day-2 (21% O_2 = 1.14±0.02 and 10% O_2 = 1.07±0.03) in 21% O_2 and 10% O_2. Similarly, in the presence of PMA, MTT slightly increased reaching a maximum at day-2 (21% O_2 = 1.07±0.03 and 10% O_2 = 0.98±0.04) and declined thereafter reaching a minimum at day-7 (21% O_2 = 0.65±0.015 and 10% O_2 = 0.5±0.026) in 21% O_2 and 10% O_2. However, PMA significantly ($P<0.05$) downregulated MTT parallel to the growth curve over 7-day time-points and in 21% O_2 and 10% O_2 conditions (Figure 5-1B). THP-1 exposure to PMA induced their M0 differentiation and hence increased their attachment to the plastic culture surface. Attached cells (cell/well) were counted in the presence and absence of PMA indicating that PMA induced significant upregulation ($p<0.001$) of cell attachment starting from day-1 [21% O_2 (GM^{-PMA} = 1000±1000 and GM^{+PMA} = 112000±10408) and 10% O_2 (GM^{-PMA} = 11000±1000 and GM^{+PMA} = 123000±15275)] with slight changes thereafter (Figure 5-1C).

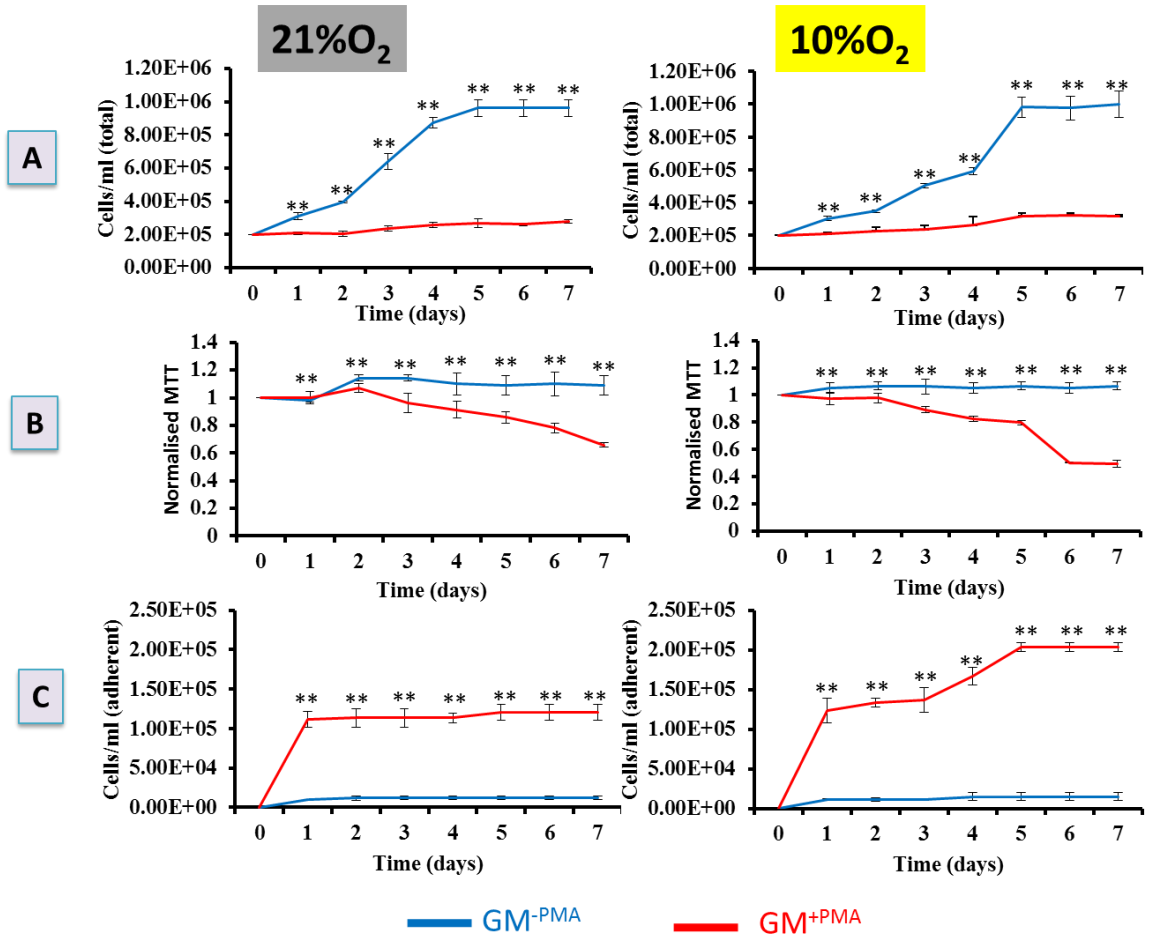

Figure 5-1. PMA inhibited THP-1 cell proliferation in GM and promoted their attachment.

Characterisation of the effects of PMA on THP-1 cell proliferation and differentiation. All experiments were performed in GM in either 21% O_2 or 10% O_2. The growth of THP-$1^{\pm PMA}$ cells was assessed using haemocytometer-based cell count (A) and confirmed by colorimetric MTT assay, 12 wells were used for each flask for a replicate of 3 flasks (n=36), Two-sample t-test were conducted to determine the significant difference between GM^{-PMA} and GM^{+PMA} (B). (C) The adherent cells were counted in all culture conditions and considered as a differentiation marker. Data expressed as mean±SD, each result represent a replicate of 3 independent experiments (n=3). Two-sample t-test were conducted to determine the significant difference, **P<0.001.

5.5.1.2 Activation/Differentiation of THP-1 cell in GM

To further characterise the role of PMA in modulation of the THP-1 behaviour in GM, IL10 and TNFa were measured in the GM over 7 days following their polarisation with PMA. To do this, THP-1 cells were seeded at a density of $5x10^5$ cells/ml in GM and exposed to

(50ng/ml of PMA) in both 21% O_2 and 10% O_2 environments and 1ml of GM were collected in replicates (n=3) over 7-days period compared to control non-treated group. Characterisation of the paracrine activity of THP-1 in GM^{+PMA} was established through measurement of both pro-inflammatory marker (TNFa (M1 marker)) or an anti-inflammatory (IL10 (M2 marker)). This indicated that PMA stimulated IL10/TNFa secretion over a 7-day period reached a maximum at day-2 [IL10 (21% O_2 = 981.7±69 and 10% O_2 = 233.7±60) and TNFa (21% O_2 = 779.9±64 and 10% O_2 = 307.6±53.3)] in 21 %O_2 and 10% O_2 environments. Significantly higher ($p<0.001$) secretion of IL10 (pg/ml) was noted in 21 %O_2 environment and versus significantly ($p<0.001$) higher secretion of TNFa (pg/ml) in 10% O_2 environment (Figure 5-2A).

For morphological assessment of THP-1 cells in GM, polarised THP-1 cells were scored according to their shape into either spindle or pancake-shaped and the subsequent percentage of total population determined. This demonstrated that polarisation of THP-1 cells leads to a significantly higher ($p<0.001$) number of pancake-shaped vs. spindle-shaped cells reaching a maximum at day-2 [21% O_2 (pancake shape = 12.2±3.6 and spindle shape = 4.7±1) and 10% O_2 (pancake shape = 14.5±4 and spindle shape = 4.5±1.1)] in both 21% O_2 and 10 %O_2 (Figure 5-2B).

Characterisation of surface markers expression by THP-1 in GM^{+PMA} was performed via assessment of a group of positive, negative, and target markers representative of monocytes and macrophages (M0, M1, and M2). The results indicated that PMA significantly upregulated ($p<0.001$) CD14 [21% O_2 (-PMA = 14.5±0.5 and +PMA = 47.1±1.4) and 10% O_2 (-PMA = 12.3±1.6 and +PMA = 40.9±0.14)] and CD73 [21% O_2 (-PMA = 15.1±1 and +PMA = 80.2±4.3) and 10% O_2 (-PMA = 13.3±3 and +PMA = 72.8±2.4)] and significantly downregulated ($p<0.001$) HLADR [21% O_2 (-PMA = 46.5±3.3 and +PMA = 25±2.5) and 10% O_2 (-PMA = 44.6±3.2 and +PMA = 30.3±2.4)]. However, PMA also displayed negative, but non-significant impacts on positive markers, such as, CD45 [21% O_2 (-PMA = 88.9±1 and +PMA = 73.6±2.1) and 10% O_2 (-PMA = 93±0.2 and +PMA = 76.7±5.6)], and CD105 [21% O_2 (-PMA = 86.3±1.1 and +PMA = 58.6±4.9) and 10% O_2 (-PMA = 84.9±3.8 and +PMA = 51.6±5.4)] (Figure 5-2C).

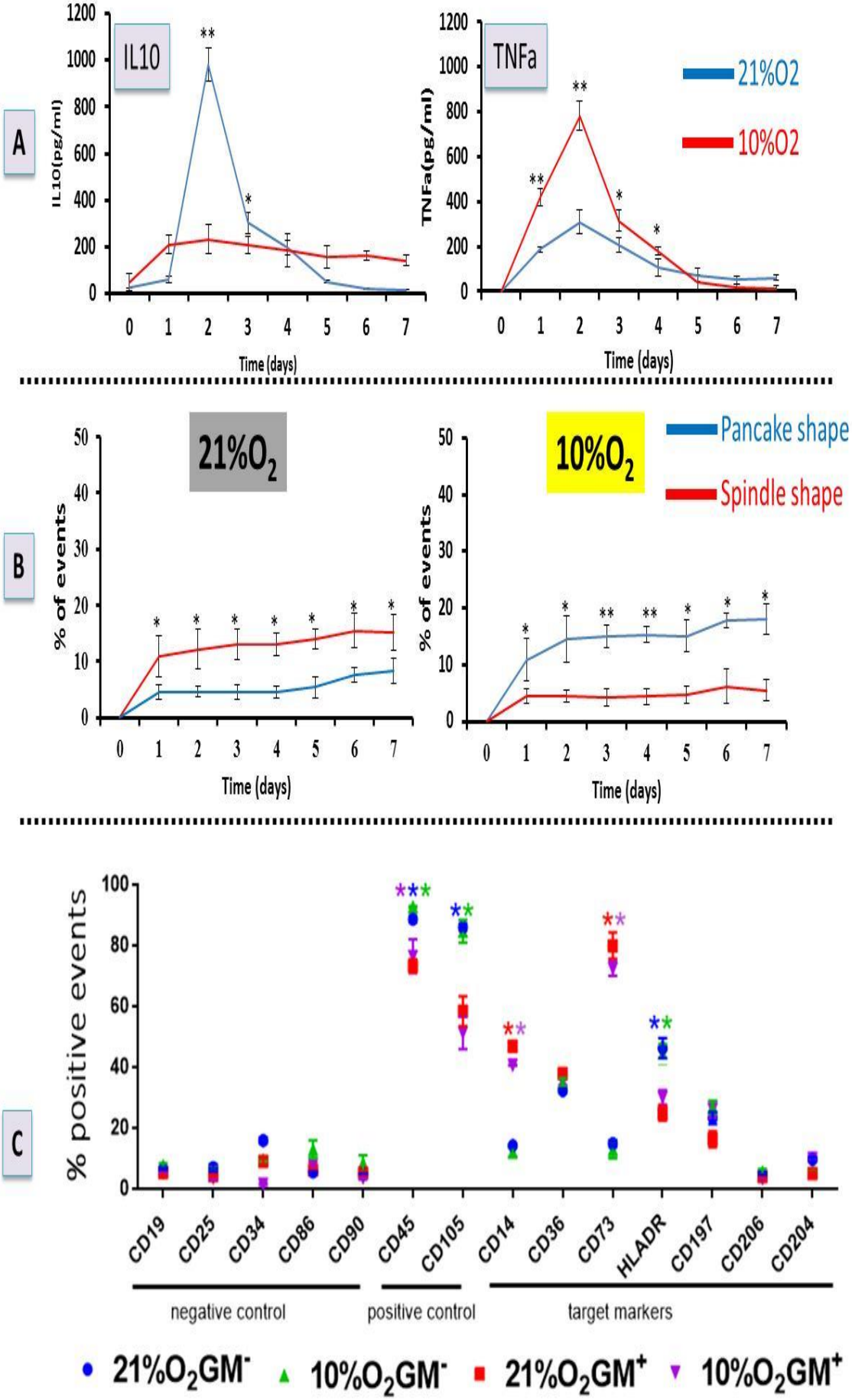
A
IL10
IL10(pg/ml)
Time (days)
TNFa
TNFa(pg/ml)
21%O2
10%O2
B
21%O2
10%O2
% of events
Pancake shape
Spindle shape
C
% positive events
CD19
CD25
CD34
CD86
CD90
CD45
CD105
CD14
CD36
CD73
HLADR
CD197
CD206
CD204
negative control
positive control
target markers
21%O2GM-
10%O2GM-
21%O2GM+
10%O2GM+

Figure 5-2 PMA induced THP-1 cell differentiation to M0 macrophages in GM.

(A) ELISA-based assay for detection of IL10/ TNFa in the THP-1^{+PMA} secretome profile following their culture in air oxygen and physioxia in GM. IL10/TNFa secretion is at basal levels in GM reflecting THP-1 de novo synthesis of these cytokines. Data expressed as mean±SD, each result represent a replicate of 3 independent experiments (n=3). Two-sample t-test were conducted to determine the significant difference, *P<0.0001. (B) Morphological assessment of THP-1 cells after being 3-days cultured in GM^{+PMA} in 21% O_2 and 10% O_2, the cells were culture in 24-wellplate in either 21% O_2 or 10% O_2 and a samples from each condition were fixed in replicate of 3 wells/day (for a 7-day period) and stained with Giemsa-May-Grunwald stain, 3 spots were considered from each well and 100 cell in the field scored according to their shape and their percentage was determined. Data expressed mean±SD, each result represent a replicate of 3 independent experiments (n=3). Two-sample t-test were conducted to determine the significant difference,*p<0.05, **p<0.001. (C) Surface markers expression by THP-1^{+PMA} including positive, negative, and target markers induced by activation, the assay were conducted after a 3-day exposure to PMA, data expressed as mean±SD, each result represent a replicate of 3 independent experiments (n=3). One-way ANOVA were conducted with a tukey's test to determine a pairwise significant difference. *P<0.001. * colour refer to relevant culture condition.

5.5.1.3 Modulation of gene expression by polarised THP-1 in GM

To identify the role of PMA in the modulation of gene expression by THP-1^{+PMA} cells in GM in 21% O_2 and 10% O_2 RTPCR was conducted on isolated RNA following their PMA-exposure across a group of chemotactic genes (CCL5, CCR5, IL8, MCP1, and MIP1A), proinflammatory genes (TNFa, IL1B, and IL12B), and an anti-inflammatory gene (IL10) compared to positive control genes (GAPDH and L32) (Figure 5-3). The result showed that PMA upregulated the expression of some genes including (IL8, MCP1, IL1B, IL12B, TNFa, and IL10) particularly in 10% O_2 compared to the positively expressed genes, GAPDH and L32, the bands were clearly expressed in early time-points over the 7-day period. In 10% O_2, IL8 showed stronger band expression in comparison to 21% O_2, similarly, CCL5 totally disappeared in 21% O_2 versus clear band expression in 10% O_2.

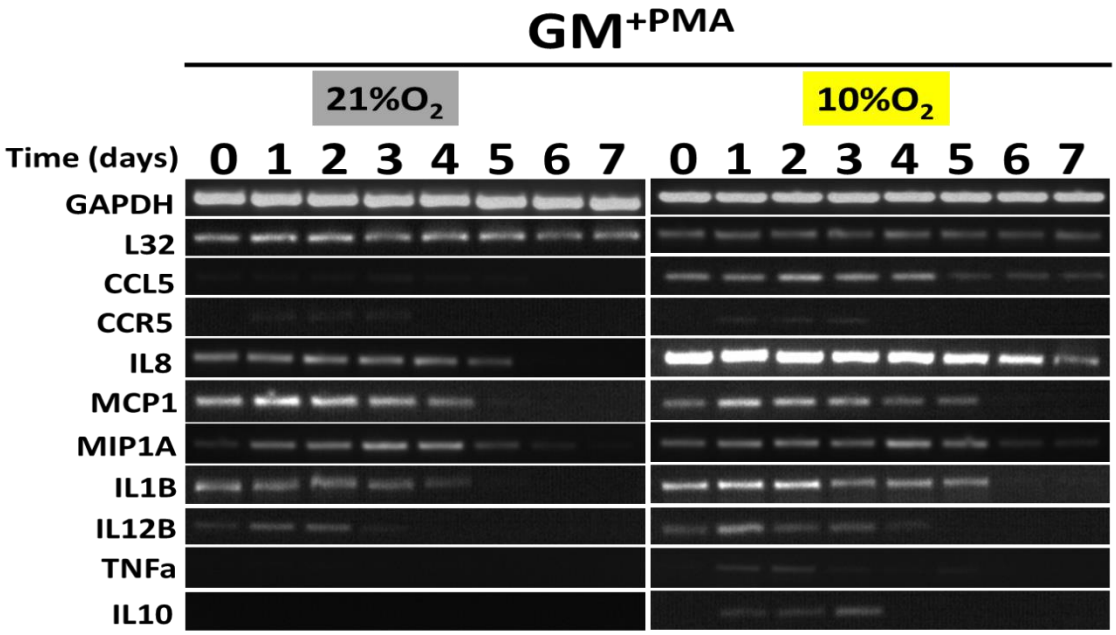

Figure 5-3. PMA modulated THP-1 gene expression profile.

Semiquantitative RTPCR for RNA of polarised THP-1 cells in GM in normoxic (21% O_2) and hypoxic (10% O_2) oxygen tension over 7-day period. Targeted genes are classified into chemotactic (CCL5, CCR5, IL8, MCP1, and MIP1A), pro-inflammatory (IL1B, IL12B, and TNFa), and anti-inflammatory genes (IL10) versus control housekeeping gene GAPDH and L32.

5.5.2 Role of SFCM in modulation of THP-1 cell line proliferation

5.5.2.1 SFCM modulated the growth curve of THP-1 cell line

The growth curve of activated and non-activated THP-1 in SFNCM and SFCM in 21% O_2 and 10% O_2 environment were characterised (Figure 5-4). In absence of PMA, growth curves followed normal proliferation patterns in 21% O_2 and 10% O_2 and in SFNCM or SFCM. The growth curve (cell/ml) of THP-1 increased gradually in SFCM reaching a stationary phase at day-5 [21% O_2 ($SFNCM^{-PMA}$ = 37000±10000, and $SFCM^{-PMA}$ = 369±20840) and 10% O_2 ($SFNCM^{-PMA}$ = 387000±20816 and $SFCM^{-PMA}$ = 345000±15000)] and plateaued thereafter. Similarly, in the presence of PMA, the growth curve gradually increased with time reaching a maximum at day-5 [21% O_2 ($SFNCM^{+PMA}$ = 343000±7637, and $SFCM^{+PMA}$ = 247000±15275) and 10% O_2 ($SFNCM^{+PMA}$ = 340000±24576 and $SFCM^{+PMA}$ = 233000±15275)]. The growth curve in SFNCM showed significant upregulation ($p<0.001$) vs. SFCM over 7-day time-points.

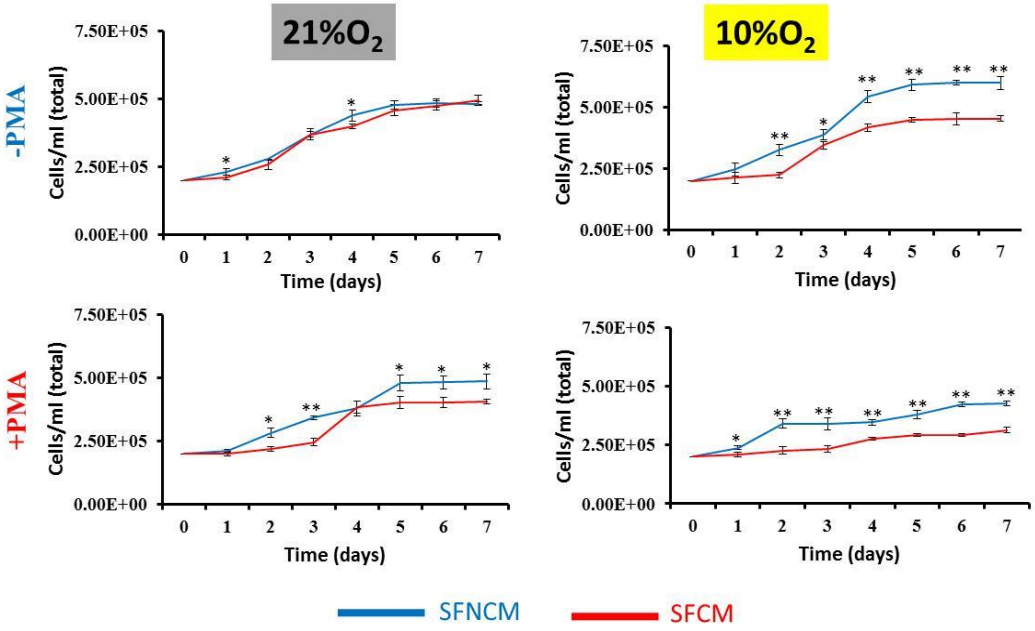

Figure 5-4. SFCM slightly suppressed the growth curve of THP-1$^{\pm PMA}$.

Growth curve of polarised and non-polarised THP-1 cells cultured in SFNCM versus SFCM in 21% O_2 and 10% O_2. The viable cells are counted over 7-days in SFNCM and SFCM and the results are compared to each other. PMA slightly suppressed THP-1 proliferation. Data expressed as mean±SD, each result represent a replicate of 3 independent experiments (n=3). Two-sample t-test were conducted to determine the significant differences. **P<0.001, *P<0.05.

5.5.2.2 SFCM modulated the MTT of THP-1 cell line

The proliferation of activated and non-activated THP-1 in SFNCM and SFCM in 21% O_2 and 10% O_2 environments were characterised via the MTT assay (Figure 5-5). In 21% O_2, THP-1^{-PMA} cell proliferation reached a maximum at day-3 (SFNCM = 1.2±0.03 and SFCM = 1.18±0.032) in both SFNCM and SFCM with no significant differences noted. However, in 10% O_2, THP-1^{-PMA} cell proliferation in SFNCM was significantly upregulated ($p<0.001$) reaching a maximum at day-3 (SFNCM = 1.2±0.02 and SFCM = 1±0.03) and declined thereafter in comparison to SFCM which showed stationary proliferation over all time-points. Moreover, in the presence of PMA, SFCM showed significant downregulation ($p<0.001$) of proliferation in comparison to SFNCM in 21% O_2 and 10% O_2 environments. Maximum differences were achieved at day-3 [21% O_2 (SFNCM = 1.1±0.04 and SFCM = 0.91±0.05) and 10% O_2 (SFNCM = 1.2±0.03 and SFCM = 0.9±0.06)].

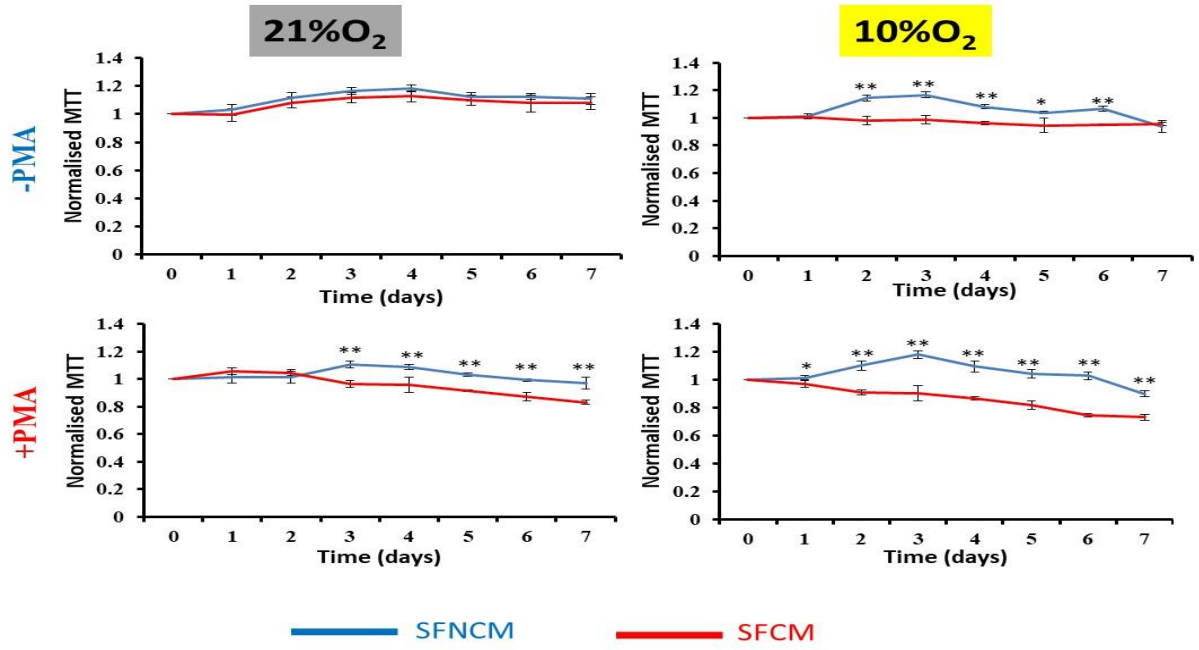

Figure 5-5. SFCM suppressed the metabolic activity (MTT) of THP-1$^{\pm PMA}$ compared to SFNCM.

MTT of activated and non-activated THP-1 cells cultured in SFNCM versus SFCM in 21% O_2 and 10% O_2. The MTT were performed over 7-days in SFNCM and SFCM and the results were normalised to day-0. PMA significantly suppressed THP-1 proliferation. Data expressed as mean±SD, each result represent a replicate of 3 independent experiments (n=3). Two-sample t-test were conducted to determine the significant differences, *P<0.05, **P<0.001.

5.5.2.3 SFCM modulation of the adherence potential of THP-1

We next sought to identify if SFCM had an impact on the differentiation potential of THP-1 as suspension monocytes. Adherent cells were counted in both SFNCM$^{\pm PMA}$ and SFCM$^{\pm PMA}$ in both 21% O_2 and 10% O_2 environments (Figure 5-6). The results showed that adherent cells were increased at day-1 [21% O_2 (SFNCM^{-PMA} = 12300±2516, SFNCM^{+PMA} = 56700±5773, SFCM^{-PMA} = 7330±5773, SFCM^{+PMA} = 150000±1000)] and 10% O_2 (SFNCM^{-PMA} = 10000±2000, SFNCM^{+PMA} = 21700±2886, SFCM^{-PMA} = 56700±5773, and SFCM^{+PMA} = 100000±1000)] and plateaued thereafter in all culture conditions. However, SFCM induced significant upregulation of adherence ($p<0.001$) over the 7-days period where this upregulation was further induced in presence of PMA starting at day-1 and thereafter.

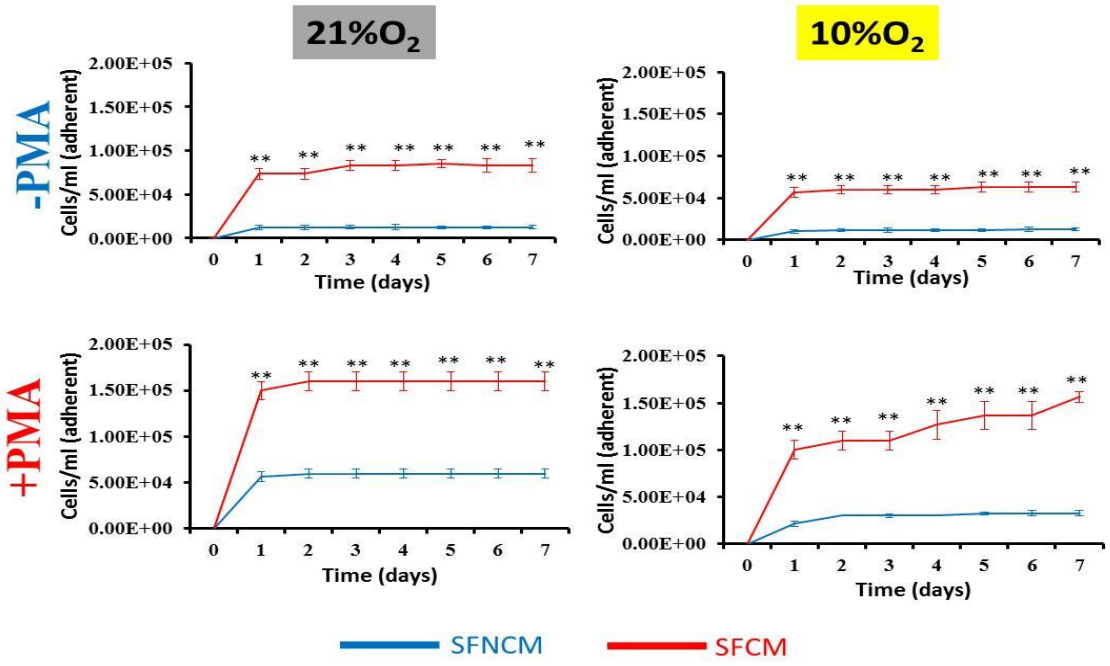

Figure 5-6. SFCM induced attachment of THP-1 cells compared to SFNCM.

Adherent cell count of activated and non-activated THP-1 cells cultured in SFNCM versus SFCM in 21% O_2 and 10% O_2. The cells were cultured and each day the suspension cells were removed leaving the attached cells to the culture plastic. Following trypsinization of the adherent cells, the viable cells are counted over 7-days in SFNCM and SFCM and the results are compared to each other. Data expressed as mean±SD, each result represent a replicate of 3 independent experiments (n=3). Two-sample t-test were conducted to determine the significant differences, **P<0.001.

5.5.3 Role of SFCM in modulation of THP-1 differentiation into M1 versus M2 in oxygen-dependent manner

5.5.3.1 SFCM induced distinct THP-1 cell morphology in an oxygen-dependent manner

To determine the differentiation patterns of the activated THP-1 in SFCM versus SFNCM, the shape of the produced macrophage was used as a baseline parameter (Figure 5-7 and 5-8). SFNCM induced a low percentage of pancake or spindle shaped THP-1 cells reaching a maximum at day-1 [21% O_2 (pancake shape = 10.5±1.8 and spindle shape = 5±1) and 10% O_2 (pancake shape = 8.4±1.5 and spindle shape = 6.8±1.3)] and plateaued thereafter. However, SFCM significantly upregulated ($p<0.001$) the percentage of the scored cells with pancake or spindle shape. THP-1 in SFCM displayed a significantly higher ($p<0.001$) pancake percentage in 21% O_2 collected SFCM versus a significantly higher ($p<0.001$) percentage of

spindle shaped cells in 10% O_2. Modulations in SFCM were achieved at day-1 [21% O_2 (pancake shape = 28±3.3 and spindle shape = 8.6±1.6) and 10% O_2 (pancake shape = 8.6±1.6 and spindle shape = 36±5.6)] and changes plateaued thereafter.

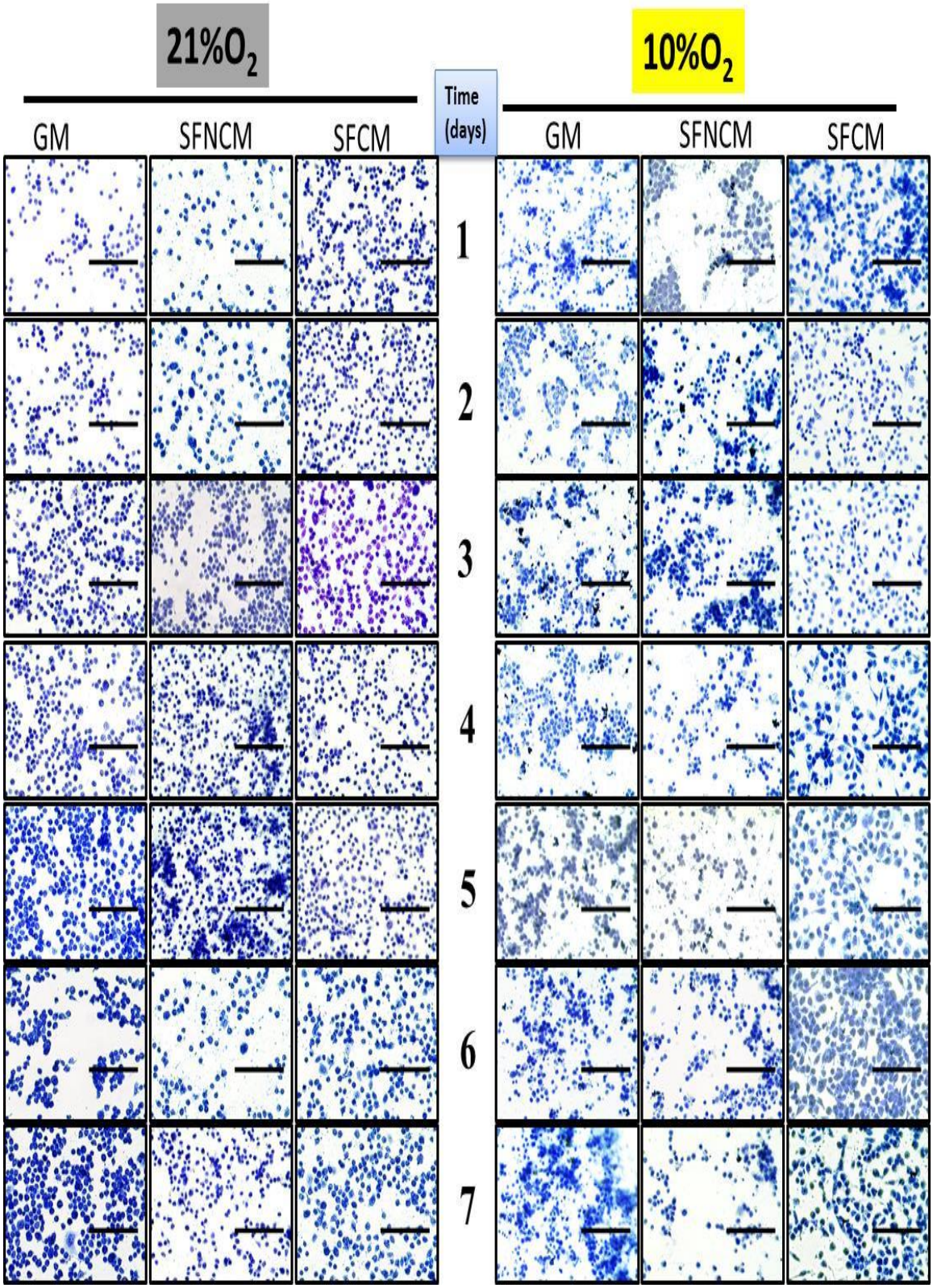

Figure 5-7. SFCM modulated the morphology of THP-1 in oxygen-dependent manner.

Representative images of activated THP-1 cells in GM, SFNCM, and SFCM in 21% O_2 and 10% O_2 over 7-days period. The cells were cultured in 24-wellplate in either 21% O_2 or 10% O_2 and samples from each condition were fixed in a replicate of 3 wells/day (for 7-days period) and stained with Giemsa-May-Grunwald stain, 3 spots were considered from each well for any subsequent analysis, scale bar 100µm.

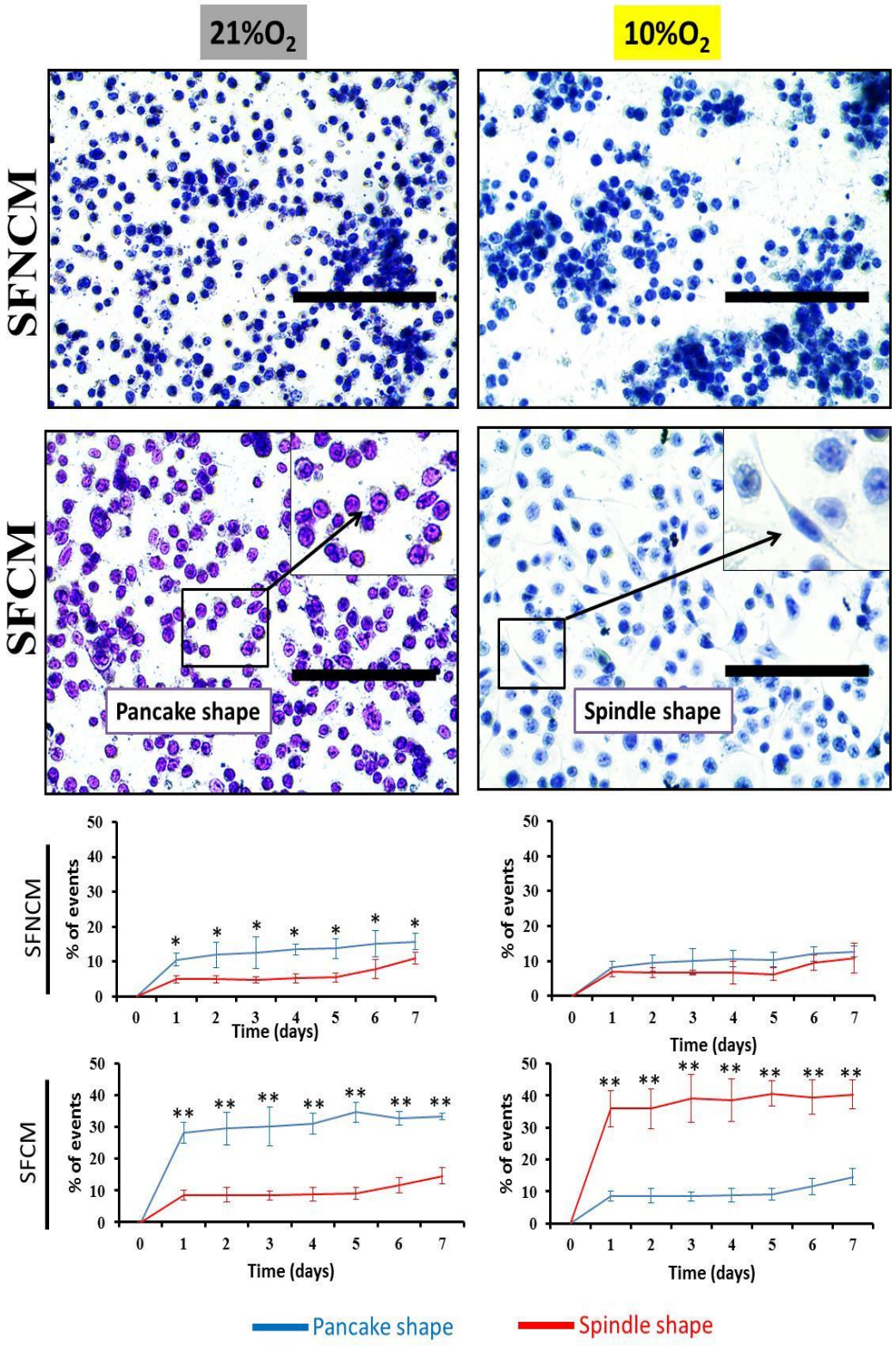

Figure 5-8. SFCM induced THP-1^{+PMA} terminal differentiation compared to SFNCM.

Representative images of polarised THP-1 cells. Images were taken following 3-days culture in SFNCM versus SFCM in 21% O_2 and 10% O_2, the cells were culture in 24-wellplate in either 21% O_2 or 10% O_2 and the samples from each condition were fixed in replicate of 3 wells/day (for a 7-day period) and stained with Giemsa-May-Grunwald stain, 3 spots were considered from each well and 100 cells in the field scored according to their shape and their percentage were determined, data expressed as mean±SD, each result represent a replicate of 3 independent experiments (n=3). Two-sample t-test were conducted to determine the significant differences, *P<0.05, ** P<0.001, scale bar 200µm.

5.5.3.2 SFCM induced distinct THP-1 cell gene transcription in an oxygen-dependent manner

We next sought to identify the role of SFCM in the modulation of gene expression by THP-1$^{±PMA}$ cells in 21% O_2 and 10% O_2 environments (Figure 5-9). The results showed that SFCM downregulates the expression of CCR5 by THP-1$^{±PMA}$ particularly in 10% O_2 versus SFNCM compared to the positively expressed genes, GAPDH and L32. SFCM downregulated a pro-inflammatory gene, such as, IL1B, IL12B, and TNFa in 21% O_2 and 10% O_2 but particularly in 10% O_2 collected SFCM. Moreover, SFCM upregulated the expression of IL10 genes in comparison to SFNCM in 21% O_2 and 10% O_2, however, 2% O_2 SFCM induced clearer band expression in comparison to 21% O_2.

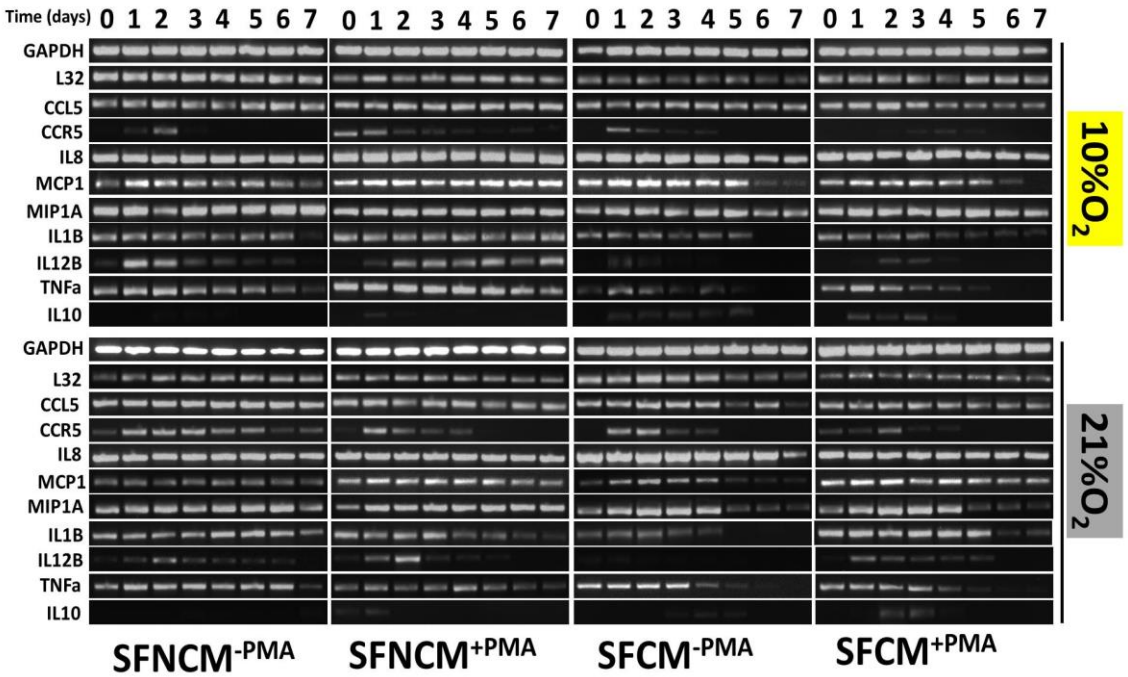

Figure 5-9. SFCM modulated the gene expression profile of THP-1^{+PMA} compared to SFNCM.

Semi-quantitative RTPCR for RNA of activated and non-activated THP-1 cells in SFNCM versus SFCM in normoxic (21% O_2) and hypoxic (10% O_2) oxygen tension over 7-day period. Targeted genes are classified into chemotactic (CCL5, CCR5, IL8, MCP1, and MIP1a), pro-inflammatory (IL1B, IL12B, and TNFa), and anti-inflammatory genes (IL10) versus control housekeeping gene GAPDH and L32.

5.5.3.3 SFCM induced distinct THP-1 cell surface marker expression in an oxygen-dependent manner

To identify the role of polarisation on the modulation of marker expression flow cytometry was conducted on THP-1$^{\pm PMA}$ in both 21% O_2 and 10% O_2 environments and in SFNCM/SFCM (Figure 5-10). The results revealed that in 21% O_2 PMA significantly upregulated ($p<0.0001$) the expression of CD73 ($SFNCM^-$ = 8.9±1.4, $SFNCM^+$ = 37.8±1.3, $SFCM^-$ = 7.3±0.43, and $SFCM^+$ = 33.4±0.5), and CD197 ($SFNCM^-$ = 9.6±1, $SFNCM^+$ = 91.5±1.2, $SFCM^-$ = 40.6±12.3, and $SFCM^+$ = 69.1±6.4), whereas 10% O_2 PMA showed no induction of specific markers.

We next sought to identify the role of SFCM in induction of terminal differentiation. The results revealed that in 10% O_2, SFCM significantly upregulated ($p<0.0001$) the expression of CD14 ($SFNCM^-$ = 10.9±0.65, $SFNCM^+$ = 13±0.4, $SFCM^-$ = 48.2±1, and $SFCM^+$ = 43.1±4.83), CD36 ($SFNCM^-$ = 52.1±0.9, $SFNCM^+$ = 25.3±1.4, $SFCM^-$ = 64.6±0.65, and $SFCM^+$ = 61.3±0.7), CD73 ($SFNCM^-$ = 7.8±0.5, $SFNCM^+$ = 14.8±1.6, $SFCM^-$ = 47±0.37, and $SFCM^+$ = 45.3±0.35), whereas 21% O_2 SFCM showed a non-specific upregulation of these markers, including modulation of CD197 ($SFNCM^-$ = 9.6±1, $SFNCM^+$ = 91.5±1.2, $SFCM^-$ = 40.6±12.3, and $SFCM^+$ = 69.1±6.4)].

To determine the differentiation patterns of THP-1$^{\pm PMA}$ in 21% O_2 versus 10% O_2 SFCM we again utilised flow cytometry. This indicated significant differences ($p<0.001$) between SFCM and SFNCM in some markers. The results revealed that in 10% O_2, SFCM significantly upregulated ($p<0.0001$) the expression of CD14 ($SFNCM^-$ = 10.9±0.65, $SFNCM^+$ = 13±0.4, $SFCM^-$ = 48.2±1, and $SFCM^+$ = 43.1±4.83), CD36 ($SFNCM^-$ = 52.1±0.9, $SFNCM^+$ = 25.3±1.4,

SFCM$^-$ = 64.6±0.65, and SFCM$^+$ = 61.3±0.7), and CD73 (SFNCM$^-$ = 7.8±0.55, SFNCM$^+$ = 14.9±1.6, SFCM$^-$ = 46.9±0.38, and SFCM$^+$ = 45.3±0.35), and CD204 (SFNCM$^-$ = 5.4±1.5, SFNCM$^+$ = 4.7±0.2, SFCM$^-$ = 11.9±5, and SFCM$^+$ = 14.9±5.9), whereas 21% O_2 SFCM significantly upregulated ($p<0.0001$) the expression of CD197 [(SFCM$^-$ = 40.6±12.3, and SFCM$^+$ = 69.1±6.4)] versus 10% O_2 [(SFCM$^-$ = 20.9±10.8, and SFCM$^+$ = 18.6±0.4)].

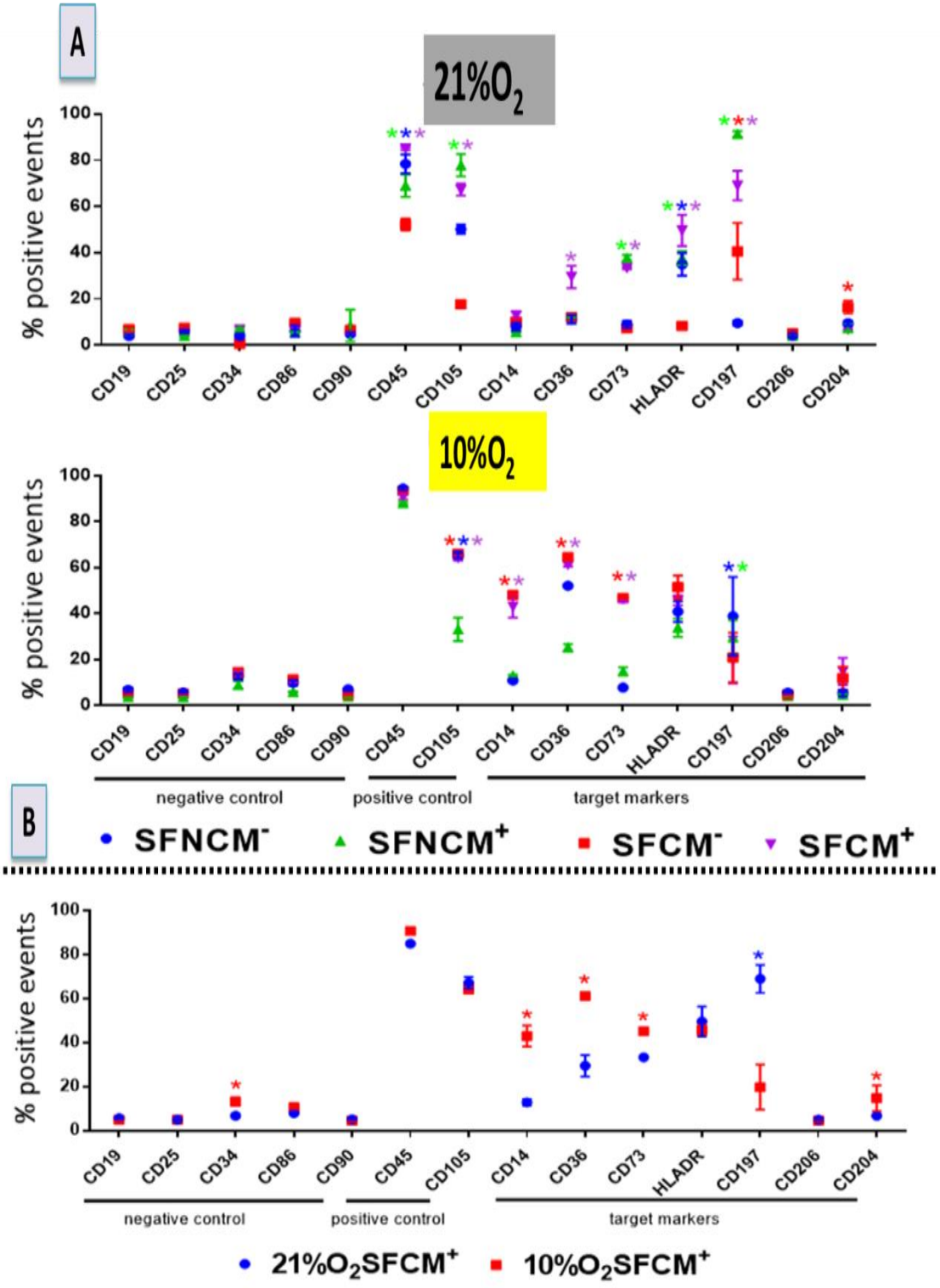

Figure 5-10. SFCM modulated surface markers expression in oxygen-dependent manner.

Flow cytometry-based surface marker expression of THP-1^{+PMA} cells cultured in 21% O_2 and 10% O_2, in different culture media; $SFNCM^-$, $SFNCM^+$, $SFCM^-$, $SFCM^+$**.** Positive and negative control markers are included in the panel, including $CD19^-$, $CD25^-$, $CD34^-$, $CD86^-$, $CD90^-$, $CD45^+$, and $CD105^+$. The target markers, include CD14, CD73, and HLA-DR (macrophage markers), CD197 (M1 macrophage marker) and CD36, CD204, CD206 (macrophage M2 markers). (A) Comparison between SFCM and SFNCM within the same oxygen tension in presence or absence of PMA. (B) Comparison between flow cytometry results of THP-1^{+PMA} cells in $SFCM^{21\%O2}$ and $SFCM^{10\%O2}$. CD197 positively induced by 21% O_2 SFCM while CD36 positively induced by 2% O_2 SFCM. Despite being M2 macrophage markers, both CD204/CD206 were weakly expressed by SFCM. Data expressed as mean±SD each result represent a replicate of 3 independent experiments (n=3). One-way ANOVA were conducted with Tukey's test to determine the pairwise significant differences. *P<0.0001. **** Colours indicate that the significant difference of relevant culture condition when compared to others.

5.5.3.4 SFCM induces distinct THP-1 cell secretome in an oxygen-dependent manner

To identify differentiation pattern of THP-1^{+PMA} cell in SFCM versus control SFNCM, the secretome profile was analysed by quantification the amount of TNFa and IL10 as a marker for M1 and M2, respectively (Figure 5-11). The results showed that the TNFa and IL10 production by polarised THP-1 was upregulated at day-1 for IL10 [SFNCM (21% O_2 = 540±248, and 10% O_2 = 2643±413) and day-2 for TNFa [SFNCM (21% O_2 = 422±26, and 10% O_2 = 304±37 and SFCM (21% O_2 = 922±49, and 10% O_2 = 373±21)] and downregulated thereafter reaching a baseline at day-7 {IL10 [SFNCM (21% O_2 = 170.6±160.7, and 10% O_2 = 78.5±23.9) and SFCM (21% O_2 = 294.8±278.3, and 10% O_2 = 33±18.7)] and TNFa [SFNCM (21% O_2 = 73±26.4, and 10% O_2 = 61±14.7) and SFCM (21% O_2 = 31.3±18.7, and 10% O_2 = 50±36)]} whether in SFNCM or SFCM and in 21% O_2 and 10% O_2. On day-1, IL10 was significantly upregulated ($p<0.001$) in SFCM collected from 10% O_2 when compared to 21% O_2 SFCM or SFNCM. Conversely, TNFa was significantly ($P<0.001$) upregulated at day-2 in normoxic (21% O_2) SFCM when compared to hypoxic (2% O_2) SFCM or SFNCM.

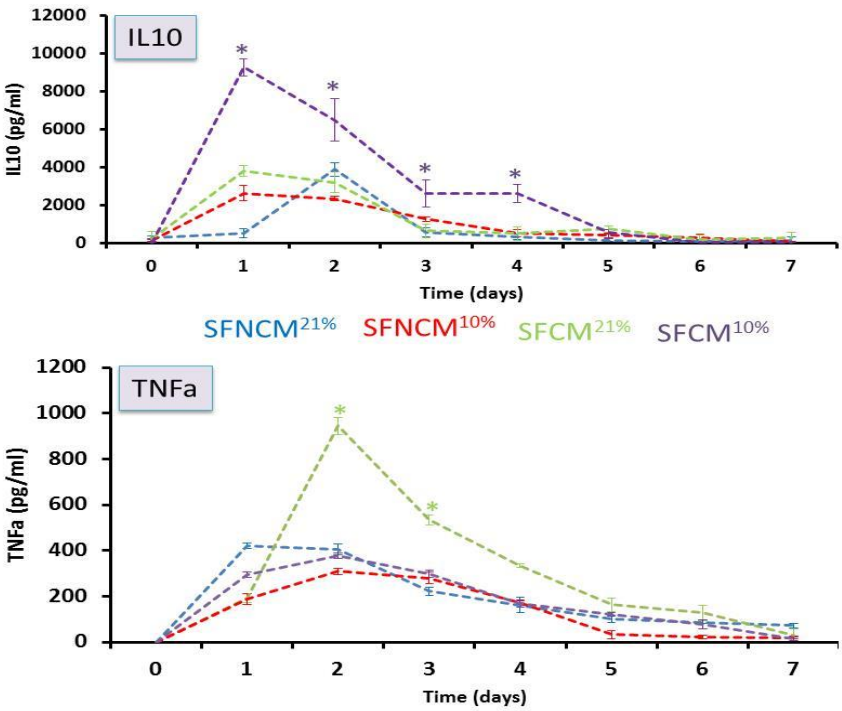

Figure 5-11. SFCM induced TNFa (M1 marker) and IL10 (M2 marker) expression in oxygen-dependent manner.

ELISA-based assay for detection of IL10/ TNFa in the THP-1^{+PMA} secretome profile following their culture in 21% O_2 and 10%O_2 under different culture media; $SFNCM^{21\%}$, $SFNCM^{10\%}$, $SFCM^{21\%}$, $SFCM^{10\%}$. IL10/TNFa secretion is at basal levels in SFNCM reflecting THP-1 *de novo* synthesis of these cytokines while their release is positively induced by SFCM in oxygen-dependent manner, 21% O_2 SFCM increases TNFa secretion (M1 marker) while 2% O_2 SFCM increases IL10 secretion (M2 marker), data expressed as mean±SD, each result represent a replicate of 3 independent experiments (n=3). One-way ANOVA were conducted with Tukey's test to determine the pairwise significant differences. *P<0.001, * colour indicates that the significant difference of relevant culture condition when compared to others.

5.5.4 Cytokine challenging THP-1 cell

5.5.4.1 Surface marker expression

In an attempt to identify the candidate biomolecule(s) responsible for driving the potential M1/M2-macrophage lineage differentiation, 4 anti-inflammatory cytokines (IL4, IL10, IL13, and TGFb) (Chapter 3) were tested by their addition to SFNCM and their subsequent neutralisation from SFCM with specific polyclonal antibodies (section 2.8) using flow cytometry to identify specific surface markers expressed by an M1/M2 macrophage (Figure

5-12 and 5-13). Negative markers included in the study included CD19, CD25, CD34, CD86, and CD90, these markers showed no more than 10% positive expression in all culture conditions in presence or absence of these cytokines and in 21% O_2 and 10% O_2 environments. CD45 and CD105 were included as positive markers and CD45 was positively expressed (>80%) in all culture conditions in presence or absence of these cytokines and in 21% O_2 and 10% O_2 environments. However, CD105 was markedly (>2 fold) downregulated in $SFCM^{+antiIL10AB}$ in 21% O_2 and 10% O_2 environments.

In addition to the negative and positive markers mentioned above, certain target markers were introduced to identify the differentiation potential of THP-1 cells toward M1 or M2 following their exposure to these cytokines (Figure 5-13). The results indicate that the combination of IL4/IL13 cytokine in SFNCM induced significant CD36-upregulation and CD197/HLA-DR-downregulation [CD36 (21% O_2 = 33.3±2.5), and (10% O_2 = 59±5.1), CD197 (21% O_2 = 50.3±2.9), and (10% O_2 = 6.4±0.3), and HLADR (21% O_2 = 18.5±2.3), and (10% O_2 = 19.2±3.1)] in comparison to control SFNCM [CD36 (21% O_2 = 12.3±0.5), and (10% O_2 = 25.3±1.4), CD197 (21% O_2 = 91.5±1.2), and (10% O_2 = 29.7±7.5), and HLADR (21% O_2 = 37.7±3) and (10% O_2 = 33.9±3.9)] ($p<0.001$). Neutralisation of IL4/Il13 from SFCM with IL4/IL13 specific polyclonal antibodies resulted in CD36-downregulation and CD197/HLA-DR-upregulation [CD36 (21% O_2 = 7.8±0.9) and (10% O_2 = 31.9±3), CD197 (21% O_2 = 59±2.4) and (10% O_2 = 71±14.3), and HLADR (21% O_2 = 69.9±2.8) and (10% O_2 = 30±4.4)] in comparison to neat SFCM [CD36 (21% O_2 = 29.5±4.9) and (10% O_2 = 61.3±0.7), CD197 (21% O_2 = 69.1±6.4) and (10% O_2 = 18.6±1.5), and HLADR (21% O_2 = 49.7±6.8) and (10% O_2 = 45.8±2.1)], in 21% O_2 and 10% O_2 environments. IL10 added to SFNCM induced non-significant ($p>0.05$) CD36-upregulation and significant ($p<0.001$) CD197/HLA-DR-downregulation [CD36 (21% O_2 = 17.3±3.6) and (10% O_2 = 32.3±1), CD197 (21% O_2 = 21.4±11) and (10% O_2 = 40.8±12.4), and HLADR (21% O_2 = 20.2±3.2), and (10% O_2 = 10±0.6)]. IL10 neutralisation from SFCM with a specific IL10 polyclonal antibody resulted in significant ($p<0.001$) CD36/CD197/HLA-DR-downregulation [CD36 (21% O_2 = 9.8±0.9) and (10% O_2 = 19±0.8), CD197 (21% O_2 = 31.8±6.2) and (10% O_2 = 20.3±3.5), and HLADR (21% O_2 = 17.5±2.5) and (10% O_2 = 18±1.5)] compared to SFCM [CD36 (21% O_2 = 29.5±4.9) and (10% O_2 = 61.3±0.7), CD197 (21% O_2 = 69±6.4)and (10% O_2 = 18.6±1.5), and HLADR (21% O_2 = 49.7±6.8) and (10% O_2 = 45.8±2.1)]. Moreover, TGFb added to SFNCM induced significant

(p<0.001) CD197-downregulation [(CD197 = 15.8±2.4)] in 21% O_2 and slight CD36-upregulation [(CD36 = 34±2.4)] in 10% O_2.

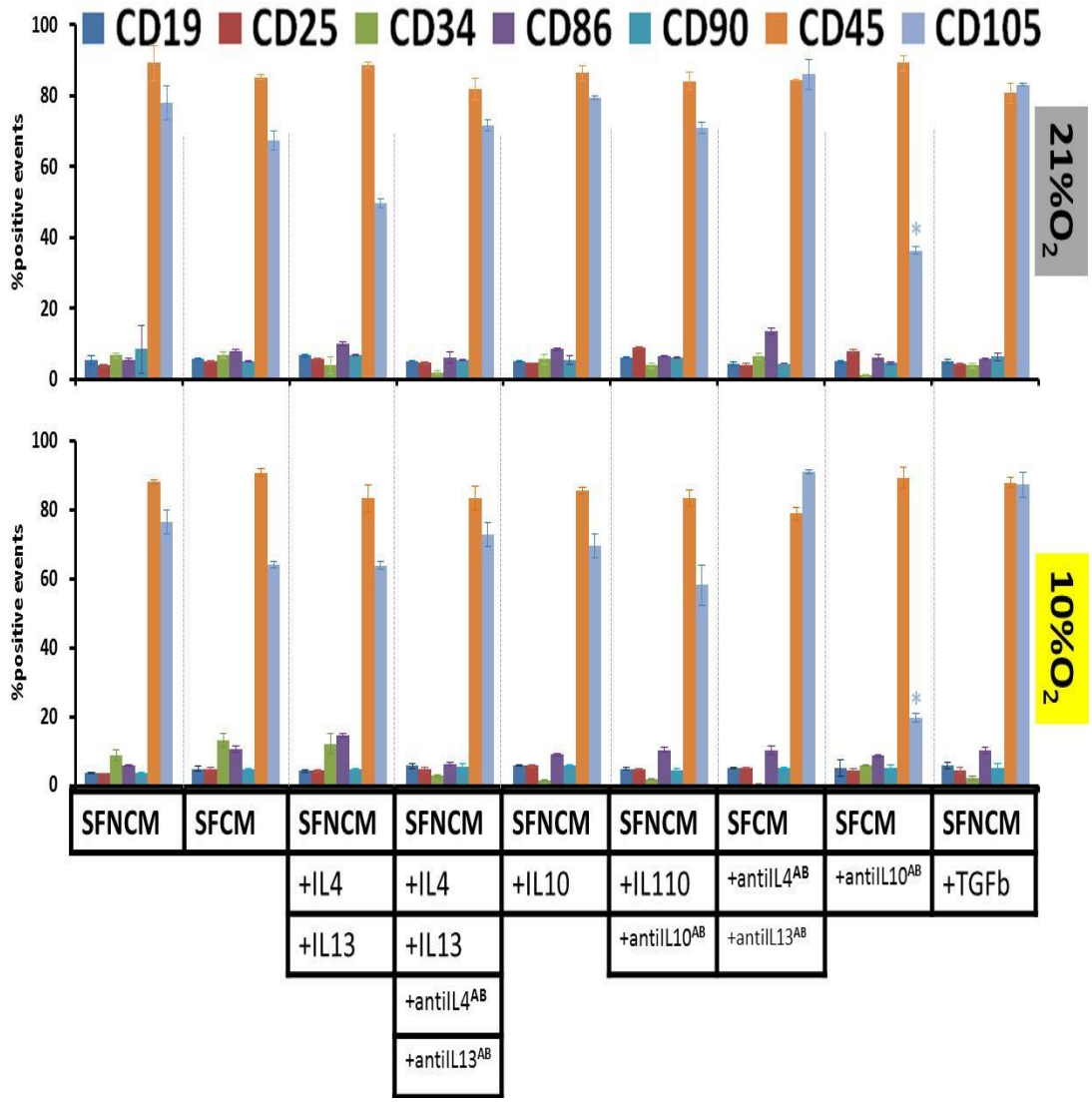

Figure 5-12. Evaluating the role of anti-inflammatory cytokines in the mode of action of SFCM based on surface markers expression (control markers).

Flow cytometry-based assay for detection of control (positive/negative) surface markers on the THP-1^{+PMA} cells following their culture in 21%O_2 and 10%O_2. THP-1 cultured under different culture media in presence or absence of 4 anti-inflammatory cytokines (IL4, IL10, IL13, and TGFb) in SFNCM and in SFCM. SFCM tested before and after neutralisation of these cytokines with their specific polyclonal antibodies in comparison to control groups (SFCM and SFNCM). Data are expressed as mean±SD, each result represent a replicate of 3 independent experiments (n=3). *>2-fold downregulation in comparison to $SFNCM^{+PMA}$. *colour indicates significant differences in this culture media compared to both SFNCM. A cytomix of IL4/IL13 was considered due to IL4/IL13-receptor overlapping.

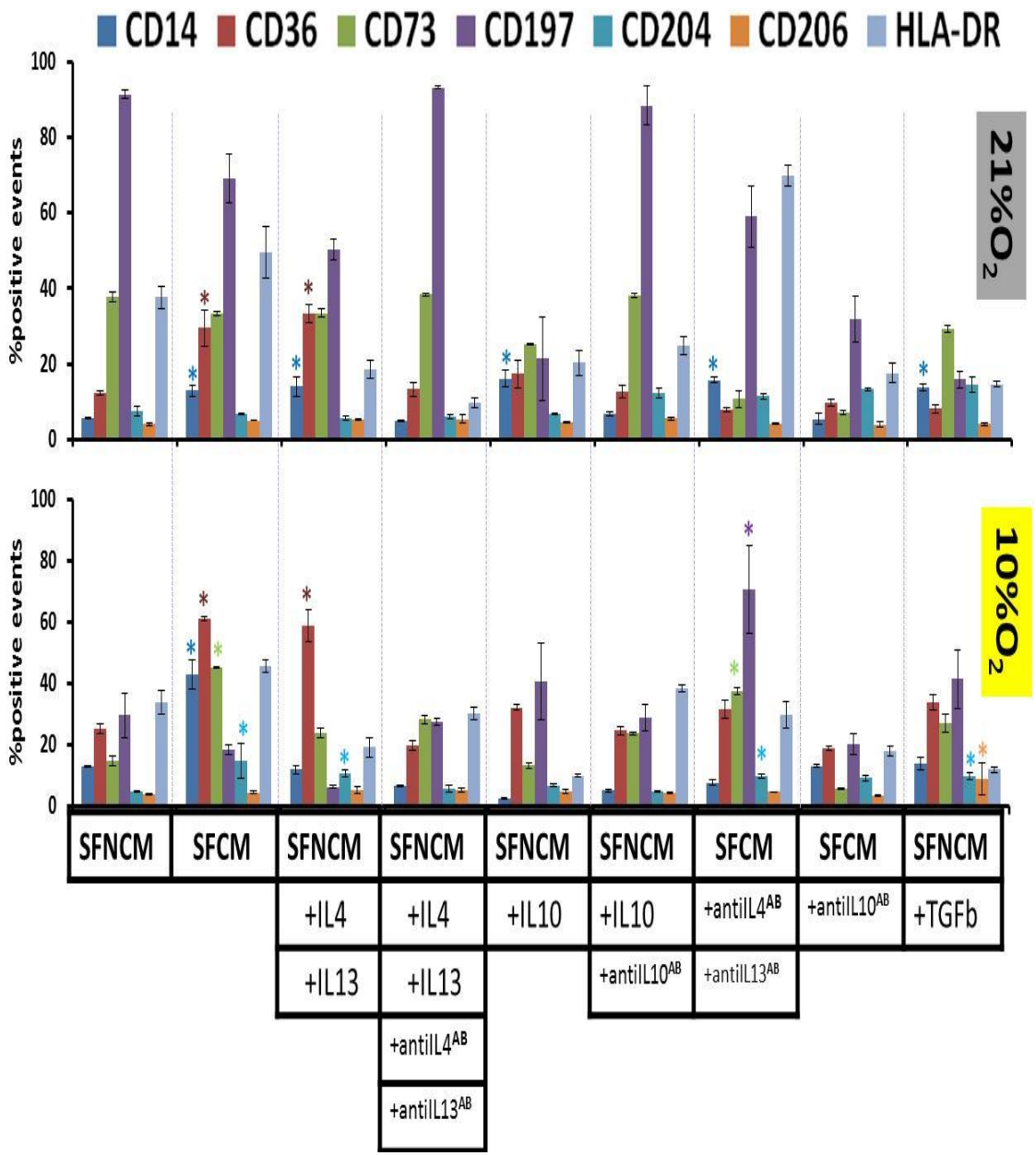

Figure 5-13. Evaluating the role of anti-inflammatory cytokines in the mode of action of SFCM based on surface markers expression (target markers).

Flow cytometry-based assay for detection of target surface markers on the THP-1^{+PMA} cells following their culture in 21%O_2 and 10%O_2. THP-1 cultured under different culture media in presence or absence of 4 anti-inflammatory cytokines (IL4, IL10, IL13, and TGFb) in SFNCM and in SFCM. SFCM tested before and after neutralisation of these cytokines with their specific polyclonal antibodies in comparison to control groups (SFCM and SFNCM). Data are expressed as mean±SD each result represent a replicate of 3 independent experiments (n=3). *>2-fold upregulation in comparison to SFNCM^{+PMA}. *colour indicates differences in this culture media compared to both SFNCM.

5.5.4.2 Secretome marker expression

In an attempt to identify the candidate biomolecule(s) responsible for the potential M1/M2-macrophage lineage differentiation, 4 anti-inflammatory cytokines were tested by their addition to SFNCM and their subsequent neutralisation from SFCM with specific polyclonal antibodies, using ELISA-based quantification of TNFa/IL10 paracrine markers secreted from the M1/M2 macrophage (Figure 5-14).

In 21% O_2, a combination of IL4/13 cytokine in SFNCM induced significant ($p<0.001$) secretion of IL10/TNFa [day-2 (IL10 = 7846.8±492) and (TNFa = 1452±335)] in comparison to control SFNCM [day-2 (IL10 = 3897.7±354.5) and (TNFa = 422.1±26.6)] and in confirmation their neutralisation from SFCM with IL4/IL13 specific polyclonal antibodies resulted in a downregulation of IL10 [day-2 (IL10 = 2505.4±192.9)] and significant ($p<0.001$) upregulation of TNFa [day-2 (TNFa = 2111.4±85.9)] compared to neat SFCM [day-2 (IL10 = 3204.4±555) and (TNFa = 922.3±49.5)]. While IL10 in SFNCM induced significant ($p<0.001$) secretion of IL10/TNFa [day-2 (IL10 = 14895.6±1481.3) and (TNFa = 2053.6±399)] in comparison to control SFNCM [day-2 (IL10 = 3897.7±354.5) and (TNFa = 422.1±26.6)]. However, IL10 neutralisation from SFCM with specific IL10 polyclonal antibody resulted in significant ($p<0.001$) downregulation of IL10 [day-2 (IL10 = 1399±122)] secretion compared to SFCM [day-2 (IL10 = 3204.4±555) and (TNFa = 922.3±49.5)] with significant upregulation ($p<0.001$) of TNFa [day-2 (TNFa = 1445±42.6)] secretion. Moreover, TGFb added to SFNCM induced significant ($p<0.001$) upregulation of both TNFa/IL10 secretion [day-2 (IL10 = 6697±411) and (TNFa = 1645.5±73)].

In 10% O_2, the results indicated that a combination of IL4/13 cytokine in SFNCM induced significant ($p<0.001$) secretion of TNFa [day-2 (TNFa = 677.3±103)] with no effect on IL10 [day-2 (IL10 = 2932.6±65.6)] secretion in comparison to control SFNCM [day-2 (IL10 = 2352.3±108.1) and (TNFa = 304.7±37)]. Conversely, their neutralisation from SFCM with IL4/IL13 specific polyclonal antibodies resulted in significant ($p<0.001$) downregulation of IL10 [day-2 (IL10 = 320.2±154.6)] and upregulation of TNFa [day-2 (TNFa = 465±118.3)] compared to neat SFCM [day-2 (IL10 = 6500±1129), and (TNFa = 373.2±21.2)]. While IL10 in SFNCM induced significant ($p<0.001$) secretion of TNFa/IL10 [day-2 (TNFa = 1779.7±327.5), and (IL10 = 5949.1±1425.9)] secretion in comparison to control SFNCM [day-2 (IL10 = 2352.3±108.1), and (TNFa = 304.7±37)]. However, IL10 neutralisation from

SFCM with specific IL10 polyclonal antibody resulted in significant ($p<0.001$) downregulation of IL10/TNFa [day-2 (IL10 = 798.4±90.5), and (TNFa = 735.6±68.6)] secretion compared to SFCM [day-2 (IL10 = 6500±1129.2), and (TNFa = 373.2±21.2)]. Moreover, TGFb added to SFNCM induced significant ($p<0.0001$) upregulation of both TNFa secretion [day-2 (TNFa = 1040.9±108.6)] with no effect ($p>0.05$) on IL10 [day-2 (IL10 = 3585.4±1700)] secretion compared to SFNCM [day-2 (IL10 = 2352.3±108.1), and (TNFa = 304.7±37)].

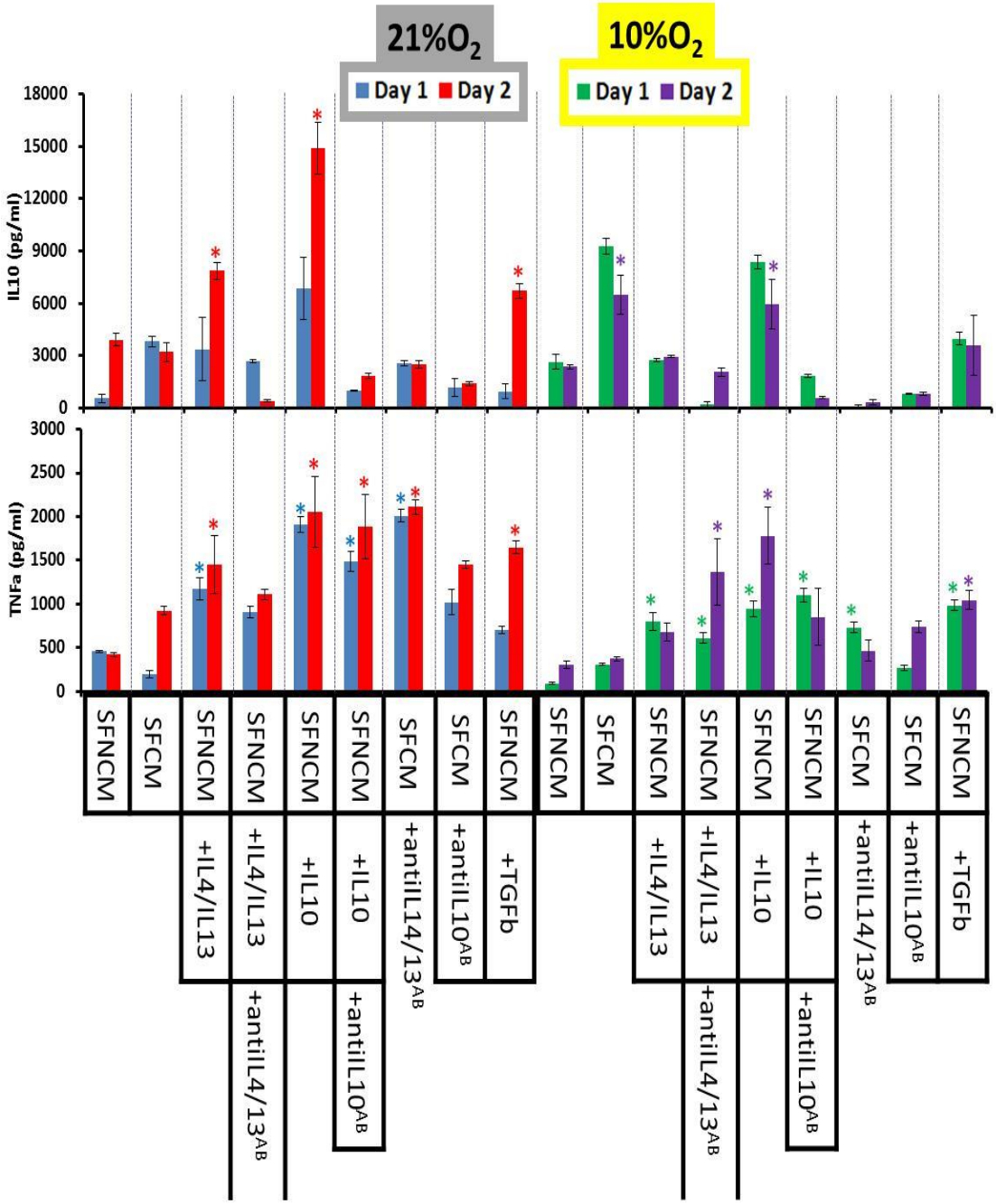

Figure 5-14. Evaluating the role of anti-inflammatory cytokines in the mode of action of SFCM based on TNFa/IL10 markers.

ELISA-based assay for detection of IL10/TNFa in the THP-1^{+PMA} secretome profile following their culture in 21%O_2 and 10%O_2. THP-1 cultured under different culture media in presence or absence of 4 anti-inflammatory cytokines (IL4, IL10, IL13, and TGFb) in SFNCM and in SFCM. SFCM tested before and after neutralisation of these cytokines with their specific polyclonal antibodies in comparison to control groups (SFCM and SFNCM). Data are expressed as mean±SD, each result represent a replicate of 3 independent experiments (n=3). One-way ANOVA were conducted with Tukey's test to determine the pairwise significant differences, *P<0.001 as compared to SFNCM and SFCM. *colour indicates significant differences in this culture media compared to both SFNCM and SFCM.

5.6 Discussion

hMSCs are currently utilised in the therapy of some chronic diseases including Graft versus Host disease[5,6], ischemic heart disease[228,229], Crohn's disease[230], diabetes mellitus[231], and rejection reaction following organ transplantation[232,233]. These diseases all share inflammation as an underlying pathology. Early *in vitro* studies on the activity of MSCs on immune cells mainly focused on cells derived from lymphoid lineages (T cells, B cells, and NK cells) with little or no attention paid for the cells from myeloid lineages particularly monocyte/macrophage system[179]. Macrophages are the key factor in initiation and propagation of an immune reaction towards antigen presentation (pro-inflammatory action) or regeneration (anti-inflammatory action)[174]. *In vitro*[234,98] and *in vivo*[96] studies have revealed that MSCs generate a macrophage with an immunoregulatory activity. The objective of this study is to confirm that SFCM could replace MSCs in the reprogramming of the differentiation of the macrophage and ultimately the fate of the immune response together with identification of the factors responsible for the mode of action. Finally, we tested the hypothesis that the *in vitro* recreation of an *in vivo*-like environment may modulate the secretome of hMSCs and ultimately the reparative action of SFCM on macrophage by reprogramming the THP-1 cell immune-phenotyping. Therefore, we explored THP-1 activated in 10% O_2 (approximately close to the circulation oxygen tension[43]) versus 21% O_2 in SFCM collected from hMSCs cultured in either 2% O_2 or 21% O_2.

Oxygen is an important parameter to consider for isolation, recovery, culture, and experimentation for both hMSCs and *in vitro* immune response models. Physioxia is the characteristic feature of the MSCs resident microenvironment, dwelling under gradient hypoxia in comparison to the systemic milieu. However, *in vivo* localised microenvironment determines the hypoxia, such as, bone marrow (1-6% O_2), adipose tissue (2-8% O_2), and neural tissues (1-8% O_2)[32]. Endogenous tissues and organs are under higher oxygen tension (4-14% O_2) than MSCs, however, it is still lower than the ambient oxygen tension (~21% O_2)[31]. Moreover, inflammation stimulates the coagulation cascade initiating a localised hypoxia environment resulting in exposure of localised macrophage to hypoxia during their activation phase[36]. Furthermore, phagocytosis is a characteristic function of macrophages and the overall processing of engulfment and digestion of invader particles is oxygen dependent, the oxygen requirement for phagocytosis increases and this phenomena is known as a respiratory burst where oxygen and nitrogen free radicals are generated serving as the bases of the defence mechanism[235]. However, an anaerobic situation has no negative impact on phagocytosis processing suggesting that the mechanism of phagocytosis is multimodal. In the hypoxia environment microbial killing is performed based on the production of toxic acidic compounds to the microbe or their deprivation from important cofactor metals, such as iron[236]. In the present study, MSCs were isolated and continuously sub-cultured in either 21% O_2 or 2% O_2 conditions and the conditioned media generated transferred to the relevant oxygen tension of the monocyte cell line model. THP-1 poorly withstood both 2% O_2 and 5% O_2 environments displayed strong culture characteristics under 10% O_2.

The stimulation of the macrophage begins with the initiation of the immune response by antigen recognition, engulfment, digestion, and processing. Macrophage responses to stimuli are associated with modulation in different cellular aspects, including morphology, polarisation, gene expression, and proliferation. Macrophages are tissue-specific showing differences in their morphology and nomenclature relevant to their resident tissues, such as Kupffer cells, microglia cells, alveolar macrophages, and Langerhans cells. Despite that, they share common properties regarding their functionalities, either eliciting (M1 macrophage) or dampening (M2 macrophage) the immune response[175]. The THP-1 cell line is a monocyte cell line that proliferated normally in growth media as suspension cells,

following a normal trend of cell line growth showing lag, log, and stationary phases. However, their proliferation is blocked by their activation upon exposure to PMA and the activated cells are attached to the culture plastic[237]. However, THP-1 activation with PMA has no impact on their differentiation, indicating that their differentiation is mainly based on localised cytokine environment, THP-1 cells exposed to PMA showed no expression of M1 or M2 markers; THP-1 cells showed minimal IL10/TNFa secretion and low CD14 expression[173] (Figure 5-15).

THP-1 macrophages are induced by PMA to differentiate into M0[227], their terminal differentiation requires the presence of cytokines; pro-inflammatory cytokines stimulate their differentiation into M1 macrophage while pro-healing cytokines stimulate their differentiation into M2[173]. In the present study, THP-1 were induced to achieve terminal differentiation in SFCM when compared to SFNCM, however, the differentiation phenotype was induced in an oxygen-dependent manner. Hence, activated THP-1 cells in SFCM collected from 21% O_2 cultured hMSCs lead to the production of an increased M1:M2 differentiation ratio while SFCM collected from hypoxia (2% O_2) cultured hMSCs lead to the production of a greater M2:M1 differentiation ratio. THP-1 activated in SFCM collected from hypoxia (2% O_2) cultured hMSCs induces more M2 macrophages indicated by their elongated spindle shape, increased IL10 secretion, and highly positive surface marker expression of CD36, and CD14, when compared with THP-1, activated in SFNCM as a control group. Conversely, THP-1 activated in SFCM collected from 21% O_2 cultured hMSCs induced more M1 macrophage differentiation indicated by their pancake-like shape, increased TNFa secretion and highly positive surface marker expression of CD197 when compared with THP-1 activated in SFNCM as a control group (Figure 5-15).

The morphological changes associated with macrophage differentiation have been related to cytoskeleton changes in the geometrical shape of the macrophage following their exposure to biochemical stimuli. A study conducted by McWhorter et al.[238] reported that macrophage differentiation is under the control of the biochemical cues from their localised environment. The study concluded that the macrophage exposure to proinflammatory factors, such as, LPS/IFNγ promoted a pancake shape phenotype while

prohealing factors, such as, IL4/IL13 promoted an elongated spindle shaped morphology. In the present study, activated THP-1 in SFNCM showed adherence potential without changing their morphological appearances, such as, shape and size. However, in SFCM the activated THP-1 cells were enlarged in size in 21% O_2 and 10% O_2. However, the hypoxic (2% O_2) SFCM promoted an elongated spindle-shape morphology indicating healing and regenerative potential of SFCM collected from hypoxia (2% O_2) while normoxic (21% O_2) SFCM modulated their morphology to a pancake-shape indicating a proinflammatory potential of normoxic (21% O_2) SFCM (Figure 5-15). These results confirm the anti-inflammatory and regenerative potential of SFCM collected from 2% O_2 versus 21% O_2. This highlights the importance of *in vitro* culture conditions on cell behaviour including their proteomic translational profile. These morphological changes were subsidised by the cell secretome profile and their characteristic surface marker panels.

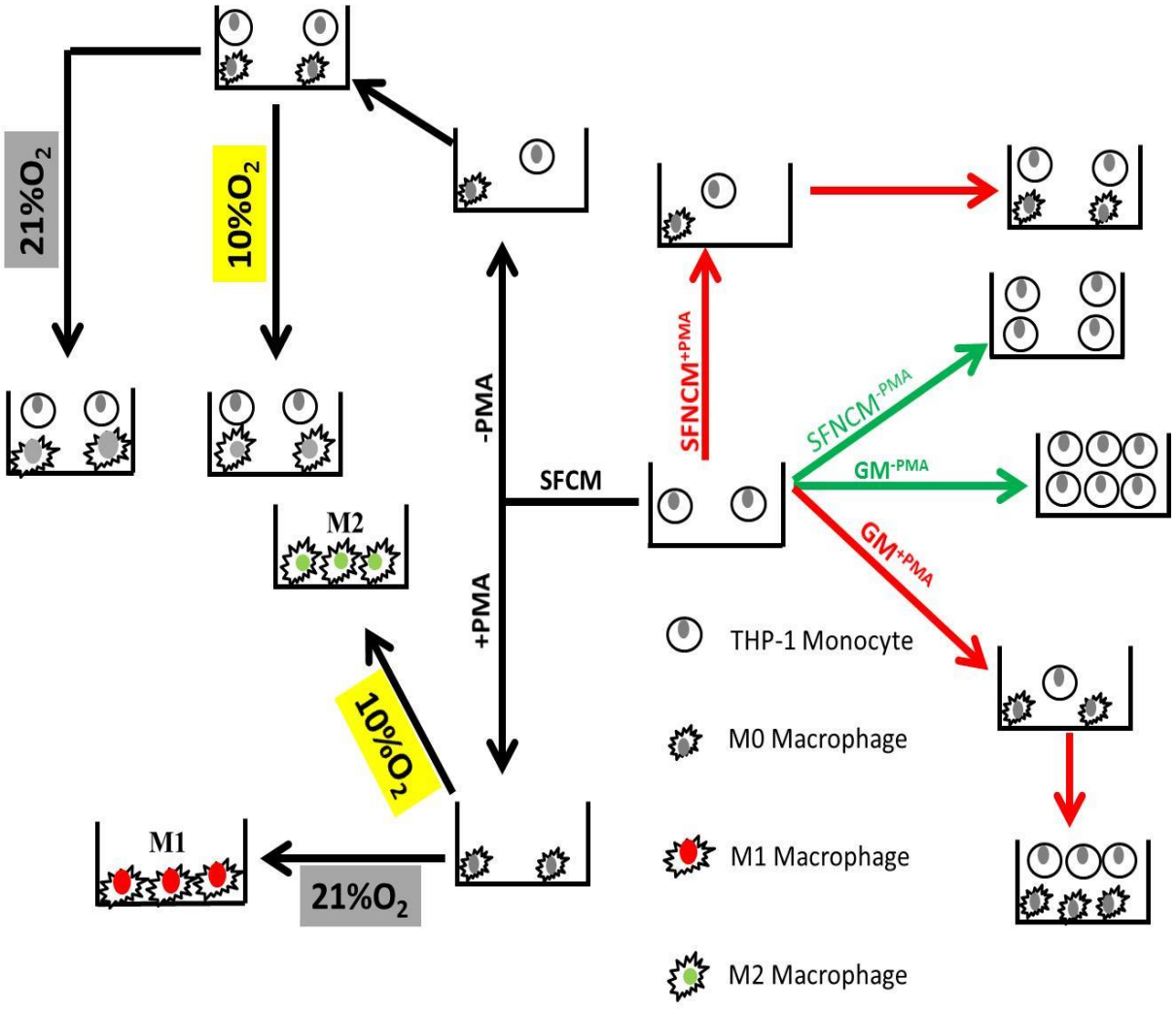

Figure 5-15. Schematic diagram simplifying the proliferation, polarisation, and differentiation of THP-1 monocyte cell line in GM, SFNCM, and SFCM.

THP-1 cells cultured in SFNCM are proliferating and their exposure to PMA results in their polarisation into M0 macrophages. SFCM promote their terminal differentiation in an oxygen-dependent manner, physioxic (10% O_2) SFCM increases M1/M2 differentiation ratio while air oxygen (21% O_2) increases M2/M1 differentiation ratio.

The differentiated macrophage exhibits modulation in their associated transcriptional profile. In the present study activated THP-1 cells were examined at the transcriptional level to detect changes in expression of chemotactic, proinflammatory and anti-inflammatory genes compared to positive control; L32 gene and GAPDH[227,237]. Activated THP-1 had a distinct chemotactic expression pattern of transcription in an oxygen-dependent manner, the measured chemotactic factors include; CCL5, CCR5, IL8, MCP1, and MIP1A, where the most affected chemotactic factor by SFCM was CCR5 showing downregulation in expression in comparison to SFNCM. This downregulation was more obvious in hypoxic (2% O_2) SFCM regardless of activation. Correspondingly, hypoxic (2% O_2) SFCM suppressed proinflammatory transcriptional profiles indicated by downregulation of TNFa, IL1B, and IL12B transcript versus normoxic (21% O_2) SFCM. Conversely, hypoxic (2% O_2) SFCM upregulated IL10 transcription versus normoxic (21% O_2) SFCM[227]. The transcriptional profile induced by SFCM has been translated into the proteomic level by measurement of IL10 and TNFa as anti-inflammatory and pro-inflammatory markers, respectively (Figure 5-15). The concentration of IL10 and TNFa were quantified using ELISA technique, the results indicated that the normoxic (21% O_2) SFCM induces THP-1 secretion of TNFa in comparison to hypoxic (2% O_2) SFCM, GM, and SFNCM while hypoxic (2% O_2) SFCM induces THP-1 secretion of IL10 in comparison to normoxic (21% O_2) SFCM, GM and SFNCM. The differences between proliferation of THP-1 in SFCM versus SFNCM should be taken to consideration. The THP-1 cell count in SFNCM was higher than that of SFCM, hence a fraction of secreted TNFa and IL10 could be related to *de novo* cellular synthesis. Therefore, the results were also presented by determination of the IL10 and TNFa per cell and plotting them against each other to exclude any extra amount of released cytokines related to their *de novo* synthesis.

Macrophage differentiation can be identified by exploring their distinct surface marker expression[98,174,175]. Activated and non-activated THP-1 cells, in SFCM versus SFNCM in both 21% O_2 and 10% O_2 conditions, were tested for their surface marker expression of a panel of antibodies, including positive ($CD45^+$, $CD73^+$, $CD105^+$, $HLADR^+$), negative ($CD19^-$, $CD25^-$, $CD34^-$, $CD86^-$, $CD90^-$), and target (CD14, CD36, CD197, CD206, CD204) markers[173]. THP-1 cultured in different conditions show no modulation in positive and negative markers while alterations were clearly observed in CD14 (macrophage marker), CD197 (M1 macrophage markers), and CD36 (M2 macrophage markers). Hypoxic (2% O_2) SFCM upregulates CD14 and CD36 surface marker expression and downregulates CD197 surface marker expression confirming its potential for THP-1 induction of terminal differentiation toward M2 macrophage. Conversely, normoxic SFCM upregulated CD14 and CD197 surface marker expression and downregulated CD36 surface marker expression confirming its potential for THP-1 induction of terminal differentiation towards the M1 macrophage. The control group showed no alteration in the expression of these markers in either 21% O_2 or 10% O_2, and the positive and negative markers were tested for comparisons. CD204 and CD206 are also commonly used as M2 macrophage markers, THP-1 displayed negative expression of these markers in 21% O_2 and 10% O_2 cultured THP-1 cells. However, different studies conducted on primary macrophages to induce their terminal differentiation into M2 macrophages have utilised CD206 and CD204 as surface markers. There is no consensus on a macrophage surface marker panel to identify the distinct differentiation toward M1 or M2 macrophage, CD36 and CD163 are considered as an M2 specific marker and CD197 as an M1 macrophage marker and CD14 as a monocyte to macrophage differentiation marker. The present study has utilised multiple cellular aspects to confirm the direction of differentiation toward M1 or M2 macrophage-based on proliferation aspects, morphological characteristic, secretome profile, and surface marker expression[96,139,236]. The consistency in the outcome of these different tests on the same cell line using various conditions could indicate the prospective direction of the subsequent steps in the future application of the SFCM and/or hMSCs in the therapeutic application of inflammatory ailments.

Previous studies have reported that the macrophage localised milieu determines their functional differentiation towards definitive types whether M1 or M2[173,139]. Studies have claimed that anti-inflammatory cytokines, such as IL4/IL13 are responsible for the direction

of the stimulated macrophages toward M2 terminal differentiation while proinflammatory factors, such as, LPS/IFNγ/TNFa are responsible for the direction of macrophages toward M1 terminal differentiation. These findings are applicable in both *in vivo* and *in vitro* studies[179,173,139,174]. In an attempt to identify the mode of action of SFCM in modulation of macrophage differentiation toward either M1 or M2, the present study characterised the role of 4 anti-inflammatory cytokines (IL4, IL10, IL13, and TGFb) on activated THP-1, either individually or in combination; To identify the mode of action, these cytokines were added to SFNCM and were blocked from SFCM by neutralising their activity using specific polyclonal antibodies. The study concluded that these cytokines induce much lower action than SFCM in the induction of terminal differentiation indicated by low TNFa/IL10 secretion and minimal CD14/CD36/CD197 surface marker expression in comparison to SFCM and SFNCM. The dose-response curve indicates that IL4/IL13 individually show minimal adherence potential, therefore, a combination of IL4/IL13 was based to identify the role of both cytokines in the induction of differentiation. IL10 and TGFb alone show a slight induction of M2 differentiation indicated by slight increase in IL10 secretion and CD36 expression (M2 markers)[139].

SFCM collected from MSCs exert their immunomodulation through several anti-inflammatory and pro-inflammatory cytokines. IL10 is present in 21% O_2 and 2% O_2 collected SFCM and appears to be the principle anti-inflammatory cytokine and exerts its immunosuppression activity on different monocytes/macrophages cellular aspects, such as chemokine synthesis, NO synthesis, and HLA-DR expression and costimulatory molecules such as IL12 and CD80/CD86[194]. Combinations or individual application of IL4/IL13 have been used extensively to direct monocytes and/or THP-1 differentiation toward regulatory rather than pro-inflammatory subtypes[139,173]. TGFb is a growth factor presents in SFCM and might have a role in modulation of immune response[139]. The post-receptor translation pathways for these individual pathways include STAT3 for IL10, STAT6 for IL4 and IL13 and TGFb induces Smad pathways. However, in the present study, these cytokines individually or in combination failed to induce THP-1 differentiation towards certain lineages in comparison to SFCM.

Collectively, the present study confirmed that SFCM induced terminal macrophage differentiation in an oxygen-dependent manner where individual anti-inflammatory cytokine or a combinational cytomix had no effect on the THP-1 secretome profile and surface marker expression. Moreover, neutralisation of these cytokines from SFCM results in incomplete restoration of pro-macrophagic status. These anti-inflammatory or pro-inflammatory cytokines have a minimal role in THP-1 differentiation when compared to SFCM and this might be partially linked to the growth factors offered by SFCM which represent important initial stimuli to induce the conversion of monocytic THP-1 cell line and their transfer to macrophage M0 status. This later step is important for subsequent direction of macrophage into either M1 or M2 based on the presence of pro-inflammatory or anti-inflammatory cues, respectively[173,139]. These findings suggested that further studies required identifying the cytokine or cytomix required to direct the macrophage-lineage differentiation.

Keele UNIVERSITY

Chapter 6

Summative discussion, conclusions, and further work

6.1 Summative discussion

Bone marrow cavity is a beehive-mimic structure composed of niches, which are highly condensed environment containing various kinds of stromal cells, including endothelial cells, reticulocytes, and osteoblasts. Niches structure play an indefinite role in maintaining cell survival, proliferation, and differentiation of hematopoietic progenitor cells[239]. A fraction of cells within the bone marrow called mesenchymal stem cells occupy the stromal compartment of bone marrow and some other tissues[86,4]. These cells are plastic-adherent, elongated cells, and have proliferation capacity forming colonies (CFU-F). They are also characterised by their multipotent differentiation potential into bone, cartilage, ligament, tendon, fat, and muscle together with the expression of MSCs surface markers [$CD73^+$, $CD90^+$, and $CD105^+$], and lack the expression of haematopoietic markers [$CD14^-$, $CD19^-$, $CD34^-$, $CD45^-$, and $HLA\text{-}DR^-$][17].

The efficacy of MSCs in regeneration might be partially linked to their released bioactive factors; such as cytokines, which are either secreted constitutively or regulatory, despite that, priming with different *in vitro* stimuli could modulate the quantity of these factors resulting in improved or modulated potency of the cell-based or cell-devoid biotherapy. Therefore, socialising MSCs with hypoxia (<5% O_2) reprogrammed their intracellular machinery to synthesise/secrete more protein-based constituents which might result in enhancement of the potency of cell-devoid biotherapy. Furthermore, it could lead to overcoming the translation drawback associated with cell-based therapy; replicative senescence, poor homing potential, and genetic instability[38]. Optimization of *in vitro* culture condition might result in production of biological product which might surrogate the cell-based therapy or might optimise the efficacy of cell-based therapy on localised target tissue, therefore, a comprehensive review of all culture condition is of paramount important and *in vitro* recreation of *in vivo* stem cell niche through application of various biochemical and biophysical stimuli on *in vitro* cultured cells might lead to production of ideal MSCs-based pharmaceutical dosage form with optimised efficacy for regenerative therapy[31].

In this study, serum free-conditioned media (SFCM) were used as a model to characterize the immune sentinels function of MSCs[156]. Proteomic analysis indicates that SFCM of hMSCs contain various cytokines which may play an important role in the suppression of inflammation and that the composition and concentration of SFCM is oxygen dependent; intermittent hypoxia (2% O_2) represents a rich resource for paracrine factors. The therapeutic effectiveness of SFCM at cellular levels reflected by its potential efficacy on *in vitro* cell line models; SFCM suppresses T cell line model in oxygen independent manner while the modulation in macrophage terminal differentiation seems to be oxygen sensitive.

The bone marrow composed of structural subunits called niches. The niche is highly sophisticated environment providing support to monitor MSCs survival, proliferation, fate, and differentiation[28]. The compartments inside the niches are characterised by low oxygen tension (1-6% O_2) in comparison to elsewhere[29,30]. Accordingly, MSCs in the *in vitro* cultured condition should be optimized to meet these *in vivo* milieu, however, most research centres are culturing their cells in normoxia (~20% O_2) environment ignoring the role of oxygen in the maintenance of survival, senescence, and genetic changes[240]. Moreover, the injured tissues are associated with activation of coagulation cascade which is reciprocally interacted with oxygen tension[36]. Interestingly, monocyte-macrophage differentiation ensues with the initiation of hypoxia in injured vicinity[43] (Figure 6-1). Therefore, culturing hMSCs under hypoxia (<5% O_2) environment to mimic the *in vivo* milieu might significantly change MSCs behaviour including their paracrine and immunomodulatory properties.

The impact of hypoxia on the stem cell biology including their transcriptional profile has been studied previously and these studies have confirmed that hypoxia dedicated to modulate the paracrine factor secretion[58,36,209]. Noteworthy to mention upregulation of VEGF, MIP, and leptin and downregulation of IGF1 by hypoxia (0.5-1.5% O_2) confirmed by microarray screening of bone marrow-derived hMSCs[58,164]. Moreover, hypoxia (1.5% O_2) modulation of stem cells paracrine activity at transcriptional level extends beyond the source of MSCs to affect umbilical cord blood-derived MSCs[164], adipose-derived MSCs[163], and MSCs derived from xenogeneic sources[162]. This effects have been translated to the proteomic levels indicated by modulation in the secretome profile following exposure to hypoxia (<5% O_2) in comparison to normoxia (21% O_2) despite differences in the source of

isolated MSCs; adipose[56,57] or bone marrow[58,59,60], variation in conditioning periods; short or long, and duration of exposure to hypoxia; transient hypoxic (O2 < 5%) exposure of adipose-derived MSCs[56]. Leptin and VEGF are considered as a hypoxia biomarkers and their overexpression in a hypoxic environment has been reported[58]. Moreover, injury of tissues has been associated with hypoxia stimulating normal endogenous compensatory defence mechanism protecting the cells from deleterious impacts of injury [153,56,54].

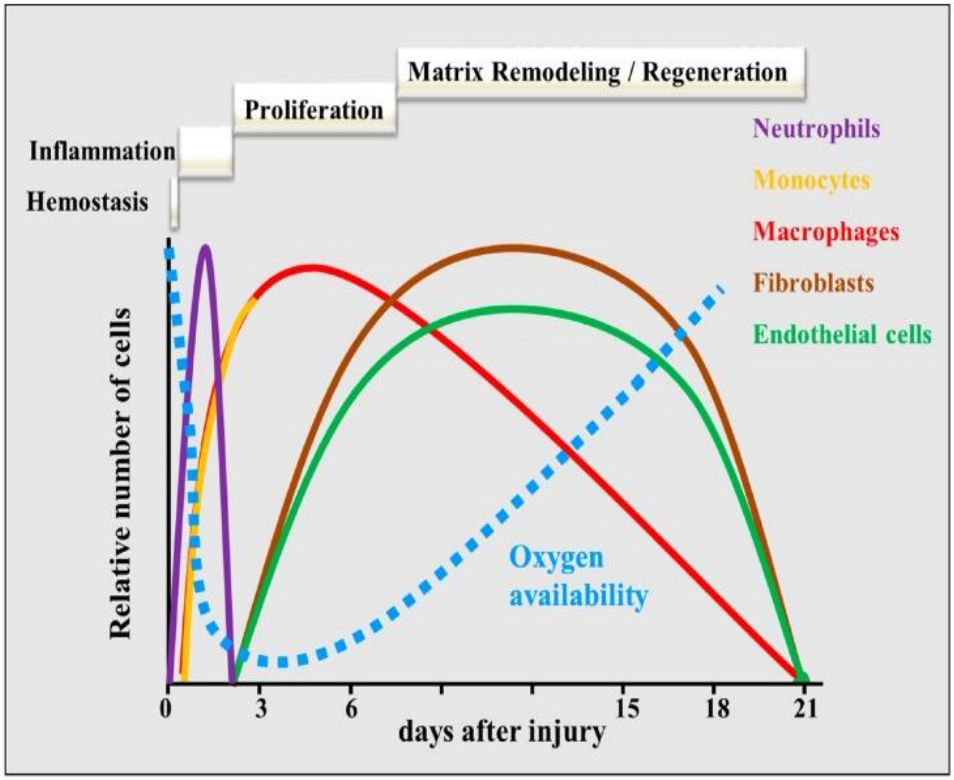

Figure 6-1. A schematic overview of the phases of wound healing over time.

After the initial homeostasis phase, neutrophils and macrophages dominate the inflammation phase, whereas fibroblasts and endothelial cells are predominant during the proliferation phase. During the remodelling phase, fibroblasts and endothelial cells undergo apoptosis or exit the wound. Finally, the granulation tissue and vascular network remodel and mature, which can last for years. The dotted blue line indicates the time course of oxygen availability.

Reprinted from Nauta TD *et al*[43], 2014, with permission from International Journal of Molecular Sciences.

Upon exposure to invader particles, resting T cell undergoes polarisation with subsequent IL2 production, the released IL2 binds to an IL2 cell surface receptor of engaged T cell inducing mTOR pathway resulting T cell proliferation[212,215]. The localised cytokine microenvironment determines the polarisation of T cell into either Th1 or Th2 cells; for

instance, presence of proinflammatory cytokine IL12 in the surrounding milieu promotes Th1 differentiation while IL4 mediates Th2 differentiation[192]. Likewise, the presence of IL10 in the T cell milieu promotes differentiation toward Treg. It has been confirmed that these cytokines promote their actions through latent proteins involving Janus Kinase (JAK) and signal transducer and activator of transcription (STAT)[168]. Different anti-inflammatory cytokines; such as, IL4, IL10, and IL12, use various post-receptor translation pathways to induce their effector function; such as, STAT6, STAT3, and STAT4, respectively[213]. The present study tested the immune response of activated Jurkat T cells in hMSCs secretome; collected as SFCM from hypoxia (2% O_2) and normoxia (21% O_2) environment. The results confirmed that SFCM effectively suppressed the overall immune response indicated by the reduction of proliferation and polarisation. The modulation of immune response was achieved in both hypoxia (2% O_2) and normoxia (21% O_2) collected SFCM. This *in vitro* model is considered as a mirror reflecting the behaviour of the SFCM application on *in vivo* T cells and might more precisely reflect the therapeutic efficacy of SFCM on the suppression of inflammatory diseases and subsequently potentiate tissue regeneration.

Immortalised cells are commonly used for research instead of primary cells. They provide several advantages, such as, they are cost-effective, easy to use, bypass the regulations and ethics associated with the use of human or animal primary cells. Moreover, cell lines are characterised by homogeneity providing pure population of cells resulting in consistent sample and reproducible results[241,242]. However, cell lines are genetically modulated which might alter their phenotype, native functions, and their responsiveness to stimuli. Moreover, cell line sub-culturing can further cause genotypic and phenotypic modification over long period of time and genetic drift can cause heterogeneity in cell culture at certain timepoint. Hence, cell lines are not a mirror reflecting the behaviour of primary cells and may provide discrepant results[241].

The limitations of long-term cell lines, such as, Jurkat are recognised, and the relative pros of mouse models for studies of T cell development and function are well authenticated. Although cultured immortalised T cell lines (e.g. Jurkat) may have lost some of their earlier characteristics, however, they keep several remarkable strengths compared with the *in vivo* model systems[243]. First, the production of transgenic and knockout mice consumes

substantial time and facilities; therefore, mouse models are not a reasonable first choice for many research centres. Second, germline gene disruptions that involve key signalling proteins frequently lead to blocks in T-cell development[244]. Although such developmental blocks provide important information in their own right, investigations into the function of the target protein in antigen-responsive, mature T cells become difficult or impossible to carry out[244]. Recently Jurkat cells were shown to be faulty in the expression of two lipid phosphatases, PTEN (phosphatase and tensin homologue) and SHIP (SH2-domain-containing inositol polyphosphate 5' phosphatase). The biological activity of SHIP deficiency in T cells are inadequately understood, however, Loss of PTEN leads to constitutive activation of the phosphatidylinositol 3-kinase (PI3K)-signalling pathway, which includes the protein serine-threonine kinase, AKT, and the PTK IL2-inducible T-cell kinase (ITK) in Jurkat cells[243,244].

A drawback of the use of cell lines is that the malignant background and the cultivation of cells under controlled conditions (outside their natural environment) might possibly result in different sensitivities and responses compared to normal somatic cells in their natural environment[245]. Also, possibly relevant interactions between the target cells and surrounding cells, as in natural tissues, cannot be easily mimicked. However, in vitro co-cultivation of THP-1 cells with neighbouring cells might be an option to overcome this drawback[246].

Unintended effects from in vitro differentiation of THP-1 macrophages, for instance, up-regulation of specific genes during the differentiation process might overwhelm mild effects of specific stimuli, particularly food-derived bioactive compounds[237], or can cause an increased sensitivity to Lipopolysaccharide (LPS)[247,248]. However, this might be less of an issue if strong stimuli, e.g. drugs or chemical compounds, are applied.

A number of publications have compared responses between the THP-1 monocytes and monocytes isolated from human peripheral blood mononuclear cells (PBMC). These studies have included a variety of stimuli and findings as shown in table 6-1. In most cases, both types showed relatively similar response patterns. However, differences have been reported in the degree of gene expression and cytokine secretion, as well as in gene expression baseline.

Table 6-1 Examples of studies with compared responses from THP-1 monocytes vs. human PBMC–monocytes.

Stimulation condition	Findings
LPS from *Pseudomonas aeruginosa* or *Escherichia coli* 10 ng/ml in time intervals up to 24 h.	PBMC monocytes produced greater amount of inflammation-related cytokines e.g. TNFa, IL6, IL8 and IL10 than do THP-1 monocytes[245].
LPS from *Salmonella minnesota* 100 ng/ml for 3 h	Up-regulation of TLRs 1, 2 and 4 in THP-1 monocytes. Up-regulation of TLRs 1–5 in PBMC monocytes[246].
Human oxidized low density lipoprotein 50 µg/ml for 48 h	Baseline expression levels of TNFa, IL1B, IL6, CD14 and CD68 were significantly higher in PBMC monocytes compared to THP-1 monocytes ($p<0.05$)[249].
Polysaccharide from *Ganoderma tsugae* 4 and 40 µg/ml for 0.5 h	PBMC monocytes produced IL1a and TNFa in a similar fashion to THP-1 cell response[250].
Hyper-branched polysaccharide from *Ganoderma sinense* 0.0001–1000 µg/ml for 72 h	Cytotoxicity of the test compounds (XTT proliferation assay) was observed to be similar for THP-1 and PBMC–monocytes[246].

Proper control of immune response in all direction should be the goal of stem cell therapy to achieve optimal improvement of injured tissue and determine the fate of the damaged organ. The healing or resolution phase is associated with either regeneration and restoration of normal tissue functionality or direction of the inflammation toward chronic stages involving stimulation of chronic inflammatory cells[127]. To ensue repair of damaged tissue or organ, both pro-inflammatory and anti-inflammatory signalling is recommended, and interruption with ether stimuli might be associated with disruption of tissue healing[251,252]. For instance, the tissue regeneration of musculoskeletal is interrupted when macrophages are spun by IL10 administration[253]. In skeletal muscle injury, the M1 macrophages recruit and stimulate deposition or proliferation progenitor cells while M2 macrophages stimulate differentiation i.e. M1 and M2 work together to achieve repair, dispelling the view of good (M2) and bad (M1) macrophage[127]. THP-1 macrophage induced by PMA to M0[227]. However, their terminal differentiation requires the presence of cytokines; pro-inflammatory cytokines stimulate their differentiation into M1 macrophage while pro-healing cytokines stimulate their differentiation into M2[173]. The present study tested the immune response of activated macrophage (THP-1 derived) in the hMSCs secretome; collected as an SFCM from hypoxia (2% O_2) and normoxia (21% O_2) environment. The outcome clarified that SFCM induced monocyte-to-macrophage

differentiation and hypoxia modulates the active constituents of SFCM and directs the net balance toward a regulatory rather than a stimulatory immune response through increasing the ratio of differentiation of M2/M1 macrophage in comparison to higher M1/M2 macrophage differentiation ratio obtained in normoxic SFCM (21% O_2). Generation of more M2 (regulatory) macrophage might provide a promised therapeutic tool for application of hMSCs-educated macrophage in treatment of inflammatory diseases and might lead to establishment of allogeneic M1 and M2 macrophage bank using signals from SFCM collect from hMSCs of third party donors; moreover, the scope might be extended to harness SFCM collected from MSCs of xenogeneic sources.

In an attempt to identify the actual biomolecule(s) modulating the regulatory macrophage differentiation in the secretome profile, the study tested those cytokines with prominent anti-inflammatory activity on the activated macrophage in order to identify the biomolecule which is responsible for the differentiation, if any. Cytokine-driven responses were individually determined via the addition of specific neutralising antibodies. The study concluded that, activated T cell IL2 secretion was blocked by SFCM itself and IL4, IL13, and IL10 when individually added to SFNCM. When these cytokines were neutralised individually in SFCM with their specific antibodies, the immune response was restored in IL10-devoided SFCM, suggesting that IL10 plays an immunosuppressive role in Jurkat T cell proliferation and activation by reducing the secretion of IL2. However, the molecular sites targeted by SFCM in order to achieve this effect remain unidentified; moreover, the present study is incompletely excluding the role of IL4/IL13 ligands in the immunosuppression achieved by SFCM. In addition, further investigation is required to determine the underlying mechanism(s) by which MSCs exert their immunomodulatory effect. This property may be harnessed to produce biological agents which have immunomodulatory actions similar to hMSCs, leading to the production of the “off-the-shelf” biological products. The production of such biological products will have important economical reflection by reducing the cost, obstacles, limitations, and complications of cell-based therapy.

The challenges which are associated with cytokines-based therapy are the main obstacle hindering the widespread application of this biotherapy including SFCM. Among these challenges are; variability of the product upon collection even from the same cells, SFCM is nutritionally depleted by the cells together with the presence of various unwanted waste biomolecules, and sterilisation and characterisation are recommended. Despite these cones, it's worthy to mention SFCM pros, such as, SFCM bypass some regulation ethics of translation therapy, SFCM is relatively cheap and can be produced in large quantities. Moreover, SFCM can be stored in (-80ºC), characterised, processed, and tested. Accordingly, the translation of SFCM required being revised wisely, to avoid translation of SFCM with different potency. Therefore, large scale production of MSCs and subsequent large scale production of SFCM is required to be batch consistent and each batch needs to be tested individually using certain markers, such as, IL10, TNFa, and CD markers as target markers to ascertain that the batch is immunosuppressing.

6.2 Conclusion:

One of the promising tools in the treatments of the disease is stem cell therapy. A number of different mechanisms have been proposed including direct cell-cell contact and paracrine factors, including cytokines, chemokines, chemical messengers, enzymes, and extracellular vesicles. Most of these factors play a great role in immune-mediated diseases, such as, graft versus host diseases, autoimmune diseases, and neurodegenerative disorders. However, the injected dose of the cells is partially retained and engrafted in the target tissues confirming that paracrine factors are the key in the mechanism of tissue regeneration and immunomodulation. To overcome the limitation of the cell count, stem cells are expanded *in vitro*; hypoxia (<5% O_2) recreation of *in vivo* mimic environment was included as one of the parameters in the present study and the achieved results show modulation in paracrine contents and potency. However, a number of different parameters were absent in the present study and represent confounding factors, such as, 3D context, extracellular matrix (structure, topology, and stiffness), and physical factors (flow shear, compression, stretch, and electrical signals). These parameters should be included in the context of stem cell translation therapy.

Testing the efficacy of SFCM on *in vitro* immune cell line models including, T cell line and macrophage cell line. The results confirmed a positive potency of SFCM on modulation of *in vitro* immune response via inhibition of T cell proliferation/polarisation and modulation of macrophage activation/differentiation toward regulatory rather than stimulatory. However, hypoxia (2% O_2) collected SFCM show more regenerative potential than normoxia (21% O_2) collected SFCM, indicated by modulation of M2:M1 macrophage differentiation. However, these results necessitate translation into primary cells to mirror the *in vivo* environment and to confirm the achievement of the same results of the cell line models.

IL10 present in SFCM in sufficient amount and is considered as an important anti-inflammatory cytokine. This thesis has confirmed the importance of IL10 in the suppression of T cell line model and its neutralisation from SFCM associated with restoration of immune response irrespective of the presence of other anti-inflammatory cytokines (IL4, IL13, and TGFb) which showed an only negligible contribution to the overall immunosuppression of SFCM. However, neutralisation of IL10 from SFCM might be associated with imbalances between pro-inflammatory/anti-inflammatory biomolecules and hence revoking the immunosuppression; suggesting that IL10 receptor gene knockout might give a clear-cut indication about the mode of action of SFCM. The role of these anti-inflammatory cytokines in macrophage M1/M2 differentiation and/or phagocytic activity showed discrepant results indicating that SFCM is a complex mixture of different biomolecules with an overall beneficial role in modulation of inflammatory ailments.

6.3 Implications for further work:

1. Identification of IL10 linked post-receptor translation pathway (STAT3) by knock-down STAT3 gene using Jurkat cell line as an *in vitro* model.

2. Identification of a chemical compound having IL10-mimic action through screening a library of chemical compounds; which have a chemical side chain that is thought to interact with IL10 receptor active epitope. Identification of such compound may change some

aspect of cell-based therapy into a small chemical compound having a therapeutic action which is partially resembling the cell-based therapy; using Jurkat cell line as an *in vitro* model (e.g. Tofacitinib, Ruxolitinib).

3. Collection of SFCM from MSCs spheroids versus monolayer might induce stronger immunosuppression; this study could be used as a template control for subsequent *in vitro* creation of *in vivo*-mimic environment.

4. Augmentation of hMSCs paracrine activity via priming with a cocktail of proinflammatory cytokines and/or modification of certain specific gene (*in vitro* hMSCs engineering).

5. Rationalization of IL4/IL13 receptor-ligand overlapping; receptor-ligand bi-specificity phenomena, using Jurkat cell line as an *in vitro* model.

6. Isolation of exosomes from SFCM, identification of its constituents and characterization of its immunomodulatory properties.

7. Translation of SFCM into *in vivo* by injecting the SFCM into a mice model of chemically-induced inflammatory diseases (e.g. rheumatoid arthritis and Crohn's disease).

8. Preparation of SFCM-based pharmaceutical dosage form with sustained release properties; due to a characteristic short duration of action of cytokines, through the incorporation of concentrated SFCM into a gel system leading to more convenient dosing intervals and suitable dosage form for topical application.

9. Translation of *in vitro* MSCs-educated primary immune cells into preclinical animal studies; application of *in vitro* hMSCs-modulated primary leukocyte (T cells and monocytes into Tregs and M2 macrophages) into mice model of chemically induced inflammatory diseases.

10. Controlling the direction of SFCM toward anti-inflammatory and regenerative direction via capturing the proinflammatory factors with their specific neutralising antibodies and vice versa.

Keele UNIVERSITY

-----References-----

1- Raoufi MF, Tajik P, Dehghan MM, Eini F, Barin A. Isolation and differentiation of mesenchymal stem cells from bovine umbilical cord blood. Reproduction in domestic animals. 2011 Feb 1;46(1):95-9.

2- Horwitz EM, Prockop DJ, Fitzpatrick LA, Koo WW, Gordon PL, Neel M, Sussman M, Orchard P, Marx JC, Pyeritz RE, Brenner MK. Transplantability and therapeutic effects of bone marrow-derived mesenchymal cells in children with osteogenesis imperfecta. Nature medicine. 1999 Mar 1;5(3):309-13.

3- Amado LC, Saliaris AP, Schuleri KH, John MS, Xie JS, Cattaneo S, Durand DJ, Fitton T, Kuang JQ, Stewart G, Lehrke S. Cardiac repair with intramyocardial injection of allogeneic mesenchymal stem cells after myocardial infarction. Proceedings of the National Academy of Sciences of the United States of America. 2005 Aug 9;102(32):11474-9.

4- Dominici ML, Le Blanc K, Mueller I, Slaper-Cortenbach I, Marini FC, Krause DS, Deans RJ, Keating A, Prockop DJ, Horwitz EM. Minimal criteria for defining multipotent mesenchymal stromal cells. The International Society for Cellular Therapy position statement. Cytotherapy. 2006 Dec 31;8(4):315-7.

5- Le Blanc K, Rasmusson I, Sundberg B, Götherström C, Hassan M, Uzunel M, Ringdén O. Treatment of severe acute graft-versus-host disease with third party haploidentical mesenchymal stem cells. The Lancet. 2004 May 1;363(9419):1439-41.

6- Le Blanc K, Frassoni F, Ball L, Locatelli F, Roelofs H, Lewis I, Lanino E, Sundberg B, Bernardo ME, Remberger M, Dini G. Mesenchymal stem cells for treatment of steroid-resistant, severe, acute graft-versus-host disease: a phase II study. The Lancet. 2008 May 16;371(9624):1579-86.

7- Donizetti-Oliveira C, Semedo P, Burgos-Silva M, Cenedeze MA, Malheiros DM, Reis MA, Pacheco-Silva A, Câmara NO. Adipose tissue-derived stem cell treatment prevents renal disease progression. Cell transplantation. 2012 Aug 1;21(8):1727-41.

8- Semedo P, Palasio CG, Oliveira CD, Feitoza CQ, Gonçalves GM, Cenedeze MA, Wang PM, Teixeira VP, Reis MA, Pacheco-Silva A, Câmara NO. Early modulation of

inflammation by mesenchymal stem cell after acute kidney injury. International immunopharmacology. 2009 Jun 30;9(6):677-82.

9- Kubo N, Narumi S, Kijima H, Mizukami H, Yagihashi S, Hakamada K, Nakane A. Efficacy of adipose tissue-derived mesenchymal stem cells for fulminant hepatitis in mice induced by concanavalin A. Journal of gastroenterology and hepatology. 2012 Jan 1;27(1):165-72.

10- Bouffi C, Bony C, Courties G, Jorgensen C, Noel D. IL-6-dependent PGE2 secretion by mesenchymal stem cells inhibits local inflammation in experimental arthritis. PloS one. 2010 Dec 7;5(12):e14247.

11- Popp FC, Eggenhofer E, Renner P, Slowik P, Lang SA, Kaspar H, Geissler EK, Piso P, Schlitt HJ, Dahlke MH. Mesenchymal stem cells can induce long-term acceptance of solid organ allografts in synergy with low-dose mycophenolate. Transplant immunology. 2008 Nov 30;20(1):55-60.

12- Omatsu Y, Sugiyama T, Kohara H, Kondoh G, Fujii N, Kohno K, Nagasawa T. The essential functions of adipo-osteogenic progenitors as the hematopoietic stem and progenitor cell niche. Immunity. 2010 Sep 24;33(3):387-99.

13- Dazzi F, Ramasamy R, Glennie S, Jones SP, Roberts I. The role of mesenchymal stem cells in haemopoiesis. Blood reviews. 2006 May 31;20(3):161-71.

14- Abumaree M, Al Jumah M, Pace RA, Kalionis B. Immunosuppressive properties of mesenchymal stem cells. Stem Cell Reviews and Reports. 2012 Jun 1;8(2):375-92.

15- Bose B. Past, Present and Future of Stem Cells in Regenerative Medicine. Feature Journal; 24-27.

16- Kim HS, Choi DY, Yun SJ, Choi SM, Kang JW, Jung JW, Hwang D, Kim KP, Kim DW. Proteomic analysis of microvesicles derived from human mesenchymal stem cells. Journal of proteome research. 2011 Dec 28;11(2):839-49.

17- Horwitz EM, Andreef M, Frassoni F. Mesenchymal stromal cells. Current opinion in hematology. 2006 Nov;13(6):419.

18- Augello A, Kurth TB, De Bari C. Mesenchymal stem cells: a perspective from in vitro cultures to in vivo migration and niches. Eur Cell Mater. 2010 Sep 1;20(121):e33.

19- Phinney DG, Prockop DJ. Concise review: mesenchymal stem/multipotent stromal cells: the state of transdifferentiation and modes of tissue repair—current views. Stem cells. 2007 Nov 1;25(11):2896-902.

20- Potian JA, Aviv H, Ponzio NM, Harrison JS, Rameshwar P. Veto-like activity of mesenchymal stem cells: functional discrimination between cellular responses to alloantigens and recall antigens. The Journal of Immunology. 2003 Oct 1;171(7):3426-34.

21- Ryan J, Barry F, Murphy JM, Mahon BP. Interferon-γ does not break, but promotes the immunosuppressive capacity of adult human mesenchymal stem cells. Clinical & Experimental Immunology. 2007 Aug 1;149(2):353-63.

22- Chan WK, Lau AS, Li JC, Law HK, Lau YL, Chan GC. MHC expression kinetics and immunogenicity of mesenchymal stromal cells after short-term IFN-γ challenge. Experimental hematology. 2008 Nov 30;36(11):1545-55.

23- William TT, Pendleton JD, Beyer WM, Egalka MC, Guinan EC. Suppression of allogeneic T-cell proliferation by human marrow stromal cells: implications in transplantation. Transplantation. 2003 Feb 15;75(3):389-97.

24- Stagg J, Pommey S, Eliopoulos N, Galipeau J. Interferon-γ-stimulated marrow stromal cells: a new type of nonhematopoietic antigen-presenting cell. Blood. 2006 Mar 15;107(6):2570-7.

25- Chan WK, Lau AS, Li JC, Law HK, Lau YL, Chan GC. MHC expression kinetics and immunogenicity of mesenchymal stromal cells after short-term IFN-γ challenge. Experimental hematology. 2008 Nov 30;36(11):1545-55.

26- Chan JL, Tang KC, Patel AP, Bonilla LM, Pierobon N, Ponzio NM, Rameshwar P. Antigen-presenting property of mesenchymal stem cells occurs during a narrow window at low levels of interferon-γ. Blood. 2006 Jun 15;107(12):4817-24.

27- Karantalis V, Hare JM. Use of mesenchymal stem cells for therapy of cardiac disease. Circulation research. 2015 Apr 10;116(8):1413-30.

28- Travlos GS. Normal structure, function, and histology of the bone marrow. Toxicologic pathology. 2006 Aug;34(5):548-65.

29- Eliasson P, Jönsson JI. The hematopoietic stem cell niche: low in oxygen but a nice place to be. Journal of cellular physiology. 2010 Jan 1;222(1):17-22.

30- Chow DC, Wenning LA, Miller WM, Papoutsakis ET. Modeling pO 2 distributions in the bone marrow hematopoietic compartment. II. Modified Kroghian models. Biophysical journal. 2001 Aug 31;81(2):685-96.

31- Haque N, Rahman MT, Abu Kasim NH, Alabsi AM. Hypoxic culture conditions as a solution for mesenchymal stem cell based regenerative therapy. The Scientific World Journal. 2013 Aug 27;2013.

32- Mohyeldin A, Garzón-Muvdi T, Quiñones-Hinojosa A. Oxygen in stem cell biology: a critical component of the stem cell niche. Cell stem cell. 2010 Aug 6;7(2):150-61.

33- Panchision DM. The role of oxygen in regulating neural stem cells in development and disease. Journal of cellular physiology. 2009 Sep 1;220(3):562-8.

34- Amorin B, Alegretti AP, Valim VD, Silva AM, Silva MA, Sehn F, Silla LM. Characteristics of mesenchymal stem cells under hypoxia. CellBio. Delaware. Vol. 2, no. 1 (Mar. 2013), p. 11-19. 2013.

35- Yoshida Y, Takahashi K, Okita K, Ichisaka T, Yamanaka S. Hypoxia enhances the generation of induced pluripotent stem cells. Cell stem cell. 2009 Sep 4;5(3):237-41.

36- Madrigal M, Rao KS, Riordan NH. A review of therapeutic effects of mesenchymal stem cell secretions and induction of secretory modification by different culture methods. Journal of translational medicine. 2014 Oct 11;12(1):260.

37- Kim HA, Rhim T, Lee M. Regulatory systems for hypoxia-inducible gene expression in ischemic heart disease gene therapy. Advanced drug delivery reviews. 2011 Jul 18;63(8):678-87.

38- Estrada JC, Albo C, Benguria A, Dopazo A, Lopez-Romero P, Carrera-Quintanar L, Roche E, Clemente EP, Enriquez JA, Bernad A, Samper E. Culture of human mesenchymal stem cells at low oxygen tension improves growth and genetic stability by activating glycolysis. Cell Death & Differentiation. 2012 May 1;19(5):743-55.

39- Fehrer C, Brunauer R, Laschober G, Unterluggauer H, Reitinger S, Kloss F, Gülly C, Gaßner R, Lepperdinger G. Reduced oxygen tension attenuates differentiation capacity of human mesenchymal stem cells and prolongs their lifespan. Aging cell. 2007 Dec 1;6(6):745-57.

40- Schächinger V, Erbs S, Elsässer A, Haberbosch W, Hambrecht R, Hölschermann H, Yu J, Corti R, Mathey DG, Hamm CW, Süselbeck T. Intracoronary bone marrow–derived progenitor cells in acute myocardial infarction. New England Journal of Medicine. 2006 Sep 21;355(12):1210-21.

41- Fischer UM, Harting MT, Jimenez F, Monzon-Posadas WO, Xue H, Savitz SI, Laine GA, Cox Jr CS. Pulmonary passage is a major obstacle for intravenous stem cell delivery: the pulmonary first-pass effect. Stem cells and development. 2009 Jun 1;18(5):683-92.

42- Rochefort YG, Vaudin P, Bonnet N, Pages JC, Domenech J, Charbord P, Eder V. Influence of hypoxia on the domiciliation of mesenchymal stem cells after infusion into rats: possibilities of targeting pulmonary artery remodeling via cells therapies?. Respiratory research. 2005 Oct 27;6(1):125.

43- Nauta TD, van Hinsbergh VW, Koolwijk P. Hypoxic signaling during tissue repair and regenerative medicine. International journal of molecular sciences. 2014 Oct 31;15(11):19791-815.

44- Grassel S, Ahmed N. Influence of cellular microenvironment and paracrine signals on chondrogenic differentiation. Front Biosci. 2007 Sep 1;12:4946-56.

45- Basciano L, Nemos C, Foliguet B, de Isla N, de Carvalho M, Tran N, Dalloul A. Long term culture of mesenchymal stem cells in hypoxia promotes a genetic program maintaining their undifferentiated and multipotent status. BMC cell biology. 2011 Mar 30;12(1):12.

46- Hass R, Kasper C, Böhm S, Jacobs R. Different populations and sources of human mesenchymal stem cells (MSC): a comparison of adult and neonatal tissue-derived MSC. Cell Communication and Signaling. 2011 May 14;9(1):12.

47- Zhang L, Peng LP, Wu N, Li LP. Development of bone marrow mesenchymal stem cell culture in vitro. Chinese medical journal. 2012 May;125(9):1650-5.

48- Liang X, Ding Y, Zhang Y, Tse HF, Lian Q. Paracrine mechanisms of mesenchymal stem cell-based therapy: current status and perspectives. Cell transplantation. 2014 Sep 15;23(9):1045-59.

49- Lönne M, Lavrentieva A, Walter JG, Kasper C. Analysis of oxygen-dependent cytokine expression in human mesenchymal stem cells derived from umbilical cord. Cell and tissue research. 2013 Jul 1;353(1):117-22.

50- Roemeling-van Rhijn M, Mensah FK, Korevaar SS, Leijs MJ, van Osch GJ, IJzermans JN, Betjes MG, Baan CC, Weimar W, Hoogduijn MJ. Effects of hypoxia on the immunomodulatory properties of adipose tissue-derived mesenchymal stem cells. Frontiers in immunology. 2013;4.

51- Das R, Jahr H, van Osch GJ, Farrell E. The role of hypoxia in bone marrow–derived mesenchymal stem cells: considerations for regenerative medicine approaches. Tissue Engineering Part B: Reviews. 2009 Oct 9;16(2):159-68.

52- Grayson WL, Zhao F, Bunnell B, Ma T. Hypoxia enhances proliferation and tissue formation of human mesenchymal stem cells. Biochemical and biophysical research communications. 2007 Jul 6;358(3):948-53.

53- Carrera S, Senra J, Acosta MI, Althubiti M, Hammond EM, de Verdier PJ, Macip S. The role of the HIF-1α transcription factor in increased cell division at physiological oxygen tensions. PloS one. 2014 May 16;9(5):e97938.

54- Tsai CC, Yew TL, Yang DC, Huang WH, Hung SC. Benefits of hypoxic culture on bone marrow multipotent stromal cells. American journal of blood research. 2012;2(3):148.

55- Cummins EP, Taylor CT. Hypoxia-responsive transcription factors. Pflügers Archiv. 2005 Sep 1;450(6):363-71.

56- An HY, Shin HS, Choi JS, Kim HJ, Lim JY, Kim YM. Adipose mesenchymal stem cell secretome modulated in hypoxia for remodeling of radiation-induced salivary gland damage. PloS one. 2015 Nov 3;10(11):e0141862.

57- Park BS, Kim WS, Choi JS, Kim HK, Won JH, Ohkubo F, Fukuoka H. Hair growth stimulated by conditioned medium of adipose-derived stem cells is enhanced by hypoxia: evidence of increased growth factor secretion. Biomedical Research. 2010;31(1):27-34.

58- Hu X, Wu R, Shehadeh LA, Zhou Q, Jiang C, Huang X, Zhang L, Gao F, Liu X, Yu H, Webster KA. Severe hypoxia exerts parallel and cell-specific regulation of gene expression and alternative splicing in human mesenchymal stem cells. BMC genomics. 2014 Apr 23;15(1):303.

59- Bakondi B, Shimada IS, Perry A, Munoz JR, Ylostalo J, Howard AB, Gregory CA, Spees JL. CD133 identifies a human bone marrow stem/progenitor cell sub-population with a repertoire of secreted factors that protect against stroke. Molecular Therapy. 2009 Nov 1;17(11):1938-47.

60- Chen L, Xu Y, Zhao J, Zhang Z, Yang R, Xie J, Liu X, Qi S. Conditioned medium from hypoxic bone marrow-derived mesenchymal stem cells enhances wound healing in mice. PloS one. 2014 Apr 29;9(4):e96161.

61- Caplan AI, Bruder SP. Mesenchymal stem cells: building blocks for molecular medicine in the 21st century. Trends in molecular medicine. 2001 Jun 1;7(6):259-64.

62- Bianco P, Robey PG, Simmons PJ. Mesenchymal stem cells: revisiting history, concepts, and assays. Cell stem cell. 2008 Apr 10;2(4):313-9.

63- Samsonraj RM, Raghunath M, Hui JH, Ling L, Nurcombe V, Cool SM. Telomere length analysis of human mesenchymal stem cells by quantitative PCR. Gene. 2013 May 1;519(2):348-55.

64- Parsch D, Fellenberg J, Brümmendorf TH, Eschlbeck AM, Richter W. Telomere length and telomerase activity during expansion and differentiation of human mesenchymal stem cells and chondrocytes. Journal of molecular medicine. 2004 Jan 1;82(1):49-55.

65- Zimmermann S, Voss M, Kaiser S, Kapp U, Waller CF, Martens UM. Lack of telomerase activity in human mesenchymal stem cells. Leukemia. 2003 Jun 1;17(6):1146-9.

66- Ouellette MM, McDaniel LD, Wright WE, Shay JW, Schultz RA. The establishment of telomerase-immortalized cell lines representing human chromosome instability syndromes. Human molecular genetics. 2000 Feb 12;9(3):403-11.

67- Teixeira FG, Panchalingam KM, Anjo SI, Manadas B, Pereira R, Sousa N, Salgado AJ, Behie LA. Do hypoxia/normoxia culturing conditions change the neuroregulatory profile of Wharton Jelly mesenchymal stem cell secretome?. Stem cell research & therapy. 2015 Jul 24;6(1):133.

68- Jaiswal N, Haynesworth SE, Caplan AI, Bruder SP. Osteogenic differentiation of purified, culture-expanded human mesenchymal stem cells in vitro. Journal of cellular biochemistry. 1997 Feb 1;64(2):295-312.

69- Xie L, Zhang N, Marsano A, Vunjak-Novakovic G, Zhang Y, Lopez MJ. In vitro mesenchymal trilineage differentiation and extracellular matrix production by adipose and bone marrow derived adult equine multipotent stromal cells on a collagen scaffold. Stem Cell Reviews and Reports. 2013 Dec 1;9(6):858-72.

70- Jung MH, Yang SE, Jin HJ, Lee MK, Song HS, Yang JY, Yang YS, Ha CW. Chondrogenic differentiation of mesenchymal stem cells from human umbilical cord blood. Journal of the Korean Orthopaedic Association. 2004 Oct 1;39(6):607-13.

71- Dale TP, de Castro A, Kuiper NJ, Parkinson EK, Forsyth NR. Immortalisation with hTERT Impacts on Sulphated Glycosaminoglycan Secretion and Immunophenotype in a Variable and Cell Specific Manner. PloS one. 2015 Jul 21;10(7):e0133745.

72- Estrada JC, Albo C, Benguria A, Dopazo A, Lopez-Romero P, Carrera-Quintanar L, Roche E, Clemente EP, Enriquez JA, Bernad A, Samper E. Culture of human mesenchymal stem cells at low oxygen tension improves growth and genetic stability by activating glycolysis. Cell Death & Differentiation. 2012 May 1;19(5):743-55.

73- Hwang JH, Shim SS, Seok OS, Lee HY, Woo SK, Kim BH, Song HR, Lee JK, Park YK. Comparison of cytokine expression in mesenchymal stem cells from human placenta, cord blood, and bone marrow. Journal of Korean medical science. 2009 Aug 1;24(4):547-54.

74- Tuan RS, Boland G, Tuli R. Adult mesenchymal stem cells and cell-based tissue engineering. Arthritis Res Ther. 2002 Dec 11;5(1):32.

75- Muraglia A, Cancedda R, Quarto R. Clonal mesenchymal progenitors from human bone marrow differentiate in vitro according to a hierarchical model. J Cell Sci. 2000 Apr 1;113(7):1161-6.

76- Karystinou A, Dell'Accio F, Kurth TB, Wackerhage H, Khan IM, Archer CW, Jones EA, Mitsiadis TA, De Bari C. Distinct mesenchymal progenitor cell subsets in the adult human synovium. Rheumatology. 2009 Jul 14;48(9):1057-64.

77- De Bari C, Dell'Accio F, Vandenabeele F, Vermeesch JR, Raymackers JM, Luyten FP. Skeletal muscle repair by adult human mesenchymal stem cells from synovial membrane. The Journal of cell biology. 2003 Mar 17;160(6):909-18.

78- Hoffmann A, Pelled G, Turgeman G, Eberle P, Zilberman Y, Shinar H, Keinan-Adamsky K, Winkel A, Shahab S, Navon G, Gross G. Neotendon formation induced by manipulation of the Smad8 signalling pathway in mesenchymal stem cells. Journal of Clinical Investigation. 2006 Apr 3;116(4):940.

79- Bossolasco P, Cova L, Calzarossa C, Rimoldi SG, Borsotti C, Deliliers GL, Silani V, Soligo D, Polli E. Neuro-glial differentiation of human bone marrow stem cells in vitro. Experimental neurology. 2005 Jun 30;193(2):312-25.

80- Di Nicola M, Carlo-Stella C, Magni M, Milanesi M, Longoni PD, Matteucci P, Grisanti S, Gianni AM. Human bone marrow stromal cells suppress T-lymphocyte

proliferation induced by cellular or nonspecific mitogenic stimuli. Blood. 2002 May 15;99(10):3838-43.

81- Bartholomew A, Sturgeon C, Siatskas M, Ferrer K, McIntosh K, Patil S, Hardy W, Devine S, Ucker D, Deans R, Moseley A. Mesenchymal stem cells suppress lymphocyte proliferation in vitro and prolong skin graft survival in vivo. Experimental hematology. 2002 Jan 31;30(1):42-8.

82- Maqbool M, Vidyadaran S, George E, Ramasamy R. Human mesenchymal stem cells protect neutrophils from serum-deprived cell death. Cell biology international. 2011 Dec 1;35(12):1247-51.

83- Klebanoff SJ, Kettle AJ, Rosen H, Winterbourn CC, Nauseef WM. Myeloperoxidase: a front-line defender against phagocytosed microorganisms. Journal of leukocyte biology. 2013 Feb 1;93(2):185-98.

84- Klebanoff SJ. Myeloperoxidase: friend and foe. Journal of leukocyte biology. 2005 May 1;77(5):598-625.

85- Lacy P. Mechanisms of degranulation in neutrophils. Allergy, Asthma & Clinical Immunology. 2006 Sep 15;2(3):98.

86- Raffaghello L, Bianchi G, Bertolotto M, Montecucco F, Busca A, Dallegri F, Ottonello L, Pistoia V. Human mesenchymal stem cells inhibit neutrophil apoptosis: a model for neutrophil preservation in the bone marrow niche. Stem cells. 2008 Jan 1;26(1):151-62.

87- Brandau S, Jakob M, Bruderek K, Bootz F, Giebel B, Radtke S, Mauel K, Jäger M, Flohé SB, Lang S. Mesenchymal stem cells augment the anti-bacterial activity of neutrophil granulocytes. PLoS One. 2014 Sep 19;9(9):e106903.

88- Plock JA, Schnider JT, Solari MG, Zheng XX, Gorantla VS. Perspectives on the use of mesenchymal stem cells in vascularized composite allotransplantation. Frontiers in immunology. 2013;4.

89- Jiang XX, Zhang Y, Liu B, Zhang SX, Wu Y, Yu XD, Mao N. Human mesenchymal stem cells inhibit differentiation and function of monocyte-derived dendritic cells. Blood. 2005 May 15;105(10):4120-6.

90- Beyth S, Borovsky Z, Mevorach D, Liebergall M, Gazit Z, Aslan H, Galun E, Rachmilewitz J. Human mesenchymal stem cells alter antigen-presenting cell maturation and induce T-cell unresponsiveness. Blood. 2005 Mar 1;105(5):2214-9.

91- Djouad F, Charbonnier LM, Bouffi C, Louis-Plence P, Bony C, Apparailly F, Cantos C, Jorgensen C, Noel D. Mesenchymal stem cells inhibit the differentiation of dendritic cells through an interleukin-6-dependent mechanism. Stem cells. 2007 Aug 1;25(8):2025-32.

92- Chen L, Zhang W, Yue H, Han Q, Chen B, Shi M, Li J, Li B, You S, Shi Y, Zhao RC. Effects of human mesenchymal stem cells on the differentiation of dendritic cells from CD34+ cells. Stem cells and development. 2007 Oct 1;16(5):719-32.

93- Ghannam S, Bouffi C, Djouad F, Jorgensen C, Noël D. Immunosuppression by mesenchymal stem cells: mechanisms and clinical applications. Stem cell research & therapy. 2010 Mar 15;1(1):2.

94- Parekkadan B, Milwid JM. Mesenchymal stem cells as therapeutics. Annual review of biomedical engineering. 2010 Aug 15;12:87-117.

95- Li YP, Paczesny S, Lauret E, Poirault S, Bordigoni P, Mekhloufi F, Hequet O, Bertrand Y, Ou-Yang JP, Stoltz JF, Miossec P. Human mesenchymal stem cells license adult CD34+ hemopoietic progenitor cells to differentiate into regulatory dendritic cells through activation of the Notch pathway. The Journal of Immunology. 2008 Feb 1;180(3):1598-608.

96- Németh K, Leelahavanichkul A, Yuen PS, Mayer B, Parmelee A, Doi K, Robey PG, Leelahavanichkul K, Koller BH, Brown JM, Hu X. Bone marrow stromal cells attenuate sepsis via prostaglandin E2–dependent reprogramming of host macrophages to increase their interleukin-10 production. Nature medicine. 2009 Jan 1;15(1):42-9.

97- François M, Romieu-Mourez R, Li M, Galipeau J. Human MSC suppression correlates with cytokine induction of indoleamine 2, 3-dioxygenase and bystander M2 macrophage differentiation. Molecular Therapy. 2012 Jan 1;20(1):187-95.

98- Maggini J, Mirkin G, Bognanni I, Holmberg J, Piazzón IM, Nepomnaschy I, Costa H, Cañones C, Raiden S, Vermeulen M, Geffner JR. Mouse bone marrow-derived mesenchymal stromal cells turn activated macrophages into a regulatory-like profile. PloS one. 2010 Feb 16;5(2):e9252.

99- Frangogiannis NG. Regulation of the inflammatory response in cardiac repair. Circulation research. 2012 Jan 6;110(1):159-73.

100- Spaggiari GM, Capobianco A, Abdelrazik H, Becchetti F, Mingari MC, Moretta L. Mesenchymal stem cells inhibit natural killer–cell proliferation, cytotoxicity, and

cytokine production: role of indoleamine 2, 3-dioxygenase and prostaglandin E2. Blood. 2008 Feb 1;111(3):1327-33.

101- Spaggiari GM, Capobianco A, Becchetti S, Mingari MC, Moretta L. Mesenchymal stem cell-natural killer cell interactions: evidence that activated NK cells are capable of killing MSCs, whereas MSCs can inhibit IL-2-induced NK-cell proliferation. Blood. 2006 Feb 15;107(4):1484-90.

102- Poggi A, Prevosto C, Massaro AM, Negrini S, Urbani S, Pierri I, Saccardi R, Gobbi M, Zocchi MR. Interaction between human NK cells and bone marrow stromal cells induces NK cell triggering: role of NKp30 and NKG2D receptors. The Journal of Immunology. 2005 Nov 15;175(10):6352-60.

103- Uccelli A, Moretta L, Pistoia V. Mesenchymal stem cells in health and disease. Nature reviews immunology. 2008 Sep 1;8(9):726-36.

104- Benvenuto F, Ferrari S, Gerdoni E, Gualandi F, Frassoni F, Pistoia V, Mancardi G, Uccelli A. Human mesenchymal stem cells promote survival of T cells in a quiescent state. Stem cells. 2007 Jul 1;25(7):1753-60.

105- Zappia E, Casazza S, Pedemonte E, Benvenuto F, Bonanni I, Gerdoni E, Giunti D, Ceravolo A, Cazzanti F, Frassoni F, Mancardi G. Mesenchymal stem cells ameliorate experimental autoimmune encephalomyelitis inducing T-cell anergy. Blood. 2005 Sep 1;106(5):1755-61.

106- Aggarwal S, Pittenger MF. Human mesenchymal stem cells modulate allogeneic immune cell responses. Blood. 2005 Feb 15;105(4):1815-22.

107- Rasmusson I, Uhlin M, Le Blanc K, Levitsky V. Mesenchymal stem cells fail to trigger effector functions of cytotoxic T lymphocytes. Journal of leukocyte biology. 2007 Oct 1;82(4):887-93.

108- Morandi F, Raffaghello L, Bianchi G, Meloni F, Salis A, Millo E, Ferrone S, Barnaba V, Pistoia V. Immunogenicity of Human Mesenchymal Stem Cells in HLA-Class I-Restricted T-Cell Responses Against Viral or Tumor-Associated Antigens. Stem Cells. 2008 May 1;26(5):1275-87.

109- Maccario R, Podestà M, Moretta A, Cometa A, Comoli P, Montagna D, Daudt L, Ibatici A, Piaggio G, Pozzi S, Frassoni F. Interaction of human mesenchymal stem cells with cells involved in alloantigen-specific immune response favors the differentiation of CD4+ T-cell subsets expressing a regulatory/suppressive phenotype. Haematologica. 2005 Jan 1;90(4):516-25.

110- Pevsner-Fischer M, Morad V, Cohen-Sfady M, Rousso-Noori L, Zanin-Zhorov A, Cohen S, Cohen IR, Zipori D. Toll-like receptors and their ligands control mesenchymal stem cell functions. Blood. 2007 Feb 15;109(4):1422-32.

111- Tomchuck SL, Zwezdaryk KJ, Coffelt SB, Waterman RS, Danka ES, Scandurro AB. Toll-like receptors on human mesenchymal stem cells drive their migration and immunomodulating responses. Stem cells. 2008 Jan 1;26(1):99-107.

112- Liotta F, Angeli R, Cosmi L, Fili L, Manuelli C, Frosali F, Mazzinghi B, Maggi L, Pasini A, Lisi V, Santarlasci V. Toll-like receptors 3 and 4 are expressed by human bone marrow-derived mesenchymal stem cells and can inhibit their T-cell modulatory activity by impairing Notch signaling. Stem cells. 2008 Jan 1;26(1):279-89.

113- Svensson M, Kaye PM. Stromal-cell regulation of dendritic-cell differentiation and function. Trends in immunology. 2006 Dec 31;27(12):580-7.

114- Krampera M, Cosmi L, Angeli R, Pasini A, Liotta F, Andreini A, Santarlasci V, Mazzinghi B, Pizzolo G, Vinante F, Romagnani P. Role for interferon-γ in the immunomodulatory activity of human bone marrow mesenchymal stem cells. Stem cells. 2006 Feb 1;24(2):386-98.

115- Corcione A, Benvenuto F, Ferretti E, Giunti D, Cappiello V, Cazzanti F, Risso M, Gualandi F, Mancardi GL, Pistoia V, Uccelli A. Human mesenchymal stem cells modulate B-cell functions. Blood. 2006 Jan 1;107(1):367-72.

116- Traggiai E, Volpi S, Schena F, Gattorno M, Ferlito F, Moretta L, Martini A. Bone marrow-derived mesenchymal stem cells induce both polyclonal expansion and differentiation of B cells isolated from healthy donors and systemic lupus erythematosus patients. Stem cells. 2008 Feb 1;26(2):562-9.

117- Augello A, Tasso R, Negrini SM, Amateis A, Indiveri F, Cancedda R, Pennesi G. Bone marrow mesenchymal progenitor cells inhibit lymphocyte proliferation by activation of the programmed death 1 pathway. European journal of immunology. 2005 May 1;35(5):1482-90.

118- Rasmusson I, Le Blanc K, Sundberg B, Ringden O. Mesenchymal stem cells stimulate antibody secretion in human B cells. Scandinavian journal of immunology. 2007 Apr 1;65(4):336-43.

119- Gerdoni E, Gallo B, Casazza S, Musio S, Bonanni I, Pedemonte E, Mantegazza R, Frassoni F, Mancardi G, Pedotti R, Uccelli A. Mesenchymal stem cells effectively

modulate pathogenic immune response in experimental autoimmune encephalomyelitis. Annals of neurology. 2007 Mar 1;61(3):219-27.

120- Ashley NT, Weil ZM, Nelson RJ. Inflammation: mechanisms, costs, and natural variation. Annual Review of Ecology, Evolution, and Systematics. 2012 Dec 1;43:385-406.

121- Rock KL, Latz E, Ontiveros F, Kono H. The sterile inflammatory response. Annual review of immunology. 2009 Apr 23;28:321-42.

122- Medzhitov R. Origin and physiological roles of inflammation. Nature. 2008 Jul 24;454(7203):428-35.

123- Kobayashi SD, Voyich JM, Whitney AR, DeLeo FR. Spontaneous neutrophil apoptosis and regulation of cell survival by granulocyte macrophage-colony stimulating factor. Journal of leukocyte biology. 2005 Dec 1;78(6):1408-18.

124- Buckley CD, Gilroy DW, Serhan CN. Proresolving lipid mediators and mechanisms in the resolution of acute inflammation. Immunity. 2014 Mar 20;40(3):315-27.

125- Park SA, Hyun YM. Neutrophil Extravasation Cascade: What Can We Learn from Two-photon Intravital Imaging?. Immune network. 2016 Dec 1;16(6):317-21.

126- Ahmed AU. An overview of inflammation: mechanism and consequences. Frontiers in Biology. 2011 Aug 1;6(4):274-81.

127- Aurora AB, Olson EN. Immune modulation of stem cells and regeneration. Cell stem cell. 2014 Jul 3;15(1):14-25.

128- Foote AK, Blakemore WF. Inflammation stimulates remyelination in areas of chronic demyelination. Brain. 2005 Feb 7;128(3):528-39.

129- Setzu A, Lathia JD, Zhao C, Wells K, Rao MS, Franklin RJ. Inflammation stimulates myelination by transplanted oligodendrocyte precursor cells. Glia. 2006 Sep 1;54(4):297-303.

130- Kyritsis N, Kizil C, Zocher S, Kroehne V, Kaslin J, Freudenreich D, Iltzsche A, Brand M. Acute inflammation initiates the regenerative response in the adult zebrafish brain. Science. 2012 Dec 7;338(6112):1353-6.

131- Miron VE, Boyd A, Zhao JW, Yuen TJ, Ruckh JM, Shadrach JL, van Wijngaarden P, Wagers AJ, Williams A, Franklin RJ. M2 microglia and macrophages drive oligodendrocyte differentiation during CNS remyelination. Nature neuroscience. 2013 Sep 1;16(9):1211-8.

132- Weber MS, Prod'homme T, Youssef S, Dunn SE, Rundle CD, Lee L, Patarroyo JC, Stüve O, Sobel RA, Steinman L, Zamvil SS. Type II monocytes modulate T cell–mediated central nervous system autoimmune disease. Nature medicine. 2007 Aug 1;13(8):935-43.

133- Vidal B, Serrano AL, Tjwa M, Suelves M, Ardite E, De Mori R, Baeza-Raja B, de Lagrán MM, Lafuste P, Ruiz-Bonilla V, Jardí M. Fibrinogen drives dystrophic muscle fibrosis via a TGFβ/alternative macrophage activation pathway. Genes & development. 2008 Jul 1;22(13):1747-52.

134- Heredia JE, Mukundan L, Chen FM, Mueller AA, Deo RC, Locksley RM, Rando TA, Chawla A. Type 2 innate signals stimulate fibro/adipogenic progenitors to facilitate muscle regeneration. Cell. 2013 Apr 11;153(2):376-88.

135- Burzyn D, Kuswanto W, Kolodin D, Shadrach JL, Cerletti M, Jang Y, Sefik E, Tan TG, Wagers AJ, Benoist C, Mathis D. A special population of regulatory T cells potentiates muscle repair. Cell. 2013 Dec 5;155(6):1282-95.

136- Porrello, Enzo R., and Eric N. Olson. Building a new heart from old parts: stem cell turnover in the aging heart. Am Heart Assoc (2010): 1292-1294.

137- Boulter L, Govaere O, Bird TG, Radulescu S, Ramachandran P, Pellicoro A, Ridgway RA, Seo SS, Spee B, Van Rooijen N, Sansom OJ. Macrophage-derived Wnt opposes Notch signaling to specify hepatic progenitor cell fate in chronic liver disease. Nature medicine. 2012 Apr 1;18(4):572-9.

138- Krizhanovsky V, Yon M, Dickins RA, Hearn S, Simon J, Miething C, Yee H, Zender L, Lowe SW. Senescence of activated stellate cells limits liver fibrosis. Cell. 2008 Aug 22;134(4):657-67.

139- Pesce JT, Ramalingam TR, Mentink-Kane MM, Wilson MS, El Kasmi KC, Smith AM, Thompson RW, Cheever AW, Murray PJ, Wynn TA. Arginase-1–expressing macrophages suppress Th2 cytokine–driven inflammation and fibrosis. PLoS pathogens. 2009 Apr 10;5(4):e1000371.

140- Shechter R, Miller O, Yovel G, Rosenzweig N, London A, Ruckh J, Kim KW, Klein E, Kalchenko V, Bendel P, Lira SA. Recruitment of beneficial M2 macrophages to injured spinal cord is orchestrated by remote brain choroid plexus. Immunity. 2013 Mar 21;38(3):555-69.

141- Epelman S, Lavine KJ, Beaudin AE, Sojka DK, Carrero JA, Calderon B, Brija T, Gautier EL, Ivanov S, Satpathy AT, Schilling JD. Embryonic and adult-derived resident cardiac

macrophages are maintained through distinct mechanisms at steady state and during inflammation. Immunity. 2014 Jan 16;40(1):91-104.

142- Hare JM, Chaparro SV. Cardiac regeneration and stem cell therapy. Current opinion in organ transplantation. 2008 Oct;13(5):536.

143- Orlic D, Kajstura J, Chimenti S, Bodine DM, Leri A, Anversa P. Bone marrow stem cells regenerate infarcted myocardium. Pediatric transplantation. 2003 Apr 1;7(s3):86-8.

144- Sato K, Ozaki K, Oh I, Meguro A, Hatanaka K, Nagai T, Muroi K, Ozawa K. Nitric oxide plays a critical role in suppression of T-cell proliferation by mesenchymal stem cells. Blood. 2007 Jan 1;109(1):228-34.

145- Chabannes D, Hill M, Merieau E, Rossignol J, Brion R, Soulillou JP, Anegon I, Cuturi MC. A role for heme oxygenase-1 in the immunosuppressive effect of adult rat and human mesenchymal stem cells. Blood. 2007 Nov 15;110(10):3691-4.

146- Selmani Z, Naji A, Zidi I, Favier B, Gaiffe E, Obert L, Borg C, Saas P, Tiberghien P, Rouas-Freiss N, Carosella ED. Human leukocyte antigen-G5 secretion by human mesenchymal stem cells is required to suppress T lymphocyte and natural killer function and to induce CD4+ CD25highFOXP3+ regulatory T cells. Stem cells. 2008 Jan 1;26(1):212-22.

147- Plotnikov EY, Khryapenkova TG, Vasileva AK, Marey MV, Galkina SI, Isaev NK, Sheval EV, Polyakov VY, Sukhikh GT, Zorov DB. Cell-to-cell cross-talk between mesenchymal stem cells and cardiomyocytes in co-culture. Journal of cellular and molecular medicine. 2008 Sep 1;12(5a):1622-31.

148- Moghadasali R, Mutsaers HA, Azarnia M, Aghdami N, Baharvand H, Torensma R, Wilmer MJ, Masereeuw R. Mesenchymal stem cell-conditioned medium accelerates regeneration of human renal proximal tubule epithelial cells after gentamicin toxicity. Experimental and toxicologic pathology. 2013 Jul 31;65(5):595-600.

149- Van Buul GM, Villafuertes E, Bos PK, Waarsing JH, Kops N, Narcisi R, Weinans H, Verhaar JA, Bernsen MR, Van Osch GJ. Mesenchymal stem cells secrete factors that inhibit inflammatory processes in short-term osteoarthritic synovium and cartilage explant culture. Osteoarthritis and Cartilage. 2012 Oct 31;20(10):1186-96.

150- Chen J, Li Y, Hao H, Li C, Du Y, Hu Y, Li J, Liang Z, Li C, Liu J, Chen L. Mesenchymal stem cell conditioned medium promotes proliferation and migration of alveolar

epithelial cells under septic conditions in vitro via the JNK-P38 signaling pathway. Cellular Physiology and Biochemistry. 2015;37(5):1830-46.

151- Walter MN, Wright KT, Fuller HR, MacNeil S, Johnson WE. Mesenchymal stem cell-conditioned medium accelerates skin wound healing: an in vitro study of fibroblast and keratinocyte scratch assays. Experimental cell research. 2010 Apr 15;316(7):1271-81.

152- Chen L, Tredget EE, Wu PY, Wu Y. Paracrine factors of mesenchymal stem cells recruit macrophages and endothelial lineage cells and enhance wound healing. PloS one. 2008 Apr 2;3(4):e1886.

153- Kinnaird T, Stabile E, Burnett MS, Shou M, Lee CW, Barr S, Fuchs S, Epstein SE. Local delivery of marrow-derived stromal cells augments collateral perfusion through paracrine mechanisms. Circulation. 2004 Mar 30;109(12):1543-9.

154- Van Poll D, Parekkadan B, Cho CH, Berthiaume F, Nahmias Y, Tilles AW, Yarmush ML. Mesenchymal stem cell–derived molecules directly modulate hepatocellular death and regeneration in vitro and in vivo. Hepatology. 2008 May 1;47(5):1634-43.

155- Dreixler JC, Poston JN, Balyasnikova I, Shaikh AR, Tupper KY, Conway S, Boddapati V, Marcet MM, Lesniak MS, Roth S. Delayed Administration of Bone Marrow Mesenchymal Stem Cell Conditioned Medium Significantly Improves Outcome After Retinal Ischemia in RatsBMSC-Conditioned Medium Rescues Ischemic Retina in Rats. Investigative ophthalmology & visual science. 2014 Jun 1;55(6):3785-96.

156- Skalnikova HK. Proteomic techniques for characterisation of mesenchymal stem cell secretome. Biochimie. 2013 Dec 31;95(12):2196-211.

157- Oskowitz A, McFerrin H, Gutschow M, Carter ML, Pochampally R. Serum-deprived human multipotent mesenchymal stromal cells (MSCs) are highly angiogenic. Stem cell research. 2011 May 31;6(3):215-25.

158- Sze SK, de Kleijn DP, Lai RC, Tan EK, Zhao H, Yeo KS, Low TY, Lian Q, Lee CN, Mitchell W, El Oakley RM. Elucidating the secretion proteome of human embryonic stem cell-derived mesenchymal stem cells. Molecular & Cellular Proteomics. 2007 Oct 1;6(10):1680-9.

159- Liu CH, Hwang SM. Cytokine interactions in mesenchymal stem cells from cord blood. Cytokine. 2005 Dec 21;32(6):270-9.

160- Ribeiro CA, Fraga JS, Grãos M, Neves NM, Reis RL, Gimble JM, Sousa N, Salgado AJ. The secretome of stem cells isolated from the adipose tissue and Wharton jelly acts

differently on central nervous system derived cell populations. Stem cell research & therapy. 2012 May 2;3(3):18.

161- Bhang SH, Lee S, Shin JY, Lee TJ, Jang HK, Kim BS. Efficacious and clinically relevant conditioned medium of human adipose-derived stem cells for therapeutic angiogenesis. Molecular Therapy. 2014 Apr 30;22(4):862-72.

162- Ohnishi S, Yasuda T, Kitamura S, Nagaya N. Effect of hypoxia on gene expression of bone marrow-derived mesenchymal stem cells and mononuclear cells. Stem cells. 2007 May 1;25(5):1166-77.

163- Baer PC, Overath JM, Urbschat A, Schubert R, Geiger H. Preconditioning of Human Adipose-derived Stromal. Stem Cells: Evaluation of Short-term Preincubation Regimens to Enhance their Regenerative Potential. J Stem Cell Res Ther. 2016;6(331):2.

164- Martin-Rendon E, Hale SJ, Ryan D, Baban D, Forde SP, Roubelakis M, Sweeney D, Moukayed M, Harris AL, Davies K, Watt SM. Transcriptional profiling of human cord blood CD133+ and cultured bone marrow mesenchymal stem cells in response to hypoxia. Stem cells. 2007 Apr 1;25(4):1003-12.

165- da Silva Meirelles L, Fontes AM, Covas DT, Caplan AI. Mechanisms involved in the therapeutic properties of mesenchymal stem cells. Cytokine & growth factor reviews. 2009 Dec 31;20(5):419-27.

166- Grötzinger J. Molecular mechanisms of cytokine receptor activation. Biochimica et Biophysica Acta (BBA)-Molecular Cell Research. 2002 Nov 11;1592(3):215-23.

167- Spangler JB, Moraga I, Mendoza JL, Garcia KC. Insights into cytokine–receptor interactions from cytokine engineering. Annual review of immunology. 2015 Mar 21;33:139-67.

168- Walter MR. The molecular basis of IL-10 function: from receptor structure to the onset of signaling. InInterleukin-10 in Health and Disease 2014 (pp. 191-212). Springer Berlin Heidelberg.

169- Cheng E, Souza RF, Spechler SJ. Tissue remodeling in eosinophilic esophagitis. American Journal of Physiology-Gastrointestinal and Liver Physiology. 2012 Dec 1;303(11):G1175-87.

170- Mueller TD, Zhang JL, Sebald W, Duschl A. Structure, binding, and antagonists in the IL-4/IL-13 receptor system. Biochimica et Biophysica Acta (BBA)-Molecular Cell Research. 2002 Nov 11;1592(3):237-50.

171- Kasaian MT, Marquette K, Fish S, DeClercq C, Agostinelli R, Cook TA, Brennan A, Lee J, Fitz L, Brooks J, Vugmeyster Y. An IL-4/IL-13 dual antagonist reduces lung inflammation, airway hyperresponsiveness, and IgE production in mice. American journal of respiratory cell and molecular biology. 2013 Jul;49(1):37-46.

172- Huang F, Chen YG. Regulation of TGF-β receptor activity. Cell & bioscience. 2012 Mar 15;2(1):9.

173- Murray PJ, Allen JE, Biswas SK, Fisher EA, Gilroy DW, Goerdt S, Gordon S, Hamilton JA, Ivashkiv LB, Lawrence T, Locati M. Macrophage activation and polarization: nomenclature and experimental guidelines. Immunity. 2014 Jul 17;41(1):14-20.

174- Labonte AC, Tosello-Trampont AC, Hahn YS. The role of macrophage polarization in infectious and inflammatory diseases. Molecules and cells. 2014 Apr 30;37(4):275.

175- Tarique AA, Logan J, Thomas E, Holt PG, Sly PD, Fantino E. Phenotypic, functional, and plasticity features of classical and alternatively activated human macrophages. American journal of respiratory cell and molecular biology. 2015 Nov;53(5):676-88.

176- Rőszer T. Understanding the mysterious M2 macrophage through activation markers and effector mechanisms. Mediators of inflammation. 2015 May 18;2015.

177- Zhao Q, Ren H, Han Z. Mesenchymal stem cells: Immunomodulatory capability and clinical potential in immune diseases. Journal of Cellular Immunotherapy. 2016 Mar 31;2(1):3-20.

178- Sato K, Ozaki K, Mori M, Muroi K, Ozawa K. Mesenchymal stromal cells for graft-versus-host disease: basic aspects and clinical outcomes. Journal of clinical and experimental hematopathology. 2010;50(2):79-89.

179- Eggenhofer E, Hoogduijn MJ. Mesenchymal stem cell-educated macrophages. Transplantation research. 2012 Sep 28;1(1):12.

180- Wimpenny I, Hampson K, Yang Y, Ashammakhi N, Forsyth NR. One-step recovery of marrow stromal cells on nanofibers. Tissue Engineering Part C: Methods. 2009 Oct 7;16(3):503-9.

181- D'Ippolito G, Diabira S, Howard GA, Menei P, Roos BA, Schiller PC. Marrow-isolated adult multilineage inducible (MIAMI) cells, a unique population of postnatal young and old human cells with extensive expansion and differentiation potential. Journal of cell science. 2004 Jun 15;117(14):2971-81.

182- Wang N, Li Q, Zhang L, Lin H, Hu J, Li D, Shi S, Cui S, Zhou J, Ji J, Wan J. Mesenchymal stem cells attenuate peritoneal injury through secretion of TSG-6. PloS one. 2012 Aug 17;7(8):e43768.

183- Kay AG, Dale TP, Akram KM, Mohan P, Hampson K, Maffulli N, Spiteri MA, El Haj AJ, Forsyth NR. BMP2 repression and optimized culture conditions promote human bone marrow-derived mesenchymal stem cell isolation. Regenerative medicine. 2015 Mar;10(2):109-25.

184- Choi JR, Pingguan-Murphy B, Abas WA, Azmi MA, Omar SZ, Chua KH, Safwani WK. Hypoxia promotes growth and viability of human adipose-derived stem cells with increased growth factors secretion. Journal of Asian Scientific Research. 2014 Jul 1;4(7):328.

185- Crisan M, Yap S, Casteilla L, Chen CW, Corselli M, Park TS, Andriolo G, Sun B, Zheng B, Zhang L, Norotte C. A perivascular origin for mesenchymal stem cells in multiple human organs. Cell stem cell. 2008 Sep 11;3(3):301-13.

186- Zannettino AC, Paton S, Arthur A, Khor F, Itescu S, Gimble JM, Gronthos S. Multipotential human adipose-derived stromal stem cells exhibit a perivascular phenotype in vitro and in vivo. Journal of cellular physiology. 2008 Feb 1;214(2):413-21.

187- Sterclova M, Matej R, Mandakova P, Skibova J, Vasakova M. R ole of interleukin 4 and its receptor in clinical presentation of chronic extrinsic allergic alveolitis: a pilot study. Multidisciplinary respiratory medicine. 2013 May 30;8(1):35.

188- Jin W, Dong C. IL-17 cytokines in immunity and inflammation. Emerging microbes & infections. 2013 Sep 1;2(9):e60.

189- Koch AE, Kunkel SL, Harlow LA, Mazarakis DD, Haines GK, Burdick MD, Pope RM, Strieter RM. Macrophage inflammatory protein-1 alpha. A novel chemotactic cytokine for macrophages in rheumatoid arthritis. The Journal of clinical investigation. 1994 Mar 1;93(3):921-8.

190- Dufour JH, Dziejman M, Liu MT, Leung JH, Lane TE, Luster AD. IFN-γ-inducible protein 10 (IP-10; CXCL10)-deficient mice reveal a role for IP-10 in effector T cell generation and trafficking. The Journal of Immunology. 2002 Apr 1;168(7):3195-204.

191- Ntaios G, Gatselis NK, Makaritsis K, Dalekos GN. Adipokines as mediators of endothelial function and atherosclerosis. Atherosclerosis. 2013 Apr 30;227(2):216-21.

192- Luzina IG, Keegan AD, Heller NM, Rook GA, Shea-Donohue T, Atamas SP. Regulation of inflammation by interleukin-4: a review of “alternatives”. Journal of leukocyte biology. 2012 Oct 1;92(4):753-64.

193- Shaikh PZ. Cytokines & their physiologic and pharmacologic functions in inflammation: A review. International Journal of Pharmacy & Life Sciences. 2011 Oct 1;2(10).

194- Moore KW, de Waal Malefyt R, Coffman RL, O'Garra A. Interleukin-10 and the interleukin-10 receptor. Annual review of immunology. 2001 Apr;19(1):683-765.

195- Ward PA. Acute and chronic inflammation. Fundamentals of inflammation. 2010 Apr 26:1-6.

196- Williams LM, Ricchetti G, Sarma U, Smallie T, Foxwell BM. Interleukin-10 suppression of myeloid cell activation—a continuing puzzle. Immunology. 2004 Nov 1;113(3):281-92.

197- Khalaf H, Jass J, Olsson PE. Differential cytokine regulation by NF-κB and AP-1 in Jurkat T-cells. BMC immunology. 2010 May 27;11(1):26.

198- Kinnaird T, Stabile E, Burnett MS, Lee CW, Barr S, Fuchs S, Epstein SE. Marrow-derived stromal cells express genes encoding a broad spectrum of arteriogenic cytokines and promote in vitro and in vivo arteriogenesis through paracrine mechanisms. Circulation research. 2004 Mar 19;94(5):678-85.

199- Park CW, Kim KS, Bae S, Son HK, Myung PK, Hong HJ, Kim H. Cytokine secretion profiling of human mesenchymal stem cells by antibody array. International journal of stem cells. 2009 May;2(1):59.

200- Griffith JW, Sokol CL, Luster AD. Chemokines and chemokine receptors: positioning cells for host defense and immunity. Annual review of immunology. 2014 Mar 21;32:659-702.

201- Wang B, Wood IS, Trayhurn P. Hypoxia induces leptin gene expression and secretion in human preadipocytes: differential effects of hypoxia on adipokine expression by preadipocytes. Journal of Endocrinology. 2008 Jul 1;198(1):127-34.

202- Chiellini C, Cochet O, Negroni L, Samson M, Poggi M, Ailhaud G, Alessi MC, Dani C, Amri EZ. Characterization of human mesenchymal stem cell secretome at early steps of adipocyte and osteoblast differentiation. BMC molecular biology. 2008 Feb 26;9(1):26.

203- Mandal P, Park PH, McMullen MR, Pratt BT, Nagy LE. The anti-inflammatory effects of adiponectin are mediated via a heme oxygenase-1–dependent pathway in rat Kupffer cells. Hepatology. 2010 Apr 1;51(4):1420-9.

204- Pawitan JA. Prospect of stem cell conditioned medium in regenerative medicine. BioMed research international. 2014 Aug 28;2014.

205- Kim JY, Song SH, Kim KL, Ko JJ, Im JE, Yie SW, Ahn YK, Kim DK, Suh W. Human cord blood-derived endothelial progenitor cells and their conditioned media exhibit therapeutic equivalence for diabetic wound healing. Cell transplantation. 2010 Dec 1;19(12):1635-44.

206- Timmers L, Lim SK, Arslan F, Armstrong JS, Hoefer IE, Doevendans PA, Piek JJ, El Oakley RM, Choo A, Lee CN, Pasterkamp G. Reduction of myocardial infarct size by human mesenchymal stem cell conditioned medium. Stem cell research. 2008 Jun 30;1(2):129-37.

207- Du Z, Wei C, Cheng K, Han B, Yan J, Zhang M, Peng C, Liu Y. Mesenchymal stem cell–conditioned medium reduces liver injury and enhances regeneration in reduced-size rat liver transplantation. Journal of Surgical Research. 2013 Aug 31;183(2):907-15.

208- Tran C, Damaser MS. Stem cells as drug delivery methods: application of stem cell secretome for regeneration. Advanced drug delivery reviews. 2015 Mar 31;82:1-1.

209- Hung SP, Ho JH, Shih YR, Lo T, Lee OK. Hypoxia promotes proliferation and osteogenic differentiation potentials of human mesenchymal stem cells. Journal of Orthopaedic Research. 2012 Feb 1;30(2):260-6.

210- Newman RE, Yoo D, LeRoux MA, Danilkovitch-Miagkova A. Treatment of inflammatory diseases with mesenchymal stem cells. Inflammation & Allergy-Drug Targets (Formerly Current Drug Targets-Inflammation & Allergy). 2009 Jun 1;8(2):110-23.

211- Zaffran Y, Destaing O, Roux A, Ory S, Nheu T, Jurdic P, Rabourdin-Combe C, Astier AL. CD46/CD3 costimulation induces morphological changes of human T cells and activation of Vav, Rac, and extracellular signal-regulated kinase mitogen-activated protein kinase. The Journal of Immunology. 2001 Dec 15;167(12):6780-5.

212- Kalekar LA, Schmiel SE, Nandiwada SL, Lam WY, Barsness LO, Zhang N, Stritesky GL, Malhotra D, Pauken KE, Linehan JL, O'sullivan MG. CD4+ T cell anergy prevents autoimmunity and generates regulatory T cell precursors. Nature immunology. 2016 Mar 1;17(3):304-14.

213- Pollizzi KN, Powell JD. Integrating canonical and metabolic signalling programmes in the regulation of T cell responses. Nature Reviews Immunology. 2014 Jul 1;14(7):435-46.

214- Heijink H. Dysregulation of T cell activity in asthma. Br J Pharmacol. 2003;138:1441-50.

215- Zhu P, Jiang W, Cao L, Yu W, Pei Y, Yang X, Wan B, Liu JO, Yi Q, Yu L. IL-2 mRNA stabilization upon PMA stimulation is dependent on NF90-Ser647 phosphorylation by protein kinase CβI. The Journal of Immunology. 2010 Nov 1;185(9):5140-9.

216- Eggenhofer E, Benseler V, Kroemer A, Popp F, Geissler E, Schlitt H, Baan C, Dahlke M, Hoogduijn MJ. Mesenchymal stem cells are short-lived and do not migrate beyond the lungs after intravenous infusion. Frontiers in immunology. 2012 Sep 26;3:297.

217- Quintana A, Kummerow C, Junker C, Becherer U, Hoth M. Morphological changes of T cells following formation of the immunological synapse modulate intracellular calcium signals. Cell calcium. 2009 Feb 28;45(2):109-22.

218- Hoogduijn MJ, Popp F, Verbeek R, Masoodi M, Nicolaou A, Baan C, Dahlke MH. The immunomodulatory properties of mesenchymal stem cells and their use for immunotherapy. International immunopharmacology. 2010 Dec 31;10(12):1496-500.

219- Mateos J, Pernas PF, Labora JF, Blanco F, Arufe MD. Proteomic applications in the study of human mesenchymal stem cells. Proteomes. 2014 Feb 7;2(1):53-71.

220- Liu YB, Qian HR, Hong DF, Wang JW, Li JT, Wang XA, Kun Y, Ma XM, Chen Y, Chen DQ, Weng WH. Mesenchymal stem cells inhibit the expression of CD25 on phytohaemagglutinin-activated lymphocytes. Zhonghua yi xue za zhi. 2007 Aug;87(30):2136-9.

221- Krampera M, Glennie S, Dyson J, Scott D, Laylor R, Simpson E, Dazzi F. Bone marrow mesenchymal stem cells inhibit the response of naive and memory antigen-specific T cells to their cognate peptide. Blood. 2003 May 1;101(9):3722-9.

222- Mori S, Matsuzaki K, Yoshida K, Furukawa F, Tahashi Y, Yamagata H, Sekimoto G, Seki T, Matsui H, Nishizawa M, Fujisawa JI. TGF-β and HGF transmit the signals through JNK-dependent Smad2/3 phosphorylation at the linker regions. Oncogene. 2004 Sep 23;23(44):7416-29.

223- Waiser J, Dell K, Böhler T, Dogu E, Gaedeke J, Budde K, Neumayer HH. Cyclosporine A up-regulates the expression of TGF-β 1 and its receptors type I and type II in rat mesangial cells. Nephrology Dialysis Transplantation. 2002 Sep 1;17(9):1568-77.

224- Vatrella A, Fabozzi I, Calabrese C, Maselli R, Pelaia G. Dupilumab: a novel treatment for asthma. Journal of asthma and allergy. 2014;7:123.

225- Prasanna JS, Gopalakrishnan D, Shankar SR, Vasandan AB. Pro-Inflammatory Cytokines, IFNc and TNFa, Influence Immune Properties of Human Bone Marrow and Whartonb Jelly Mesenchymal Stem Cells Differentially. PLos One. 2010 Feb 2;5(2).

226- Gordon SB, Irving GR, Lawson RA, Lee ME, Read RC. Intracellular Trafficking and Killing ofStreptococcus pneumoniae by Human Alveolar Macrophages Are Influenced by Opsonins. Infection and immunity. 2000 Apr 1;68(4):2286-93.

227- Traore K, Trush MA, George M, Spannhake EW, Anderson W, Asseffa A. Signal transduction of phorbol 12-myristate 13-acetate (PMA)-induced growth inhibition of human monocytic leukemia THP-1 cells is reactive oxygen dependent. Leukemia research. 2005 Aug 31;29(8):863-79.

228- Chen SL, Fang WW, Ye F, Liu YH, Qian J, Shan SJ, Zhang JJ, Chunhua RZ, Liao LM, Lin S, Sun JP. Effect on left ventricular function of intracoronary transplantation of autologous bone marrow mesenchymal stem cell in patients with acute myocardial infarction. The American journal of cardiology. 2004 Jul 1;94(1):92-5.

229- Bang OY, Lee JS, Lee PH, Lee G. Autologous mesenchymal stem cell transplantation in stroke patients. Annals of neurology. 2005 Jun 1;57(6):874-82.

230- Dalal J, Gandy K, Domen J. Role of mesenchymal stem cell therapy in Crohn's disease. Pediatric research. 2012 Feb 8;71(4-2):445-51.

231- Abdi R, Fiorina P, Adra CN, Atkinson M, Sayegh MH. Immunomodulation by mesenchymal stem cells. Diabetes. 2008 Jul 1;57(7):1759-67.

232- Perico N, Casiraghi F, Introna M, Gotti E, Todeschini M, Cavinato RA, Capelli C, Rambaldi A, Cassis P, Rizzo P, Cortinovis M. Autologous mesenchymal stromal cells and kidney transplantation: a pilot study of safety and clinical feasibility. Clinical Journal of the American Society of Nephrology. 2011 Feb 1;6(2):412-22.

233- Tan J, Wu W, Xu X, Liao L, Zheng F, Messinger S, Sun X, Chen J, Yang S, Cai J, Gao X. Induction therapy with autologous mesenchymal stem cells in living-related kidney transplants: a randomized controlled trial. Jama. 2012 Mar 21;307(11):1169-77.

234- Kim J, Hematti P. Mesenchymal stem cell–educated macrophages: A novel type of alternatively activated macrophages. Experimental hematology. 2009 Dec 31;37(12):1445-53.

235- Breznan D, Goegan P, Chauhan V, Karthikeyan S, Kumarathasan P, Cakmak S, Nadeau D, Brook JR, Vincent R. Respiratory burst in alveolar macrophages exposed to urban particles is not a predictor of cytotoxicity. Toxicology in Vitro. 2013 Jun 30;27(4):1287-97.

236- Orihuela R, McPherson CA, Harry GJ. Microglial M1/M2 polarization and metabolic states. British journal of pharmacology. 2016 Feb 1;173(4):649-65.

237- Park EK, Jung HS, Yang HI, Yoo MC, Kim C, Kim KS. Optimized THP-1 differentiation is required for the detection of responses to weak stimuli. Inflammation research. 2007 Jan 14;56(1):45-50.

238- McWhorter FY, Wang T, Nguyen P, Chung T, Liu WF. Modulation of macrophage phenotype by cell shape. Proceedings of the National Academy of Sciences. 2013 Oct 22;110(43):17253-8.

239- Yin T, Li L. The stem cell niches in bone. The Journal of clinical investigation. 2006 May 1;116(5):1195-201.

240- Scadden DT. The stem-cell niche as an entity of action. Nature. 2006 Jun 28;441(7097):1075.

241- Kaur, Gurvinder, and Jannette M. Dufour. "Cell lines: Valuable tools or useless artifacts." (2012): 1-5.

242- Stacey G. Primary cell cultures and immortal cell lines. eLS. 2006.

243- Bartelt RR, Cruz-Orcutt N, Collins M, Houtman JC. Comparison of T cell receptor-induced proximal signaling and downstream functions in immortalized and primary T cells. PloS one. 2009 May 4;4(5):e5430.

244- Abraham RT, Weiss A. Jurkat T cells and development of the T-cell receptor signalling paradigm. Nature Reviews Immunology. 2004 Apr;4(4):301.

245- Schildberger A, Rossmanith E, Eichhorn T, Strassl K, Weber V. Monocytes, peripheral blood mononuclear cells, and THP-1 cells exhibit different cytokine expression patterns following stimulation with lipopolysaccharide. Mediators of inflammation. 2013;2013.

246- Chanput W, Mes JJ, Wichers HJ. THP-1 cell line: an in vitro cell model for immune modulation approach. International immunopharmacology. 2014 Nov 1;23(1):37-45.

247- Takashiba S, Van Dyke TE, Amar S, Murayama Y, Soskolne AW, Shapira L. Differentiation of monocytes to macrophages primes cells for lipopolysaccharide stimulation via accumulation of cytoplasmic nuclear factor κB. Infection and immunity. 1999 Nov 1;67(11):5573-8.

248- Zarember KA, Godowski PJ. Tissue expression of human Toll-like receptors and differential regulation of Toll-like receptor mRNAs in leukocytes in response to microbes, their products, and cytokines. The journal of immunology. 2002 Jan 15;168(2):554-61.

249- Bruckmeier M, Kuehnl A, Culmes M, Pelisek J, Eckstein HH. Impact of oxLDL and LPS on C-type natriuretic peptide system is different between THP-1 cells and human peripheral blood monocytic cells. Cellular Physiology and Biochemistry. 2012;30(1):199-209.

250- Han XQ, Chung Lap Chan B, Dong CX, Yang YH, Ko CH, Gar-Lee Yue G, Chen D, Wong CK, Bik-San Lau C, Tu PF, Shaw PC. Isolation, structure characterization, and immunomodulating activity of a hyperbranched polysaccharide from the fruiting bodies of Ganoderma sinense. Journal of agricultural and food chemistry. 2012 Apr 18;60(17):4276-81.

251- Arnold L, Henry A, Poron F, Baba-Amer Y, Van Rooijen N, Plonquet A, Gherardi RK, Chazaud B. Inflammatory monocytes recruited after skeletal muscle injury switch into antiinflammatory macrophages to support myogenesis. Journal of Experimental Medicine. 2007 May 14;204(5):1057-69.

252- Ruffell D, Mourkioti F, Gambardella A, Kirstetter P, Lopez RG, Rosenthal N, Nerlov C. A CREB-C/EBPβ cascade induces M2 macrophage-specific gene expression and promotes muscle injury repair. Proceedings of the National Academy of Sciences. 2009 Oct 13;106(41):17475-80.

253- Perdiguero E, Sousa-Victor P, Ruiz-Bonilla V, Jardí M, Caelles C, Serrano AL, Muñoz-Cánoves P. p38/MKP-1–regulated AKT coordinates macrophage transitions and resolution of inflammation during tissue repair. J Cell Biol. 2011 Oct 10:jcb-201104053.